YIP1 family member 4 (YIPF4) is a novel cellular binding partner of the papillomavirus E5 proteins

Marietta Müller

Submitted in accordance with the requirements for the degree of
Doctor of Philosophy

The University of Leeds
School of Molecular and Cellular Biology

January, 2014

The candidate confirms that the work submitted is her own and that appropriate credit has been given where reference has been made to the work of others.

Für

Philip Simeon Müller

Acknowledgement

I would like to thank my two supervisors Dr Andrew Macdonald and Prof Nicola Stonehouse for their support and guidance throughout this project. I would also like to thank all past and present members of the Macdonald and Stonehouse labs for their helpful discussions and advice. In particular, thank you to Dr Christopher Wasson for the primary cell work and lab entertainment and to 'team lunch' Özlem Cesur and Dr Emma Prescott for invaluable chats. Thank you to Hussein Abdul-Sada for interesting perspectives and challenging questions. Many thanks to Gareth Howell and Jamel Mankouri for help with microscopy and flow cytometry. Thank you to Dr Cheryl Walter for help with the vaccinia virus expression system and Rosella Doble and Dr Sophie Forrest for help with qPCR. I would also like to thank Dr Tobias Lamkemeyer for granting insights into his expertise in mass spectrometry. Thank you to my advisor Prof G. Eric 'Excuse me, you are on fire' Blair for his advice and support. Many thanks to Susan Matthews and Rajni Bhardwaj for keeping the lab organised – you are truly invaluable!
I would also like to thank Yorkshire Cancer Research for funding my PhD.

Ich danke meinen Eltern und Geschwistern für Ihre Unterstützung während der ganzen Promotion und speziell der letzten Monate. Auch meinen Taufpaten Maria und Andreas möchte ich für Ihre Unterstützung danken. Ich danke Sandra und Kerstin für eine unvergessliche Zeit in Leeds. Ich danke allen meinen Freunden für Ihr Verständnis und Ihre Motivation. Im Besonderen möchte ich Nadine danken – ohne Dich hätte ich es nicht so weit gebracht!

Eugene moratuwa wa pelo yaka, ke leboha tshehetso le rotlohetso eo o mphang yona ka dinako tsohle ke kahoo ke o ratang ka lerato le ke keng ja lekangwa le bophara ba lefatshe le tswang botebong ba pelo yaka.

Abstract

Papillomaviruses (PVs) are capable of causing a broad spectrum of diseases with the human PVs (HPVs) being responsible for a great portion of cervical, anogenital and head and neck cancers worldwide. The PV oncoprotein E5 plays roles in host cell transformation, the PV life-cycle and viral immune evasion. However, the mechanisms by which E5 achieves this are unclear. A yeast two-hybrid screen identified a novel Golgi protein, YIPF4, as a potential interactor of 16E5. YIPF4 is a member of the integral membrane protein family YIP1 that is thought to mediate intracellular trafficking. Quantitative polymerase chain reaction, Western blot and immuno-histochemistry analysis confirmed that YIPF4 is expressed in host cells of HPV infection in cell culture systems and in clinical samples of HPV16 induced cervical lesions. This implies that YIPF4 could be a relevant *in vivo* binding partner of E5. Upon the differentiation of HPV18 positive keratinoctyes in semisolid medium, the YIPF4 expression levels were stabilised compared to control cells suggesting that YIPF4 might play a role during the productive viral life-cycle. A differential, detergent permeabilisation assay provided the first experimental evidence for a three trans-membrane domain model of YIPF4. Co-immuno-precipitation revealed a conserved interaction of YIPF4 with E5 proteins from clinically important PVs indicating a potentially invaluable role of this complex for the virus. A flow cytometry approach unexpectedly revealed that neither E5 nor YIPF4 proteins modulate the trafficking of human leukocyte antigen class I molecules to facilitate viral immune evasion. A preliminary cellular interactome of YIPF4 was determined in a label free mass spectrometry experiment to facilitate the search for the function of the highly conserved E5/YIPF4 protein complex. This knowledge might contribute to elucidating new targets for the development of therapeutic agents against the broad spectrum of PV associated diseases.

Table of contents

List of tables

List of illustrative material

Abbreviations

α-	anti-
°C	degrees Celsius
µ	micro
16E5	human papillomavirus type 16 E5 oncoprotein
16K	16 kDa subunit of the vacuolar H^+ - ATPase
3'	three prime
5'	five prime
5-HT_{1A}R	serotonin receptor
A or a	adenine
A31-3T3	murine fibroblast cell line
ADP	adenosine diphosphate
ANOVA	analysis of variance
APS	ammonium persulphate
Arf1	ADP-ribosylation factor 1
ArfGAP1	ADP-ribosylation factor GTPase-activating protein 1
ARS	age standardised rate
ATP	adenosine triphosphate
AU	arbitrary units
Bap31	B-cell receptor-associated protein 31
BF	bright field
BLAST	basic local alignment search tool
BLASTN	nucleotide-nucleotide basic local alignment search tool
Bos1	bet one suppressor 1
bps	base pairs
BPV	bovine papillomavirus
C or c	cytosine
c.o.	codon optimised
C127	murine epithelial tumour cell line
CCDC136	coiled-coil domain containing 136
CDK	cyclin-dependent kinase
cDNA	complementary deoxyribonucleic acid
CECAD	cluster of excellence in cellular stress responses in aging- associated diseases
cervix	uterine cervix
CIN	cervical intraepithelial neoplasia
CLMN	calmin
CMV	cytomegalovirus
Co-IP	co-immuno-precipitation
COPI	coat protein complex 1
COPII	coat protein complex 2
COX-2	cyclooxygenase-2
CPV	*Canis familiaris* Papillomavirus
CR	coding region
CR1	conserved region 1
CR2	conserved region 2
Crm-1	chromosome region maintenance 1 protein homolog
C-terminus	carboxyl-terminus
DAPI	4',6-diamidino-2-phenylindole
DBD	DNA-binding domain
ddH_2O	double-distilled water

DMEM	Dulbecco’s modified Eagle’s medium
DMSO	dimethyl sulphoxide
DNA	deoxyribonucleic acid
DP1	DRTF1-polypeptide 1
dpi	dots per inch
DTT	dithiothreitol
E	early
e.g.	exempli gratia
E2BS	E2 binding site
E4	E1^E4
E6AP	E6 associated protein
EDTA	ethylenediaminetetraacetic acid
EGF	epidermal growth factor
eGFP	enhanced green fluorescent protein
EGF-R	epidermal growth factor receptor
EMI1	early mitotic inhibitor 1
ER	endoplasmatic reticulum
ErbB2	epidermal growth factor receptor-related protein 2
ErbB3	epidermal growth factor receptor-related protein 3
ErbB4	epidermal growth factor receptor-related protein 4
ERGIC	ER-Golgi intermediate compartment
ERK 1/2	extracellular signal-regulated kinase 1/2
EV	epidermodysplasia verruciformis
EVER1	epidermodysplasia verruciformis protein 1
EVER2	epidermodysplasia verruciformis protein 2
FACS	fluorescence-activated cell sorting
FdPV	*Felis domesticus* Papillomavirus
FinGER	five-pass trans-membrane protein localising to the Golgi and ER
FL	fluorescence
FLAG	octapeptide DYKDDDDK
FRET	fluorescence resonance energy transfer
fwd	forward
g	gramme
G or g	guanine
GAP	nucleotide dissociation inhibitor
GAPDH	glyceraldehyde 3-phosphate dehydrogenase
GDF	GDI dissociation factor
GDI	guanine nucleotide dissociation inhibitor
GDP	guanosine diphosphate
GEF	guanine nucleotide exchange factor
GFP	green fluorescent protein
GGT	geranylgeranyl transferase
GM130	Golgi matrix protein 130
GO	gene ontology
Golgi	Golgi apparatus
Grd19p	Golgi retention deficient protein 19
GTP	guanosine-5'-triphosphate
GW	genital wart
h	hour(s)
H&E	haematoxylin and eosin
H^+	proton
HA	haemagglutinin
HC	heavy chain
HCMV	human cytomegalovirus

HEK293	Human embryonic kidney 293
HEK293T	Human embryonic kidney 293 T antigen cells
HEPES	N-2-hydroxyethylpiperazine-N'-2-ethanesulfonic acid
HFK	human foreskin keratinocytes
HIV	human immunodeficiency virus
HLA	human leukocyte antigen
HNSCC	head and neck squamous-cell carcinoma
HPV	human papillomavirus
HSIL	high-grade squamous intra-epithelial lesion
ICC	immuno-cytochemistry
ICO	Institut Catala d'Oncologia
ID	identification tag
IFN	interferon
IgG	immunoglobulin G
IHC	immuno-histochemistry
IP	immuno-precipitation
IRE1α	Inositol-requiring protein 1 alpha
k	kilo
K^+	potassium ion
kDa	kilo dalton
Kif5B	kinesin-1 heavy chain
KNβ3	karyopherin β3
KO	knock out
L	late
l	litre
LAMP-1	lysosome-associated membrane glycoprotein 1
LAMP-2	lysosome-associated membrane glycoprotein 2
LB	Luria-Bertani
LCR	long control region
LDS	lithium dodecyl sulphate
LFQ	label free quantification
log	logarithmic
LSIL	low-grade squamous intra-epithelial lesion
LSM	laser scanning microscope
LUMIER	luminescence-based mammalian interactome mapping
M	molar concentration
m	milli
m	metre
m/z	mass-to-charge ratio
MAML1 or 3	mastermind-like protein 1 or 3
mann. II	mannosidase II
MAP	mitogen-activated protein
MaPV	*Mesocricetus auratus* Papillomavirus
MF	membranous fraction
mg	milligram(s)
MHC	major histocompatibility complex
min	minute(s)
ml	millilitre(s)
mM	millimolar
MnPV	*Mastomys natalensis* Papillomavirus
mRNA	messenger ribonucleic acid
MS	mass spectrometry
n/a	not applicable
n/doc.	not documented

n/n	not named
n/s	not stated
Na^+	sodium ion
nano-LC ESI-MS/MS	nano-liquid chromatography electrospray ionisation tandem mass spectrometry
NCR	non-coding region
NES	nuclear export signal
NF-κB	nuclear factor of kappa light polypeptide gene enhancer in B-cells
ng	nanogramme
NIH 3T3	murine fibroblast cell line
NLS	nuclear localisation signal
nm	nanometre
No	number
N-terminus	amino-terminus
o/n	overnight
OaPV	*Ovis aries* Papillomavirus
OcPV	*Oryctolagus cuniculus* Papillomavirus
OD_{600}	optical density measured at 600 nm
ORF	open reading frame
ori	origin of replication
OSCC	oropharyngeal squamous-cell carcinoma
OvPV	*Odocoileus virginianus* Papillomavirus
p	probability
PAE	early polyadenylation site
PAL	late polyadenylation site
PANTHER	protein annotation through evolutionary relationship
Pap smear	Papanicolaou smear test
PBS	phosphate buffered saline
PCC	Pearson correlation coefficient
PCR	polymerase chain reaction
PDGFβ-R	platelet-derived growth factor receptor beta
PDZ	post synaptic density protein, Drosophila disc large tumor suppressor, zonula occludens-1 protein
PepV	*Psittacus erithacus* Papillomavirus
pH	-log10 concentration of hydrogen ions
PI	propidium iodide
PIN	penile intraepithelial neoplasia
PpPV	*Pan paniscus* Papillomavirus
pRB	retinoblastoma-associated protein
PSC	Pearson and Spearman correlation coefficients
PV	papillomavirus
qPCR	quantitative real-time polymerase chain reaction
Ref	reference
rel.	relative
REP	Rab escort protein
rev	reverse
RNA	ribonucleic acid
RRP	recurrent respiratory papillomatosis
SCC	squamous-cell carcinoma
SDM	standard deviation of the mean
SDS	sodium dodecyl sulphate
SDS-PAGE	sodium dodecyl sulphate polyacrylamide gel electrophoresis
sec	second(s)
SF	soluble fraction
SfPV	*Sylvilagus floridanus* Papillomavirus

shRNA	short hairpin ribonucleic acid
SILAC	stable isotope labelling by/with amino acids in cell culture
siRNA	small interfering RNA
siRNA NC	small interfering ribonucleic acid negative control
STAT1	signal transducer and activator of transcription 1
SV40	simian vacuolating virus 40
T or t	thymine
TAD	transactivation domain
TAP	transporter associated with antigen processing
TAP-MS	tandem affinity purification followed by mass spectrometry analysis
TBS	Tris buffered saline
TBST	Tris buffered saline containing Tween-20
TBX2	T-box transcription factor 2
TBX3	T-box transcription factor 3
TEMED	tetramethylethylenediamine
TfR	transferrin receptor
TGN46	*trans*-Golgi network integral membrane protein 2
TM	trans-membrane
TMD	trans-membrane domain
t-SNARE	target soluble N-ethylmaleimide-sensitive facto attachment protein receptor
Tvp18	T-SNARE affecting a late Golgi compartment protein 2 compartment vesicle protein of 18 kDa
Tvp23	T-SNARE affecting a late Golgi compartment protein 2 compartment vesicle protein of 23 kDa
TXNDC	thioredoxin domain-containing protein 15
UK	United Kingdom
US11	unique short glycoprotein 11
US2	unique short glycoprotein 2
US6	unique short glycoprotein 6
USA	United States of America
UVB	ultraviolet B
V	volts
v/v	volume per volume
Vam7p	vacuolar morphogenesis protein 7
VAPB	vesicle-associated membrane protein (VAMP) associated protein B (VAPB
v-ATPase	vacuolar ATPase
VLP	virus-like particle
Vps17	vacuolar protein sorting-associated protein 17
Vps5	vacuolar protein sorting-associated protein 5
v-SNARE	vesicle soluble N-ethylmaleimide-sensitive facto attachment protein receptor
w/v	weight per volume
WHO	World Health Organization
WT	wildtype
x g	times gravitational force
XBP-1	X-box-binding protein 1
Y2H	yeast two-hybrid
Yif1	Yip1 interacting factor
YIF1A	YIP1-interacting factor homolog A
YIF1B	YIP1-interacting factor homolog B
Yip	Ypt interacting protein
YIPF4	YIP1 family member 4
Yop1	Yip one partner
Yos1	Yip one suppressor 1
ZnT-1	zinc transporter 1

Chapter 1. Introduction

1.1. Family of Papillomaviruses

The family of papillomaviruses (PV) or *Papillomaviridae* is one of the largest and evolutionarily most successful family of viruses in vertebrates (Van Doorslaer, 2013, Van Doorslaer et al., 2013). It could be derived from an ancient ancestral PV that segregated into four to six more specialised viruses (Bravo and Alonso, 2007, Shah et al., 2010). Due to their genetic stability, the evolutionary selection in PVs is slow. Co-evolution with their hosts as well as recombination and host-switching events during several millions of years resulted in highly species and tropism specific viruses (Gottschling et al., 2011). The PVs infect distinct niches of the epithelium of reptiles, birds and mammals and the infections can show no symptoms or cause a variety of disease ranging from warts to cancer.

1.2. Classification of PVs

The first PV was isolated by Shope from cottontail rabbits in 1933 (Shope and Hurst, 1933). The viral particles from skin papillomas were first visualised by electron microscopy 16 years later (Strauss et al., 1949). Since then a total of 241 PV types have been discovered and new putative HPV types are identified frequently (Ekström et al., 2013). The classification of PVs has been a continuing debate over many decades (de Villiers, 2013).

The classification system currently used was initiated by the Reference Centre for Papillomaviruses, Heidelberg, Germany (Bernard et al., 2010, de Villiers, 2013). Its nomenclature is similar but not identical to the nomenclature used by the International Committee on the Taxonomy of Viruses (Fauquet et al., 2005). According to the currently used classification system, the 241 types of PVs form the *Papillomaviridae*, which are categorised according to sequence similarity of the capsid protein L1 open reading frame (ORF). The PVs of the 29 genera

share less than 60% sequence identity and are biologically diverse. The 170 HPV types identified so far are members of the α-, β-, γ-, μ- and ν-genera with the α-HPV types being responsible for the heaviest clinical burden (Figure 1.1) (Bernard et al., 2010, de Villiers, 2013, de Villiers et al., 2004, Van Doorslaer, 2013).

The genera are subdivided into species that share 60% - 70% sequence identity. The members of a species have coherent biological properties. The HPV types belonging to the α-9 species, like HPV type 16 (HPV16), infect the mucosal epithelium and are associated with malignant lesions. These are therefore characterised as 'high-risk' HPV types. 'Low-risk' HPV types, like HPV6 and 11 of the α-10 species, only cause benign lesions in the mucosal epithelium. The PV types that cause lesions of the skin like HPV2 of the α-4 species are 'cutaneous' HPV types.
The PV types have to show more than 10% sequence differences to any other PVs to be considered a distinct PV type. A PV with only 2% - 10% sequence difference is called a subtype and with less than 2% sequence difference a variant.

1.3. HPV induced diseases

1.3.1. Cutaneous lesions

Most of the HPV types that infect the cutaneous epithelium in humans belong to the β-genus of PVs but some are also classified as α-, γ-, μ-, ν-genera PVs (Bernard et al., 2010). They cause benign lesions like warts that are characterised by an increase in the horny layer (hyperkeratosis) as well as thickening (acanthosis) and folding (papillomatisis) throughout all layers of the dermis (Cubie, 2013). The common wart is mainly caused by the α-4 HPV2 and is remarkably persistent. The development of plantar warts or verrucas is induced by the μ-1 HPV1, α-4 HPV2 and the γ-1 HPV4 while flat plane warts predominantly originate from infections with the α-2 HPV types 3 and 10. Especially the deep plantar warts can be extremely painful for the patient. Up to

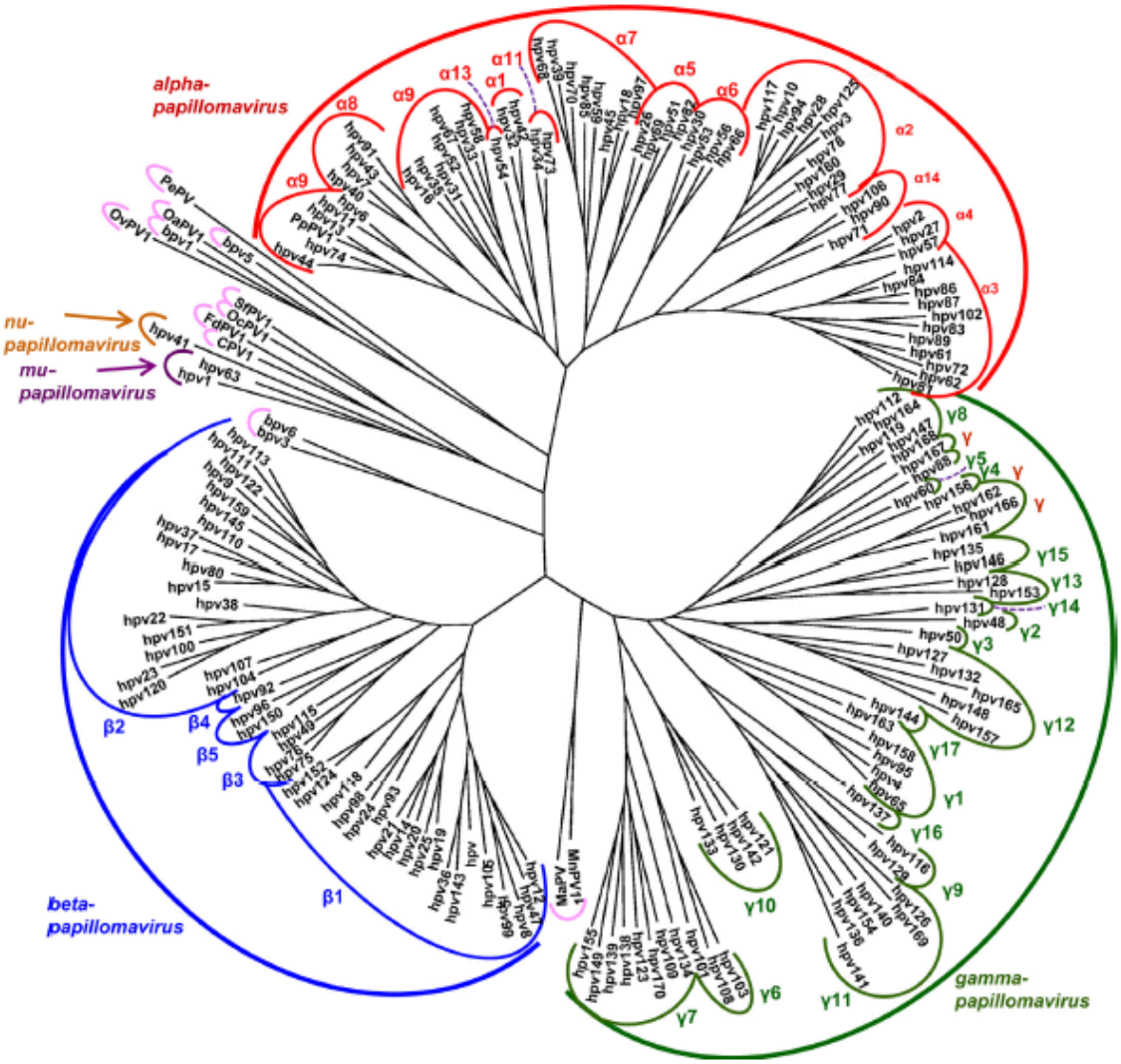

Figure 1.1 Phylogenetic tree of 170 HPV types including some animal PV types. The phylogenetic analysis is based on the L1 ORF. PV genera, species and types are shown. Animal PV types highlighted in pink belong to θ-, ε-, δ-, κ-, λ-, ξ-, π-genera, respectively. Adapted from de Villiers, 2013.

80% of cutaneous warts spontaneously resolve within 2 years (Cubie, 2013, Sterling et al., 2001)

Epidermodysplasia verruciformis (EV) patients suffer from a rare disorder of the innate immune system that mediates susceptibility to β-PVs, with HPV5 and 8 being the most prevalent HPV types. (Kiviat, 1999, Lazarczyk et al., 2009, Ramoz et al., 2002). EV patients develop plane warts and verrucous lesions with childhood onset and are likely to develop squamous cell carcinomas (SCCs) before the age of 40 (Sterling, 2005). EV is caused by an autosomal

recessive mutation of the EV proteins 1 or 2 (EVER1 or EVER2) genes which encode trans-membrane channel-like proteins. The wildtype EVER proteins interact with the zinc transporter 1 (ZnT-1) and are thus responsible for zinc homeostasis (Lazarczyk et al., 2008). HPV16 E5 (16E5) binds EVER and ZnT-1 and alters their function to enhance the downstream activator protein 1 mediated expression of the HPV oncoproteins E6 and E7 (Lazarczyk et al., 2009). The defective EVER genes in EV patients achieve similar downstream affects which favour the infection with β-PVs that do not encode an E5 gene.

1.3.2. Benign mucosal lesions

Mucosal infections by α-HPV types are more common than cutaneous infections but the majority of these do not show any symptoms (Cubie, 2013, Winer et al., 2005). Infections of the genital mucosa can, however, lead to the development of condylomata acuminate or genital warts (GWs). Ninety-seven per cent of GWs are caused by the low-risk HPV types 6 and 11 (Ball et al., 2011). These evoke the characteristic acanthosis and papillomatosis resulting in thickening of the epithelia similar to cutaneous warts but without hyperkeratosis (Cubie, 2013). GWs are mainly found in the regions traumatised during sexual intercourse. GWs can be painful and have a great impact on health-related quality of life (Woodhall et al., 2008). In rare occasions vaginal warts were shown to obstruct the birth canal (Cubie, 2013). A third of GWs manifestations will spontaneously regress within four months (Yanofsky et al., 2012).

HPV infections of the laryngeal mucosa can lead in rare occasions to recurrent respiratory papillomatosis (RRP). The majority (92%) of RRP is associated with the low-risk HPV types 6 and 11 (Abramson et al., 1987). The disease is characterised by exophytic warty lesions in the laryngeal area, which are usually benign but recur after surgical removal. The symptoms range from hoarseness or stridor to obstruction of the airways depending on disease severity (Gillison et al., 2012). In 1.6% of patients the benign lesions progress into cancer (Dedo and Yu, 2001), however, in HPV11 positive RRP with pulmonary involvement the malignant conversion rate can be as high as 80% (Gerein et al., 2005).

1.3.3. Malignant mucosal lesions

High-risk HPV types cause malignant mucosal lesions in several anogenital sites like the uterine cervix (cervix), penis, vulva, vagina, anus and in the head and neck area (Figure 1.2) (Bouvard et al., 2009).

Cervical cancer is the most studied HPV related cancer to date. Professor Harald zur Hausen was awarded the Nobel Prize in Physiology or Medicine in 2008 for the discovery of the association between HPV and cervical cancer.
Twelve high-risk HPV types are associated with this type of cancer namely HPV16, 18, 31, 33, 35, 39, 45, 51, 52, 56, 58, and 59 (Bouvard et al., 2009). HPV16 and HPV18 alone account for 70% - 76% of cervical cancer cases worldwide (de Sanjose et al., 2007, Li et al., 2011). There is limited evidence for a further 8 HPV types (26, 53, 66, 67, 68, 70, 73, 82) to be the causative agents of cervical cancer (Bouvard et al., 2009).

The majority of cervical cancers arise in the transformation zone of the cervix and are SCCs (80% - 90%). The remaining cervical cancer cases are adenocarcinomas (Cubie, 2013). However, 50% of the initial HPV infections spontaneously resolve within 6 months and ~90% of infections clear within a few years (Rodriguez et al., 2010, Winer et al., 2011).

Persistent HPV infections can progress into precancerous lesions called cervical intraepithelial neoplasia (CIN) (Cubie, 2013). These do not cause any apparent symptoms. Characteristic histological features of CINs are highly vacuolated cells with hyperchromatic nuclei, the koilocytes. The CIN lesions are graded. CIN1 lesions contain 1/3 abnormal cells, CIN2 lesions feature 2/3 cells with abnormalities and in CIN3 lesions all cells are highly abnormal. Further viral persistence can lead to invasive cancer.

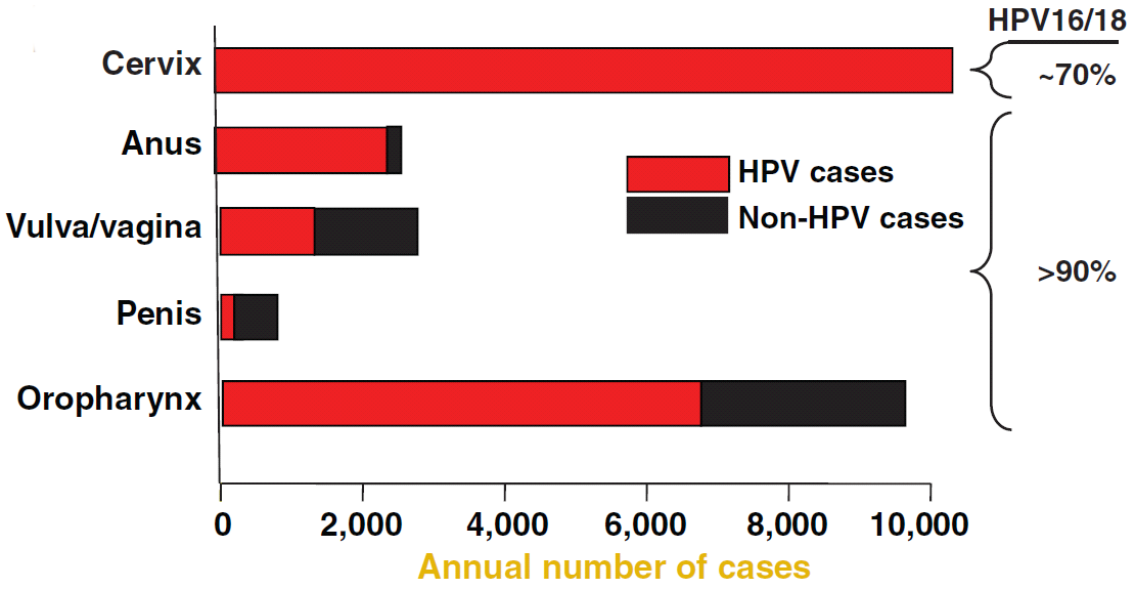

Figure 1.2 Distribution and incidences of cancers associated with HPV in the USA. The HPV associated cancer cases (red) are contrasted with HPV-unrelated cancer cases (black). The approximate percentage of cancers attributable to the most common HPV types 16 and 18 is shown on the right. Adapted from Lowy and Schiller, 2012.

It was initially believed that the integration of the viral DNA into the host genome is crucial for the progression into invasive cancer (Corden et al., 1999, Cullen et al., 1991). However, several invasive cancer samples only contain episomal HPV genomes which challenges this episteme of cervical cancer aetiology (Badaracco et al., 2002).

Early stage SCCs are mostly asymptomatic while pelvic pain, vaginal bleeding and discharge as well as pain during intercourse can be symptoms of later stage SCCs. Co-factors for the progression into cervical cancer are long-term use of oral contraceptives, smoking, co-infections with human immunodeficiency virus (HIV) and multiparity (Moscicki et al., 2012).

HPVs are also associated with carcinoma of the penis with 90% of *in situ* penile carcinomas and 52% of invasive penile carcinomas being positive for HPV (Krustrup et al., 2009). This illustrates that HPV prevalence differs amongst carcinoma subtypes, e.g. 82% of warty-basaloid cancers are HPV positive while no association has been observed with verrucous penile carcinomas (Chaux

and Cubilla, 2012). HPV16 is found in 91% of high-risk HPV induced carcinomas (Krustrup et al., 2009). The patient might present with discharge or bleeding, flat brown-blue growths, warty papules or red rashes which are usually painless (Cubie, 2013). Pre-cancerous lesions defined as penile intraepithelial neoplasia (PIN) precede the development into cancer. Also, certain risk factors for cancerous progression have been identified like lack of condom use, not being circumcised, number of lifetime sexual partners and smoking (Moscicki et al., 2012).The natural history of HPV infections in men is, however, largely unknown and urgently needs further investigations (Hartwig et al., 2012).

HPV also causes less common forms of anogenital cancer. Four per cent of gynaecological cancers worldwide are carcinomas of the vulva (Castellsagué et al., 2013). This rare cancer is attributable to HPV (43%) with HPV16 being the most prevalent HPV type (Lowy and Schiller, 2012, Rumbold et al., 2012). The majority of vaginal (70%) and anal (92%) cancers are also associated with HPV (Ouhoummane et al., 2013, Stern et al., 2012). In 90% of anal cancer samples high-risk HPV16 was identified as the causative agent.

A remarkable 72% of oropharyngeal SCCs (OSCCs) can be associated with HPV in the USA (Chaturvedi et al., 2011, Mehanna et al., 2013) but as for penile cancer, the prevalence of HPV in head and neck SCCs (HNSCCs) is subtype specific. Worldwide, 36% of OSCCs is HPV positive while only 24% of oral SCCs and 24% of laryngeal SCCs are attributable to HPV (Kreimer et al., 2005). The great majority (~90%) of HPV associated HNSCC is caused by HPV16. The viral DNA is often but not always integrated into the host genome (Lace et al., 2011). Co-factors for the development of HNSCC could be alcohol, smoking, genetic variations as well as diet and nutrition and dental hygiene (Gillison et al., 2012). Notably, patients with HPV positive HNSCC have a 28% reduced risk of death compared to HPV negative HNSCC patients (Ragin and Taioli, 2007).

1.3.4. BPV induced pathology

To date, 10 bovine PV (BPV) types have been identified and classified amongst the δ-, ε-, ξ-genera of PVs (Bernard et al., 2010). The BPV types 1 and 2 form an exception to the epithelia tropism and species specificity of the *Papillomaviridae*. They are the only known PVs that also infect the fibroblasts in the dermis and are not confined to the infection of cattle but cross-species infection of horses and other ungulates has been described (Shafti-Keramat et al., 2009). Their pathology is diverse with tumour formation being observed in the genital and paragenital area and the skin, but also the eye, upper gastrointestinal tracts and the urinary bladder (Roperto et al., 2010). The formation of urinary bladder and lower gastrointestinal carcinomas correlates with the ingestion of bracken-fern (Nasir and Campo, 2008). BPV1 and BPV2 are associated with the formation of urinary bladder cancer while BPV4 is predominant causative agent of gastrointestinal carcinomas.

1.3.5. Epidemiology of malignant HPV associated lesions

HPV associated cancers have a high impact on the world population. The probability of a woman acquiring a HPV infection during her life is remarkably high, at 80% - 90% (Bosch et al., 2012), however, the HPV prevalence differs greatly amongst populations. In Africa, Central America and Mexico it is estimated to be ≥20% while in Europe and Asia only 8% of women are assumed to be HPV infected (de Sanjose et al., 2007). This puts more than 2 billion women worldwide older than 15 years at risk of developing cervical cancer. Interestingly, the prevalence of high-risk HPV types does not vary greatly between regions of the world. Fifty-four per cent of invasive cervical cancers are caused by HPV16 and 16.5% by HPV18.

Cervical cancer is the second most common cancer in women worldwide with 86% of cases occurring in developing countries (Figure 1.3, Table 1.1) (WHO and ICO, 2010). Almost half of the patients die from the disease. Until the year 2030, a worldwide 2% increase in incidence of cervical cancers is predicted, which is in balance with the rate of decline (Forman et al., 2012).

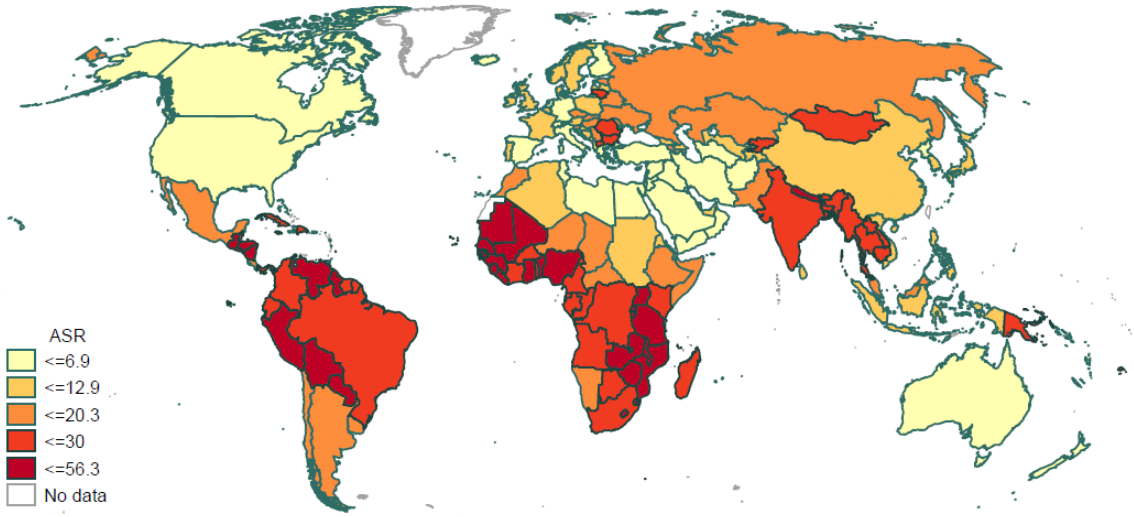

Figure 1.3 Age standardised rate of cervical cancer worldwide. Age standardised rates (ARS) indicated are per 100, 000 women per year. The heavieast burden of cervical cancer is carried by developing countries. Adapted from WHO and ICO, 2010.

Table 1.1 Extent of HPV associated cancers worldwide (rounded numbers), in the UK and Yorkshire and the North (Castellsagué et al., 2013, de Sanjose et al., 2007, WHO and ICO, 2010).

type of cancer	annual cases worldwide	cases in the UK, 1998 - 2002	cases in Yorkshire and the North, 1998 - 2002	age group mostly affected [years]
cervical	530,000	14,393	2081	<35; >45
head and neck	400,000	4,705	583	n/s
vulva	27,000	4,812	637	n/s
anal	27,000	1,449	205	n/s
penile	22,000	1,916	256	50 - 70
vagina	13,000	1,041	137	n/s

n/s = not stated

HPV associated cancers of the penis are rare and account for 0.5% of cancers in men (Castellsagué et al., 2013, WHO and ICO, 2010). Incidences rates correlate with cervical cancer and are higher in Latin America, India and Thailand than in Western countries (Castellsagué et al., 2013, de Martel et al., 2012). Cancer of the vulva is another rare form of HPV related cancer with ~60% of vulva cancers occurring in developed countries (WHO and ICO, 2010). HPV induced cancer of the vagina accounts for 2% of all gynaecological cancers worldwide with 68% cent of them occurring in developing countries. HPV positive cancer of the anus is more common in women than in men but it is especially high in women with cervical or vulva cancer, men who have sex with men and immunosuppressed populations including HIV infected people (Castellsagué et al., 2013).

The number of HPV related OSCC is on the rise with 72% of them being positive for HPV today compared to only 16% in the 1980 (Chaturvedi et al., 2011, Mehanna et al., 2013). According to estimates, in 2020 the number of HPV positive OSCCs will exceed the numbers of HPV-related cervical cancers. This dramatic rise in HPV positive OSCCs was described as a cancer epidemic (Marur et al., 2010).

1.3.6. Transmission

HPVs are generally transmitted by contact with a contaminated person or object and facilitated by minor injuries to the epidermis of the recipient.

Cutaneous warts in childhood are easily spread because person to person contact is frequent as well as suckling on contaminated surfaces like fingers is common (Cubie, 2013).

Mucosal HPV types can be spread horizontally by sexual and non-sexual contact as well as vertically by mother to infant contact.

The primary route of mucosal HPV transmission is either direct or indirect sexual contact where skin to skin contact is more crucial than penetration (Stanley, 2010). Oral sex and potentially open mouth kissing can also facilitate the spread of HPV (D'Souza and Dempsey, 2011) although the latter is controversial (Meyer et al., 2013).

The transmission of HPV frequently occurs via autoinoculation. The same HPV types were identified on hands and fingers of patients with genital HPV which can promote the infection of other mucosal sites of their bodies (Winer et al., 2010).

The vertical transmission rate from mother to infant is approximately 20% - 30% (Castellsague et al., 2009, Erickson et al., 2013, Rombaldi et al., 2008, Rombaldi et al., 2009). The virus can be spread via the placenta, amniotic fluid or during delivery. The great majority (up to 100%) of infant HPV infections are cleared within the first year of life and the juvenile onset of RRP and GWs is rare (Obalek et al., 1990, Silverberg et al., 2003).

1.3.7. HPV and the immune system

The virus-host co-evolution selected for a diverse range of HPV immune evasion strategies (Amador-Molina et al., 2013). The HPV life-cycle which is confined to the epithelial layers (1.4.2) minimises the exposure to cells of the innate immune system (Stanley, 2012). The release of new virus particles coincides with the natural death of the differentiated keratinocyte and cytolysis and the subsequent initiation of the inflammatory response is avoided. This type

of viral life-cycle bypasses a viraemia which exacerbates detection by the host's immune system.
The viral proteins are encoded with suboptimal codons for the expression in mammalian host cells. This hampers their expression and keeps the viral protein expression low to further evade recognition by the host's T cells (Kanodia et al., 2007, Liu et al., 2002, Zhao et al., 2005). High levels of viral proteins are only expressed in the upper layers of the stratified epithelium which approach terminal differentiation (Middleton et al., 2003, Stanley, 1994, Sterling et al., 1993).

Despite its hidden life-cycle, HPV employs further strategies to evade the immune system. The viral oncoproteins E5 and E7 actively down-regulate the cell surface expression of human leukocyte antigen (HLA) class I and II as well as CD1d (Ashrafi et al., 2006a, Bottley et al., 2008, Miura et al., 2010, Zhang et al., 2003) to avoid recognition by T cells. The E5 mediated down-regulation of HLA class I molecules is common to all tested PV types so far (Ashrafi et al., 2006a).
High-risk HPV types down-regulate a wide array of pro-inflammatory cytokines (Amador-Molina et al., 2013, Karim et al., 2011). Especially E6 and E7 actively inhibit the interferon (IFN) signalling pathways to escape from innate immunity (Barnard and McMillan, 1999, Ronco et al., 1998).

In the majority of cases the immune system eventually clears the HPV infections. In GWs and CIN1 lesions this is achieved by infiltration of both CD4+ and CD8+ T cells and macrophages into the infected epithelium which promote clearance by the expression of pro-inflammatory cytokines (Coleman et al., 1994). This cell-mediated immune response is predominantly directed against the E2 and E6 proteins (de Jong et al., 2002, Welters et al., 2003).

The adaptive immune response supports HPV clearance although seroconversion is only observed in 60% - 69% of women depending on the HPV type (Carter et al., 2000). The generation of antibodies specific to the major viral capsid protein L1 in HPV16 positive patients can require 6 – 12 months. In HNSCCs antibodies to HPV16 E6 and E7 can be detected in ~20%

of patients (Smith et al., 2007). High antibody levels against HPV16 and 18 protect from reinfection or reactivation (Safaeian et al., 2010). This was exploited for the development of prophylactic vaccines (1.3.8).

1.3.8. Prevention and treatment of HPV induced lesions

There are two prophylactic vaccines available to prevent infection from the most common mucosal HPV types. Cervarix (GlaxoSmithKline Biologicals) is a bivalent virus-like particle (VLP) vaccine against the most frequent high-risk HPV types 16 and 18 while Gardasil (Merck) is a quadrivalent VLP vaccine against the high-risk HPV types 16 and 18 and the low-risk HPV types 6 and 11. Both vaccines are highly effective against infections with the targeted HPV types and additional cross protection against other HPV types (Cervarix: HPV31, 33, 45, Gardasil: HPV31) was observed (De Vincenzo et al., 2013, Kjaer et al., 2009, Paavonen et al., 2009). Their safety profile as well as immunogenicity and long-term protection are excellent (Bosch et al., 2012, Denny, 2013, Schiller et al., 2012). When sufficient vaccination levels are achieved globally, 70% of cervical cancers can be prevented (Bosch et al., 2012).

In the UK, girls between 12 – 13 years of age are vaccinated through secondary school vaccination programmes with the quadrivalent vaccine. This national vaccination schedule is highly effective and some herd-immunity is provided (Mesher et al., 2013). Vaccination of boys is effective but currently not part of the UK vaccination schedule (Castellsagué et al., 2013, Schiller et al., 2012).

Limitations to the vaccines include (i) lack of therapeutic effect (ii) targeting of few HPV types only (iii) high cost and therefore not accessible to everyone, which make further preventative measures necessary.

A cervical screening programme was launched in the UK in 1988 with great success. Women between the ages of 25 – 64 years are recruited once every 3 years and potentially 80% of cervical cancer related deaths were prevented this way (Peto et al., 2004). In 2008, screening coverage was 69% UK-wide. Yorkshire and the Humber achieved 80% screening coverage between 2006 and 2007.

Screening assays comprise the cytology-based Pap smear and liquid-based cytology assays, which detect microscopic abnormalities in exfoliated patient cells. These can be visualised with acetic acid or Iodine solution during a colposcopy examination of the patient's cervix. Biopsies of the affected areas can be tested for HPV DNA or messenger RNA (mRNA). To date more than 125 commercial HPV DNA tests are available, including self-sampling home tests (Poljak et al., 2012, Seiwert, 2013). However, the clinical performances of the majority of the HPV DNA tests are not standardised which might cause bias in the correct diagnosis.
Notably, all the screening tools in place are focused on the prevention of cervical cancer only. No nationwide screening schedule for the remaining HPV associated cancers (Table 1.1) exists.

Treatment options for CIN lesions are curing the symptom rather than the causative HPV infection due to the lack of HPV specific antivirals. Various methods of surgical removal of the affected area are employed (loop electrosurgical excision procedure, cold knife cone biopsy, electrofulgaration, cold-coagulation, cryotherapy) (Stern et al., 2012). Advanced cervical cancer is treated with hysterectomy and chemoradiotherapy. The treatment of other HPV induced anogenital cancers and HNSCCs is confined to surgery and chemotherapy and radiotherapy (Stern et al., 2012). GWs are successfully treated by topical application of the immune modifier imiquimod or the cytomegalovirus (CMV) antiviral cidofovir. Also cutaneous warts are treated with the topical application of salicyl acid but cryotherapy is also commonly employed (Sterling et al., 2001).

Overall, effective prevention and treatment options only exist for HPV induced cervical cancers in developed countries. Global and national managing of the significant incidences of other HPV related cancers is poor. Further effort has to be spent on expansion of health care systems and basic research to successfully prevent a greater number of HPV related cancers.

1.4. PV virology

1.4.1. PV genome organisation

PVs are non-enveloped DNA viruses with a double-stranded and circular genome of approximately 8000 bps (Figure 1.4) (Zheng and Baker, 2006). It encodes for the core proteins E1, E2, L1 and L2 and the oncoproteins E5, E6 and E7 that have been gained and lost during evolution and are therefore not encoded by all PV types (Van Doorslaer, 2013). The genome is packaged in an icosahedral capsid of 60 nm in diameter, which consists of major, L1, and minor, L2, structural proteins (Buck et al., 2008, Finnen et al., 2003).

The compact genome is organised into three main regions. The early region comprises 50% of the viral genome and encodes the ORFs of the six early (E) proteins E1, E2, E4, E5, E6 and E7 (Zheng and Baker, 2006). An E8 ORF is also encoded in BPV, HPV31 and several rabbit PVs (Han et al., 1998, Stubenrauch et al., 2001, Tomita et al., 2007). The late region is located down-stream of the early region and constitutes 40% of the PV genome (Zheng and Baker, 2006). It encodes for the late (L) proteins L1 and L2. The remaining 10% of the PV genome is designated the long control region (LCR; also upstream regulatory region) which contains the origin of replication (*ori*). PVs possess two main promoters. In the HPV16 genome the early promoter, P97, is situated upstream of the E6 ORF and facilitates expression of the early genes (Zheng and Baker, 2006). The late promoter, P670, is localised in the E7 ORF and is active during the productive phase of the viral life-cycle (Grassmann et al., 1996).

PVs employ a variety of transcriptional and post-transcriptional regulation mechanisms to coordinate viral gene expression during the complex life-cycle (Bernard, 2013, Johannsen and Lambert, 2013, Schwartz, 2013). The transcription from the PV genome can be regulated by viral DNA methylation. Also, alternative splicing and polyadenylation of various polycistronic mRNAs regulates the timely expression of viral proteins. The translation efficiency of the RNA is intentionally limited by use of rare codons (1.3.7).

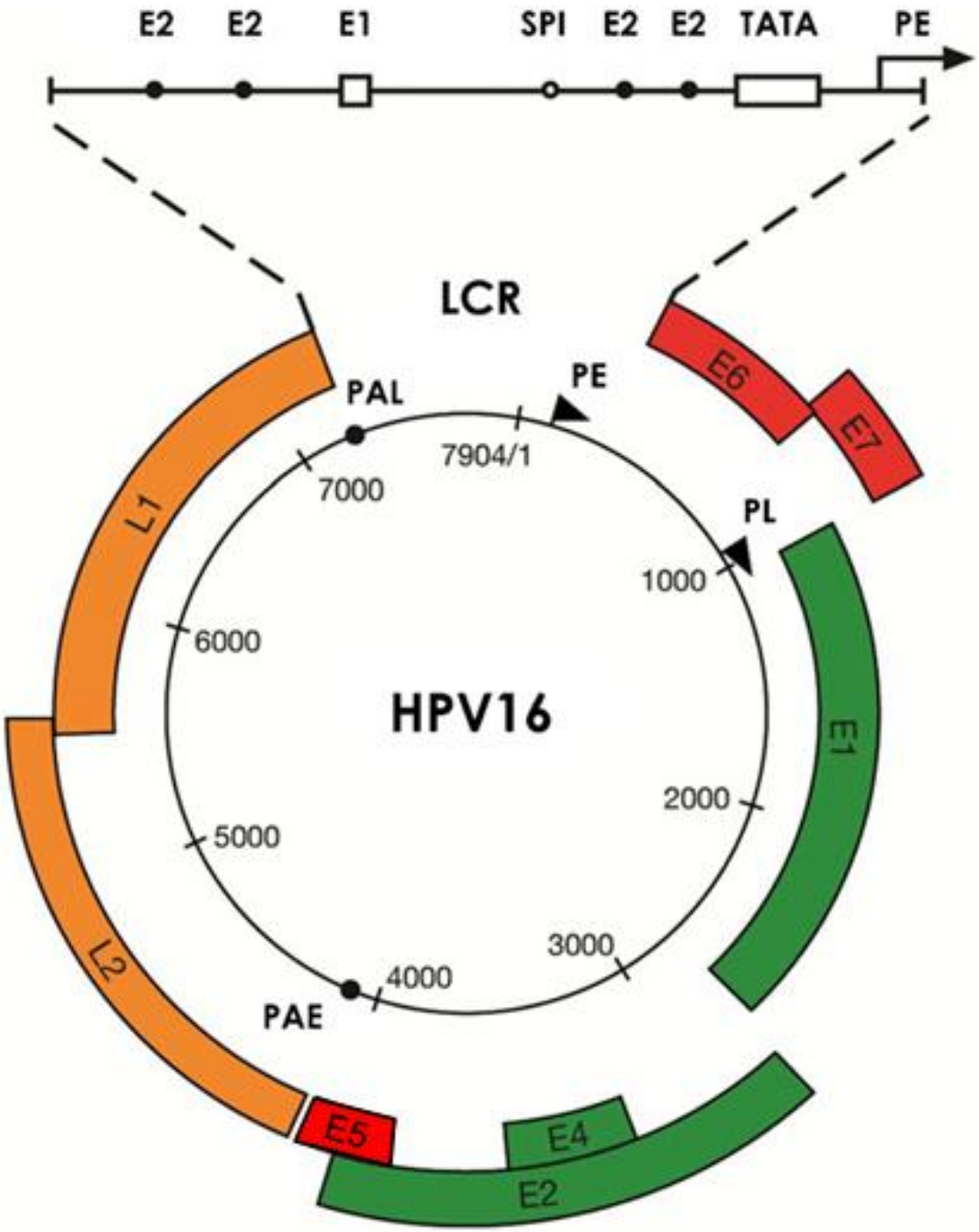

Figure 1.4 Genome organisation of HPV16. The 7904 bps of the genome are organised into three regions: early region (red and green), late region (orange) and the LCR. HPV oncoproteins are depicted in red. A simplified LCR is illustrated showing the binding sites of the viral proteins E1 and E2 and of cellular transcription factors (SP1) only. PE = P97, PL = P670, PAE = early polyadenylation site, PAL = late polyadenylation site. Adapted from Doorbar et al., 2012.

1.4.2. PV life-cycle

The life-cycle of PVs completely depends on the differentiation of the epithelial keratinocytes they infect. Its completion takes approximately three weeks (Stanley, 2006). This is the same time that basal keratinocytes require for complete differentiation. The life-cycle of HPV16 is relatively well understood for cervical tissue (Doorbar, 2006) but less so for other sites of infection and other PV types, respectively (Doorbar et al., 2012).

1.4.2.1. Attachment and entry

PVs infect mitotically active basal stem cells of the epithelium (Pyeon et al., 2009b). Access to these cells is facilitated by epithelial wounding or micro-wounding and first requires binding of L1 to heparan sulphate proteoglycans and possibly laminin at the basal membrane (Richards et al., 2013, Schiller et al., 2010). The conformation of the viral capsid changes and exposes the amino-terminus (N-terminus) of L2 for furin cleavage (Richards et al., 2006). Cleavage exposes a segment of L1 that interacts with an unidentified cell surface receptor (Schiller et al., 2010). The endocytic uptake is facilitated by the tetraspanin CD151 and the integrins α3β1 and α6β1/4 (Scheffer et al., 2013). The virus is uncoated in late endosomes and the major capsid protein L1 is degraded. A complex of L2 and the PV genome escapes the endocytic pathway, enters the nucleus and localises to nuclear domain 10 bodies as episomes (Bergant Marusic et al., 2012, Day et al., 2004). With 12 – 24 h until first transcription from the PV genome, the attachment and entry phase of the PV life-cycle is remarkably slow (Day et al., 2003, Schiller et al., 2010).

In accordance with the diversity of PVs, multiple mechanisms for entry into the cell have been described for different PV types (Bousarghin et al., 2003, Day et al., 2003, Hindmarsh and Laimins, 2007, Schelhaas et al., 2012, Smith et al., 2008).

1.4.2.2. Initial genome amplification and subsequent genome maintenance

The PVs replication and virion assembly (1.4.2.4) is completely confined to the nucleus (Doorbar et al., 2012). Upon entry into the keratinocyte nucleus, the PV genome is rapidly amplified to an estimated 100 - 200 copies/cell (Figure 1.5). The viral E2 protein binds to the E2 binding sites (E2BS) in the LCR and recruits the viral helicase E1 to the *ori* to achieve the amplification. After this initial amplification phase, the viral episome replication is maintained without the contribution of the viral E1 protein (Egawa et al., 2012). Only the viral E2 protein with some of its cellular interaction partners tethers the episomes to the host's chromatin to ensure retention and equal partitioning during cell division (Dao et al., 2006, McBride et al., 2006, Parish et al., 2006, Van Tine et al., 2004).

High-risk HPV types are thought to drive these basal and parabasal keratinocytes into cell proliferation by expression of their potent E6 and E7 oncoproteins (Doorbar, 2006). The low-risk types with less potent E6 and E7 proteins are most likely dependent on the wound healing response to the micro-wound (1.4.2.1) to facilitate proliferation of these cells (Doorbar, 2006, Schiller et al., 2010, Valencia et al., 2008). The proliferation of the infected cell(s) not only helps to spread the viral infection in the proximal tissue but is also necessary for completion of the viral life-cycle (1.4.2.3).

1.4.2.3. Productive phase of the viral life-cycle

In uninfected epithelium only the basal stem cells are capable of DNA synthesis and mitosis (Fuchs, 1990). Upon cell division the daughter cells migrate towards the epithelial surface and undergo a differentiation process that involves biochemical and morphological changes resulting in dead and superficial cells that are sloughed from the surface eventually.

Initially, the basal daughter cells enter the suprabasal layer, which is comprised of mitotically inactive but metabolically active cells. These express keratins that contribute to the formation of cytoskeletal filaments as well as the envelope protein involucrin. In the overlying granular layer, expression of keratins discontinues but the production of filaggrin supports the bundling of the keratin filaments into larger fibres. The influx of calcium into these permeable cells

activates transglutaminase, which links the envelope proteins to a cage-like structure. This results in the terminally differentiated cells of the overlying cornified layer. These cells completely abandon metabolic activity and consist of dead cage-like structures filled with keratin fibres.

The PV life-cycle, however, depends on the cellular replication machinery in the suprabasal layer of the epithelium. Therefore, PVs uncouple the differentiation process from the DNA replication process in these cells which is characterised by the simultaneous expression of differentiation markers like keratins and cell cycle entry markers including cyclin A (Doorbar et al., 2012).
The expression of the viral proteins E6 and E7 facilitates re-entry into the cell cycle by interacting with tumour suppressor proteins. E7 causes degradation of members of the retinoblastoma-associated protein (pRB) family and E6 proteins mediate inactivation of p53 (Doorbar et al., 2012). Different properties of high-risk and low-risk oncoproteins might explain distinct pathologies caused by high-risk and low-risk HPV types.
The expression of the E5 oncoprotein modifies the cellular environment to facilitate cell cycle re-entry and subsequent viral genome amplification (1.6.2). Also the E4 protein is thought to contribute indirectly to viral genome amplification and cell cycle re-entry (Peh et al., 2004, Wilson et al., 2005, Wilson et al., 2007).
The progressing differentiation of the host cells initiates transcription from the late viral promoter with increased expression of the viral replication proteins E1 and E2. This results in a ~2 log increase in episomal copy number that is primarily achieved when suprabasal cells move towards a G2-like phase of the cell cycle (Banerjee et al., 2011, Doorbar et al., 2012, Maglennon et al., 2011, Wang et al., 2009).

1.4.2.4. Virus assembly and release

The emergence of new infectious virions requires packaging of the newly amplified PV genomes (1.4.2.3). The E2 protein promotes the expression of the necessary structural proteins L1 and L2 from the late viral promoter by use of alternative splicing sites and the late polyandenylation signal (Doorbar et al.,

2012, Johansson et al., 2012). The E2 protein recruits the viral genomes to the sites of assembly which is directed by the minor capsid protein L2 (Day et al., 1998). The genome is encapsidated and new virions emerge.

The viral E4 protein accumulates in cells that are undergoing virus synthesis and assembles into amyloid fibres (Doorbar et al., 1997, Doorbar et al., 2012, McIntosh et al., 2008). These rupture the cage-like structures filled with keratin fibres of the cornified cells and thus enable release of the virions (Doorbar et al., 1991, Doorbar et al., 2012, Wang et al., 2004).

1.4.2.5. Deregulation of the HPV life-cycle in carcinogenesis

The increasing severity of cervical neoplasia and progression into cancer correlates with the de-regulated expression of the viral oncoproteins E6 and E7 (Doorbar et al., 2012). This could be caused by epigenetic modifications since the LCR is distinctly methylated in the HPV induced lesions (Ding et al., 2009, Doorbar et al., 2012, van Kempen et al., 2013). Also, the hormone oestrogen plays a role in the progression into cancer as the LCR region comprises hormone response elements (Arbeit et al., 1996, Gariglio et al., 2009).

These elevated levels of the oncoproteins E6 and E7 induce aneuploidisation and chromosomal instability which are necessary for progression into cancer (Melsheimer et al., 2004). The genomic instability promotes integration of the viral episome into the host genome at common fragile sites (Dall et al., 2008, Thorland et al., 2003, Wilting et al., 2009). This is observed for up to 90% of cervical cancers (Pett and Coleman, 2007, Yu et al., 2005). Integration usually retains the LCR and the ORFs for the oncoproteins E6 and E7 while the ORFs for the regulatory proteins E1, E2 as wells as E4, E5 and L2 are disrupted or lost (Choo et al., 1987, Doorbar, 2006). Since the E2 protein can act as transcriptional repressor for E6 and E7, its loss during integration promotes transcriptions of these oncogenes (Thierry, 2009). However, 30% of HPV16 positive cancer contain episomal genomes only, thus, the integration is not the sole crucial factor for progression to cancer but rather the persistent expression of the viral oncoproteins E6 and E7 (Doorbar et al., 2012).

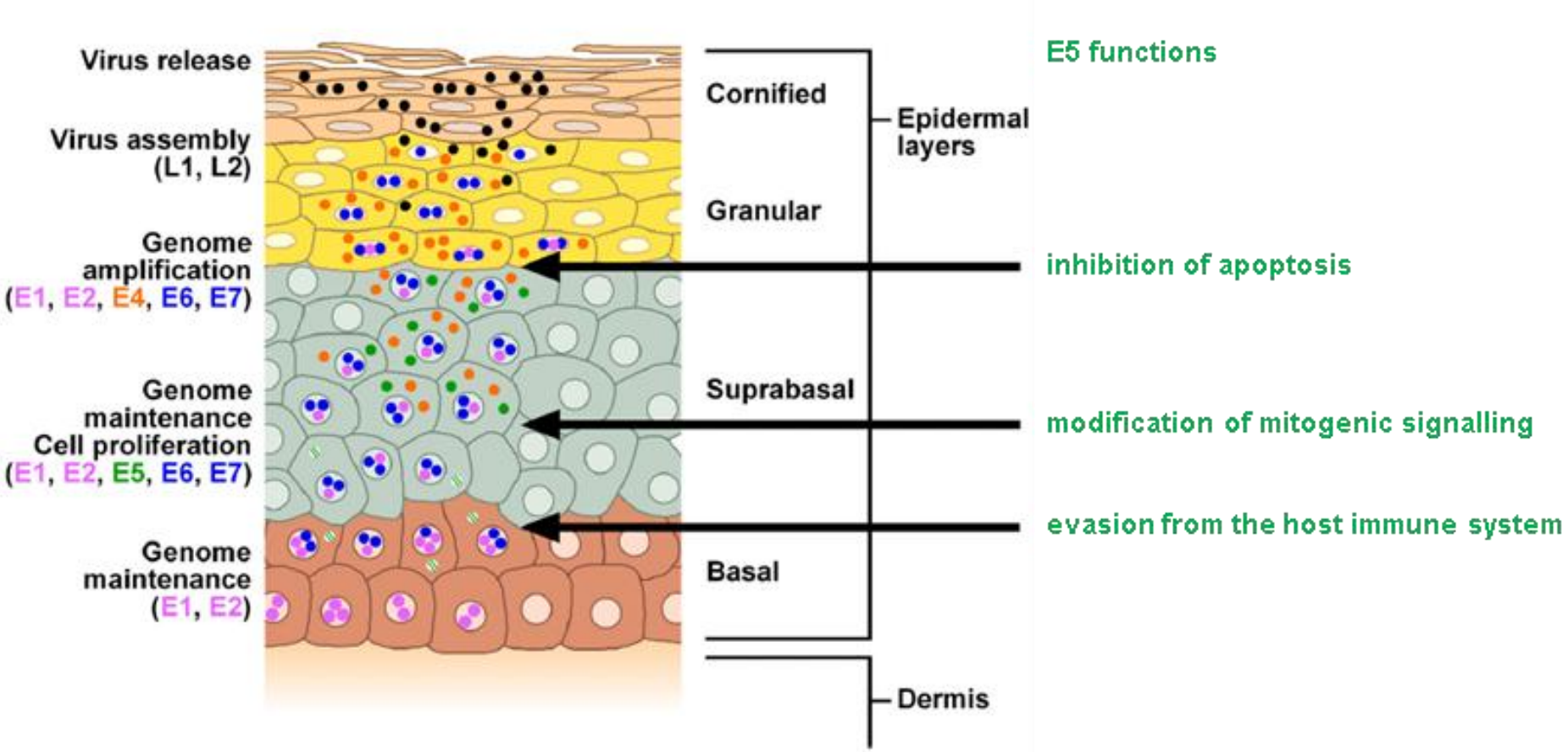

Figure 1.5 Schematic drawing of the PV life-cycle. The differential expression of the viral proteins is shown in context of the epidermal layers. For a description of the viral proteins see main text (1.5 and 1.6). Some of the functions of E5 are indicated on the right. Adapted from Venuti et al., 2011

1.5. PV proteins

1.5.1. E1 regulatory protein

The PV E1 protein is a homo-hexameric DNA helicase of the superfamily III (Hickman and Dyda, 2005, Singleton et al., 2007). It is the most conserved and the only protein with enzymatic function encoded by PVs (Bergvall et al., 2013). The E1 proteins are unstable proteins that are degraded by the ubiquitin-proteasome pathway (Malcles et al., 2002). They range in size between 600 – 650 amino acids and are highly post-translationally modified by phosphorylation, caspase cleavage and sumoylation to regulate E1 function, although the role of sumoylation is not understood yet (Bergvall et al., 2013).

The E1 protein is comprised of three functional sections. The regulatory domain at the N-terminus contains motifs that mediate the nuclear import/export of the protein. The adjacent DNA-binding domain (DBD) recognises the viral *ori* and binds it via its DNA-binding loop and DNA-binding helix (Enemark et al., 2000). The DBD also mediates dimerisation of E1 proteins as well as interaction with replication factors of the host. The carboxyl-terminus (C-terminus) comprises the helicase domain, which contains three functional subdomains. The oligomerisation domain facilitates the formation of a homo-hexamer (Titolo et al., 2000). The adenosine triphosphate (ATP) binding domain binds and hydrolyses ATP to provide energy for the DNA unwinding while the most C-terminal brace domain promotes the stability of the homo-hexamer during this process (Whelan et al., 2012).

The E1 helicase is responsible for establishing a sufficient viral genome copy number upon cell infection and to promote genome amplification during the productive viral life-cycle (Bergvall et al., 2013). It is controversial whether E1 is also required for maintenance of the viral copy number in undifferentiated cells (Egawa et al., 2012). In undifferentiated cells, E1 establishes a bi-directional replication fork while in differentiating cells during the productive phase of the viral life-cycle, it employs a rolling-circle mechanism for viral replication (Flores

and Lambert, 1997). Cleavage of the N-terminal region of E1 by caspases promotes this amplification phase of the viral genome (Moody et al., 2007).
The E1 dependent viral genome replication is regulated by shuttling the protein between the nucleus and the cytoplasm. The nuclear import is facilitated by importins that bind to the nuclear localisation signal (NLS) at the N-terminus of E1 (Bian et al., 2007). Phosphorylation at the NLS disrupts the association with importins and prevents nuclear import and the subsequent replication. However, the phosphorylation by mitogen-activated protein (MAP) kinases can also promote the import into the nucleus and stimulate viral DNA replication (Yu et al., 2007).
The nuclear export of E1 is mediated by binding of Crm-1 exportin to the nuclear export signal (NES) at its N-terminus (Deng et al., 2004). This can be inhibited by cyclin-dependent kinase 2 (CDK) induced phosphorylation. In contrast, phosphorylation of BPV1 E1 by CDK2 can promote the export from the nucleus (Hsu et al., 2007) and E1 phosphorylation may also reduce its sequence-specific DNA binding activity resulting in discontinuing of replication (Schuck et al., 2013).

The viral *ori* comprises a palindromic E1 binding region, two to three E2 binding regions and an AT-rich region (Figure 1.4) (Bergvall et al., 2013, Lee et al., 1997, Sun et al., 1996, Titolo et al., 2003). These elements allow the correct assembly of the double-hexameric E1 conformation required for viral genome replication via intermediate protein complexes. First, the E2 protein recruits E1 to the *ori* and forms an E1-E2-*ori* ternary complex (Bergvall et al., 2013, Sanders and Stenlund, 2001, Stenlund, 2003). This complex is converted into an E1 double-trimer in head-to-head configuration (Enemark et al., 2000, Enemark et al., 2002, Sedman and Stenlund, 1996) which melts the DNA at the *ori* requiring ATP hydrolysis (Schuck and Stenlund, 2005, Schuck and Stenlund, 2011). The single DNA strands allow for the formation of two E1 hexamers each encircling one DNA strand which then moves in 3' to 5' direction to unwind the DNA further. The viral DNA is replicated by utilising the cellular replication machinery that is recruited by E1 like the polymerase α-primase complex (Park et al., 1994), the replication protein A (Han et al., 1999) and the topoisomerase I (Clower et al., 2006).

1.5.2. E2 regulatory protein

The E2 protein is an essential regulatory protein of PVs and is therefore encoded by all known PV types (McBride, 2013, Van Doorslaer, 2013). They form stable homo-dimers (McBride et al., 1989) with the monomer of HPV16 comprising 365 amino acids. E2 proteins are localised in the nucleus but not the nucleolus of the host cell (Zou et al., 2000). This is mediated by importin molecules (Bian and Wilson, 2010) which recognise its NLS (Klucevsek et al., 2007). Also, acetylation of E2 promotes the localisation in the nucleus (Quinlan et al., 2013). The half-life of E2 proteins is very short (Hubbert et al., 1988) but protein stability is regulated by phosphorylation and sumoylation (Penrose et al., 2004, Sekhar and McBride, 2012, Wu et al., 2009).

There are three domains in the E2 proteins. The N-terminal transactivation domain (TAD) contains approximately 200 amino acids and is highly conserved (McBride, 2013). It plays important roles in viral genome replication and the activation or repression of viral transcription. It can also self-interact and promote dimer formation (Antson et al., 2000).
The C-terminal domain is the DBD and dimerisation domain which comprises approximately 85 – 100 amino acids (McBride, 2013). It binds to consensus motifs ($ACCN_6GGT$) on the DNA (Androphy et al., 1987b) and plays the main role in dimerisation of the protein (McBride et al., 1989).
The TAD and DBD are linked by a hinge region (Gauthier et al., 1991). This is an unstructured, not well conserved domain that varies in length (McBride et al., 1989). It prevents steric hindrance between the TAD and DBD (Winokur and McBride, 1992). In α-PVs a motif in this region also promotes nuclear localisation and association of E2 with the nuclear matrix (Zou et al., 2000).

The E2 ORF is expressed from the early and late promoter of PVs during their life-cycle (Burnett et al., 1990, Johansson and Schwartz, 2013). E2 expression levels accomplished by transcription from the late promoter are higher since E2 is required for the productive phase of the viral life-cycle (Ozbun and Meyers, 1998).

The E2 proteins exert their various roles by interacting with viral and cellular proteins (McBride, 2013). The interaction of E2 with the viral protein L2 facilitates the establishment of the viral genome upon infection (Day et al., 2004, Day et al., 1998). E2 also loads the viral helicase E1 onto the *ori* to promote genome replication. E2 functions as the main transcriptional regulator of the viral ORFs (Chin et al., 1988) by recruiting cellular proteins that activate or repress their transcription. Whether E2 activates or represses transcription depends on its concentration within the cell (Bouvard et al., 1994b).

During mitosis, E2 tethers the viral genomes to the host chromosomes to ensure equal partitioning amongst the daughter cells (Bastien and McBride, 2000). For this, the E2 DBD binds to the consensus DNA sequence on the viral genome and its TAD mediates binding to the host chromosome by interacting with cellular proteins like bromodomain-containing protein 4 (Ilves et al., 2006, Wang et al., 2013). PVs of different genera bind to distinct regions of the host chromosomes (Oliveira et al., 2006).

E2 might play a role in processing of the viral RNA because interactions with serine/arginine splicing factors were observed (Lai et al., 1999). It was also shown that E2 regulates the expression of cellular proteins (Ramirez-Salazar et al., 2011) but this is controversial (Jang et al., 2009, Võsa et al., 2012). E2 might also be involved in the packaging of the viral genome into virion particles (Zhao et al., 2000).

Alternative splicing of the N-terminal domain results in shorter isoforms of the E2 protein (Stubenrauch et al., 2000). These function as repressors of viral transcription and replication (Ammermann et al., 2008, Stubenrauch et al., 2007), which is important for maintaining of the genome copy number. The E2 isoform can dimerise with the full-length E2 protein. These hetero-dimers can mediate transcription and initiation of replication but not partitioning of viral genomes (Kurg et al., 2006, Kurg et al., 2010).

Very importantly, the E2 ORF can be lost or disrupted during viral genome integration into the host genome (Schwarz et al., 1985). This removes the repression from the transcription of the oncogenes E6 and E7 which promotes host cell transformation (1.4.2.5) (Bernard et al., 1989).

1.5.3. E4 protein

The E4 regulatory proteins vary in size and are not well conserved amongst PV types regarding its primary amino acid sequence (Doorbar, 2013). In papillomas they can make up to 30% of total cellular protein (Doorbar et al., 1986). They predominantly localise to the cytoplasm but nuclear localisation was also observed (Doorbar, 2013, Nicholls et al., 2001). E4 of cutaneous HPV types localises primarily in cytoplasmic inclusion granules and much less in inclusion granules in the nucleus (Egawa, 1994).

Although the primary amino acid sequence of E4 is not conserved, the proteins have similar modular structures (Doorbar, 2013). The N-terminus comprises a leucine cluster that mediates binding to cytokeratin. This is followed by a proline rich region and a region with predominantly positively charged amino acids. The adjacent loop domain might mediate interaction with cellular proteins. The C-terminal multimerisation domain follows after a negatively charged and a second proline rich domain. The multimerisation domain mediates self-association of the E4 proteins into amyloid fibres (McIntosh et al., 2008).

The E4 ORF is located in the early region of the viral genome within the E2 ORF (Danos et al., 1982) (Figure 1.4), but it is expressed from the viral late promoter in the suprabasal and granular epithelial layers during the productive phase of the viral life-cycle (Doorbar et al., 1997). It is expressed from a spliced transcript containing the initiation codon of the E1 ORF as well as a few down-stream codons and the complete E4 ORF (Doorbar et al., 1990). The protein is thus referred to as E1^E4 (here abbreviated as E4). Recently, three splicing variants have been detected in HPV16; E6*^E4 (Milligan et al., 2007), E2^E4S and E2^E4L (Tan et al., 2012a) and one in HPV18, E1^E4S (Kho et al., 2013) but their functions are not yet known.

The function of E4 is regulated by the proteases and kinases that become activated during the life-span of the host cell (Doorbar, 2013). E4 is initially expressed from the late promoter in the suprabasal epithelial layers as a protein of short half-life. It is phosphorylated by MAP kinases during the S phase of the

host cell, which condenses the loop structure and enhances binding to cytokeratin. In the upper suprabasal and granular epithelial layers, E4 is additionally phosphorylated by CDK. This opens the loop structure and allows the access of calpain to the E4 N-terminus. In the granular epithelial layer, calpain sequentially cleaves amino acids from the N-terminus and E4 is phosphorylated further by protein kinase C. This structural change facilitates the formation of amyloid fibres.

The late expression of E4 implies a role in the productive phase of the viral life-cycle. Indeed, E4 has been shown to contribute to viral genome amplification (Nakahara et al., 2005, Wilson et al., 2005, Wilson et al., 2007). E4 causes arrest of host cells in a G2-like phase, which promotes the amplification of the viral genome (Davy et al., 2005, Davy et al., 2002, Knight et al., 2004, Knight et al., 2006). In addition to that, E4 associates with E2 (Davy et al., 2009) which could contribute to viral genome amplification, however, this remains to be elucidated.

Notably, infectious virions are exclusively produced in host cells expressing E4 (Doorbar, 2013), thus E4 is involved in the synthesis of new virions (Nakahara et al., 2005, Wilson et al., 2005, Wilson et al., 2007).

Low-risk E4 proteins are cross-linked by cellular transglutaminase, which compromises the cornified envelope and might facilitate the release and thus transmission of the virus (Brown et al., 2006, Doorbar, 2013). This is also achieved by formation of amyloid fibres and the association with and disruption of the cytokeratin filament network (Doorbar, 2013, Doorbar et al., 1991, Doorbar et al., 1997) or its reorganisation to the cell periphery (Roberts et al., 1997).

The E4 protein might be exploited in the future as a biomarker for active HPV disease and HPV disease severity (Borgogna et al., 2012, Griffin et al., 2012).

1.5.4. L1 structural protein

L1 is the major structural protein of the PVs. HPV16 L1 (16L1) is a protein of 506 amino acids accounting for a molecular weight of ~56 kDa that is expressed from the late viral promoter during the productive stage of the viral life-cycle (Wang et al., 2011). The transcribed ORF is not altered by splicing events. The L1 protein localises to the nucleus of the host cells. The phosphorylation of tyrosine 129 and 340 of the 16L1 in a L1/2 pseudovirion has been reported but a function was not attributed so far (Buck et al., 2013). L1 proteins can self-assemble into VLPs which are similar to the native virion and potent immunogens (Buck et al., 2013). For these reasons the HPV vaccines are based on the L1 VLPs (1.3.8).

Three-hundred-and-sixty L1 proteins are organised into 72 pentameric capsomers in the mature virus capsid as well as an unknown number of L2 proteins (1.5.5) (Wolf et al., 2010). The L1 protein constitutes the entire exterior surface of the capsid. The N- and C-termini of each L1 protein face towards the virion lumen. The pentameric capsomers are connected via disulphide bonds between cysteine 175 of 16L1 with cysteine 428 of the neighbouring 16L1 (Modis et al., 2002). These cysteine residues are conserved amongst PVs L1 proteins. However, the surface loops of the pentameric capsomers are not well conserved which explains the limited cross-reactivity of neutralising antibodies against the vaccine HPV types (1.3.8) (Kemp et al., 2011, Kemp et al., 2012).

As the sole surface protein on the PV capsid surface, L1 facilitates virus entry into the host cell by interacting with heparan sulphate proteoglycans on the extracellular basement membrane (Johnson et al., 2009). HPV16 L1 promotes this interaction via its lysine residues at positions 278, 356 and 361 (Knappe et al., 2007). This induces a conformational change to the capsid that allows the cleavage of L2 by furin (1.5.5). A further change to the capsid formation mediates binding of L1 to an unknown cell surface receptor which was initially thought to be integrin (Evander et al., 1997) but this is controversial (Huang and Lambert, 2012).

Upon completion of the viral life-cycle, L1 is preassembled into pentameric capsomers in the cytoplasm (Bird et al., 2008) and then imported into the nucleus via karyopherins (Nelson et al., 2002). This requires a NLS at the C-terminus of L1 (Zhou et al., 1991). The assembly into the new virions takes place in the nucleus with the NLS playing a role in the encapsidation of the viral genome (Schäfer et al., 2002). The capsid slowly matures into a stable form needed for successful transmission by forming the disulphide bonds between neighbouring L1 proteins (Buck et al., 2005, Conway et al., 2009b).

1.5.5. L2 structural protein

The L2 protein is the minor capsid protein of PVs (Wang and Roden, 2013). HPV16 L2 (16L2) is comprised of 473 amino acids and migrates at ~ 73kDa on electrophoretic gels which is greater than its predicted molecular weight of ~50kDa (Xi and Banks, 1991). In contrast to L1, L2 cannot self-assemble into VLPs. There are up to 72 L2 proteins in the PV capsid (Buck et al., 2008), but the precise number is not known. It is mostly hidden below the L1-composed surface of native virions (Wang and Roden, 2013), however, the actual configuration has not been established yet. The 16L2 protein is heavily phosphorylated (Xi and Banks, 1991) and sumoylated on the lysine at position 35 which affects its stability and binding ability to L1 (Bergant Marusic et al., 2010).

The domain structure of L2 is highly conserved (Wang and Roden, 2013). It holds two cysteine amino acids towards the N-terminus that form an intra-molecular disulphide hairpin loop (Campos and Ozbun, 2009). Mutation of these cysteines have been shown to result in non-infectious virions (Campos and Ozbun, 2009) but others observed improvement of infectivity (Conway et al., 2009a). All L2 proteins contain a consensus furin cleavage motif (Richards et al., 2006) and a sortin nexin 17 binding motif (Bergant and Banks, 2013). The C-terminus of L2 has a proline motif that functions as a L1 binding site (Finnen et al., 2003). In addition to that, the N- and C-termini are comprised of positively charged amino acids that can not only function as DBD but also as NLS (Doorbar et al., 2012).

Because of its nature as a structural protein, L2 is expressed only in the upper most layers of the epithelium after the onset of E4 expression (Doorbar et al., 2012). It localises to the nucleus of those terminally differentiated cells.

L2 is required for virus entry and establishment of infection. Upon exposure of the virus to heparan sulphate of the extracellular matrix, a conformational change exposes the L2 N-terminus for furin cleavage (1.4.2.1) (Day and Schiller, 2009). Further conformational changes to the capsid facilitate internalisation of the virus via an unknown receptor. It is controversial, whether L2 could mediate binding to the unknown receptor (Kawana et al., 2001, Yang et al., 2003b), e.g. a hetero-tetramer of annexin A2 (Woodham et al., 2012). But further research is needed to determine the PV entry mechanism.

After cell entry, the virus accesses the early and then the late endosomes as well as the *trans*-Golgi which requires the previous furin cleavage of L2 (Day et al., 2013). The interaction of L2 with the chaperone cyclophilin B facilitates the uncoating of the capsid by dissociating the L1 protein from the L2/viral genome complex (Bienkowska-Haba et al., 2012). The binding to sortin nexin 17 may help the complex to escape degradation by the lysosomes (Bergant and Banks, 2013). The furin cleavage is also required for the L2/viral genome complex to exit from the endosomal compartment (Richards et al., 2006). This might be supported by L2-induced membrane destabilisation (Kämper et al., 2006) or by a trans-membrane like domain at the N-terminus of L2 which associates into higher order structures that penetrate the endosomal membrane (Bronnimann et al., 2013).

The L2 protein promotes the trafficking of the L2/genome complex to the nucleus by interacting with the motor protein dynein and thus enables the complex to traverse the cytoplasm on the actin/microtubule network (Florin et al., 2006). During the establishment of initial infection, the L2/genome complex enters the nucleus requiring the breakdown of the nuclear envelope during mitosis (Pyeon et al., 2009a). During the productive phase of the viral life-cycle, L2 can most likely enter the nucleus mediated by its interaction with karyopherins (Bordeaux et al., 2006).

L2 regulates transcription by interacting with transcription factors like TBX2 and TBX3 (Schneider et al., 2013). This could inhibit transcription of the early viral genes and promotes transition towards viral assembly. L2 binds non-specifically to DNA via its DBD (Mallon et al., 1987, Wang and Roden, 2013) and thus recruits the viral genome as well as L1 and E2 to the nuclear domain 10 bodies of the nucleus to facilitate genome encapsidation and assembly of the virion (Day et al., 1998). Thereby, L1 and L2 binding is mediated by hydrophobic interactions (Finnen et al., 2003).

1.5.6. E6 oncoprotein

The E6 oncoproteins are not encoded by all PV types (1.4.1). High-risk HPV E6 proteins have a more distinct oncogenic effect than the low-risk HPV E6 proteins (Vande Pol and Klingelhutz, 2013). The sequence conservation amongst the E6 proteins is limited to for example 24% between HPV16 E6 (16E6) and BPV1 E6, however, their structure is similar (Zanier et al., 2013).
The E6 ORF is transcribed from the early PV promoter and the protein exists at low levels in the host cell with a half-life of approximately 4 h (Androphy et al., 1987a, Vande Pol and Klingelhutz, 2013). The cellular localisation between high-risk and low-risk E6 proteins differs with high-risk E6 proteins being distributed throughout the cell while low-risk E6 proteins are predominantly confined to the nucleus (Guccione et al., 2002).

Both, the N- and C-terminus of E6 comprise a zinc-binding domain. The N-terminal domain also mediates dimerisation of the protein (Lipari et al., 2001) which is required for the degradation of p53 (Zanier et al., 2012). The interconnecting α-helical tube between the N- and C-terminus contains an LXXLL motif binding pocket (Zanier et al., 2013). The high-risk E6 proteins also contain an eight amino acid PDZ (post synaptic density protein, Drosophila disc large tumor suppressor, zonula occludens-1 protein) ligand motif at its C-terminus. This sequences varies amongst HPV types and facilitate the targeting of different PDZ domain containing proteins (Thomas et al., 2005). The PDZ ligand motif can be phosphorylated which prevents PDZ domain containing proteins from binding.

The transformation efficiency of high-risk E6 proteins is moderate. It can expand the life-span of transfected keratinocytes, but only the co-expression with E7 mediates immortalisation of the cells (Hudson et al., 1990). In agreement with this, 16E6 transgenic mice did not develop neoplasia or cancer (Riley et al., 2003). This could only be observed in E6 and E7 transgenic mice. A weak transforming activity of human foreskin keratinocytes (HFKs) was detected for 6E6 in combination with 16E7 (Halbert et al., 1992). In PV infection, E6 and E7 are co-expressed in the host cell and have complementary functions. The E7 oncoprotein degrades the RB protein p105, which results in stabilisation of p53 and induction of apoptosis. To counteract, E6 mediates degradation of p53 and thus inhibits cell cycle arrest and apoptosis to allow completion of the HPV life-cycle (Vande Pol and Klingelhutz, 2013), however, the precise cooperation between E6 and E7 differs between PV types.

To exert its function, the E6 protein requires binding to a LXXLL motif containing binding partner. This modifies its structure and stabilises it which facilitates the interaction with cellular binding partners like p53 (Ansari et al., 2012). High-risk E6 proteins interact with the LXXLL motif of the cellular ubiquitin ligase E6 associated protein (E6AP) (Brimer et al., 2007, Huibregtse et al., 1993). This promotes dimerisation of E6 via its N-terminal domain and the E6/E6AP complex can interact with the core DBD of native p53 (Ansari et al., 2012). E6AP provides the ubiquitination of p53 and thus its degradation (Scheffner et al., 1993, Zanier et al., 2012). Other cellular ubiquitin ligases like HERC3 could regulate the ubiquitin ligase activity of E6AP in the E6/E6AP/p53 complex (Kühnle et al., 2011).

Low-risk E6 proteins can also interact with E6AP and activate its ubiquitin ligase activity but this does not lead to p53 degradation (Brimer et al., 2007). They inhibit the acetylation of p53 (Thomas and Chiang, 2005) and thus the transcription of pro-apoptotic genes (Giampieri et al., 2004).

Studies in E6AP null mice have shown that E6 can degrade p53 via an E6AP independent pathway (Shai et al., 2007) but the mechanism remains to be investigated.

The β-PV, μ-PV and v-PVs predominantly bind to the LXXLL motif of the transcriptional co-activators mastermind-like protein 1 and 3 (MAML1 and

MAML3) (Tan et al., 2012b) and only poorly to the LXXLL motif of E6AP. This leads to repression of the Notch transcriptional activation complex.

Interestingly, high-risk E6 and some cutaneous E6 can activate telomerase (Klingelhutz et al., 1996) by transcriptionally up-regulating the human telomerase reverse transcriptase component (Veldman et al., 2001). The benefit for this function are unknown since the completion of the viral life-cycle does not require the immortalisation of the host cell (Vande Pol and Klingelhutz, 2013).

A large-scale microarray analysis of tissue from 16E6 transgenic mice revealed the alteration of the expression of a multitude of genes compared to control mice (Mendoza-Villanueva et al., 2008). According to this analysis, E6 deregulates genes involved in cell cycle progression, apoptosis and immune response. Some of these alterations are mediated by direct interaction of E6 with specific transcription factors (Vande Pol and Klingelhutz, 2013).

The E6 protein plays a role in the amplification of the viral genome because the viral genome amplification and L1 production were reduced in an organotypic raft culture system with an E6 mutant HPV18 genome (Wang et al., 2009). In β-PVs, E6 might delay the differentiation of the host cell to favour the completion of the viral life-cycle by down-regulating the Notch pathway. Their interaction with the MAML1 and MAML3 proteins of the Notch transcription complex inhibits the transcription of genes that promote cellular differentiation (Meyers et al., 2013).

To further support the viral life-cycle, the E6 proteins of low-risk and high-risk α-PVs and β-PVs bind the pro-apoptotic protein Bak and mediate its degradation (Thomas and Banks, 1999, Underbrink et al., 2008). Also, E6 interacts with procaspase-8 to prevent it from responding to apoptotic stimuli (Filippova et al., 2007, Tungteakkhun and Duerksen-Hughes, 2008).

In order to escape the immune surveillance of the host, E6 proteins promote resistance to IFN (Beglin et al., 2009) by down-regulating multiple IFN responsive genes (Nees et al., 2001).

Notably, there is an E6* isoform in high-risk HPV types which results from alternative splicing and comprises the N-terminal portion of the full-length E6 protein. It counteracts the effects of the full-length E6 protein by binding to E6AP but inhibiting the degradation of p53 (Pim et al., 1997) and by stabilising procaspase 8 instead of mediating its degradation (Tungteakkhun et al., 2010).

1.5.7. E7 oncoprotein

The E7 protein of high-risk HPVs exerts oncogenic functions (Phelps et al., 1988) but not every PV encodes an E7 ORF (1.4.1). E7 is a small, acidic protein of ~100 amino acids and a predicted molecular weight of ~11 kDa (Roman and Münger, 2013, Smotkin and Wettstein, 1986). With less than 1 h, the half-life of E7 is very short (Smotkin and Wettstein, 1987) because the protein is subject to proteasomal degradation (Reinstein et al., 2000).
The E7 proteins are localised in the nucleus of the host cell (Guccione et al., 2002) but have also been observed in the cytoplasm (Smotkin and Wettstein, 1987). Indeed, E7 can shuttle between the nucleus and the cytoplasm. A hydrophobic motif at the C-terminus interacts with the central channel nucleoporin Nup62 and mediates its nuclear import (Eberhard et al., 2013). Another explanation for the localisation pattern observed might be the differential cellular localisation of three isoforms of HPV16 E7 (16E7): 16E7a1, 16E7a and 16E7b (Valdovinos-Torres et al., 2008).

The E7 protein structure is characterised by a flexible N-terminus and a more structured C-terminus (Calçada et al., 2013). The N-terminus contains two conserved regions (CR1 and CR2) that are similar to regions of simian vacuolating virus 40 (SV40) large T antigen and adenovirus E1A (Phelps et al., 1988, Roman and Münger, 2013) and are conserved between HPV types. The CR2 domain contains a LXCXE motif which mediates binding to pRB and other pocket proteins like p107, p130 (Dyson et al., 1992, Münger et al., 1989). The N-terminus comprises a NLS between amino acids 1 – 37 (Knapp et al., 2009). There are two CXXC domains at the C-terminus of E7 that constitute a zinc-binding site (Barbosa et al., 1989) that can also mediate dimerisation of the protein (Clements et al., 2000). However, it is not known yet whether E7

functions as a dimer *in vivo* (McLaughlin-Drubin and Münger, 2009). Moreover, the C-terminus possesses a NES and another NLS (Eberhard et al., 2013, Knapp et al., 2009).

The stability of 16E7 is increased by phosphorylation of threonines at positions 5 and 7 (Liang et al., 2008). The CR2 domain contains another phosphorylation motif that is targeted by casein kinase II (Barbosa et al., 1990). This is phosphorylated during the early cell cycle (Massimi and Banks, 2000). The serine at position 71 is phosphorylated during the S phase implying that E7 is differentially regulated during the cell cycle (Massimi and Banks, 2000).

As an oncoprotein, E7 inhibits the differentiation of keratinocytes and facilitates cellular immortalisation (McLaughlin-Drubin and Münger, 2009), with high-risk E7 proteins having greater oncogenic potential than low-risk E7 proteins (Halbert et al., 1992). A characteristic feature of E7 is its binding and subsequent degradation of pRB which disrupts the differentiation process of the host cells and renders them competent for DNA synthesis (Collins et al., 2005). *In vivo*, E7 cooperates with E6 to achieve transformation of cells (1.5.6).

The binding of E7 to pRB disrupts the pRB/E2F repressor complex, which then allows entry into S phase (Huang et al., 1993, Wu et al., 1993). The high-risk E7 proteins destabilise pRB through proteasomal degradation (Boyer et al., 1996) to accomplish cell transformation. In agreement with its lower oncogenic potential, low-risk E7 proteins bind pRB with less affinity (Münger et al., 1989).

HPV16 E7 can also bind E2F transcription factor directly to enhance its transcriptional activity (Hwang et al., 2002). This increases the expression of the transcriptional repressor E2F6. However, 16E7 abrogates its repressor activity to ensure the S phase state of the cell (McLaughlin-Drubin et al., 2008). E7 enhances the expression of the E2F regulated early mitotic inhibitor 1 (EMI1) and stabilises the protein (Yu and Münger, 2013). EMI1 functions as an inhibitor of the ubiquitin ligase complex anaphase promoting complex/cyclosome. This inhibition could promote cellular DNA replication in favour of the viral life-cycle and may cause prometaphase delay and centrosome overduplication. E7 also

affects expression of cyclin A and E (Zerfass et al., 1995) and inhibits the growth-inhibitory activities of tumour suppressors $p21^{CIP1}$ (Funk et al., 1997) and $p27^{KIP1}$ (Zerfass-Thome et al., 1996) to instigate entry into S phase. It is conceivable that the abrogation of $p21^{CIP1}$ and $p27^{KIP1}$ function could be responsible for the resistance to transforming growth factor-β mediated growth inhibition observed in E7 expressing keratinocytes (Pietenpol et al., 1990).

The E7 proteins are also involved in the viral life-cycle, prevention of apoptosis and immune evasion strategies. During the viral life-cycle, high-risk 16E7 and 18E7 proteins were shown to be required for the productive stage (Flores et al., 2000, McLaughlin-Drubin et al., 2005). In contrast, the low-risk 11E7 and the high-risk 31E7 proteins appear to play a role in maintenance of the viral genome in the non-productive phase of the viral life-cycle (Oh et al., 2004, Thomas et al., 1999).

One way 16E7 can inhibit apoptosis of the host cell is by interacting with the actin-binding protein gelsolin (Mileo et al., 2013). This interaction prevents its cleavage by caspase-3, which reduces the amount of the pro-apoptotic N-terminal cleavage product but also the anti-apoptotic C-terminal cleavage product. However, 16E7 can also directly interact with the N-terminal cleavage product to decrease its pro-apoptotic effect.

The E7 proteins employ many strategies to evade the host's immune surveillance. HPV16 E7 was shown to disrupt the function of the double stranded DNA sensor toll-like receptor 9 of the innate immune system (Hasan et al., 2013). This is achieved by down-regulating the expression of toll-like receptor 9 through epigenetic regulation. In addition to this, E7 disrupts the response to IFN-α signalling by binding to p48, the DNA-binding component of the IFN-stimulated gene factor 3 transcription complex (Barnard and McMillan, 1999). The interaction retains p48 in the cytoplasm and thus prevents the transcription of IFN-α response genes.

With the down-regulation of major histocompatibility complex (MHC) class I molecules from the cell surface, the E7 proteins also modulate the adaptive immune response. HPV16 E7 was shown to inhibit IFN-γ induced

phosphorylation of STAT1 (Zhou et al., 2013). This blocked the IFN regulatory factor-1 and the transporter associated with antigen processing (TAP) and prevented the cell surface expression of MHC class I molecules and lysis by T cells.

Notably, E7 causes chromosomal instability in multiple ways (McLaughlin-Drubin and Münger, 2009). It was recently observed that 16E7 enhances the expression of the DNA replication initiation factor Cdt1 (Fan et al., 2013). The up-regulation of Cdt1 leads to cell cycle arrest in the G2 phase and many rounds of host cell replication without entering mitosis. This facilitates genomic instability and might promote the integration of the viral genome into the host chromosomes (Kessis et al., 1996); a progress that is often associated with HPV induced cancer development (1.4.2.5).

1.6. E5, a multifunctional oncoprotein

The E5 protein is one of the PV oncoproteins but not every PV type encodes for an E5 gene (1.4.1). It is, however, expressed in the clinically most relevant α–genus HPV types as well as in PVs of the δ– and κ–genera including the carcinogenic BPV types. Compared to the well-studied E6 and E7 oncoproteins its properties and functions are poorly understood.

Bravo and Alonso classified 110 E5 sequences of α-HPV types into four separate families namely E5α, -β, -γ, and -δ according to their phylogenetic relationships as well as chemical characteristics (Bravo and Alonso, 2004). The E5α family is represented in the α5, α6, α7, α9, and α11 PV species and comprises all high-risk HPV types including HPV16, 18 and 31. The E5α ORF is approximately 240 base pairs (bp) in length and encodes highly hydrophobic amino acids that potentially form three trans-membrane domains (TMDs). The amino acid sequences, however, are poorly conserved. The homology amongst E5β proteins is relatively high. Its ORF is much smaller with 140 bp and encodes a protein with one potential TMD. The E5β proteins can be found in HPV types of the α2, α3, α4, and α12 PV species with HPV2a E5 being a representative. HPV6b and HPV11 E5 represent the E5γ family, which is extremely well conserved. It is encoded by a 270 bp ORF, which expresses a protein of approximately 90 amino acids with three putative TMDs. These E5 proteins are exclusively found amongst the α10 PV species. The E5δ proteins can also be found amongst the α10 species besides the α1 and α8 species. These are encoded by an ORF of approximately 150 bp in length which translated into a protein with one putative TMD represented by HPV13 E5. Thus, the E5 proteins of the 4 families appear to have very diverse characteristics, but they share common functions (1.6.1, 1.6.2, 1.6.3).

The best characterised E5 protein to date is the E5α protein 16E5. It consists of 83 amino acids that are predicted to form three α- helical TMDs (Figure 1.6) (Bubb et al., 1988, Wetherill et al., 2012a). The C-terminal domain reaches into the cytoplasm while the N-terminal domain projects into the compartment lumen/extracellular space (Krawczyk et al., 2010, Wetherill et al., 2012a),

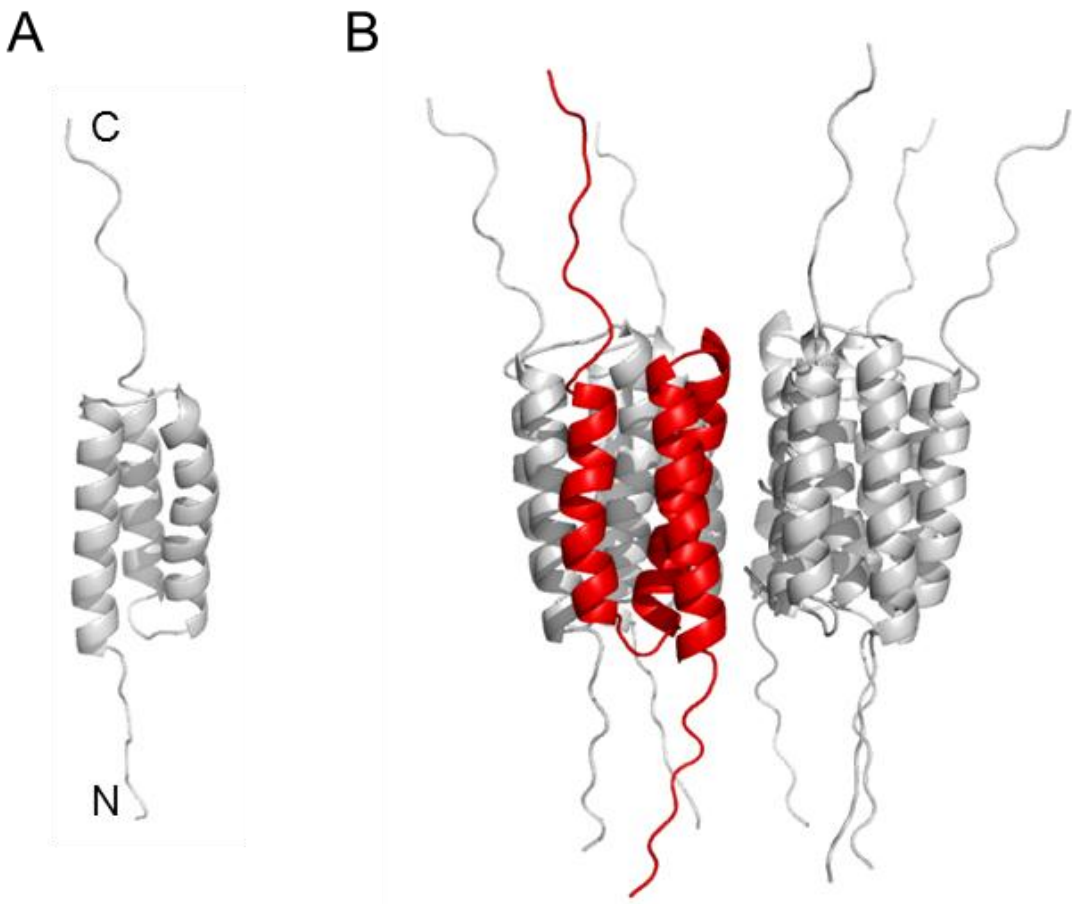

Figure 1.6 Model of the 16E5 monomer (A) and homo-hexamer (B). The 16E5 monomer is predicted to have three TMDs with the C-terminus facing the cytoplasm and the N-terminus facing the compartment lumen. Six monomers can associate into a homo-hexamer that has viroporin functions. Adapted from Wetherill et al., 2012a.

although one group noted the opposite orientation (Hu and Ceresa, 2009). There is evidence that 16E5 forms dimers by interactions of their hydrophobic regions (Gieswein et al., 2003, Kell et al., 1994). Also, the formation of a homo-hexamer that constitutes a viroporin was observed (Wetherill et al., 2012a). Twelve naturally occurring 16E5 protein variants have been identified with an increased usage of mammalian codons correlating with severity of pathogenesis (Bible et al., 2000, Nath et al., 2006). Post-translational modifications of 16E5 are not known (Rodriguez et al., 2000) but 18E5 is likely to be phosphorylated at a serine residue in its second TMD (communicated by Prof L. Chow at Molecular Biology of DNA Tumour Viruses Conference, 2010).

The E5 proteins of BPV are not classified amongst the E5α – E5δ families. They are small with BPV1 E5 constituting 44 amino acids (Burkhardt et al., 1987, Schiller et al., 1986, Schlegel et al., 1986) and BPV4 comprising 42 amino acids

(Pennie et al., 1993). This short length allows for the formation of one TMD only which is orientated with the C-terminus towards the lumen and the N-terminus facing the cytoplasm (Burkhardt et al., 1989). Like 16E5, BPV1 E5 forms dimers via hydrophobic interactions but with additional formation of disulphide bonds (King et al., 2011, Oates et al., 2008, Windisch et al., 2010).

HPV16 E5 was detected with a specific antibody in HPV16 positive cervical tissue as well as CIN1 and CIN2 samples (Chang et al., 2001, Kell et al., 1994). Sixty per cent of cervical cancer samples with episomal HPV16 genome and 80% of low-grade squamous intra-epithelial lesions (LSILs) as well as 90% of high-grade squamous intra-epithelial lesions (HSILs) showed 16E5 protein expression. However, antibodies to the 16E5 proteins are limited in their applications and despite several attempts (Adam et al., 2000, Chang et al., 2001, Chen and Mounts, 1989, Hwang et al., 1995, Kell et al., 1994, Sahab et al., 2012), there is no reliable and specific 16E5 antibody available to date. This limits the study of the 16E5 protein to epitope tagged, exogenously expressed protein.

For detection of endogenous E5, mRNA is frequently used as surrogate for the presence of the protein. HPV16 E5 mRNA is clearly expressed in cervical cancer samples and LSILs and HSILs with 16E5 and 16E6 mRNA being linked to decreased patient survival (Schrevel et al., 2011, Stoler et al., 1992). A similar study in HPV16 positive cervical pre-cancerous lesions showed that 76% of LSILs and 70% of HSILs express varying levels of 16E5 mRNA (Lorenzon et al., 2011). Also, the HPV16 positive CaSki cell line expresses E5 mRNA as well as E5 protein as determined by mass spectrometry analysis (Sahab et al., 2012, Schmitt and Pawlita, 2011).
The BPV E5 protein was detected in bovine cutaneous warts and urinary bladder tumours (Borzacchiello et al., 2003, Borzacchiello et al., 2006). Additionally, fibropapillomas of water buffalos and sarcoids of horses showed BPV E5 expression (Carr et al., 2001, Silvestre et al., 2009).

Due to the lack of a specific antibody, the cellular localisation of 16E5 was determined with overexpressed and epitope tagged 16E5. As a highly

hydrophobic protein with three TMDs, 16E5 was shown to localise mainly to endomembrane compartments. The majority of 16E5 proteins were detected at the endoplasmic reticulum (ER) and the Golgi apparatus (Golgi) (Ashrafi et al., 2006b, Auvinen et al., 2004, Conrad et al., 1993, Gruener et al., 2007, Lewis et al., 2008) with occasional detection at the nuclear membrane and the plasma membrane (Gieswein et al., 2003, Hu et al., 2009, Hu and Ceresa, 2009). The BPV1 E5 protein shows similar distribution to cellular membranes (Schlegel et al., 1986).

No intrinsic enzymatic activity is known for the E5 proteins, however, future research might reveal an intrinsic function of the 16E5 viroporin. So far, it is assumed that E5 exerts its roles via interaction with host cell proteins. In fact, the expression of 16E5 in cultured cells affects the expression of 25 to 179 host genes depending on cell types and experimental conditions (Kivi et al., 2008, Sudarshan et al., 2010). This indicates a significant but poorly investigated impact of E5 on its host cells. Roles of E5 have been identified in host cell transformation (1.6.1), the PV life-cycle (1.6.2) and viral immune evasion (1.6.3). The PV E5 protein is therefore a multifunctional oncoprotein.

1.6.1. Oncogenic potential of E5

The E5 protein of BPV is the main oncogenic protein of these PV types (Dimaio et al., 1986, Schiller et al., 1986, Schlegel et al., 1986). It is capable of transforming mouse fibroblasts and mortal human fibroblasts (Bergman et al., 1988, Petti and Ray, 2000). The E5 protein of HPV is a weaker transforming protein and is most likely not essential for carcinogenesis since it is not expressed in all HPV16 positive tumours (Venuti et al., 2011).

The first evidence of the weak transforming property of an HPV E5 protein came from 6E5 which induced anchorage independent growth in murine NIH 3T3 cells and formation of small colonies in C127 cells (Chen and Mounts, 1990). Shortly afterwards, 16E5 was shown to induce anchorage-independent growth in various established cell lines (Leechanachai et al., 1992, Leptak et al., 1991, Pim et al., 1992) and to have mitogenic effects in primary human foreskin epithelial cells (Straight et al., 1993). Further evidence for the transforming

property of 16E5 was gathered when its expression enhanced the proliferation and colony formation of primary baby rat kidney cells achieved by 16E7 (Bouvard et al., 1994a, Valle and Banks, 1995).

This effect was confirmed in transgenic mouse models which expressed a codon optimised 16E5 sequence in the basal compartment of the stratified squamous epithelia as well as a combination of 16E5, 16E6 and 16E7 oncoproteins (Maufort et al., 2010, Maufort et al., 2007). The formation of tumours was greater in 16E5/16E6 and 16E5/16E7 expressing mice than in mice expressing 16E6 and 16E7 individually. Mice expressing 16E5 only showed development of cancers when additionally treated with oestrogen with 16E5 contributing to the promotion and progression of cancer, not to its initiation. An oncogenic potential of the HPV E5 proteins is therefore firmly established in physiologically relevant cell lines *in vitro* and in transgenic mouse models *in vivo*.

1.6.1.1. E5 promotes transformation via EGF-R and down-stream mitogenic signalling

The *in vitro* transformation by 16E5 is facilitated by epidermal growth factor (EGF) and its receptor (EGF-R) (Leechanachai et al., 1992, Pim et al., 1992, Straight et al., 1993, Tomakidi et al., 2000b). Also, the formation of skin tumours *in vivo* in 16E5 transgenic mice requires expression of EGF-R (Genther Williams et al., 2005). Thus, the ability of HPV E5 to transform host cells could be associated with the manipulation of EGF-R and its down-stream signalling. Indeed, 70% - 90% of cervical cancers show increased levels of EGF-R (Kim et al., 2004, Mathur et al., 2000, Oh et al., 2000, Schrevel et al., 2011) suggesting that the manipulation of EGF-R mitogenic pathways is crucial for HPV E5 induced transformation.

The exact mechanism of EGF-R dependent transformation by 16E5 is highly controversial. The initial widely accepted hypothesis was based on the interaction of E5 with the 16K subunit of the vacuolar H^+ - ATPase (Figure 1.7) (Conrad et al., 1993). This interaction was proposed to lead to a decline of endosomal acidification and thus decreased EGF-R degradation after

stimulation (Straight et al., 1995, Straight et al., 1993). This way, the receptor recycles to the cell surface resulting in constitutive mitogenic signalling. The interaction with the 16K is conserved for the BPV1 E5 protein, the main BPV oncoproteins, and would therefore support this hypothesis (Schapiro et al., 2000).

A more recent study however showed that the binding of 16E5 to the 16K subunit is independent of its effects on EGF-R (Rodriguez et al., 2000). It was also observed that 16E5 promotes the activity of EGF-R by increasing its phosphorylation which can lead to increased expression of the prostaglandin E2 receptor EP4 (Oh et al., 2009, Straight et al., 1993). Other studies reported a direct binding between 16E5 and EGF-R that might be responsible for increased EGF-R activity (Hwang et al., 1995), but this finding could only be reproduced for 6E5 and not for 16E5 (Conrad et al., 1994). Very interestingly, one study even indicated a 16E5-induced EGF-R down-regulation (Pedroza-Saavedra et al., 2010).

Another concept emerges which proposes that E5 prevents the fusion of early endosomes with late endosomes and thus interferes with the correct receptor trafficking (Figure 1.7). One study suggests that endosome fusion is prevented by reorganisation of the actin cytoskeleton (Thomsen et al., 2000) but a later study could not confirm alterations to the cytoskeleton and suspects a direct disruption of membrane fusion by 16E5 (Suprynowicz et al., 2010). In addition to modifying receptor trafficking, 16E5 disrupts the binding of EGF-R to its ubiquitin ligase the cellular casitas B-lineage lymphoma proto-oncogene (Zhang et al., 2005). This reduces its ubiquitination and subsequent proteasomal degradation and facilitates receptor recycling.

A modification of cellular trafficking by 16E5 could be responsible for the increased plasma membrane expression of caveolin-1 and ganglioside GM1 that has been observed (Suprynowicz et al., 2008). Elevated ganglioside GM1 expression promotes mitogenic signalling by the EGF-R at low ligand concentrations (Figure 1.7) (Nishio et al., 2005). Thus, it is possible that the E5

induced alteration of cellular trafficking enhances ligand dependent EGF-R signalling in multiple complementary ways.

An involvement of 16E5 in cellular trafficking events is indeed conceivable since 16E5 interacts with karyopherin β3 (KNβ3) which plays an important role in the exocytic trafficking pathway (Krawczyk et al., 2008a) although the function of the KNβ3/16E5 complex has not been determined yet. Bravo and colleagues discovered that 16E5 alters the lipid composition of cellular membranes and proposes that this effect of 16E5 precedes the modification of cellular trafficking (Bravo et al., 2005).

Importantly, the cellular localisation of E5 at the ER and Golgi predestine it for roles in trafficking events but the cellular proteins that are involved in exocytic/endocytic trafficking and interact with E5 are still to be identified.

HPV16 E5 was shown to activate down-stream MAP kinases dependent and independent of EGF (Gu and Matlashewski, 1995). The treatment of A31-3T3 fibroblasts expressing 16E5 with EGF increased the activation of EGF-R and the down-stream MAP kinases extracellular signal-regulated kinase 1/2 (ERK1/2) (Crusius et al., 1997). But 16E5 also promotes the translocation of the phorbol ester PMA-dependent protein kinase C to the cellular membranes which results in a down-stream activation of the MAP kinase ERK1/2 independent of EGF (Crusius et al., 1997, Crusius et al., 1999, Crusius et al., 2000). This is achieved by the induction of stress on the human keratinocyte expressing 16E5. Notably, 16E5 also activates further MAP kinases like p38 in response to stress which, however, are not involved in mitogenic signalling pathways.

The activation of MAP kinases facilitates their translocation into the nucleus and promotes the activation of transcription factors. Indeed, the expression of 11E5a mRNA in GW samples correlated with the increased expression of *c-jun* (Chen et al., 1996a). In accordance with this, 16E5 enhanced the expression of *c-jun* in A31-3T3 fibroblasts and human keratinocytes (Chen et al., 1996a, Chen et al., 1996b, Chen et al., 1996c) as well as the expression of *c-myc* in A31-3T3 fibroblasts (Crusius et al., 1997). HPV16 and 11E5 can also transactivate the *c-fos* promoter (Chen et al., 1996c). The down-stream effect of these proteins is

progression through the cell cycle (see below) and the stimulation of the E6 and E7 oncogene transcription (Venuti et al., 2011).

The progression through the cell cycle is mediate by decreased expression of tumour suppressors. HPV11E5 and 16E5 were shown to down-regulate the transcription of $p21^{Waf1/Sdi1/Cip1}$ in NIH 3T3 cells and immortal human keratinocytes (Tsao et al., 1996). It is conceivable that this is achieved by the up-regulation of *c-jun* expression since *c-jun* can repress $p21^{Waf1/Sdi1/Cip1}$ transcription. Also, 16E5 can reduce the half-life of $p27^{KIP1}$ (Pedroza-Saavedra et al., 2010). This effect is enhanced by stimulation with EGF. The decreased cellular levels of the tumour suppressor proteins $p21^{Waf1/Sdi1/Cip1}$ and $p27^{Kip1}$ can mediate the exit from cell cycle arrest.

HPV16 E5 was also shown to interact with further EGF-R family members (Crusius et al., 1998). Upon stimulation of 16E5 expressing cells with EGF the EGF-R related proteins 2 and 3 (ErbB2 and ErbB3) receptors exhibited increased phosphorylation. No effect was seen on the ErbB4 receptor. In contrast, in CIN samples the expression of 16E5 correlated with the expression of ErbB4 receptor and EGF-R (Chang et al., 2001). Later it was revealed that the ErbB4 (JM-b/CYT-1) isoform forms a complex with 16E5 which leads to a ligand-independent activation of the down-stream pathway (Chen et al., 2007).

Another mitogenic pathway activated by 16E5 is the G-protein coupled endothelin-1 receptor A pathway. This constitutes an autocrine loop where HPV transfected keratinocytes express and secrete endothelin-1 to stimulate their own growth via their endothelin A receptors (Venuti et al., 1997). HPV16 E5 is thought to increase signalling via this pathway (Venuti et al., 1998) but the mechanism remains to be elucidated.

1.6.1.2. Further oncogenic functions of E5

A different mechanism for the oncogenic effect of 16E5 is cell-cell fusion (Gao and Zheng, 2010, Hu et al., 2009, Hu and Ceresa, 2009). The formation of bi-nucleated cells required the expression of 16E5 on both cells with the C-termini facing the extracellular space. And indeed, tetraploidy was described as an early event in cervical cancer development (Olaharski et al., 2006). In accordance with this, the low-risk 6E5 was not able to produce bi-nucleated cells. However, the orientation of 16E5 with the C-terminus facing the extracellular space is controversial (Krawczyk et al., 2010, Wetherill et al., 2012a) and more research is needed to investigate the involvement of 16E5 in the introduction of tetraploidy in cervical cancer development.

HPV16 E5 also contributes to cancer progression indirectly by facilitating viral episome integration into the host genome which is frequently observed in cervical cancer (1.4.2.5). The expression of 16E5 in keratinocytes induced the expression of the IFN regulatory factor-1 transcription factor which promoted transcription of the IFN-β gene and other IFN-stimulated genes like caspase 8 and RNA-dependent protein kinase R (Muto et al., 2011). In the HPV16 positive W12 cell line the treatment with IFN-β accelerated the progression from an episomal cell population into a cell population with integrated viral genomes (Herdman et al., 2006). Thus, it is conceivable that 16E5 promotes progression into cancer by facilitating the integration of the viral genome by expression of IFN-β. However, this role of 16E5 is not in favour for the virus, since the integration of the viral genome means the abortion of the viral life-cycle.

BPV1 E5 exerts its transformational ability via the platelet-derived growth factor β-receptor (PDGFβ-R) (Klein et al., 1999, Lai et al., 2005). The BPV1 E5 dimer binds directly to two PDGFβ-R inducing their dimerisation and activation (Cohen et al., 1993, Drummond-Barbosa et al., 1995, Goldstein et al., 1994, Nilson and Dimaio, 1993, Petti et al., 1991). The PDGFβ-R activation is strictly independent of the receptor ligand since the activation of mutant PDGFβ-R lacking the extracellular ligand binding domain is possible (Drummond-Barbosa et al., 1995, Staebler et al., 1995). Instead the receptor dimerisation induces auto-

transphosphorylation and promotes the down-stream mitogenic signalling (Lai et al., 1998, Petti and Dimaio, 1994). The interaction of BPV1 E5 – PDGFβ-R is highly specific because BPV1 E5 cannot bind the closely related PDGFα-R (Goldstein et al., 1994). It is thought that BPV E5 can transform the host cells independently of the PDGF-R by activating *c-src* (Suprynowicz et al., 2002) but this is controversial (Lai et al., 2005).

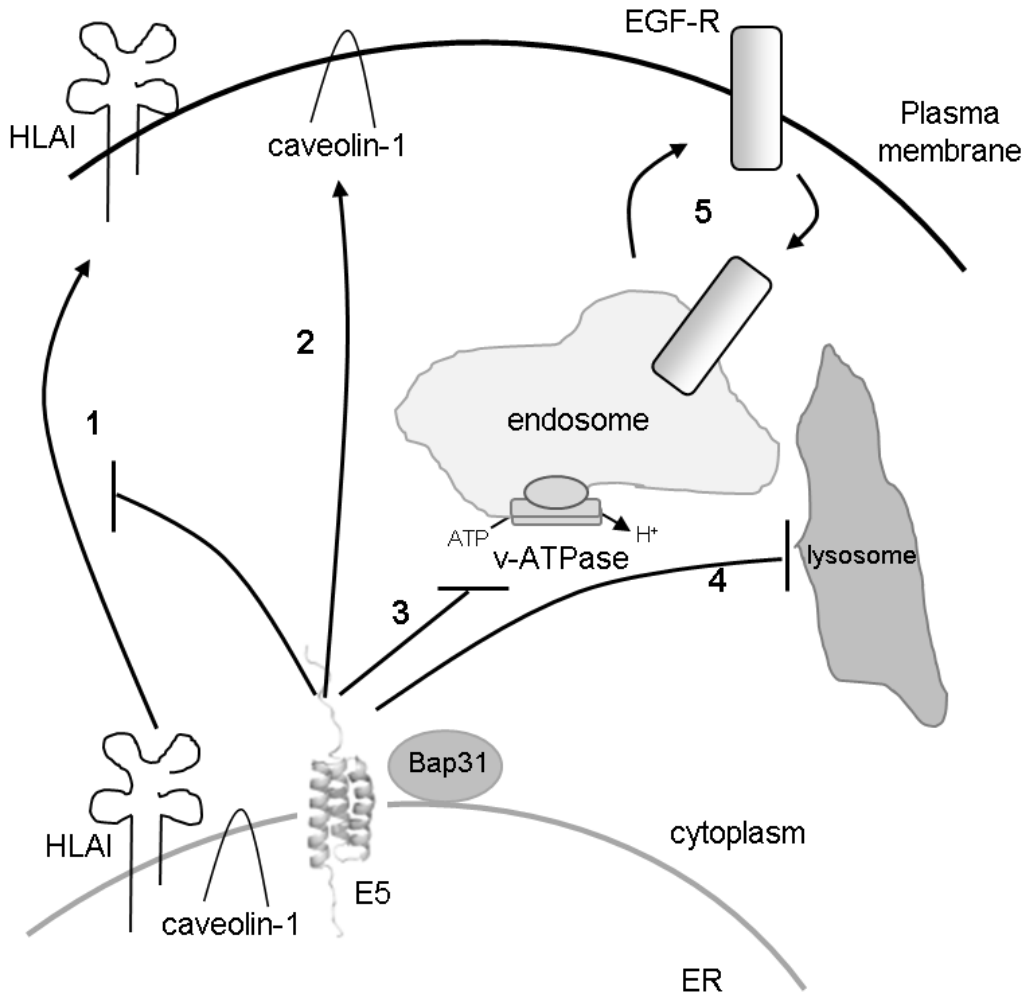

Figure 1.7 E5 modulates cellular trafficking pathways. Schematic showing the potential effects of E5 on host cell trafficking pathways. E5 down-regulates HLA class I, II and CD1d from the cell surface (1.) but up-regulates the cell surface expression of caveolin-1 and ganglioside GM1 (2.). The inhibition of endosome acidification (3.) or the perturbation of endosome fusion to acidic lysosomes (4.) may promote EGF-R recycling to the cell surface (5.). v-ATPase = vacuolar ATPase. Adapted from Wetherill et al., 2012b.

1.6.2. E5 and the viral life-cycle

The E5 protein is not expressed in all PV types (1.4.1). Therefore its role in the viral life-cycle is presumably not essential. It is thought to indirectly contribute to the completion of the viral life-cycle by generating the adequate cellular environment (Venuti et al., 2011).

The HPV E5 ORF is only expressed at low levels in the early stages of the viral life-cycle (Longworth and Laimins, 2004) because it is at position 4 on the polycistronic viral mRNA and is unlikely to be translated by the leaky ribosome-scanning mechanism employed. Upon alternative splicing in differentiating host cells (1.4.2.3) the E5 ORF constitutes the second ORF on the late polycistronic RNA and is therefore thought to be expressed highly in suprabasal epithelial cells (Figure 1.5). Similar expression patterns were observed for BPV1 and BPV4 E5 proteins (Araibi et al., 2004, Burnett et al., 1990).

The involvement of high-risk HPV E5 proteins in the viral life-cycle was investigated with human keratinocytes transfected with a wildtype (WT) and an E5 knock out (E5 KO) viral genome, respectively. In undifferentiated cells the KO of 16E5 and 31E5, respectively, did not show any phenotype implying that 16E5 and 31E5 do not play a role in the non-productive phase of the viral life-cycle (Fehrmann et al., 2003, Genther et al., 2003). This is in accordance with its potentially low expression level at this stage.
Differentiating NIKS, an immortalized keratinocyte cell line, with the 16E5 KO genotype only showed a minor reduction in unscheduled DNA synthesis compared to control cells. No effects were seen on the viral genome amplification, expression of late viral genes and alteration of normal keratinocyte differentiation (Genther et al., 2003). Therefore, 16E5 might only play a minute role in the productive stage of the HPV16 life-cycle.
Interestingly, the KO of 31E5 in differentiating primary human foreskin keratinocytes significantly reduced the amplification of the viral genome and the expression of late genes (Fehrmann et al., 2003). A decrease in the expression of cyclins A and B implies that 31E5 KO cells do not re-enter the cell cycle efficiently upon cell differentiation.

Thus, there is general consensus that E5 functions in the late, productive stages of the viral life-cycle, but the scope of the involvement appears to deviate between different HPV types. However, this observation could be due to different cell types used in these two studies (Fehrmann et al., 2003, Genther et al., 2003) so further research is needed to identify conserved and individual functions in the viral life-cycle of the E5 proteins from different HPV types.

HPV16 E5 inhibits apoptosis of the host cell which favours the completion of the HPV life-cycle indirectly (Figure 1.5). Cells expressing 16E5 showed reduced apoptosis when stimulated with Fas ligand and tumour necrosis factor-related apoptosis-inducing ligand compared to control cells (Kabsch and Alonso, 2002b). This is achieved by down-regulation of the Fas receptor and impaired formation of the death-inducing signalling complex, respectively. This function of 16E5 was confirmed in a physiologically more relevant organotypic raft culture system (Kabsch et al., 2004).

HPV16 E5 also reduces apoptosis after exposure to UVB irradiation which is facilitated by the activation of ERK1/2 and phosphatidylinositol 3-kinase-protein kinase B (1.6.1) (Zhang et al., 2002). The apoptotic response to hydrogen peroxide is reduced by targeting the apoptosis regulator BAX for proteasomal degradation (Oh et al., 2010). A co-localisation of 16E5 with the apoptosis regulator Bcl-2 was also observed, however, an interaction of the two proteins or a function of the potential complex was not investigated (Auvinen et al., 2004).

One study showed that 16E5 inhibits the ER stress pathway by decreasing the expression of cyclooxygenase-2 (COX-2), the transcription factors x-box-binding protein (XBP-1) and the serine/threonine-protein kinase/endoribonuclease IRE1α (Sudarshan et al., 2010). However, others saw an up-regulation of COX-2 by 16E5 (Kim et al., 2009, Subbaramaiah and Dannenberg, 2007) and by 6bE5 and 11E5, respectively (Wu et al., 2005, Wu et al., 2007c). A lack of effect of 6bE5 on COX-2 and XBP-1 was also observed (Condjella et al., 2009). Thus, the impact of E5 on the ER stress pathway is still controversial.

Interestingly, 16E5 expressing cells promote apoptosis in response to osmotic stress (Kabsch and Alonso, 2002a). It is conceivable that this is facilitated by its

viroporin conformation (Wetherill et al., 2012a), however, further research is needed to investigated this possibility.

The potential expression of 16E5 at the plasma membrane was shown to inhibit cell-cell communication in monolayer cell cultures and organotypic raft cultures (Oelze et al., 1995, Tomakidi et al., 2000a). This is achieved by dephosphorylation and possibly down-regulation of connexin 43, a major gap junctional protein and could lead to decreased sensitivity to growth signals from adjacent cells and consequential increased cell proliferation. The 16K subunit of the vacuolar H^+ - ATPase also forms part of gap junctions and is a conserved binding partner of PV E5 proteins. It is therefore highly likely that this interaction contributes to the PV life-cycle by enhancing cell proliferation (DiMaio and Petti, 2013). An inhibition of cell-cell communication was also observed for BPV E5 proteins with connexin 26 and calpain3 potentially playing roles (Ashrafi et al., 2000, Roperto et al., 2010, Silva et al., 2013). Notably, the E5 induced loss of cell-cell communication might be in contrast to the E5 induced cell-cell fusion observed by others (Hu et al., 2009). This underlines that the functions of E5 are poorly understood and further research is needed for clarification.

HPV16 E5 was shown to interact with the cellular EVER and ZnT-1 proteins (1.3.1) (Lazarczyk et al., 2008). This causes a disruption of the zinc homeostasis that is pivotal for the HPV life-cycle (Lazarczyk and Favre, 2008). In EV patients the zinc imbalance is caused by the mutated *EVER1* or *EVER2* genes which makes patients extremely susceptible for β-genus HPV types that do not encode an E5 protein (Lazarczyk et al., 2009, Orth, 2008).

In contrast to activation of mitogenic pathways (1.6.1.1), 16E5 reduces the proliferation and with it the differentiation of keratinocytes (Belleudi et al., 2011). To achieve this, 16E5 decreases the transcript and protein levels of the keratinocyte growth factor receptor/fibroblast growth factor receptor 2b and modulates its endocytic trafficking. The exact mechanism of alteration of endocytic trafficking remains to be elucidated.

It was also proposed that 16E5 plays a role in viral egress. The exit of the virions could be facilitated by the formation of koilocytes which emerge from cells expressing 16E5 in combination with E6 (DiMaio and Petti, 2013, Krawczyk et al., 2008b). For this, 16 E5 interacts with the calpactin I protein complex and drives it to the peri-nuclear region where it induces the formation of the characteristic peri-nuclear vacuoles by promoting membrane fusion (Krawczyk et al., 2011). The typical enlarged nuclei could originate from the 16E5 induced endoreplication (Hu et al., 2010).

Taken together, PV E5 proteins do not play a role in the early non-productive phase of the viral life-cycle but in the later productive stage. It contributes indirectly by promoting host cell proliferation and by preventing apoptosis. Maybe the formation of koilocytes facilitates the exit of the assembled virions from the nucleus.

1.6.3. E5 and PV immune evasion

The establishment of a persistent infection is crucial for the PV life-cycle (1.4.2) and requires evasion from the host's immune system (1.3.7). A common mechanism for viruses to avoid recognition by the host's immune cells is the prevention of antigen presentation by HLA/MHC class I molecules on the cell surface (Piguet, 2005). This mechanism is also employed by HPV since the surface down-regulation of HLA class I molecules can be observed in SCCs of the cervix (Cromme et al., 1993, Ritz et al., 2001).

The cell surface down-regulation of HLA class I molecules was shown to be mediated by the E5 protein (Figure 1.5 and Figure 1.7) (Ashrafi et al., 2006a). This function is highly conserved amongst all PV E5 proteins tested (2aE5, 6bE5a, 16E5, 83E5, BPV1 E5, BPV4 E5) (Ashrafi et al., 2006a, Ashrafi et al., 2005, Ashrafi et al., 2002, Cartin and Alonso, 2003).
The impact of E5 is specific to certain HLA class I types. HPV16 E5 expressing cells only down-regulate the HLA-A and HLA-B types from the cell surface to prevent recognition by cytotoxic T lymphocytes (Ashrafi et al., 2005). The HLA-

C and HLA-E types are not affected because they function as inhibitory ligands for natural killer cells.

E5 employs various strategies to achieve the down-regulation of HLA/MHC class I from the cell surface. Upon 16E5 expression, HLA class I molecules are retained in the Golgi (Ashrafi et al., 2005). There, 16E5 interacts with the HLA class I heavy chain (HC) via its 1st TMD, which could be responsible for its retention (Ashrafi et al., 2006b, Cortese et al., 2010). Others observed a ternary complex of 16E5, HLA HC and its chaperone calnexin (Gruener et al., 2007) and indeed, in calnexin deficient cells, 16E5 cannot prevent HLA class I expression on the cell surface. Also, the interaction of 16E5 with the HLA class I chaperone B-cell receptor-associated protein 31 (Bap31) could play a role in the HLA class I retention (Regan and Laimins, 2008), but this remains to be elucidated. The reduced cell surface expression of HLA class I was shown to successfully prevent recognition of 16E5 expressing cells by CD8+ T cells (Campo et al., 2010).
Notably, 16E5 does not repress the expression of the HLA class I HC and the required TAP. Its inhibitory effect on HLA class I presentation on the cell surface is reversible by treatment with IFN-β (Ashrafi et al., 2005). In contrast, BPV4 E5 represses the expression of the MHC class I HC in addition to binding to its HC and preventing its transport through the Golgi (Marchetti et al., 2005, Marchetti et al., 2002). The total amount of cellular MHC class I can be increased by treatment with IFN but the expression on the cell surface cannot be rescued (Araibi et al., 2004). This implies that the E5 proteins disturb the correct trafficking of the HLA/MHC class I molecules to the cell surface. Further research is needed to identify the exact mechanism of E5 mediated HLA/MHC class I cell surface down-regulation.

Further studies revealed the down-regulation of HLA class II molecules (Zhang et al., 2003) as well as CD1d (Miura et al., 2010) by 16E5 which are likely to contribute to immune evasion. Thus, E5 employs multiple strategies to prevent detection by the host’s immune system.

In summary, the E5 proteins are multifunctional oncoproteins that play roles in host cell transformation, the PV life-cycle and viral immune evasion, but the precise mechanisms employed by the E5 proteins are still poorly understood. It is striking that most functions of E5 are mediated by alterations to the cellular trafficking system. E5 modifies not only the endocytosis of receptors responsible for mitogenic signalling (EGF-R) but also decreases the exocytosis of immune modulators (HLA class I and II, CD1d) or increases the exocytosis of lipid raft components (caveolin-1, ganglioside GM1). Further research is needed to determine how E5 mediates these functions.

1.7. Work leading to this project

The E5 proteins do not have an intrinsic enzymatic function so they exert their roles in the host by interacting with cellular proteins. A yeast two-hybrid (Y2H) screen was performed with the E5 protein of the clinically most relevant HPV16 to determine further cellular binding partners (Gundurao and Haas, University of Edinburgh, UK). In a semi-automated Y2H assay (Albers et al., 2005), the 16E5 bait was screened against a human testis epithelial cell and a HeLa cell library, respectively. This resulted in the identification of eight potential 16E5 interacting proteins (Table 1.2). The zinc transporter ZnT-1 identified in the human testis cell library is already confirmed as a 16E5 interaction protein (Lazarczyk et al., 2008), thus serving as a positive control for this assay.

Table 1.2 Binding partners of 16E5 identified by Y2H screen against a human testis and HeLa cell library. The Y2H screen was performed by Gundurao and Haas, University of Edinburgh, UK.

UniProt ID	protein name (abbreviation)
Q13200	26S proteasome non-ATPase regulatory subunit 2 (PSMD2)
Q96JQ2	calmin (CLMN)
Q96JN2	coiled-coil domain containing protein 136 (CCDC136)
O76003	glutaredoxin-3 (GLRX3)
Q9P258	protein RCC2
Q96J42	thioredoxin domain-containing protein 15 (TXNDC)
Q9BSR8	YIP1 family member 4 (YIPF4)
Q9Y6M5	zinc transporter 1 (ZnT-1)

Four of the potential 16E5 biding partners were further investigated with a co-immuno-precipitation (Co-IP) approach called the luminescence-based mammalian interactome mapping (LUMIER) assay (Gundurao and Haas, University of Edinburgh, UK). For this, CCDC136, CLMN, YIPF4 and TXNDC were tagged with *Staphylococcus aureus* protein A and served as bait while 16E5 was tagged with *Renilla reniformis* luciferase and was used as prey (Figure 1.8). The interaction of JUN and FOS served as positive control. Bait

and prey were co-expressed in HEK293 cells and their lysates were analysed with the LUMIER assay. The bioluminescence was used as read out for interaction and normalised interaction signals were Z-transformed. Statistical analysis showed significant differences between the 16E5 binding partners and the positive control ($p \leq 0.01$). However, YIPF4 constituted the most promising novel 16E5 binding partner. YIPF4 was also observed as a 16E5 binding partner by tandem affinity purification followed by mass spectrometry (Tap-MS) analysis using IMR-90 normal human diploid fibroblasts transfected with tandem epitope tagged 16E5 (Rozenblatt-Rosen et al., 2012). Thus, YIPF4 is extremely likely to be an authentic 16E5 binding partner since the interaction was observed in three different experimental approaches.

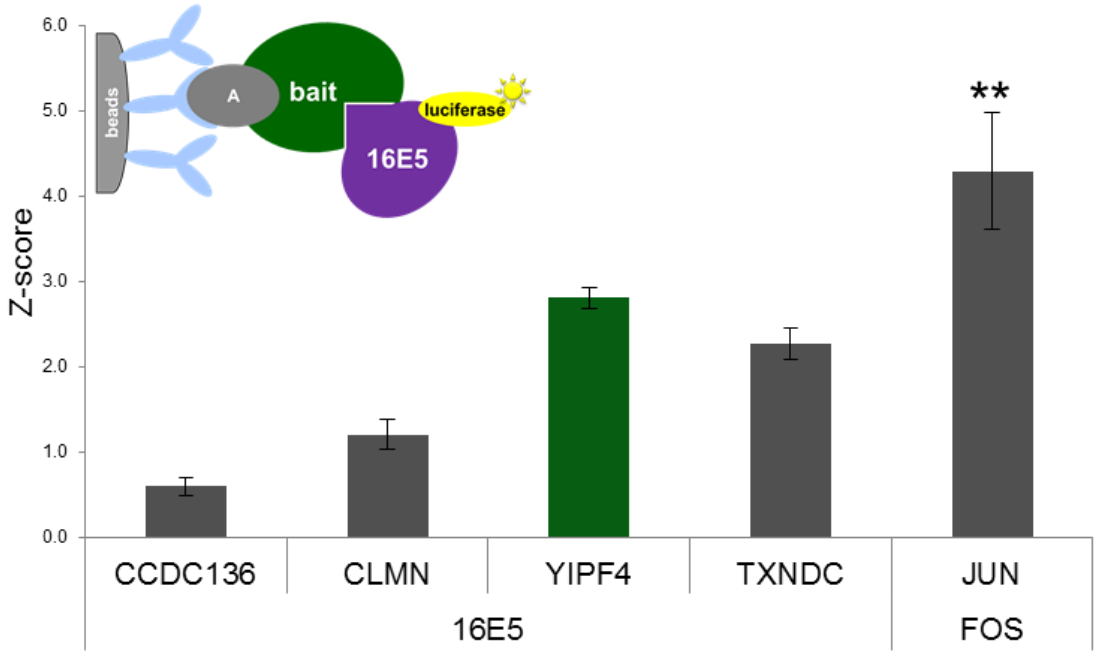

Figure 1.8 LUMIER assay for 16E5 interactors. The potential 16E5 interactors identified in the Y2H screen were tagged with Protein A and used as bait in the LUMIER assay to precipitate the *Renilla*-luciferase tagged 16E5 (schematic drawing). The bioluminescence emitted from the luciferase was normalised and Z-transformed to indicate protein interaction. The ineracting proteins JUN and FOS served as positive control. The highlighted protein YIPF4 (green) was chosen as subject of this PhD project. *$p \leq 0.01$. A = Protein A. The LUMIER assay was performed by Gundurao and Haas, University of Edinburgh, UK.

1.8. YIP1 protein family

The YIP1 proteins form a highly conserved family of integral membrane proteins in eukaryotes (Calero et al., 2002). They are characterised by (I) a common domain topology that consist of a hydrophilic N-terminus facing the cytoplasm and a hydrophobic C-terminus predicted to form several TMDs (Figure 1.9) (II) they interact with Rab GTPases (1.8.1) requiring their dual C-terminal prenylation and (III) the family members associate amongst each other (Calero et al., 2002, Chen and Collins, 2005b). Phylogenetic analysis of the protein family revealed two conserved motifs (P and GY) and a third motif (DLYGP) that has variations (ELYGP, DLYIP, DLWGP, DFWGP, DLAGP) (Stolle et al., 2005).

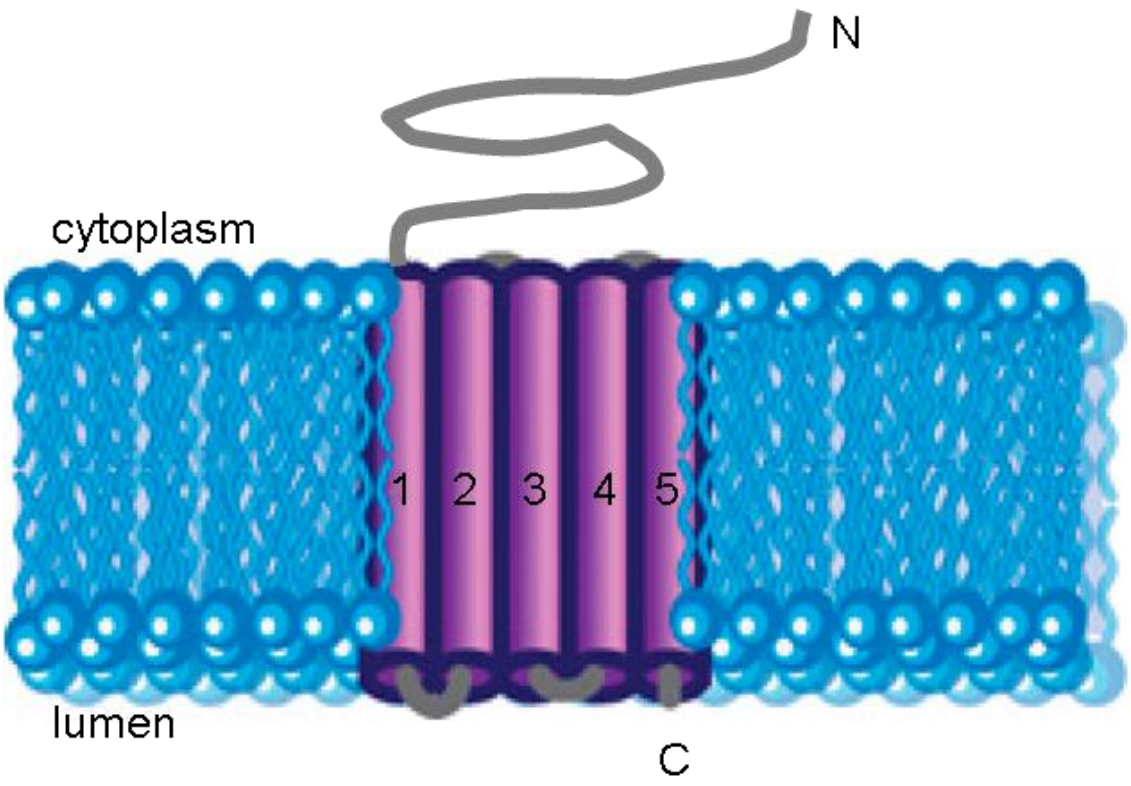

Figure 1.9 YIP1 protein membrane topology. This model of mammalian YIPF6 represents the characteristic topology of the YIP1 family members: A hydrophilic N-terminus exposed to the cytoplasm and a hydrophobic C-terminus predicted to form several TMDs. Adapted from Brandl et al., 2012.

According to the definition above, the YIP1 family has 4 members in yeast and 9 members in mammals (Table 1.3). Others also consider Yip2p and Yip3p in yeast as well as the prenylated Rab acceptors 1 and 2 (PRA1, PRA2) in mammals as members of the YIP1 family (Barrowman et al., 2003, Jin et al., 2005, Kano et al., 2009, Pfeffer and Aivazian, 2004, Stolle et al., 2005). However, their sequences and topology are too dissimilar compared to the other YIP1 family members and Yip3p/PRA1 can interact with mono-prenylated Rab GTPases which deviates from the YIP1 family criteria (Calero et al., 2002, Chen et al., 2004, Chen and Collins, 2005b, Figueroa et al., 2001, Geng et al., 2005, Heidtman et al., 2005, Shakoori et al., 2003). Thus, in the following, these proteins are not considered part of the YIP1 family.

Table 1.3 YIP1 family members in yeast and their mammalian orthologues. The table is based on reviewed UniProt entries.

YIP1 family member		**synonyms**	**mammalian species**
yeast	**mammals**		
Yip1	**YIPF4**	FinGER4	human, bovine, chicken, dog, mouse, rat, rhesus macaque
	YIPF5	FinGER5, SMAP-5, Yip1A	human, bovine, crab-eating macaque, dog, mouse, pig, rat, Sumatran orang-utan
	YIPF7	FinGER9, Yip1B	human, bovine, mouse
Yip4	**YIPF3**	FinGER3	human, mouse, rat,
	YIPF6	FinGER6	human, bovine, mouse, rat
Yip5	**YIPF1**	FinGER1	human, mouse, rat, Sumatran orang-utan
	YIPF2	FinGER2	human, mouse, rat
Yif1p	**YIF1A**	FinGER7, 54TMp	human, bovine, mouse
	YIF1B	FinGER8	human, mouse, rat

1.8.1. Rab GTPases

Small Rab GTPases belong to the superfamily of Ras GTPases that are known to play regulatory roles in membrane trafficking i.e. vesicle budding, movement, tethering and fusion (Hutagalung and Novick, 2011). There are 66 different Rab GTPases encoding genes in humans and eleven in yeast (called Ypt GTPases) (Calero et al., 2001, Garcia-Ranea and Valencia, 1998, Lazar et al., 1997, Pfeffer, 2013). The Rab proteins comprise a globular N-terminus that mediates binding and hydrolysis of guanosine triphosphate (GTP). Upon translation, the Rab GTPases associate with Rab escort proteins (REPs) that mediate binding to the Rab geranylgeranyl transferases (RabGGT) (Figure 1.10). These covalently attach one or two prenyl groups to unstructured and hypervariable C-terminal domain of the Rab GTPase.

Rab GTPase proteins function as molecular switches changing between an active, GTP-bound state and an inactive, guanosine diphosphate (GDP)-bound state (Hutagalung and Novick, 2011, Lee et al., 2009). In the active state, Rab GTPases are associated with their specific target membrane recruiting effector proteins that execute vesicle budding, movement, tethering and fusion, respectively. A Rab GTPase accessory protein called ‘GTPase accelerating protein’ (GAP) catalyses the hydrolysis of GTP to GDP and thus converts the Rab GTPase into its inactive state. Another accessory protein called ‘GDP dissociation inhibitor’ (GDI) binds to the inactive Rab GTPase and extracts it from the membrane creating a cytosolic pool of inactive Rab GTPase-GDP-GDI complexes. When required, Rab GTPases are recruited back and inserted to its target membrane by a membrane ‘GDI displacement factor’ (GDF). GDF catalyses the release of GDI and facilitates the access for the ‘guanine nucleotide exchange factor’ (GEF) which exchanges GDP for GTP and thus converts the Rab GTPase back to its active state.

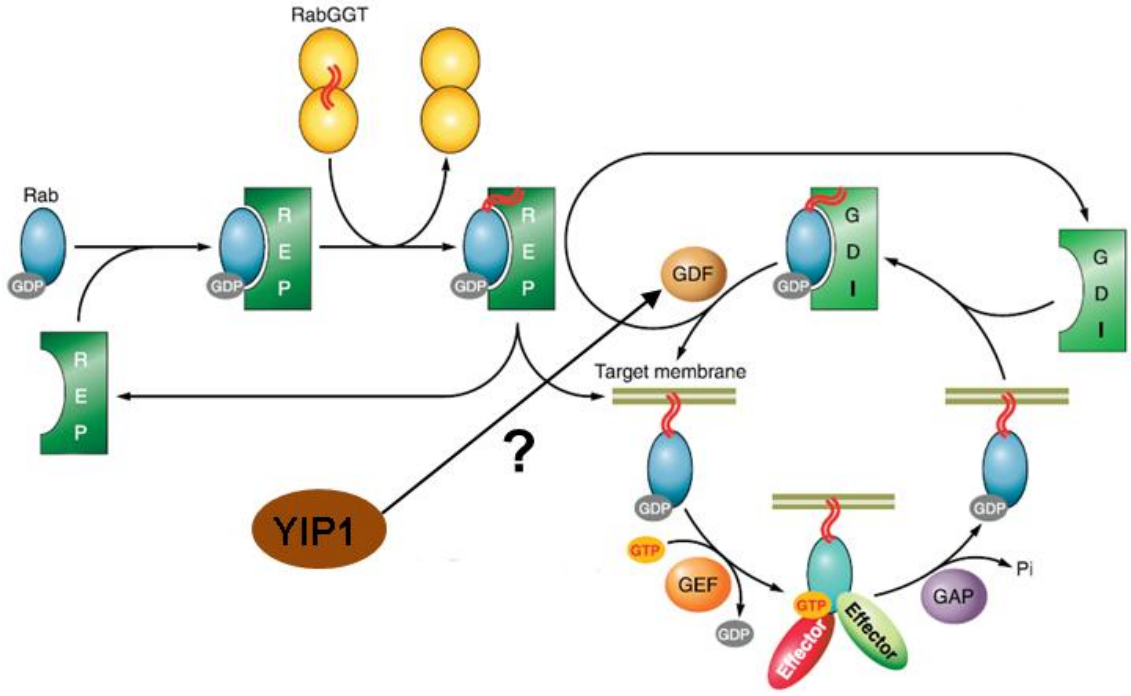

Figure 1.10 The Rab GTPase cycle. Rab GTPases are molecular switches that cycle not only between a GTP-bound active state and a GDP-bound inactive state but also between a free cytosolic pool and a membrane bound pool. They exert their functions by recruiting effector proteins. YIP1 family members are proposed to function as Rab GDFs. For detailed description see main text (1.8.1). Adapted from Hutagalung and Novick, 2011.

1.8.2. YIP1 proteins in yeast

1.8.2.1. Yip1p

The Ypt-interacting protein 1 (Yip1p) is an essential protein in yeast and the founder member of the YIP1 family that was first identified 16 years ago (Yang et al., 1998). It was confirmed as an integral membrane protein with a hydrophilic N-terminus facing the cytoplasm. It is predicted to have 3 TMDs towards the C-terminus and localises at the *cis*-Golgi or cycles between the ER and Golgi (Heidtman et al., 2003, Yang et al., 1998).

Yip1p interacts with di-geranylgeranylated and not mono-prenylated Ypt GTPases (Calero et al., 2003) in accordance with the YIP1 family criteria. In *in vitro* assays, Yip1p binds a myriad of Ypt GTPases (Ypt1p, Sec4p, Vps21p, Ypt6p, Ypt7p, Vps21p, Ypt31p, Ypt51p, Ypt52p, Ypt53p) (Calero et al., 2003, Matern et al., 2000, Yang et al., 1998). Besides the requirement for dual-prenylation, Yip1p preferentially binds the GDP bound form of the Ypt GTPases (Yang et al., 1998), although others saw no preference for GTP or GDP bound Ypt GTPases (Calero et al., 2003). However, in *in vivo* assays Yip1p exclusively interacts with Ypt GTPases localised at the Golgi like Ypt1p which plays a role in anterograde ER to Golgi trafficking as well as Ypt31p that is involved in intra-Golgi and Golgi to vacuole trafficking (Chen et al., 2004, Yang et al., 1998). Yip1p also binds Ypt6p, which is linked to retrograde trafficking from the Golgi to the ER indicating a function of Yip1p in ER to Golgi anterograde or Golgi to ER retrograde trafficking. Indeed, a defective Yip1p protein results in disruption of membrane trafficking and vesicle budding from the ER and the function of Yip1p in trafficking events was shown to be dependent on Ypt GTPases and their GDIs (Chen et al., 2004).

Because of its integral membrane property, Yip1p is thought to function as GDF to recruit the soluble Ypt GTPase/GDI complex from the cytoplasm to the Golgi membrane (Chen and Collins, 2005b, Yang et al., 1998). In agreement with this, Calero and colleagues observed an increase in the soluble pool of Ypt1p in Yip1p defective cells (Calero et al., 2003). Barrowman and colleagues, however, did not notice an increase of the soluble Ypt1p pool in Yip1p defective

cells and Ypt1p could still associate with its target membrane under these conditions (Barrowman et al., 2003). Thus, more research is needed to determine whether Yip1p functions as a GDF for Ypt GTPases of the early secretory pathway.

Yip1p forms a tetrameric complex consisting of one other YIP1 family member Yif1p (YIP1 interacting factor) (1.8.2.2) and the unrelated proteins Yop1p (YIP one partner) and Yos1p (Yip one suppressor 1) (Andrulis et al., 1998, Calero et al., 2001, Heidtman et al., 2005, Ito et al., 2001, Ito et al., 2000). The interaction of Yip1p with the small integral membrane protein Yop1p is mediated by their hydrophilic N-termini (Calero et al., 2001). The overexpression of Yop1p causes disruption of the early secretory pathway as well as membrane accumulation and cell death. It is therefore conceivable that Yip1p and Yop1p mediate a common stage in membrane trafficking even because Yop1p was also shown to interact with Ypt6p.
Yos1p is bound by Yip1p and Yif1p (Heidtman et al., 2005). It is a very small integral membrane protein that localises to the ER and Golgi and is packed into coat protein complex 2 (COPII) transport vesicles. Depletion of Yos1p blocks the trafficking between ER and Golgi. The Yip1p/Yif1p/Yop1p/Yos1p complex therefore plays a role in the anterograde trafficking from ER to Golgi.

Yip1p is known to function in COPII vesicle trafficking which could be mediated by the interaction with Ypt GTPases (Chen and Collins, 2005b). The Yip1p/Yif1p complex binds to the ER to Golgi SNARES bet one suppressor 1 and Sec22p and is thought to promote fusion of ER-derived vesicles to the Golgi (Barrowman et al., 2003). Others did not observe an involvement of Yip1p in COPII vesicle fusion but rather in COPII vesicle budding from the ER and this process was independent of Ypt1p (Heidtman et al., 2003). Also, a role in Golgi structure maintenance and function is conceivable. Clearly, further research is needed to determine the precise role of Yip1p in intracellular trafficking.

The Yip3p protein which is not a member of the Yip1p family (1.8) interacts with Yip1p and binds to Ypt GTPases *in vitro* in an non-specific manner (Calero and Collins, 2002, Ito et al., 2001, Ito et al., 2000). Because the human orthologue

of Yip3p, PRA1, interacts with v-SNARES and functions as a Rab GTPase GDF, the Yip1p/Yip3p complex could contribute to the regulation of intracellular trafficking (Sivars et al., 2003). But further research is needed to allocate a function to this protein complex.

The hydrophilic N-terminal domains of Yip1p and Yif1p interact with the phox homology domain of proteins, which is a phosphoinositide binding domain (Vollert and Uetz, 2004). Amongst these are Grd19p, Vam7p, Vps5p, Vps17p, and Ypt35p which are involved in the endocytic pathway. Thus, it is conceivable that Yip1p functions in the endocytic trafficking pathway in addition to the secretory pathway but this remains to be confirmed.

1.8.2.2. Yif1p

Yip1p interacting factor Yif1p, is an integral membrane protein with the characteristic hydrophilic N-terminus and a hydrophobic C-terminus predicted to form three TMDs (Andrulis et al., 1998, Matern et al., 2000). This essential protein co-localises with its interaction partner Yip1p at the *cis*- and *medial*-Golgi and in COPII vesicles (Otte et al., 2001). The overexpression of Yif1p can compensate for the loss of Yip1p indicating that it might perform similar functions as Yip1p (Calero et al., 2002).

Indeed, in a Y2H assay, Yif1p weakly interacted with the Yip1p binding partners Ypt1p and Ypt31p (Matern et al., 2000) and is proposed to function as a Ypt GTPase GDF (Figure 1.10) (Cardoso and Calonje, 2003, Matern et al., 2000, Otte et al., 2001). It is conceivable that Yif1p recruits the Ypt GTPases to COPII vesicles to mediate fusion with the target membrane.
Yif1p interacts with Yip3p and co-localises with it at ER derived vesicles (Andrulis et al., 1998, Otte et al., 2001). Also, an interaction with the batten disease protein 2 was observed, a protein that is involved in intracellular protein transport (Chattopadhyay et al., 2003). Defective Yif1p results in a disruption of trafficking between the ER and Golgi whereby ER membranes accumulate and the glycosylation in the Golgi is reduced (Matern et al., 2000). Thus, Yif1p as part of a larger protein complex plays a role in the early secretory pathway.

1.8.2.3. Yip4p and Yip5p

Yip4p and Yip5p are non-essential proteins and the most recent YIP1 family members in yeast. They are predicted to have a hydrophilic N-terminus and several C-terminal TMDs (Calero et al., 2002).

In a Y2H assay and a pull down assay they were shown to interact with several Ypt GTPases requiring their C-terminus (Calero et al., 2002). Deletion of Yip4p and Yip5p did not alter the membrane bound and soluble pool of various tested Ypt GTPases which implies that Yip4p and Yip5p do not function as Ypt GDFs (Geng et al., 2005).

Yip4p and Yip5p both interact with Yip1p but their overexpression cannot compensate for the loss of Yip1p (Calero et al., 2002). This might indicate that they exert different functions to Yip1p. An interaction between Yip4p and Yip5p and a self-association of Yip4p was also observed. In addition to that, Yip4p and Yip5p interact with the Golgi membrane proteins Tvp23 and Tvp18 but the functions of these proteins are largely unknown (Inadome et al., 2007).

1.8.3. YIP1 proteins in mammals

A Psi-basic local alignment search tool (BLAST) search identified homologues of Yip1p, Yip4p, Yip5p and Yif1p in humans, mice, insects, nematodes and plants (Shakoori et al., 2003). In humans, eight YIP1 family members were initially detected with the ninth family member YIPF7 only being discovered in a homology search for YIPF5 (Stolle et al., 2005) (Table 1.3).
All human YIP1 family members are predicted to have a hydrophilic N-terminus and five TMDs towards the C-terminus (Shakoori et al., 2003). The N-terminus domain was shown to face the cytoplasm.

The mRNA of the YIP1 family members was expressed in all tested human tissues (heart, brain, placenta, lung, liver, skeletal muscle, kidney, pancreas, spleen, thymus, prostate, testis, ovary, small intestine, colon, peripheral blood leukocyte) with especially high expression levels in the skeletal muscle and testis (Shakoori et al., 2003).

Like for the yeast YIP1 family members (1.8.2), the human YIP1 family members are likely to function in cellular trafficking processes but their precise functions are still poorly chracterised.

1.8.3.1. YIPF1 and YIPF2

YIPF1 and YIPF2 are orthologues of the yeast Yip5 protein (Table 1.3) but compared to their orthologue (1.8.2.3) they are poorly studied yet. YIPF1 is translated from one mRNA but there are two splicing variants of YIPF2 mRNA in certain tissues (Shakoori et al., 2003). In a Y2H screen YIPF1 and YIPF2 were identified as binding partners and both proteins bind YIPF6 and could therefore form a trimeric complex. YIPF1 can also bind to itself. The interactions are mediated by the TMDs of the proteins, not their hydrophilic N-termini. The functions of these potential protein complexes are not known.

Interestingly, two single-nucleotide polymorphisms (dbSNP Reference IDs (rs6588492 --> A/G and rs6680026 --> C/T) in YIPF1 correlate with a susceptibility to treatment with angiotensin II receptor blocker in patients with mild/moderate hypertension (Kamide et al., 2013). Whether YIPF1 has a causative effect in the susceptibility to treatment with the angiotensin II receptor blocker remains to be investigated.

1.8.3.2. YIPF3 and YIPF4

YIPF3 is the orthologue of Yip4p in yeast (Table 1.3). YIPF3 is translated from one mRNA splicing variant while there are multiple splicing variants for its paralogue YIPF4 (Shakoori et al., 2003; 3.1.1). In an immuno-fluorescence approach, it was confirmed that the hydrophilic N-terminus of YIPF3 faces the cytoplasm and the hydrophobic C-terminus the lumen (Tanimoto et al., 2011). Both proteins are localised at the *cis*-Golgi.

YIPF3 is post-translationally modified (Tanimoto et al., 2011). Its asparagine at position 337 is N-glycosylated while the threonines at positions 333, 334, 339 and 346 are O-glycosylated (Halim et al., 2012a, Halim et al., 2012b, Tanimoto et al., 2011). The functional implications of these modifications are not known but are likely to be required for protein maturation. Interestingly, glycosylated YIPF3 is secreted in the human urine but whether it can serve as a biomarker is not yet known (Halim et al., 2012a).

The YIPF4 protein was detected as a single entity on a Western blot and thus post-translational modifications were excluded (Tanimoto et al., 2011). In contrast, large-scale mass spectrometry analysis suggests the phosphorylation of tyrosines at positions 10 and 60 as well as ubiquitination of lysines at positions 47 and 91 (Hornbeck et al., 2004). Further research is needed to confirm this and to determine the functions of these potential modifications.

YIPF3 and YIPF4 interact and form protein complexes of four different sizes (520kDa, 450kDa, 260kDa, 220 kDa) but the exact stoichiometry or composition of these complexes is not known (Tanimoto et al., 2011). Interestingly, small interfering RNA (siRNA) mediated knock down of YIPF4 reduces the YIPF3 expression levels. It is therefore possible that YIPF4 stabilises the YIPF3

protein. The knock down of YIPF3 did not alter YIPF4 expression levels but rather promoted its localisation to the ER indicating that YIPF3 might be responsible for YIPF4 localisation at the *cis*-Golgi.
Initially, YIPF4 was identified as a binding partner of the YIP1 family member YIF1A in a Y2H assay (Shakoori et al., 2003) but this interaction could not be confirmed in a Co-IP assay (Tanimoto et al., 2011) underlining the importance of verifying Y2H data.

The knock down of YIPF3 and YIPF4, respectively, results in the fragmentation of the Golgi (Tanimoto et al., 2011). Interestingly, this does not affect the anterograde transport and the sialylation of test proteins. Even the simultaneous knock down of the YIP1 family members YIPF3, YIPF4, YIPF5 and YIPF1A does not affect the functionality of the Golgi. Thus, these proteins appear not to play an essential role in the regulation of Golgi structure and function.

1.8.3.3. YIPF5

YIPF5 is the orthologue of yeast Yip1p (Table 1.3). A total of 9 splicing variants have been identified for YIPF5 but their role *in vivo* might be less important (Stolle et al., 2005). YIPF5 transcripts were detected in all of 37 tested human tissues as well as 5 different human cell types. It is predicted to be transcribed from a TATA-box less promoter which is characteristic for housekeeping genes. With regard to its ubiquitous expression, YIPF5 is indeed likely to be a housekeeping gene (Stolle et al., 2005, Tang et al., 2001).

The YIPF5 protein consists of 257 amino acids and possesses the characteristic hydrophilic N-terminus and hydrophobic C-terminus with several predicted TMDs (Stolle et al., 2005, Tang et al., 2001). In HeLa cells, YIPF5 showed ER-like localisation (Shakoori et al., 2003). Others observed a juxtanuclear and ER exit site localisation as well as a co-localisation with components of COPII vesicles (Tang et al., 2001). Indeed, green fluorescent protein (GFP) tagged YIPF5 was used as an ER exit site marker in a study of mitosis (Kano et al., 2004). YIPF5 was also detected at the ER - Golgi intermediate compartment (ERGIC) (Dykstra et al., 2010, Kano et al., 2009,

Yoshida et al., 2008) and the *cis*-Golgi (Kano et al., 2009, Stolle et al., 2005, Yoshida et al., 2008). Kano and colleagues observed YIPF5 localisation at the *trans*-Golgi (Kano et al., 2009) but Yoshida and colleagues excluded its localisation at the *medial*- or *trans*-Golgi (Yoshida et al., 2008). Because different studies observed YIPF5 at various locations between the ER and the Golgi, it is likely that YIPF5 cycles between the ER and Golgi.

YIPF5 interacts with the YIP1 family member YIF1A (1.8.3.5) and forms protein complexes of three different sizes (320 kDa, 160 kDa and 120 kDa) but the stoichiometry and composition of these complexes is not known (Dykstra et al., 2013, Yoshida et al., 2008). Knock down of YIPF5 reduced the expression levels of its interaction partner YIF1A and vice versa. It is conceivable that the proteins stabilise each other in those complexes. YIPF5 also interacts with the mammalian homologue of Yop1p (1.8.2.1), DP1 and the related DPL1, but a function was not allocated to these protein complexes (Dykstra et al., 2010).

Independent of binding to YIF1A and DP1, YIPF5 plays a role in ER network organisation (Dykstra et al., 2010, Dykstra et al., 2013, Yoshida et al., 2008). Knock down of YIPF5 resulted in rearrangement of the ER into stacked and concentrically whorled structures. The glutamic acid at position 95 and the neighbouring leucines at positions 91 and 96 of the N-terminal domain and the lysine at position 146 and the valine at position 152 of the C-terminal domain are crucial for the correct organisation of the ER (Dykstra et al., 2013).
Interestingly, others did not observe a disruption of the ER network upon YIPF5 knock down but a fragmentation of the Golgi (Dykstra et al., 2010, Yoshida et al., 2008) and Kano and colleagues did not detect any alterations in ER, ERGIC and Golgi morphology (Kano et al., 2009). This might be due to different knock out efficiencies in the individual experiments.

YIPF5 binds to the COPII components Sec23 and Sec24 via its highly conserved amino acids 75 – 106 and is efficiently packaged into COPII transport vesicles (Tang et al., 2001). In agreement with this, YIPF5 knock down disrupted the ER to Golgi trafficking. Dykstra and colleagues, however, only saw a delay and not a disruption of the secretory trafficking in YIPF5 knock

down cells (Dykstra et al., 2010) and others could not detect an involvement of YIPF5 in anterograde transport (Kano et al., 2009, Yoshida et al., 2008). Interestingly, the treatment of vascular smooth muscle cells with the transforming growth factor β-1 elevated the expression of YIPF5 (Stolle et al., 2005). YIPF5 could therefore play a role in the secretion of components of the extracellular matrix.

YIPF5 might also function in retrograde transport. The knock down of YIPF5 decreased the rate of COPI-independent but not the COPI-dependent retrograde transport between the Golgi and ER (Kano et al., 2009). This was caused by the reduced recruitment of Rab6 GTPase to the membranes. However, YIPF5 does not bind to Rab6 and is therefore unlikely to function as its GDF (Figure 1.10). Further research is needed to determine the precise role of YIPF5 in anterograde and retrograde trafficking.

1.8.3.4. YIPF6 and YIPF7

YIPF6 is the orthologue of the yeast Yip4 protein and YIPF7 is the orthologue of Yip1 protein (Table 1.3). YIPF6 mRNA is expressed ubiquitously in human and mouse tissues and a multitude of splicing variants have been detected on a Northern blot (1.8.3) (Brandl et al., 2012, Shakoori et al., 2003). In contrast, YIPF7 was only discovered after the initial identification of the YIP1 family in mammals (Shakoori et al., 2003, Stolle et al., 2005) and murine YIPF7 is exclusively expressed in the heart (Tang et al., 2001). It therefore forms an exception from the otherwise ubiquitously expressed YIP1 proteins. Overexpressed murine YIPF6 localises to the *cis*- and *trans*-Golgi (Brandl et al., 2012). It also co-localises with the COPII component Sec31a and could therefore play a role in anterograde ER to Golgi transport.

In a Y2H assay, YIPF6 interacted with YIPF1 and YIPF2 with the interaction being mediated by their hydrophobic C-terminal domains (Shakoori et al., 2003). The binding of these proteins was, however, not investigated further nor was a function allocated. Interestingly, a thymine to adenine transversion in the YIPF6 gene in mice correlated with intestinal inflammation (Brandl et al., 2012).

The mutation leads to the skipping of intron 4 during splicing and results in a frameshift with a premature stop codon. The expression of WT YIPF6 in these mice rescues the intestinal inflammatory phenotype. The responsible mechanism was not determined.

1.8.3.5. YIF1A

YIF1A is the orthologue of yeast Yif1 protein (Table 1.3). There is only one splicing variant known in human tissues (Shakoori et al., 2003). The YIF1A protein was predcited to have 4 - 5 TMDs and its hydrophilic N-terminus was shown to face the cytoplasm (Jin et al., 2005, Kuijpers et al., 2013). It localises to the ER (Kuijpers et al., 2013), the ERGIC (Breuza et al., 2004, Kuijpers et al., 2013), and the *cis*- and *trans*-Golgi (Jin et al., 2005) and was indeed shown to cycle between the ER and Golgi (Breuza et al., 2004, Kuijpers et al., 2013).

In a Y2H assay, YIF1A bound to YIPF4 (Shakoori et al., 2003), however, this could not be confirmed in a Co-IP assay (Tanimoto et al., 2011). In contrast, the interaction between YIF1A and YIPF5 is well established (Jin et al., 2005, Young, 1998) and could function in the maintenance of the Golgi structure, although further research is needed to confirm this.
The TMDs and the N-terminal amino acids 31 – 41 of YIF1A mediate binding to the ADP-ribosylation factor GTPase-activating protein 1 (ArfGAP1) (Akhter et al., 2007). This is thought to be involved in COPI vesicle formation by regulation of the GTP-binding protein Arf1. Thus, YIF1A is likely to play a role in COPI-dependent retrograde vesicle transport.
The first two potential TMDs of YIF1A bind to the single TMD of VAPB (vesicle-associated membrane protein (VAMP) associated protein B (VAPB)) (Kuijpers et al., 2013). Short hairpin RNA (shRNA) interceded knock down of YIF1A in neurons resulted in aberrant dendrite morphology since YIF1A mediates the transfer of membranes from the soma to dendrites. Thus, YIF1A plays a specific role in the dendrite development of neurons. The cellular localisation of YIF1A is altered in neurons with the mutant VAPB-P56S allele and could therefore be linked to the VAPB-associated motor neuron diseases.

1.8.3.6. YIF1B

YIF1B is an orthologue of the yeast Yif1p protein (Table 1.3). There are several YIF1B splicing variants expressed in a variety of human tissues (Shakoori et al., 2003). Rat YIF1B is 89% identical to human YIF1B and transcripts and proteins are expressed in brain, heart, kidney, lung, spleen, muscle and intestine (Carrel et al., 2008). It is predicted to have the characteristic hydrophilic N-terminus and 5 TMDs. The human YIF1B localises to the ER (Shakoori et al., 2003) while the rat YIF1B localises to ER and the *median*-Golgi and the transport vesicles in-between these organelles (Carrel et al., 2008).

Like YIF1A (1.8.3.5), YIF1B interacts with ArfGAP1 with the tryptophan at position 211 being essential for this interaction (Akhter et al., 2007). Therefore, YIF1B could play a role in COPI-dependent retrograde vesicle transport. Also, YIF1B interacts with VAPB and might be associated with the VAPB-associated motor neuron disease (1.8.3.5) (Kuijpers et al., 2013).

YIF1B plays another essential role in neurons. It partially co-localises with the serotonin receptor 5-HT_{1A}R in rat hippocampal neurons (Carrel et al., 2008). The two proteins interact with high affinity via two aspartic acids at the N-terminus of YIF1B and three basic amino acids at the C-terminus of 5-HT_{1A}R (Al Awabdh et al., 2012). YIF1B promotes the trafficking of 5-HT_{1A}R to the distal section of the dendrites (Carrel et al., 2008). Others, however, could not confirm the involvement of YIF1B in 5-HT_{1A}R trafficking (Kuijpers et al., 2013). In contrast to this, Al Awabdh and colleagues proposed a model of a YIF1B trafficking complex for 5-HT_{1A}R (Figure 1.11) (Al Awabdh et al., 2012). Co-IP assays and immuno-fluorescence approaches suggest a model where YIF1B binds 5-HT_{1A}R and YIPF5 and mediates association with Rab6 GTPase. Rab6 GTPase facilitates the bi-directional movement on the tubulin cytoskeleton via 2 motor proteins: Kinesin-1 HC (Kif5B) and dynein. Further research is needed to support this first detailed model of YIP1 family member mediated trafficking.

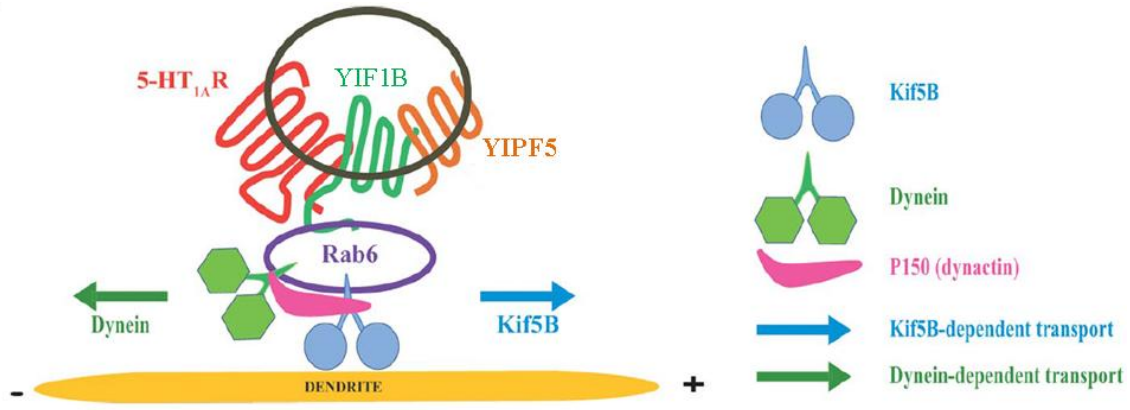

Figure 1.11 YIF1B mediated trafficking of the serotonin receptor 5-HT_{1A}R in dendrites. YIF1B functions as a scaffolding protein to assembly the trafficking complex that allows plus-and minus-end directed trafficking of 5-HT_{1A}R in dendrites. The dynactin subunit P150 facilitates switching between the two trafficking directions. More research is needed to confirm this first precise trafficking model of a YIP1 family member. Adapted from Al Awabdh et al., 2012.

In summary, the YIP1 proteins are a family of integral membrane proteins, which is highly conserved in eukaryotes. Notably, their characteristic membrane topology is largely based on bioinformatic predictions and has not been experimentally validated.

YIP1 proteins play a role in cellular trafficking processes, which could be facilitated by their Ypt/Rab GTPase binding partners. Because YIP1 proteins are integral membrane proteins they are proposed to function as GDFs for those Ypt/Rab GTPases (Figure 1.10) but this remains to be proven.

YIP1 family members interact with each other and form large protein complexes of partially redundant functions, which are not well understood to date. Most YIP1 family members are ubiquitously expressed, only YIPF7 expression is limited to heart tissue. Because of the high conservation and ubiquitous expression, it is conceivable that the YIP1 family members are housekeeping proteins but then specific functions in the development and trafficking of neuronal receptors have been identified. Also, mutations in some mammalian YIP1 proteins correlate with specific clinical disorders.

Thus, despite their small size and limited number, the YIP1 family members play crucial roles in eukaryotic cells. The prospect of YIPF4 interacting with a viral protein could be extremely elucidative not only for the YIP1 family but also for the pathogenesis of PVs.

1.9. Aims and objectives

Preliminary work suggests that YIPF4 is a new cellular target of the 16E5 oncoprotein (1.7). The properties and functions of both proteins are only poorly understood but it is conceivable that both proteins play roles in cellular trafficking pathways. The aim of this PhD study was therefore to characterise the potential interaction between 16E5 and YIPF4 and investigate the function of this protein complex. To this end, the specific objectives of this study were:

1. To verify and asses the expression of YIPF4 in HPV infected cells and tissue.

2. To produce experimental evidence for the membrane topology of YIPF4 as the first representative of the YIP1 family.

3. To confirm the interaction of 16E5 with YIPF4.

4. To investigate the interaction of YIPF4 with E5 proteins of other PV types and HPV16 oncoproteins.

5. To allocate a function to the 16E5/YIPF4 protein complex.

Chapter 2. Materials and Methods

2.1. Bacterial cell culture

2.1.1. Bacteria growth and storage

The *Escherichia coli* strain NEB5α (New England BioLabs (NEB), USA) was used as host for the amplification of DNA vectors. *E. coli* were grown on semisolid medium (0.75% w/v agar in LB Medium) and in liquid shaking cultures (Luri-Bertani (LB) medium: 3% w/v tryptone soya broth, 0.5% w/v yeast extract), respectively, overnight (o/n) at 37°C. Appropriate antibiotics were added for selection (50 µg/µl Kanamycin, 100 µg/µl Ampicillin). Semisolid cultures were stored for short periods of time at 4°C. For long-term storage, cells were frozen at -80°C in freezing medium (23% glycerol in liquid o/n culture).

2.1.2. Preparation of chemically competent bacteria

Ultra competent NEB5α cells were prepared according to the Inoue Method (Sambrook and Russell, 2006). Briefly, single colonies were grown in SOB-medium (2% peptone, 0.5% yeast extract, 10 mM NaCl, 2.5 mM KCl, pH 7.5, autoclaved) at 18°C to an optical density measured at 600 nm (OD_{600}) of 0.6. The culture was incubated on ice before harvesting the cells by centrifugation at 2500 x g for 10 min at 4°C. Cells were washed once in transformation buffer (10 mM PIPES, 15 mM $CaCl_2$, 250 mM KCl, 55 mM $MnCl_2$, pH 6.7, filter sterilised). Cells were resuspended in ice-cold transformation buffer and dimethyl sulphoxide (DMSO) was added to a final concentration of 7%. Aliquots were prepared which were frozen at -80°C for long-term storage.

2.1.3. Transformation of competent bacteria with plasmid DNA

Transformation of NEB5α cells was based on the method described by Hanahan (Hanahan, 1983). Plasmid DNA (2 µl) was added to 50 µl of competent NEB5α (2.1.2) cells and incubated on ice for 20 min. Cells

underwent heat shock treatment at 42°C for 30 sec. Cultures were incubated on ice for 2 min followed by the addition of 200 µl of LB medium and an 1 h incubation at 37°C shaking at 180 rpm. The cultures were streaked out onto selective semisolid medium (2.1.1).

2.1.4. Preparation of plasmid DNA

2.1.4.1. Small scale preparation

To purify plasmid DNA on a small scale, 5 ml of selective LB medium were inoculated with a single colony previously grown on semisolid medium. The culture was shaken o/n at 37°C. Cells were harvested by centrifugation of 2 ml of culture for 5 min at 16100 x g. The plasmid DNA was purified using the sodium dodecyl sulphate (SDS)-alkaline denaturation method employed by the Wizard® Plus SV Minipreps DNA Purification System (Promega, UK). Purification was conducted according to the manufacturer's protocol. DNA was eluted from the Wizard® SV Minicolumns with 30 µl ddH_20.

2.1.4.2. Large-scale preparation

To purify plasmid DNA on a larger scale, a starter culture was prepared by inoculating 2 ml of selective LB medium with a single colony grown on semisolid medium. The culture was shaken for 4 h at 37°C and diluted (1:500) in 100 ml of selective LB medium. This large-scale culture was shaken o/n at 37°C. Cells were harvested by centrifugation at 6000 x g for 15 min at 4°C. The plasmid DNA was purified using the Plasmid Maxikit (Qiagen, Germany) according to the manufacturer's protocol. Plasmid DNA was resuspended in 100 µl – 300 µl ddH_2O.

The concentration of the plasmid DNA was determined using a Nanodrop spectrophotometer (Thermo Fisher Scientific, USA).

2.2. Molecular Cloning

2.2.1. Plasmid DNA vectors and oligonucleotides

See Table A. 1 and Table A. 2 in Appendix.

2.2.2. Polymerase chain reaction

The polymerase chain reactions (PCR) were performed based on the method developed by Mullis and colleagues (Mullis et al., 1986). Amplifications of the target sequences were conducted using a KOD DNA polymerase (Merck, UK) in a 50 µl reaction volume containing: 1 x KOD DNA Polymerase Buffer, 1 unit KOD DNA Polymerase, 200 µM dNTP, 2.5 nM $MgCl_2$, 10% DMSO, 100 pmol forward and reverse primer (Table A. 1 and Table A. 2), respectively and 100 – 500 ng DNA template. The reactions were conducted in a MJ research PTC-200 Thermal Cycler (GMI) according to the following protocol: hot start for 60 sec at 94°C followed by 30 - 40 cycles of denaturation for 20 sec at 95°C, annealing for 20 sec and elongation at 74°C. The annealing temperature and elongation time were adjusted according to the melting temperature (T_M) of the oligonucleotides and length of target sequence, respectively (Table A. 1 and Table A. 2). The amplification products were purified from the reaction using the Qiaquick PCR purification kit (Qiagen, Germany) according to the manufacturer's protocols. DNA integrity was verified by agarose gel electrophoresis (2.2.3).

2.2.3. Agarose gel electrophoresis

PCR amplification products and restriction digest products were separated by agarose gel electrophoresis. For this, a 1.6% agarose gel was prepared (1.6% w/v agarose in TAE (40 mM Tris base, 20 mM Acetic acid, 1 mM EDTA)) with the addition of 1 x SYBR safe DNA gel stain (Invitrogen, USA). Gel loading dye (5 x: 10% Glycerol, Orange G in TAE) was added to the samples to obtain a 1 x final concentration. Electrophoresis was carried out at 180 V for 37 min in TAE buffer. The agarose gel was viewed and documented using a Syngene InGenius gel documentation system (Syngene Bioimaging, UK).

2.2.4. Restriction enzyme digestion

Purified PCR amplification products and destination vectors were digested with two high fidelity enzymes (NEB, USA). In a reaction volume of 30 µl, 1 µg of DNA was digested with 10 units of enzyme I and enzyme II (Table A. 1 and Table A. 2), respectively in 1 x NEB Buffer 4. Samples were incubated for 1 h at 37°C.

2.2.5. Antarctic Phosphatase treatment of destination vectors

Linearised destination vectors were treated with 1 unit Antarctic Phosphatase (NEB, USA) for 30 min at 37°C followed by inactivation at 65°C for 5 min.

2.2.6. DNA ligation reactions

Ligations of PCR amplification products into their destination vectors were accomplished using T4 DNA ligase (NEB, USA). In a total volume of 10 µl, 400 units of T4 DNA ligase in 1 x T4 DNA ligase buffer were used to ligate a PCR amplification product and a destination vector in a ratio of 3:1. The ligation reaction was incubated for 30 min at room temperature (RT). Ligation products were transformed into competent NEB5*α* cells (2.1.2).

2.2.7. Screening clones and sequencing

The integrity of the sequences of all clones prepared for this project was confirmed by sequencing. All sequencing reactions were conducted by GATC-Biotech (Germany) using provided vector-specific sequencing primers. The resulting DNA sequences were analysed with the online accessible Basic Local Alignment Search Tool (BLAST; National Center for Biotechnology Information, USA) and a pairwise alignment tool (European Molecular Biology Laboratory – European Bioinformatics Institute, EMBL-EBI, UK). Sequences were formatted using ‘DNATools’ (Department of Biology, Southeast Missouri State University, USA).

2.2.8. Basic bioinformatics

The molecular weights of 16E5 and YIPF4 truncation mutants (Table A. 1, Table A. 2) were predicted using the Protein Molecular Weight Calculator (Science Gateway, USA).

Multiple sequence alignments of YIPF4 sequences from various species (Table A. 3) were aligned using the ClustalW2 online tool (EMBL-EBI, UK).

The YIPF4 gene sequence (NT_022184.15|:11324845-11353545) was searched for the HPV E2BS ($ACCN_6GG$, Hines et al., 1998) using the 'pattern search' function of GeneQuest (DNASTAR, USA). Sequence logos of the potential E2BSs were generated with the WebLogo tool (Crooks et al., 2004).

The membrane topology of YIPF4 (UniProt ID: Q9BSR8) was predicted using the SOSUI online tool (Hirokawa et al., 1998, Shakoori et al., 2003).

2.3. Protein Biochemistry

2.3.1. Bicinchoninic acid assay for protein concentration determination

Protein concentrations of mammalian cell lysates were determined with a detergent-compatible bicinchoninic acid (BCA) protein assay kit (Thermo Fisher Scientific, USA) according to the manufacturer's protocol for microplates. Briefly, a series of standard dilutions (0 µg/ml – 2 µg/ml) of bovine serum albumin (BSA) was prepared using the lysis buffer of the samples. Mammalian cell lysates were diluted 1:10 and 1:100. The BSA standards and the diluted samples were added into a 96-well plate in duplicates and the BCA working reagent was added. After 10 min incubation at RT, the absorbance at 562 nm was determined on a PowerWave XS2 Microplate Spectrophotometer (BioTek, UK). A standard curve was generated using the accompanying software (Gen5 1.07.5, BioTek, UK) to determine the samples' total protein concentration taking into account the dilution factor.

2.3.2. SDS polyacrylamide gel electrophoresis (SDS-PAGE)

Proteins were separated according to molecular weight using a minigel system (BioRAD, USA). 10%, 12%, 13.5% and 15% SDS-polyacrylamide gels were prepared according to required protein resolution (separating gel: 10%; 12%, 13.5%; 15% Acrylamide, 375 mM Tris/Cl, pH 8.8; 0.1% SDS, 0.1% APS, 0.01% TEMED; stacking gel: 6% Acrylamide, 125 mM Tris/Cl, pH 6.8; 0.1% SDS, 0.1% APS, 0.01% TEMED). Protein samples, 30 µl, with lithium dodecyl sulphate (LDS) sample buffer (Invitrogen, USA) and 0.1% 2-mercapoethanol, were loaded alongside 5 µl SeeBlue prestained protein marker (Invitrogen, USA) or ColorPlus Prestained Protein Marker (NEB, USA). Electrophoresis was carried out at 100 - 120 V in 1 x SDS running buffer (34.7 mM SDS, 250 mM Tris Base, 1.92 M Glycine) until the desired protein resolution was achieved.

2.3.3. Western blot analysis

Separated proteins were transferred from the SDS-polyacrylamide gels to HybondTM-C Extra mixed ester nitrocellulose membranes (Amersham BioSciences, UK) on a semi-dry Transfer Cell (BioRAD, USA) or a wet transfer XCell II™ Blot Module (Invitrogen, USA). For this, the membranes were equilibrated in transfer buffer (192 mM Glycine, 25 mM Tris Base, 20% methanol) before conducting the semi-dry transfer at 15 V for 45 – 60 min and the wet transfer at 30 V for 60 – 150 min according to protein size. Membranes were then blocked by incubation in blocking solution (5% Marvel dried skimmed milk in TBS-T (TBS: 25 mM Tris/Cl, pH 7.5; 138 mM NaCl and 0.1% Tween-20)) for at least 30 min at RT. Primary antibody (Table A. 4) diluted in blocking solution was added to the membrane and incubated o/n at 4˚C on a shaking platform or alternatively for 1 h at RT. Membranes were then washed briefly with TBS-T at RT. The secondary antibody, which is conjugated to horseradish peroxidase (Table A. 5), was diluted in blocking solution (1:5000) and incubated for 1 – 3 h at RT. The membranes were washed 3 x 10 min in TBS-T. To detect the chemiluminescent signal, membranes were briefly incubated in equal amounts of enhanced chemiluminescent solution 1 (2.5 mM Luminol, 40 nM p-coumaric acid, 100 mM Tris/Cl, pH 8.5) and solution 2 (0.02% H_2O_2, 100 mM

Tris/Cl, pH 8.5) or SuperSignal West Femto Chemiluminescent Substrate (Thermo Fisher Scientific, USA). Membranes in a protective sleeve were exposed to CL-Xposure film (Thermo Fisher Scientific, USA) or Amersham Hyperfilm ECL (GE Healthcare, UK) for an appropriate length of time. The film was automatically developed using a table top processor (Konica SRX-101A) with few exceptions of manually development. The Blot Restore Membrane Rejuvination kit (Millipore, UK) was used according to the manufacturer's instructions to allow reprobing of the membrane (see above).

2.3.4. Densitometry analysis of Western blots

Western blot films (2.3.3) were digitalised by scanning on an Epson Perfection V600 Photo Scanner as a 24 bit image and a resolution of 600 dpi. Protein levels were quantified using ImageJ (National Institutes of Health, USA). For this, the Western blot images were inverted and protein bands were selected with a square. The same square surface was selected for every protein band. Band intensity was determined with the 'measure' function. Areas of the film with no protein bands were measured and deducted as background. The resulting data was entered into OriginPro8.6 (MicroCal Inc., USA) to perform a one-way analysis of variance (ANOVA).

2.4. Mammalian cell culture

2.4.1. Cell lines and their maintenance

Mammalian cell lines (Table 2.1) were maintained in Dulbecco's modified Eagle medium (DMEM; Lonza, Switzerland) supplemented with 10% foetal bovine serum (FBS; GIBCO, UK) and 50 U/ml penicillin and streptomycin (Lonza, Switzerland), respectively. Huh7 cell medium was additionally supplemented with 1 x non-essential amino acids (HyClone, USA). All cell lines were typically kept in 75 cm^3 flasks (Sarstedt, Germany) and grown in a CO_2 incubator (Sanyo, USA) at 37°C and 5% CO_2.

All cell culture work was conducted in an Airstream Class II Biological Safety Cabinet (ESCO, UK).

Table 2.1 Mammalian cell lines used in this study.

cell line	organism	cell types and comments
BHK-21	*Mesocricetus auratus* (syrian golden hamster)	fibroblast-like cells derived from kidney tissue
C33A	*Homo sapiens* (human)	epithelial cells, derived from cervical cancer biopsies
CaSki	*Homo sapiens* (human)	cervical epithelial cells from metastatic site: small intestine; epidermoid carcinoma, reported to contain integrated HPV16 (~600 copies per cell) as well as sequences related to HPV18
Cos-7	*Cercopithecus aethiops* (vervet monkey)	kidney fibroblast-like cell line transformed with SV40 T antigen
HaCaT	*Homo sapiens* (human)	*in vitro* spontaneously transformed keratinocytes from histologically normal skin
HEK293T	*Homo sapiens* (human)	epithelial kidney cells expressing the transforming gene of adenovirus 5
HeLa	*Homo sapiens* (human)	epithelial cells from cervical adenocarcinoma, have been reported to contain HPV18 sequences
Huh7	*Homo sapiens* (human)	epithelial-like cells derived from liver carcinoma
Saos-2	*Homo sapiens* (human)	bone tissue of osteosarcoma patient, epithelial morphology
SiHa	*Homo sapiens* (human)	epithelial cells of cervical SCC, reported to contain integrated HPV16 genomes (~1 - 2 copies per cell)
U-2 OS	*Homo sapiens* (human)	bone tissue of osteosarcoma patient, epithelial morphology
Vero	*Cercopithecus aethiops* (vervet monkey)	SV40 T antigen un-transformed kidney cells
3T3 J2	*Homo sapiens* (human)	fibroblasts

2.4.2. Passaging of cell lines

Cells were passaged when the monolayers reached 80% - 90% confluence. For passaging, medium was aspirated off and cells were washed once with sterile phosphate buffered saline (PBS; Oxoid, UK). To detach cells from the culture flask, 1 x TrypLE^{TM} Express (GIBCO, UK) was added and incubated at 37°C, 5% CO_2 until cells were dislodged. TrypLE^{TM} Express was inactivated by addition of 9 ml complete DMEM. If required, cells were counted using a haemocytometer. All cell lines were split in a ratio of 1:10 and 1:5.

2.4.3. Freezing and thawing of cells

Cells were harvested for long term storage from an 80% - 90% confluent flask as described (0). The cell suspension was centrifuged at 420 x relative centrifugal force (RCF), 4°C for 5 min and the supernatant removed. The cell pellet was resuspended in 5 ml freezing medium (10% DMSO in FBS). Aliquots of 1 ml were transferred to cryogenic tubes (Cole-Parmer, UK), which were placed into a Mr. Frosty Cryo 1°C Freezing Container (Nalgene, UK) for stepwise temperature reduction to -80°C. For long-term storage cells were kept at -80°C.

For recovery, the cryogenic tubes were incubated at 37°C until cell suspension was thawed. Cells were transferred into 5 ml of complete DMEM and centrifuged 420 x RCF, 4°C for 5 min. The supernatant was removed and the cell pellet resuspended in 13 ml complete DMEM and transferred to 75 cm^3 flasks. Cells were maintained as described (2.4.1, 2.4.2).

2.4.4. Transient transfections with polyethylenimine

HEK293T cells were seeded into 10 cm cell culture dishes (Corning, USA) at a density of 2 x 10^5 cells/ml and incubated o/n at the afore-mentioned conditions (2.4.1). Plasmid DNA (10 µg) was added to 1 ml of 1 x Opti-MEM I Reduced Serum Medium - with GlutaMAX™ I (GIBCO, UK) in a polysterene round-bottom test tube (BD Falcon, UK). After 5 min incubation at RT, 20 µg of the chemical transfection reagent polyethylenimine (PEI in H_2O, pH 7.4;

Polysciences, UK) (DNA:PEI ration = 1:2) was added and incubated for a further 20 - 40 min at RT. For co-transfections of two plasmids, 10 µg of each plasmid was incubated with 40 µg of PEI in 1 ml 1x Opti-MEM I Reduced Serum Medium. Complete DMEM in culture dishes was replaced with Opti-MEM I Reduced Serum Medium - with GlutaMAX™ I and the DNA-PEI mixture was added dropwise. Cells were incubated for 16h – 24h as described (2.4.1). The expression of enhanced GFP (eGFP)-fusion proteins was confirmed by epifluorescence microscopy (Nikon Eclipse TS 100) before processing the cells.

2.4.5. Transient transfections with Lipofectin

SiHa cells were seeded into 6-well dishes (Sarstedt, Germany) at a density of 1 x 10^5 cells/ml and incubated for 48 h at the afore-mentioned conditions (2.4.1). To transiently transfect, 5 µl of Lipofectin (Invitrogen, USA) were diluted in 100 µl of 1 x Opti-MEM I Reduced Serum Medium and 1 µg of DNA were dispensed separately in 100 µl 1 x Opti-MEM I Reduced Serum Medium. For co-transfections a total of 2 µg of DNA and 10 µl of Lipofectin per well were used. Both mixtures were incubated at RT for 40 min before combining them and incubating for another 20 min at RT. Celle were washed once with PBS and were grown in 1 x Opti-MEM I plus transfection mixture for 16 h before they were harvested for lysis (2.4.8), immuno-fluorescent analysis (2.6) or functional analysis (2.11).

2.4.6. Transfection of siRNA with HiPerFect Transfection reagent

SiHa cells were plated into 6-well dishes at a density of 1 x 10^5 cells/ml and incubated for 48 h. Under RNase free conditions, cells were transfected with 4 FlexiTube siRNA (Table 2.2) (Qiagen, Germany) specifically targeted to YIPF4 and an AllStars negative control siRNA (siRNA NC) (Qiagen, Germany), respectively, as follows: per well of transfection, 300 ng of siRNA and 12 µl HiPerFect transfection reagent (Qiagen, Germany) were dissolved in 100 µl Opti-MEM I Reduced Serum Medium. The transfection mixture was briefly mixed and incubated at RT for 15 min. It was then added to the cells in fresh complete DMEM. Cells were harvested and lysed (2.4.8) at 0 h, 16 h, 24 h, 40

h, 48 h and 72 h post-transfection. Cleared cell lysate was subject to BCA assay (2.3.1) and Western blot analysis (2.3.2, 2.3.3) to determine knock down efficiencies. Cells treated with YIPF4 specific siRNA under the most efficient conditions were analysed by flow cytometry (2.11)

Table 2.2 FlexiTube siRNA specific to YIPF4. The sequences were searched with the BLASTN online tool (NCBI, USA) and unspecific targeting of other cellular proteins was excluded.

name	siRNA sequence	alignment with YIPF4 sequence [bp]
siRNA1	aagcacctggattggtaatta	1301-1321 → NCR
siRNA3	agggtggtctcatggattata	670-690 → CR
siRNA4	aagaattggacattgatctaa	503-523 → CR
siRNA5	taagtggtacttctaaatcat	1842-1862 → NCR

NCR = non-coding region, CR = coding region

2.4.7. Determination of protein half-life using cycloheximide

U-2OS cells were plated into a 6-well dish at a density of 1 x 10^5 cells/ml and incubated under standard conditions (2.4.1) for 24 h. Complete DMEM was supplemented with 100 µg/ml cycloheximide (Sigma, USA) and cells were incubated under afore-mentioned conditions (2.4.1). Cells were harvested at 0 h, 6.5 h, 24 h, 30 h, 48 h and 72 h of cycloheximide treatment and lysed and analysed as described (2.4.8, 2.3).

2.4.8. Harvesting of cells and lysis

Cells in 6-well dishes were harvested by incubation with 0.5 ml 1 x TrypLE^{TM} Express at 37°C after washing with PBS until cells lifted off the dish. To neutralise the 1 x TrypLE^{TM} Express, 1 ml of complete DMEM was added and cell suspension was transferred to a centrifugation tube. Cell pellet was obtained by centrifugation at 400 x g and 4°C and was washed once with PBS before it was used for RNA extraction (2.10.1), functional analysis (2.11) or lysis. To lyse, 100 µl lysis buffer (10 mM Tris/Cl, pH7.5; 150 mM NaCl, 0.5 mM EDTA, 0.5% NP40, 1 x Protease inhibitor cocktail, EDTA-free (Roche,

Switzerland)) was added and incubated on ice for 30 min with frequent, extensive vortexing. Unwanted cell debris was removed by centrifugation at 17000 x g for 15 min at 4ºC. The pellets were discarded.

To lyse cells from a 10 cm dish, medium was aspirated off the cells and washed once with PBS. PBS was replaced by ice-cold lysis buffer and cells were scraped into solution, incubated on ice and cell lysate cleared as described above.

The total protein content of the cleared cell lysates was determined by BCA assay (2.3.1) before it was further analysed by SDS-PAGE (2.3.2) and Western blot analysis (2.3.3).

2.4.9. Vaccinia virus VTF7-3 expression system

2.4.9.1. Recombinant vaccinia virus VTF7-3 stock preparation

BHK-21 cells were plated into 60 mm dishes (Corning, USA) at a density of 5 x 10^5 cells/ml and incubated o/n. A recombinant vaccinia virus stock (VTF7-3 with a T7 RNA polymerase gene), kindly provided by Dr Cheryl Walter, University of Leeds, UK, was diluted in PBS to obtain a multiplicity of infection of 1 when added to the cells. The virus was absorbed during 1 h of incubation with occasional shaking. Two millilitre of minimum essential medium (MEM; Sigma, USA) plus supplements was added and the cells incubated until an extensive cytopathic effect became visible which usually took 3 to 4 days. Cells were transferred to a centrifugation tube and centrifuged at 17000 x g for 5 min. The pellet was resuspended in 2 ml of Tris/Cl, pH 8.8 and snap frozen with liquid nitrogen. To obtain the cell-associated virus, cells were thawed and sonicated for 2 min. The freeze-thaw-sonication cycle was repeated 5 x before cell debris was spun down at 17000 x g for 5 min. Supernatant was saved on ice and pellet was resolved in 0.5 ml Tris/Cl followed by another freeze-thaw-sonication cycle. The cell debris was spun down again and this supernatant combined with the previous supernatant saved on ice and stored at -80˚C until use.

2.4.9.2. Plaque assay for virus titre determination

BHK-21 cells were seeded into a 6-well plate and grown to 80% confluence. Media was removed and 2 ml of MEM plus 10% FBS added containing the following dilutions of the supernatant containing VTF7-3 (2.4.9.1): 5 x 10^{-6}, 5 x 10^{-7} and 5 x 10^{-8}. Cells were incubated for 1 h with frequent gentle shaking and then for further 48 h without shaking. Cells were then stained with 1 x Gentian Violet (1% w/v crystal violet, 4% v/v formaldehyde, 5% v/v ethanol in PBS) for 15 min at RT. After rinsing with H_2O, plaques could be counted and virus titre determined.

2.4.9.3. Infection and transfection of BHK-21 cells for virus mediated protein expression

BHK-21 cells were plated into 60 mm dishes and grown to a confluence of 70% – 90%. To recover the VTF7-3 virus from its -80°C storage, the vials were rapidly thawed at 37°C and sonicated for 2 min. For infection of BHK-21 cells, VTF7-3 virus was diluted in PBS to 5 plaque forming units per cell and added to the cells for a 50 min incubation with gentle shaking every 10 min.

The subsequent transient transfection was carried out with Lipofectin, as described elsewhere (2.4.5). Briefly, 1 ml of 1 x Opti-MEM I Reduced Serum Medium - with GlutaMAX™ I (GIBCO, UK) was dispensed in a polysterene round-bottom test tube (BD Falcon, UK). Twenty-two microliter of Lipofectin (Invitrogen, USA) transfection agent were added and the mixture left at RT. Two to four micrograms of DNA per plasmid were dispensed in a 1.5 ml Eppendorf tube, which was diluted with 500 µl Opti-MEM with GlutaMAX. The DNA was then added to the round-bottom test tubes and incubated for 15 min at RT after shaking gently. The virus was aspirated off and the cells were washed 2 x with 2 ml of Opti-MEM with GlutaMAX. The transfection mixtures from the round-bottom tubes were added to the cells and incubated for 20 h - 24 h. Cells were lysed and analysed as described above (2.4.8, 2.8.2).

2.5. Human foreskin keratinocytes (HFKs)

Primary HFKs (Table 2.3) were obtained from Dr Sally Roberts, University of Birmingham, UK. HFK cell lines stably transfected with the HPV18 genome (WT) and HPV18 genome with a stop codon following the E5 ORF start codon (E5 KO) were prepared by Drs Christopher Wasson and Rebecca Ross, University of Leeds, UK (Table 2.3). The presence of the stop codon was confirmed by sequence analysis (2.2.7).

Table 2.3 Human foreskin keratinocyte cell lines used in this study

name	description
HFK HPV18_1 WT	HFKs of donor 1, transfected with WT HPV18 genome
HFK HPV18_1 E5 KO	HFKs of donor 1, transfected with E5 KO HPV18 genome
HFK HPV18_2 WT	HFKs of donor 2, transfected with WT HPV18 genome
HFK HPV18_2 E5 KO	HFKs of donor 2, transfected with E5 KO HPV18 genome
HFK_3	HFKs of donor 3, untransfected

2.5.1. Maintaining and passaging untransfected HFKs

HFKs were maintained in serum free medium (SFM; GIBCO, UK) supplemented with 25 µg/ml bovine pituitary extract (GIBCO, UK) and 0.2 ng/ml recombinant EGF (GIBCO, UK) whereby the medium was replaced with fresh medium every 2 days. Cells were only grown to a confluence of ≤ 80% in 10 cm dishes. The incubation conditions were the same as described for established cell lines (2.4.1).

To passage, the medium was removed and replaced by PBS-EDTA solution (1% PBS, 0.1% EDTA). After 3 min incubation at 37°C, the PBS-EDTA was removed and replaced by 1 ml Trypsin-EDTA solution (Sigma, USA) which was left to incubate for 5 min - 10 min until cells detached. Trypsin was inhibited by

the addition of SFM supplemented with 1% Trypsin inhibitor (GIBCO, UK). HFKs were transferred to a falcon tube and centrifuged at 538 x g for 5 min at 4°C. The pellet was resuspended in SFM, cells were counted on a haemocytometer and re-seeded at a density of 2 x 10^5 cells per dish.

2.5.2. Maintaining and passaging HFKs with HPV18 genomes

The HFK HPV18 cell lines of both donors (Table 2.3) were maintained in 10 cm dishes with 3T3 J2 fibroblasts as feeder cells in E-medium (see below) supplemented with 2 mM L-glutamine (Lonza, Switzerland) and 5 ng/ml EGF (BD Biosciences, UK).

3T3 J2 fibroblasts were pre-treated with 8 µg/ml mitomycin-C (Roche, Switzerland) in DMEM for 2 h - 4 h and 2 x 10^6 cells were seeded in E-medium in 10 cm dishes 24 h prior to addition of transfected HFKs.

HFKs containing the HPV18 WT and HPV18 E5 KO genomes were passaged as described (2.5.1) and seeded into the dishes containing the mitomycin-C treated 3T3 J2 fibroblasts.

One litre of E-medium was prepared as follows: 600 ml of DMEM Hepes (Sigma, USA) were mixed with 320 ml Hams-F-12 (GIBCO, UK), 20 ml Penicillin/Streptomycin (GIBCO, UK), 5% FBS, 10 µg Cholera Toxin (Sigma, USA), 1 x hydrocortisone (Sigma, USA) and 1 x cocktail. One-hundred millilitre of 100 x cocktail was prepared by mixing 10 ml of 0.18 M Adenine (Sigma, USA), 10 ml of 5 mg/ml Insulin (Invitrogen, USA), 10 ml 5 mg/ml transferin (Sigma, USA), 10 ml 2 x 10-8 M 3,3`,5-Triiodo-L-thyronine (T3) (Sigma, USA) in PBS. The cocktail was filter-sterilised before use.

2.5.3. Methylcellulose differentiation of HFKs

Differentiation of HFKs and HFK HPV18 cell lines (Table 2.3) was induced by growing in a methylcellulose (MC) matrix according to the method described by Wilson and Laimins (Wilson and Laimins, 2005). Cells were grown in a 10 cm cell culture dish as described (2.5.1, 2.5.2) until 80% confluent. As in passaging, cells were lifted off the dish and the medium was removed by centrifugation.

One millilitre of E-medium (no EGF) was added to resuspend the cells. The cells from one dish were frozen at -80°C at this point to obtain the 0 h time point of differentiation The remaining cell suspensions were homogeneously mixed with 25 ml of MC matrix (1.5% w/v MC (Sigma, USA), 5% FBS in E-medium) in a 10 cm dish. The cultures were then incubated as described (2.4.1)
Further time points for differentiation were collected at 48 h and 72 h. Semisolid medium containing differentiated cells were transferred to Falcon tubes and diluted with ice-cold PBS. Cells were spun down by centrifugation at 537 x g for 10 min at 4 °C. The medium was discarded and the cell pellet washed three more times with ice-cold PBS. The cell pellet was stored at -80°C.

2.5.4. Cell lysis of differentiated HFKs

Cell pellets (2.5.3) were thawed on ice and resuspended in 500 µl lysis buffer (8 M Urea, 2 mM phenylmethanesulfonylfluoride (PMSF), 10% 2-mercaptoethanol). Cells were lysed mechanically by forcing through a syringe (gauge 19 needle, 1.5'') 5 times. Cell debris was removed by centrifugation at 17000 x g for 20 min at 4°C. The supernatant was taken forward for Western blot analysis (2.3.3, 2.3.4).

2.5.5. RNA extraction from differentiated HFKs

The cell pellets (2.5.3) were resuspended in 7.2 ml Trizol (GIBCO, UK) and incubated for 5 min at RT. Chloroform (1.4 ml) (Invitrogen, USA) was added and the mixture was shaken for 15 sec followed by incubation at RT for 3 min. Phase separation was achieved by centrifuging the samples at 12000 x g for 15 min at 4°C. The aqueous phase was transferred to a fresh tube and the RNA precipitated by adding 3.6 ml isopropanol. After inversion, samples were incubated for 10 min at RT. The RNA was precipitated by centrifugation at 12000 x g for 10 min at 4°C. The RNA was washed with 75% ethanol. The pellet was air-dried and resuspended in 50 µl TE (10 mM Tris/Cl, pH 8; 1 mM EDTA, pH 8.0) which was resolved by incubation at 55°C - 60°C for 10 min. The amount and quality of RNA samples was examined by spectrophotometry (2.1.4.2).

2.5.6. Organotypic raft cultures

Organotypic raft cultures of HFK HPV18 cell lines (Table 2.3) were prepared according to the protocol by Wilson and Laimins (Wilson and Laimins, 2005). Briefly, keratinocytes were grown on a matrix of 8 mg/ml rat tail collagen (BD Biosciences, UK) and 2 x 10^6 3T3 J2 fibroblasts in E-medium supplemented with 2 mM L-glutamine and 5 ng/ml EGF. After 4 days, the matrix and keratinocytes were transferred onto a sterile wire mesh. An air-liquid interface was created by addition of E-medium without EGF. The organotypic raft cultures were grown for 13 days at 37°C and 5% CO_2 with media changes every other day. Rafts were fixed by flooding in 4% paraformaldehyde (PFA; 4% PFA in PBS, pH 7.4). Rafts were embedded in paraffin and sectioned into 5 µm slices by Propath, UK. Haematoxylin and eosin (H&E) staining of the sections was also carried out by Propath, UK. Raft cultures were prepared and H&E samples imaged by Dr Christopher Wasson, University of Leeds, UK.

2.5.7. Immuno-histochemistry

Paraffin embedded organotypic raft cultures slices (2.5.6) or CIN1 and CIN3 pathological sections (kindly provided by Prof Sheila Graham, University of Glasgow, UK) were stained as follows. Paraffin was removed by submersing in 100% Xylene (BDH, UK) for 3 x 5 min. Rehydration of samples occurred by serial incubation for 1 min each in 100% ethanol, 90% ethanol and 70% ethanol followed by 5 min incubation in H_2O. Antigens were retrieved by 15 min boiling in sodium citrate buffer (10 mM Tri-sodium citrate, pH 6; 0.05% Tween-20). After cooling, samples were washed in H_2O followed by blocking in 10% normal goat serum (NGS) in PBS for 1 h at RT. In a humidity chamber, the primary antibody (Table A. 4) was incubated for 1 h at RT in 1.5% NGS buffer. Slides were washed 5 x in PBS prior to incubation with AlexaFluor labelled secondary antibody (Table A. 6) for 1 h in 1.5% NGS buffer. Unbound antibodies were removed by further washing and the samples mounted using ProLong Gold Antifade Reagent with 4',6-diamidino-2-phenylindole (DAPI) (Molecular Probes, UK) or UltraCruz™ Hard-set Mounting Medium (SantaCruz, UK). Edges were sealed with nail varnish and slides stored at 4°C until viewing (2.6.4).

2.5.8. Fluorescent intensity profiles

Fluorescent intensity profiles across the height of the stained organotypic raft culture sections (2.5.7) were generated with ImageJ using the 'Plot Profile' function. Plot values were exported into Microsoft excel to generate plots with trendlines of the 'moving average' type and a period of 15.

2.6. Immuno-cytochemistry

2.6.1. Growing cells on coverslips

Immuno-cytochemical staining was conducted in 12-well dishes (PAA, UK). Huh7 and SiHa cells, respectively, were seeded into the wells containing circular cover slips (No 1.5; Appleton Woods, UK) at a density of 1 x 10^5 cells/ml. Cells were taken forward for staining (2.6.2, 2.6.3) when approximately 70% confluent.

2.6.2. Fixation of cells

The medium was aspirated off the cells followed by one wash with PBS. Cells were then fixed by incubation with 4% PFA in PBS, pH 7 – 7.5 at RT for 10 min. Cells were washed again in PBS and stored at 4°C for short periods of time until use.

2.6.3. Immuno-labelling

Fixed cells were permeabilised with Triton X-100 (0.1% Triton X-100 in PBS) or 0.5% Saponin (AlfaAesar, USA) for 10 min at RT. In case of Saponin permeabilisation, 0.5% Saponin was maintained throughout the staining procedure in the blocking and antibody buffers as well as the wash buffer (0.5% Saponin in PBS). Coverslips were incubated in blocking buffer (0.2% gelatine, 10% NGS in PBS) for 15 min at RT. After a washing step in PBS, the primary antibody (Table A. 4) was diluted in antibody solution (0.2% gelatine in PBS) and incubated for 1 h at RT or at 4°C o/n. Followed by 4 washing steps with

PBS, the secondary antibody (Table A. 6) was diluted in antibody solution and incubated for 1.5 h at RT. After a final 4 washing steps, the coverslips were mounted onto glass slides (0.8 - 1.0 mm thick: VWR, USA) using the mounting agent ProLong Gold Antifade Reagent with DAPI (Molecular Probes, UK) or UltraCruz™ Hard-set Mounting Medium (SantaCruz, UK). When co-staining, the primary and secondary antibody incubations were repeated after the last washing step before mounting the coverslips. Edges of coverslips were sealed with nail varnish and slides were stored at 4°C until viewing. Analysis of co-localisation of two proteins was conducted with the 'Pearson–Spearman correlation co-localisation' (PSC) plug-in (2.7.4) for ImageJ.

2.6.4. Microscopy

Samples were imaged with a Zeiss laser scanning confocal microscope (510-META and 700; Zeiss, Germany) under an oil-immersion 63 x objective lens (NA = 1.40). Pinholes were adjusting for each channel to yield equal optical sections. The LSM700 operates a 405 nm, 488 nm, 555 nm and 639 nm laser, which allowed for 4 colour observations. Representative images were processed using the Zen 2011 software (Zeiss, Germany).

2.7. Differential, detergent permeabilisation assay

2.7.1. Transfection of Huh7 cells on coverslips

Huh7 cells were seeded into 12-well plates containing circular cover slips at a density of 7 x 10^4 cells/ml and incubated o/n as described (2.4.1). Lipofectin (Invitrogen, USA) transfection was conducted as described (2.4.5). Briefly, 1 µg DNA was added to 50 µl Opti-MEM I Reduced Serum Medium - with GlutaMAX™ I. Also, 5 µl Lipofectin (Invitrogen, USA) was added to another aliquot of 50 µl Opti-MEM I Reduced Serum Medium - with GlutaMAX™ I. The DNA containing medium was added to the Lipofectin containing medium and incubated for 40 min at RT. Complete DMEM was replaced with fresh complete DMEM. Transfection mixture (DNA:Lipofectin ration = 1:5) was added to the cell dropwise and incubated o/n as described (2.4.1). The DMEM was replaced with

complete DMEM containing 10 µM of the proteasome inhibitor MG132 (Calbiochem, UK). After incubation for up to 6 h, cells were fixed (2.6.2) and immuno-labelled under selective permeabilisation (2.7.2).

2.7.2. Immuno-labelling under selective permeabilisation

Cells were completely permeabilised with Triton X-100 and selectively permeabilised with Digitonin, respectively. In cells completely permeabilised, co-staining with FLAG (EnoGene, UK) and haemagglutinin (HA) (Sigma, USA) antibodies was conducted as described above (2.6.3). When selectively permeabilising the plasma membrane, cells were incubated with 5 µg/ml Digitonin in PBS (Cayman Chemical, USA), which was maintained in the blocking buffer, washing buffer and antibody solutions. In addition, samples were subject to control staining with no detergent present.

2.7.3. Microscopy of selectively permeabilised samples

Samples were imaged as described (2.6.4). Gain settings were set up for the Triton X-100 permeabilised samples for each sample and then maintained for the Digitonin permeabilised and control cells.

2.7.4. Quantification of co-localisation and statistical analysis

Quantification of co-localisation of FLAG and HA staining was conducted using the PSC ImageJ plug-in (French et al., 2008). The threshold was set to 25. A macro was written to standardise the analysis process (6.1).

To determine the co-localisation of the two protein tags or two proteins in a specific area of the cell, a blue mask was applied that selected the area to investigate and excluded the remaining pixels from the analysis.

The Pearson correlation coefficients (PCC values) were transferred into the data analysis software OriginPro8.6 (MicroCal Inc., USA) to perform a one-way ANOVA. The significance level was set to 0.05 and 0.01 respectively. The Tukey means comparison method and the Levene test for equal variances were applied.

2.8. Subcellular fractionations

2.8.1. Crude fractionation

HEK293T cells were separated into a nuclear and a cytoplasmic fraction. For this, cell pellets were lysed in 200 µl cytoplasmic lysis buffer (20 mM Tris/Cl, pH 7.4; 100 mM NaCl, 5 mM $MgCl_2$, 0.5% NP40, 1 x Protease inhibitor cocktail) by incubation on ice for 30 min with frequent vortexing. Cell nuclei were removed by centrifugation at 9600 x g for 20 min at 4°C. The supernatant accounted for the cytoplasmic fraction. The pellet was washed twice in cytoplasmic lysis buffer before resuspending in 200 µl radioimmuno-precipitation assay buffer (50 mM Tris/Cl, pH 7.5; 150 mM NaCl; 1% NP40; 0.5% w/v sodium deoxycholate; 0.1% SDS, 1 x Protease inhibitor cocktail). Debris was removed by centrifugation at 96000 x g for 10 min at 4°C. The supernatant accounted for the nuclear fraction. Both fractions were subject to Western blot analysis (2.3.3). An antibody against Lamin B1 (Table A. 4) was used to identify the nuclear fraction while an antibody against glyceraldehyde 3-phosphate dehydrogenase (GAPDH) (Table A. 4) was used as a marker for the cytoplasmic fraction.

2.8.2. Membrane fractionation

HEK293T cells expressing GFP-YIPF4 fusion protein (2.4.4) and BHK-21 cells expressing full-length FLAG-YIPF4-HA V244 and truncation mutants (2.4.9.3) were scraped into 1 ml of buffer M1 (10 mM PIPES, pH 7.4; 0.5 mM $MgCl_2$; 1 x Protease Inhibitor Cocktail (Roche, Switzerland)) and lysed by sonication (Grant Ultrasonic bath XUBA1; Thermo Fisher Scientific, USA). Salt concentrations were adjusted by adding 250 µl of buffer M2 (10 mM PIPES, pH 7.4; 600 mM KCl; 150 mM NaCl; 22.5 mM $MgCl_2$). Samples were centrifuged at 3000 x g for 10 min at 4°C to remove cell nuclei and unbroken cells. The supernatant was subject to ultra-centrifugation at 100000 x g for 10 min at 4°C to pellet the membranous fraction. The pellet was washed once in adjusted buffer M1 and resuspended in 2 x LDS sample buffer (Invitrogen, USA) plus 0.1% 2-mercaptoethanol. The supernatant depicting the soluble fraction was subject to o/n acetone precipitation at -20°C. After washing the pelleted soluble fraction

once in 70% ethanol, these samples were also resuspended in 2 x LDS sample buffer plus 01% 2-mercaptoethanol. Both fractions were examined by Western blot analysis (2.3.2, 2.3.3). An antibody against GAPDH (Table A. 4) identified the soluble fraction, while an antibody against *trans-Golgi* network integral membrane protein 2 (TGN46) (Table A. 4) or against human transferrin receptor (TfR) (Table A. 4) served as marker for the membranous fraction.

2.9. Immuno-precipitation

Co-IPs of epitope/GFP-tagged overexpressed proteins and endogenous YIPF4, respectively, were performed using dynabeads protein G (Invitrogen, USA). HEK293T cells in 10 cm cell culture dishes were transfected (2.4.4) and lysed (2.4.8) as described. Total protein concentration was determined (2.3.1) and the concentrations adjusted to the sample with the lowest concentration using binding buffer (50 mM Tris/Cl, pH 7.4; 100 mM KCl, 0.1 mM EDTA, 0.2% NP40, 0.1% BSA, 2.5% Glycerol, 2 mM dithiothreitol (DTT), 1 x Protease inhibitor cocktail, EDTA-free (Roche, Switzerland)). Magnetic dynabeads protein G slurry (15 µl) was equilibrated with binding buffer and was then incubated with 2 µl – 2.5 µl of respective antibody (α-FLAG, α-GFP, α-YIPF4; Table A. 4) and a 1:1 mixture of adjusted cell lysate and binding buffer for 1 h at RT. After 4 washes with wash buffer (100 mM Tris/Cl, pH 7.4; 100 mM NaCl, 0.5% NP40, 2 mM DTT, 1 x Protease inhibitor cocktail, EDTA-free (Roche, Switzerland)) beads were transferred to a fresh tube. Proteins were eluted by boiling for 10 min in 35 µl of 2 x LDS sample buffer (Invitrogen, USA) plus 0.1% 2-mercaptoethanol. Eluates were examined by Western blot analysis (2.3.2, 2.3.3).

2.10. Quantitative Real-time PCR

2.10.1. RNA extraction

Total RNA was extracted from cell pellets (2.4.8) using the Quick-RNA™ MiniPrep (Zymo Research, USA) and RNeasy Plus Mini Kit (Qiagen, Germany) according to the manufacturers protocols. RNA from HFK cell lines were extracted as described (2.5.5). The RNA yield was determined using a Nanodrop spectrophotometer (Thermo Fisher Scientific, USA).

2.10.2. Reverse transcription

Five hundred nanogramme of total RNA (2.10.1) was reverse transcribed (RT) into complementary DNA (cDNA) using the RevertAid First Strand cDNA Synthesis Kit (Thermo Fisher Scientific, UK) according to the manufactures protocol. Briefly, 500 ng of RNA (2.10.1) was pre-incubated with 0.5 µg oligo $(dT)_{18}$ primers for 5 min at 65°C. Reaction buffer, 20 units RiboLock RNase Inhibitor, 1 mM dNTP mix and 40 units M-MuLV Reverse Transcriptase were added and the reverse transcription performed for 60 min at 37°C. The reaction was terminated by heating to 70°C for 5 min.

2.10.3. Quantitative Real-time PCR

The quantitative real-time PCR (qPCR) reaction was conducted using the QuantiFast® SYBR® Green PCR kit (Qiagen, Germany) and a Corbett Rotor-Gene 6000 (Qiagen, Germany). Briefly, 2.5 µl of RT-reaction mix (2.10.2) (equals 62.5 ng of cDNA) and 1 µM of each forward and reverse primer (Table 2.4) were added to the 2 x QuantiFast SYBR Green PCR Master Mix. The PCR reaction was conducted as follows: initial activation step for 5 min at 95°C and a two-step cycle of denaturation (10 sec at 95°C) and combined annealing and extension (30 sec at 60°C) which was repeated 40 times. A melting curve from 60°C – 95°C with 5 sec at every 1°C interval was performed at the end of the last cycle.

Table 2.4 Primers used for qPCR analysis

primers	fwd 5' – 3'	rev 5' – 3'
YIPF4	AGATCTCAGTGGTTCAATAGCATC	TCCAAGAGTGGCTTGTTATC
cyclin A	CTGGCTGGTGGAGGTTGGG (Müller et al., 1999)	CCCTCTCAGAACAGACATACA
HPV18 E7	GACCTAAGGCAACATTGCA	GCTCGTGACATAGAAGGTCAA
U6	CTCGCTTCGGCAGCACA	GCAAATTCGTGAAGCGTT

HPV18 E7 primers were kindly provided by Dr Christopher Wasson and U6 primers were kindly provided by Rosella Doble, University of Leeds, UK. The YIPF4 qPCR primers amplify the bp 78 – 236 of the YIPF4 cDNA sequence (NCBI Reference Sequence: NM_032312.3). fwd = forward, rev = reverse.

2.10.4. Analysis of q-PCR results

The data obtained (2.10.3) was analysed according to the $\Delta\Delta$ C_t method (Livak and Schmittgen, 2001) using the Rotor-Gene 6000 software. U6 served as normaliser gene.

2.10.5. Determination of q-PCR primer efficiency

The efficiency of primer pairs was determined by qPCR as described (2.10.3) using 1 µM of each primer (Table 2.4) and a dilution series of cDNA (62.5 ng, 6.25 ng, 0.625 ng 0.0625 ng). The primer pair efficiencies (Table 2.5) were calculated using the 'quantitation analysis' function of the Rotor-Gene6000 software.

Table 2.5 Efficiencies for the qPCR primers used in this study

primers	efficiency
YIPF4	1.13
cyclin A	0.99
HPV18 E7	1.09
U6	1.26

The efficiency of the U6 primer pair was determined by Rosella Doble, University of Leeds, UK.

2.11. FACS assays for determination of cell surface HLA class I expression

2.11.1. Transfection of SiHa cells with siRNA

SiHa cells were plated into 6-well dishes at a density of 1 x 10^5 cells/ml and grown under normal conditions (2.4.1) for 48 h. Effective YIPF4 specific siRNA4 (Table 2.2) and siRNA NC, respectively, were transfected with HiPerFect Transfection reagent as described (2.4.6) using 300 ng siRNA per well. Two wells were transfected per siRNA. SiHa cells were harvested 40 h post-transfection (2.4.8). The cells were counted using a haemocytometer and the cell number was adjusted to 15 x 10^5 cells/sample for staining with HLA class I antibody (2.11.4).

2.11.2. Transfection of SiHa cells with GFP fusion-protein encoding plasmids

SiHa cells were plated and grown as above (2.11.1). The transfections were performed with Lipofectin as described (2.4.5) using 1 µg of peGFP-C1, peGFP-16E5 and peGFP-US6 (kindly provided by Dr Eric Hewitt, University of Leeds, UK), respectively. Four wells were transfected per constructs. Sixteen hours post-transfection cells were harvested (2.4.8) and the cell number was determined using a haemocytometer. Total cell number was adjusted to approximately 22 x 10^5 cells/sample for staining with HLA class I antibody (2.11.4).

2.11.3. Co-transfection of SiHa cells with GFP fusion-protein constructs and HLA-A201

SiHa cells were prepared for Lipofectin mediated transfection as described (2.11.2). Cells were transfected with a total of 2.1 µg DNA/well and 10.5 µl Lipofectin/well. The ration of peGFP-C1 and peGFP-16E5, respectively, to pcDNA3.1(-)Pac-HLA-A201 (kindly provided by Dr Eric Hewitt, University of Leeds, UK) was 1:2 (700ng peGFP-C1/peGFP-16E5 : 1400 ng pcDNA3.1(-

)Pac-HLA-A201). A control sample transfected with 700 ng peGFP-C1 and 3.5 µl Lipofectin was included. Cells were harvested 16 h post-transfection and the cell number was determined and adjusted to a total cell number of 22 x 10^5 cells/sample. Cells were stained according to the protocol described (2.11.4), however, using the HLA-A201 type specific antibody clone BB7.2 (1:100; Biolegend, USA).

2.11.4. Staining live cells with HLA class I antibody for flow cytometry analysis

All subsequent treatment was carried out on ice, with ice-cold buffers and in a cooled centrifuge. All incubation steps were carried out on a tube roller at 4°C. Samples with adjusted total cell number (2.11.1, 2.11.2, 2.11.3) were centrifuged at 400 x g for 5 min and the cell pellet was washed in PBS. Blocking was performed by incubating cells in blocking buffer (10% NGS in PBS) for 1 h. The blocking buffer was replaced with antibody solution (1.5% NGS in PBS) with HLA class I antibody (W6/32; 1:100; Abcam, UK). After 1 h incubation, cells were washed once in PBS before incubating with antibody solution and secondary Alexa Fluor® 647 goat anti-mouse immunoglobulin G (IgG) antibody (1:500, Invitrogen, USA; kindly provided by Prof G. Eric Blair) for 1 h. Samples were washed three times in PBS and eventually resuspended in 350 µl PBS. A viability marker, propidium iodide (PI; Invitrogen, USA) was added to a final concentration of 2.4 µg/ml 5 min before analysis on the flow cytometer (2.11.5).

2.11.5. Flow cytometer analysis of HLA class I cell surface expression

Samples were analysed on an LSRFortessa (BD Biosciences, USA) flow cytometer using the accompanied software (FACSDiva Version 6.2). All cell populations were gated to contain live cells only by excluding PI positive cells.
The cells surface HLA class I expression of cells transfected with YIPF4 specific siRNA4 (2.11.1) was determined for 100 000 live cells per sample and was repeated three times.

The HLA class I cell surface levels of SiHa cell expressing GFP, GFP-16E5 and GFP-US6 (2.11.2) was determined for 500 000 live cells which were sequentially gated to include GFP expressing cells only. The experiment was repeated three times, once in triplicate and twice in duplicate.

SiHa cell samples co-expressing GFP, GFP-16E5 and HLA-A201 (2.11.3) were gated to include 10 000 live and GFP positive cells for analysis of cell surface HLA-A201 class I expression. The experiment was conducted three times in duplicate.

For each sample, the mean fluorescence of the HLA/HLA-A201 class I detecting channel was determined using the FACSDiva software. The mean fluorescence values were compared by one-way ANOVA using OriginPro8.6 software. Histograms of fluorescence intensity in HLA/HLA-A201 class I detecting channel versus cell count were compiled with FlowJo software version 7.6.4 (TreeStar, USA) expressing the cell count as percentage of maximum cell count (= relative cell number).

2.12. Label free quantification of YIPF4 binding partners

2.12.1. Co-IPs using the GFP-Trap® system

Co-IPs for label free quantification (LFQ) of GFP-YIPF4 binding partners were performed with the GFP-Trap system (Chromotek, Germany) according to the manufacturer's protocol. To avoid contamination of samples with keratin, all buffers used were prepared freshly and filter sterilised. All steps of the Co-IP protocol were conducted in an Airstream Class II Biological Safety Cabinet (ESCO, UK). Briefly, GFP-YIPF4 and GFP (control) were overexpressed in HEK293T cells (2.4.4). Sixteen hours post-transfection, GFP-YIPF4 expressing cells were treated with 10 µM MG132 for 4.5 hours. All cells were then lysed and total protein concentration determined and adjusted as described (2.3.1, 2.4.8). Fifty microliters of GFP-Trap beads slurry per sample were equilibrated with dilution buffer (10 mM Tris/Cl, pH 7.5; 150 mM NaCl, 0.5 mM EDTA, 1 x Protease inhibitor cocktail, EDTA-free (Roche, Switzerland)). One millilitre of adjusted protein sample was diluted with the same amount of dilution buffer and the o/n incubation was carried out at 4ºC with end-over-end rotation. The samples were washed once in ice-cold dilution buffer and once in ice-cold wash buffer (10 mM Tris/Cl pH7.5; 500 mM NaCl; 0.5 mM EDTA). Proteins were eluted in 100 µl elution buffer (50 mM Tris/Cl, pH 8.8; 0.1% SDS, 1% DTT) by heating to 70°C for 10 min. Eluate was transferred to a fresh tube and send for LFQ to Dr Tobias Lamkemeyer, CECAD, Cologne, Germany (2.12.2, 2.12.3, 2.12.4). An aliquot of the samples was analysed by Western blot for presence of GFP-YIPF4 and GFP.

For a second attempt to determine the YIPF4 interactome, the transfected HEK293T cells were subject to crude subcellular fractionation (2.8.1) before Co-IP and LFQ.

2.12.2. Tryptic in-solution digest

Immuno-precipitated proteins (2.12.1) were digested with Lys-C followed by trypsin according to the filter aided sample preparation method developed by Wisniewski and colleagues (Wisniewski et al., 2009). Ten kilo dalton filters were

used. Peptides were desalted with stop-and-go-extraction tips according to the method by Rappsilber and colleagues (Rappsilber et al., 2007). Eluted peptides were concentrated by vacuum-centrifugation and diluted to a volume of 10.0 µl with 0.5% acetic acid.

2.12.3. Nano-liquid chromatography electrospray ionisation tandem mass spectrometry (nano-LC ESI-MS/MS)

Sample analysis was performed on a LTQ Orbitrap Discovery mass spectrometer (Thermo Fisher Scientific, USA) coupled to an EASY-nLC II nano-LC system (Proxeon/ Thermo Fisher Scientific, USA). Four microliter of each sample were separated on a C18 reversed phase column (length: 15 cm, internal diameter: 75 µm, Proxeon/ Thermo Fisher Scientific, USA) for 120 min (10% - 40% acetonitrile) at a flow rate of 250 nl/min (buffer A: 0.1% formic acid in H_2O; buffer B: 0.1% formic acid in acetonitrile). Masses of intact peptides were detected in the Orbitrap at 30,000 resolution in the mass-to-charge (m/z) range 350–2000 using m/z 445.12003 as a lock mass. Up to 10 CID spectra were acquired in the linear ion trap following each full scan.

2.12.4. Protein identification and label free quantification

Data obtained from the nano-LC ESI-MS/MS were analyzed using the Progenesis LC-MS software (version 4.0, Nonlinear Dynamics, UK). Raw data files were imported in profile mode and automatically aligned resulting in 194 vectors. To increase alignment quality, 87 vectors were added manually. Raw abundances of features were normalized using the “normalise to all proteins” function (factor 0.98). All peptide features with 2 - 4 charges (z = 2 - 4) and MS/MS data were used for quantitation and identification. Peak-list files containing MS/MS spectra were created and subsequently used for database search using an in-house Mascot server (version 2.2, Matrixscience, London, U.K., Perkins et al., 1999) and the UniProt database of *Homo sapiens*. The following search parameters were applied: trypsin as proteolytic enzyme, up to two missed cleavages, carbamidomethylation at cysteine residues was set as fixed modification and oxidation at methionine as a variable modification.

Peptide mass tolerance was 10‰ for intact peptide masses detected in the Orbitrap and 0.8 Da for fragment ions in the linear ion trap.

The lists of identified peptides were treated to achieve a false positive rate of 4%. Peptides were then filtered for mass error of ≤ 5‰ and sequence length of at least 6 amino acid residues. Entries containing the description “keratin” were removed. Protein quantitation was performed on all peptides as well as only on non-conflicting peptides. In addition, peptides were filtered for highest mean in the test condition and a fold change of ≥ 1.5.

The list of UniProt protein IDs was analysed for molecular functions and biological processes using the PANTHER classification system (Mi et al., 2013). Results were illustrated in pie charts with Microsoft excel.

Chapter 3. Exploration of the basic properties of YIPF4

3.1. Introduction

3.1.1. Expression profile of YIPF4

Despite identification a decade ago as a member of the YIP1 family of proteins, YIPF4 has received little scrutiny (Shakoori et al., 2003). Thus, we hold very little experimental evidence of the properties and functions of this protein. The YIPF4 gene region is located on chromosome 2 in humans (bp 32,502,979 - 32,537,002 = 34,024 bp), but no promoter region or transcription factors responsible for expressional regulations are identified to date. Northern blot analysis identified two splicing variants of YIPF4 mRNA (Shakoori et al., 2003) most likely corresponding to the 1982 bp mRNA (NCBI ref. NM_032312.3) and 1390 bp mRNA (NCBI ref. XM_005264600.1) entered into the NCBI database. Automated computational analysis predicts a third splicing variant of 1760 bp (NCBI ref. XM_005264599.1). However, only one YIPF4 protein of 244 amino acids and 27 kDa was identified with an antibody raised against the recombinant full-length YIPF4 protein (Tanimoto et al., 2011, Yoshida et al., 2008). Large scale mass spectrometry analysis suggests the phosphorylation of tyrosines at positions 10 and 60 and the ubiquitination of lysines at positions 47 and 91 (Hornbeck et al., 2004). Others did not observe any major post-translational modifications of YIPF4 (Tanimoto et al., 2011) and further research is needed to resolve this seeming contradiction.

Northern blot analysis showed that YIPF4 mRNA of the two splicing variants is expressed in all human tissues tested (heart, brain, placenta, lung, liver, skeletal muscle, kidney, pancreas, spleen, thymus, prostate, testis, ovary, small intestine, colon, peripheral blood leukocyte) (Shakoori et al., 2003). In addition, human YIPF4 mRNA was part of several large-scale microarray projects that confirmed expression in a multitude of normal and diseased human tissues (MGC, 2004, Ohira et al., 2003, Ota et al., 2004) (uploaded at http://biogps.org/).

Contrary to the large-scale YIPF4 mRNA expression data, little is known about the expression of YIPF4 protein. YIPF4 protein was detected in HeLa cells in addition to normal rat kidney cells and rat liver Golgi lysates with a specific antibody (Tanimoto et al., 2011). The expression in HeLa cells provides some evidence that YIPF4 protein is present in cells infected with HPV. No further evidence is available on the expression of YIPF4 protein in HPV susceptible and permissive cells or in pathological sections of HPV infected sites. The expression profile of YIPF4 protein in differentiating cells is also unknown.

The subcellular localisation of YIPF4 protein is firmly established in HeLa cells (Tanimoto et al., 2011). Co-localisation with the *cis*-Golgi marker Golgi matrix protein 130 (GM130) in immuno-fluorescence microscopy and density gradient centrifugation in addition to immuno-electron microscopy analysis demonstrated its localisation to the *cis*-Golgi. YIPF4 is thought to be involved in maintenance of the Golgi structure since siRNA knock down of YIPF4 causes fragmentation of the Golgi (Tanimoto et al., 2011).

3.1.2. Topology of YIPF4

The topology of YIPF4 was never formally investigated but its membrane topology was predicted from the physiochemical properties of its amino acids (Shakoori et al., 2003). Further clues towards the topology can theoretically be derived from homologue YIP1 family members.

When the YIP1 family members were first identified in humans (Shakoori et al., 2003) they were predicted to be ‘five-pass trans-membrane proteins localising to the Golgi and ER’ (FinGERs) with YIPF4 being family member 4. The predictions were made with the online tool SOSUI which is based on the Kyte and Doolittle hydropathy index (Kyte and Doolittle, 1982), amino acid charges, amino acid amphiphilicity and the length of the protein sequence (Hirokawa et al., 1998). It is highly accurate (>99%) in predicting whether a protein is a membrane or soluble protein and in predicting the number of trans-membrane helices (accuracy ~97%). In this 5 TMD model, the hydrophilic N-terminus is exposed to the cytosol and the hydrophobic C-terminus is buried within the

membrane in accordance with the YIP1 family characteristics (1.8). This orientation was experimentally confirmed for the human YIP1 family members YIPF1, YIPF2 and YIPF3 in an immuno-fluorescence microscopy approach (Shakoori et al., 2003). The topology model of YIPF4 entered in the UniProt database (ID: Q9BSR8) is based on the application of several predictive tools (Eisenberg et al., 1984, Jones, 2007, Käll et al., 2004, Krogh et al., 2001) and is almost identical to the SOSUI tool generated model (Shakoori et al., 2003).

Another way of approaching YIPF4 membrane topology is by deriving it from better-studied homologues. The yeast homologue Yip1p, founder of the Yip1 domain family, was first identified by Yang and colleagues in 1998 (Yang et al., 1998) and is therefore amongst the better-studied proteins of this family (1.8.2.1). It is thought to have three TMD (Yang et al., 1998) although this topology model is also purely based on computational predictions. The UniProt database entry of Yip1p (ID: P53039) favours a 5 TMD model based on a consensus model of the predictive tools mentioned above. These contradictory models underline the fact that no experimental data is available on the TMDs of YIP1 family members which illustrates the urgent need for experimental examination.

The aim of this chapter is to explore some essential properties of YIPF4 to form a basis for further research on this protein. The expression of YIPF4 protein and mRNA in cell lines relevant to HPV research is examined as well as the presence of YIPF4 protein in organotypic raft cultures and pathological sections of HPV induced cervical lesions. Its subcellular localisation is investigated and its predicted 5 TMD topology sought to be experimentally verified

3.2. Results

3.2.1. YIPF4 was expressed in various established cell lines

In order to investigate YIPF4 protein expression in various established cell lines of the cervix (CaSki, SiHa, HeLa, C33A), skin (HaCaT), kidney (HEK293T (human), Vero (monkey), Cos-7 (monkey), BHK-21 (hamster)), liver (Huh7) and bone tissue (U-2 OS, Saos-2), cell pellets were lysed and total protein separated by SDS-PAGE. The corresponding Western blots were probed with a commercial YIPF4 antibody. It confirmed the presence of YIPF4 in every sample by showing a clear band at the expected size of approximately 27 kDa (Figure 3.1A). Overexpressed, myc epitope tagged YIPF4 in HEK293T cells (lane 6) was successfully detected with the YIPF4 antibody confirming that the detected protein is YIPF4. It showed an additional higher order oligomeric form, which according to its size (approximately 58 kDa), corresponds to a YIPF4 dimer. The endogenous YIPF4 was hardly detectable in this sample.
Three different passages per cell lines were examined on Western blots and densitometry analysis was performed with ImageJ (Figure 3.1B). The relative YIPF4 protein amounts were determined by calculating the ratio of YIPF4 band intensities to the loading control tubulin (Figure 3.1B). Overall, the relative amount of YIPF4 did not vary significantly between the human cell lines tested (mean values between 0.2 – 5.4). Only the hamster kidney BHK-21 cells expressed significantly more YIPF4 protein than U-2 OS and HeLa cells ($p \leq 0.05$).

The YIPF4 transcript amounts were determined by qPCR relative to the housekeeping gene, U6. These showed markedly more variation (Figure 3.2A). Amongst the human cell lines tested, U-2 OS cells expressed significantly more YIPF4 mRNA than the cervical cell lines C33A and HeLa ($p \leq 0.05$ and $p \leq 0.01$, respectively) and the liver cell line Huh7 ($p \leq 0.01$). The monkey kidney cells Vero expressed significantly more YIPF4 mRNA compared to the same cervical and liver cell lines ($p \leq 0.05$). BHK-21 cells expressed significantly less YIPF4 mRNA than Vero ($p \leq 0.05$) and U-2 OS cells ($p \leq 0.01$). Thus, the observations

made on protein (Figure 3.1B) and transcript levels (Figure 3.2A) do not correlate directly.

The qPCR primers were positioned to amplify bp 78 – 236 of YIPF4 cDNA. There is no indication for splicing variants in this region since only one PCR product of the expected size (159 bp) was obtained (Figure 3.2B).

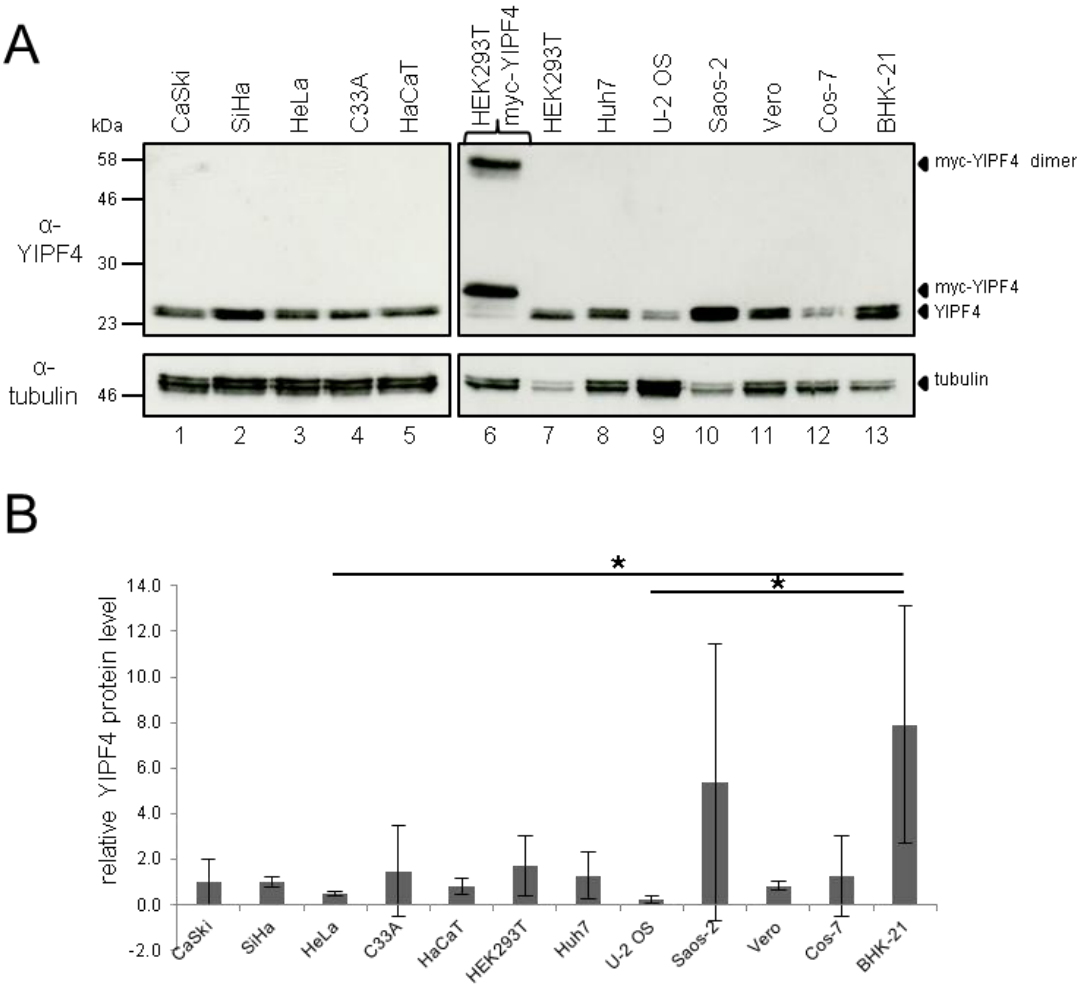

Figure 3.1 YIPF4 protein was expressed in various cell lines. A. Lysates from twelve cell lines were separated by SDS-PAGE and the endogenous YIPF4 protein detected with the YIPF4 antibody on the Western blot. Also, myc epitope tagged YIPF4 was overexpressed in HEK293T cells (lane 6). Apparent double bands are artefacts of the electrophoresis B. The relative YIPF4 protein levels were determined by densitometry analysis. For this, the ratios of YIPF4 and tubulin band intensities (A) were determined using the ImageJ software. Each bar represents the mean (± standard deviation of the mean (SDM)) of three experimental replicates. The data were analysed by one-way ANOVA. * $p \leq 0.05$

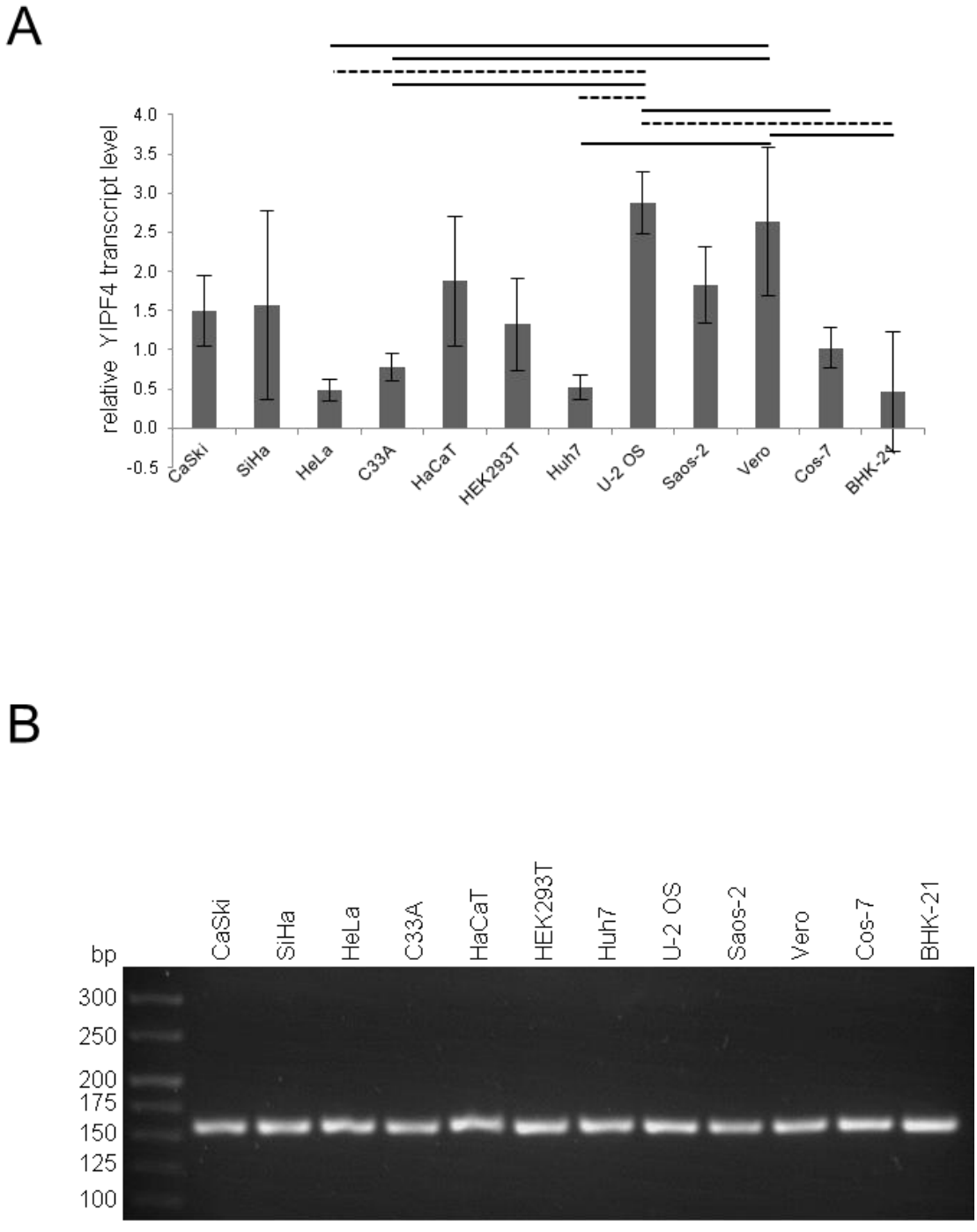

Figure 3.2 YIPF4 mRNA was expressed in various cell lines. A. Total RNA from twelve cell lines was extracted and YIPF4 transcript levels were determined by qPCR. Transcript levels were analysed with the $\Delta\Delta C_t$ method, normalised to the housekeeping gene U6 and presented in relation to the HEK293T samples. Each bar represents the mean (± SDM) of three experimental replicates. A one-way ANOVA was performed. Solid line = $p \leq 0.05$, dashed line = $p \leq 0.01$ B. Representative qPCR amplification products (A) spanning bp 78 - 236 of YIPF4 cDNA sequence were separated on a 3% agarose gel.

3.2.2. YIPF4 was expressed in human foreskin keratinocytes cell lines to similar levels

YIPF4 was successfully detected in cervix and skin established cell lines, which are infected by or theoretically susceptible and permissive to HPV. YIPF4 expression also needed confirmation in HFK cell lines generated from three donors of primary HFKs, which were untransfected or transfected with WT HPV18 genomes (HFK_3, HFK HPV18_1 WT, HFK HPV18_2 WT). Also, cells derived from the same donors were transfected with E5 knock out (KO) HPV18 genomes (HFK HPV18_1 E5 KO, HFK HPV18_2 E5 KO). They were included in the experiment to establish a possible effect on YIPF4 protein and/or transcript levels by the E5 protein. The presence of the HPV18 WT and E5 KO genotypes were validated by sequencing of the E5 ORF (data not shown).

Total protein from these cell lines was separated by SDS-PAGE and the corresponding Western blot probed with the YIPF4 antibody. YIPF4 was clearly detectable in every cell line as a band of approximately 27 kDa (Figure 3.3A). Relative quantification of YIPF4 protein was performed by densitometry analysis of three different passages per cell line (Figure 3.3B). It revealed no significant differences in YIPF4 protein levels amongst the three donors. Notably, the YIPF4 protein levels were similar between cell lines with the HPV18 WT and HPV18 E5 KO genotype, respectively, indicating that 18E5 does not have an effect on the YIPF4 protein levels.

The YIPF4 encoding mRNA was quantified relative to U6 by qPCR (Figure 3.3C). In agreement with the protein data (Figure 3.3B), there was no marked difference in YIPF4 transcript levels amongst the cell lines.

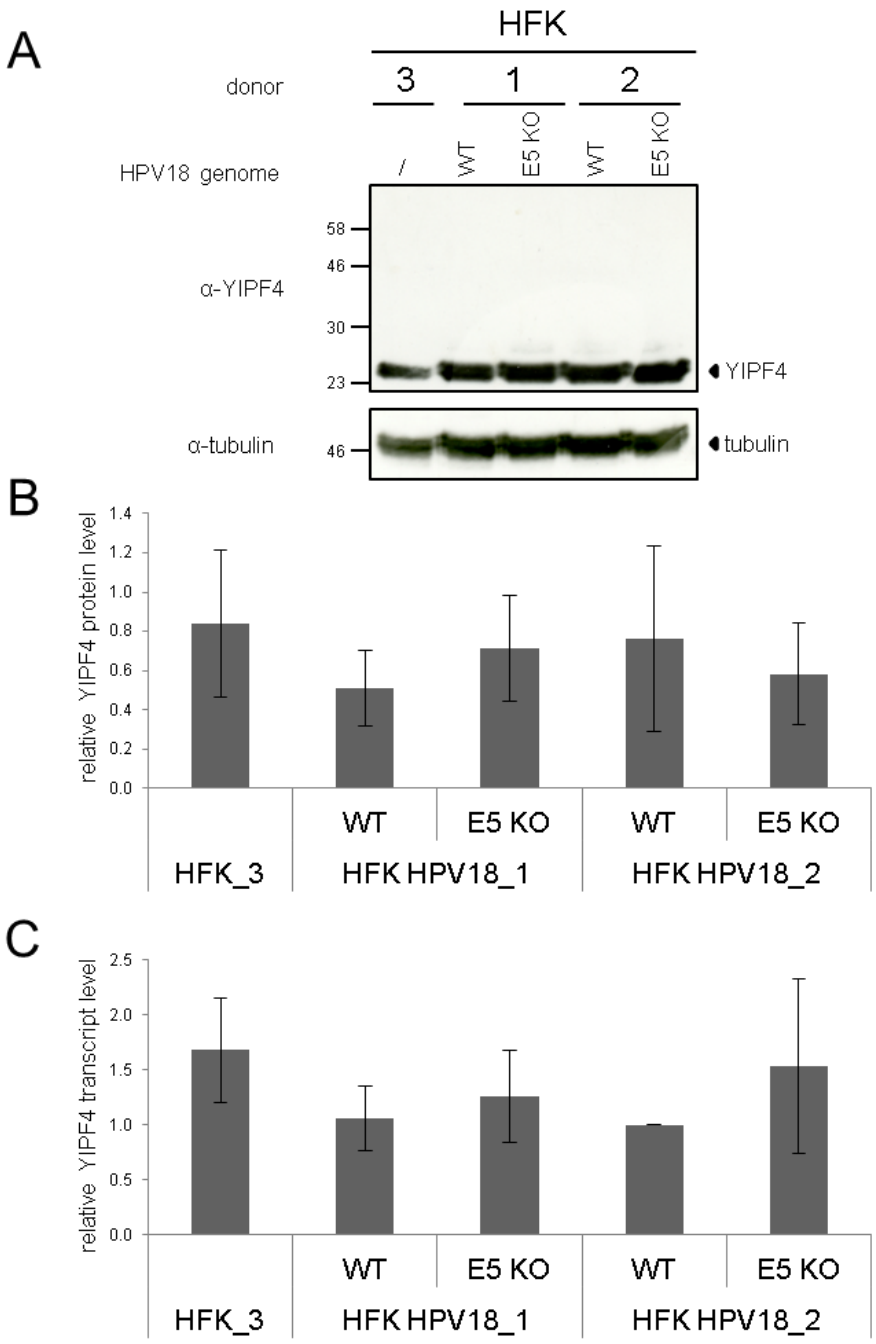

Figure 3.3 YIPF4 was expressed in HFK cell lines. A. Total protein from HFK cell line lysates was separated by SDS-PAGE. The endogenous YIPF4 protein was detected with the YIPF4 antibody on the Western blot. '/' = no HPV18 genome. Marker in kDa. B. The relative YIPF4 protein levels are illustrated by the ratios of YIPF4 and tubulin band intensities (A) as determined with the ImageJ software. C. Total RNA was extracted from HFK cells and YIPF4 transcript levels were determined by qPCR and normalised to the housekeeping gene U6. Transcript levels are expressed in relation to the HFK HPV18_2 WT samples. Analysis of transcript levels was performed using the $\Delta\Delta C_t$ method. Each bar (B, C) represents the mean (± SDM) of three independent replicates. A one-way ANOVA of YIPF4 protein (B) and transcript (C) levels showed no significant differences of YIPF4 levels in these HFK cell lines.

3.2.3. YIPF4 was expressed in organotypic raft cultures and localised at the Golgi

To date, detection of YIPF4 expression has been confined to monolayer cell culture systems. The HPV life cycle, however, depends on cell differentiation so the investigation of YIPF4 expression in organotypic raft cultures was essential.
The HFK cell lines of the three donors (3.2.2) were grown in the organotypic raft culture system. Haematoxylin and eosin (H&E) staining of their histological sections allowed the observation of successful stratification into the basal, suprabasal, granular and cornified cell layers (Figure 3.4A, upper panel).
Immuno-histochemistry with the YIPF4 antibody clearly showed equal staining of histological sections of organotypic raft cultures of all cell lines (Figure 3.4A, middle panel). YIPF4 was expressed throughout the basal, suprabasal and granular layers but absent in the cornified layer. The amount of YIPF4 protein was similar throughout those layers concluding from the fluorescence intensity profile spanning the height of the raft culture in the microscopy image (Figure 3.4A, lower panel). This intensity profile was similar for raft cultures of all cell lines. This implies that 18E5 and other HPV proteins do not affect the expression levels of YIPF4 during keratinocyte differentiation.

Since subcellular localisation of proteins is difficult to determine in sections of three dimensional culture systems, the subcellular localisation of YIPF4 was investigated in monolayer cell culture. Others observed a co-localisation of YIPF4 with the *cis*-Golgi marker GM130 in HeLa cells (Tanimoto et al., 2011). In our hands, staining with a GM130 antibody was not successful (data not shown). The yeast homologues of YIPF4, Yip4p and Yip5p, were shown to localise to the *trans*-Golgi (Inadome et al., 2007). Also, the mammalian paralogues, YIPF5 (Kano et al., 2009), FLAG-YIPF6 (Brandl et al., 2012) and GFP-YiF1 (Jin et al., 2005) co-localised with *trans*-Golgi network proteins like TGN46. Thus, SiHa cells were co-stained with YIPF4 and TGN46 antibodies (Figure 3.4B). A clear co-localisation between YIPF4 and TGN46 could be observed implying that YIPF4 at least partially localised to the *trans*-Golgi network in SiHa cells.

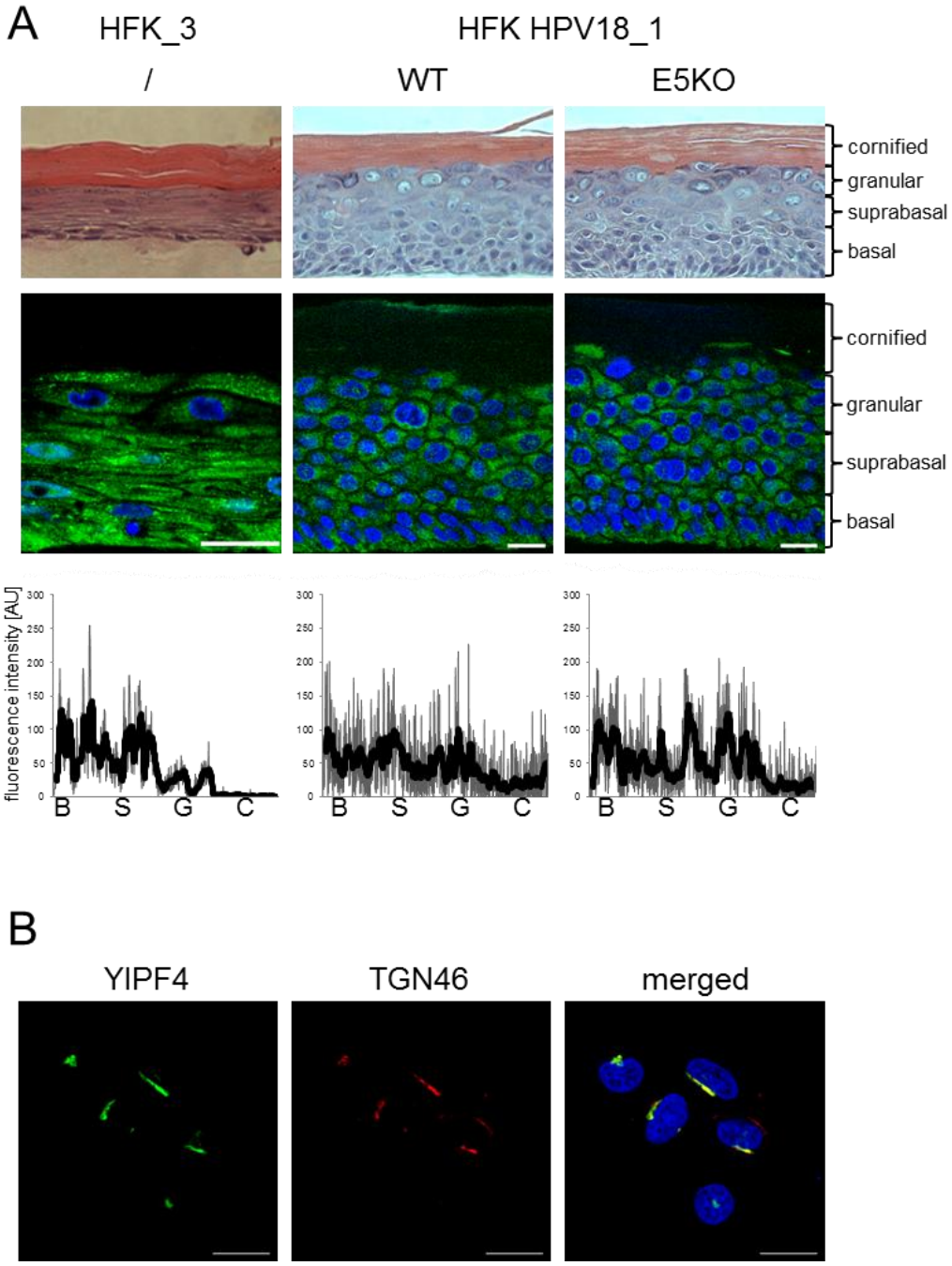

Figure 3.4 Immuno-fluorescent detection of YIPF4. A. HFK cell lines were grown in organotypic raft cultures for 13 days. Their histological sections were H&E stained (upper panel) and stained for endogenous YIPF4 (green; middle panel). Representative images of donor 1 and 3 are shown. Cell layers as identified by morphology are indicated on the right. The fluorescent intensity profiles were determined with ImageJ across the basal (B), suprabasal (S), granular (G) and cornified (C) layers (lower panel) and a trend line fitted. '/' = no HPV18 genome. B. SiHa cells were grown on cover-slips, fixed as above and stained for YIPF4 and the *trans*-Golgi network marker TGN46. Immuno-fluorescent images were acquired with Zeiss LSM700 confocal microscope and H&E images were acquired with Zeiss AxioVert 200 inverted microscope. Cell nuclei were labelled with DAPI (blue, A + B). Scale bars = 20 µm

3.2.4. YIPF4 was expressed in pathological sections of CIN1 and CIN3 lesions

With the YIPF4 expression verified in the three dimensional model of HPV infected sites it was important to investigate whether it was also present in clinical samples of HPV induced lesions. For this, pathological sections of HPV16 positive CIN1 and CIN3 lesions were examined. Most lesions of CIN1 and CIN3 grade express 16E4 protein (Griffin et al., 2012). The presence of HPV16 in these pathological samples was therefore confirmed by successful staining of both samples for 16E4 protein (Figure 3.5). Co-staining with the YIPF4 antibody showed a clear expression of YIPF4 in the CIN1 and CIN3 lesions confirming that YIPF4 is expressed in HPV induced cervical lesions.

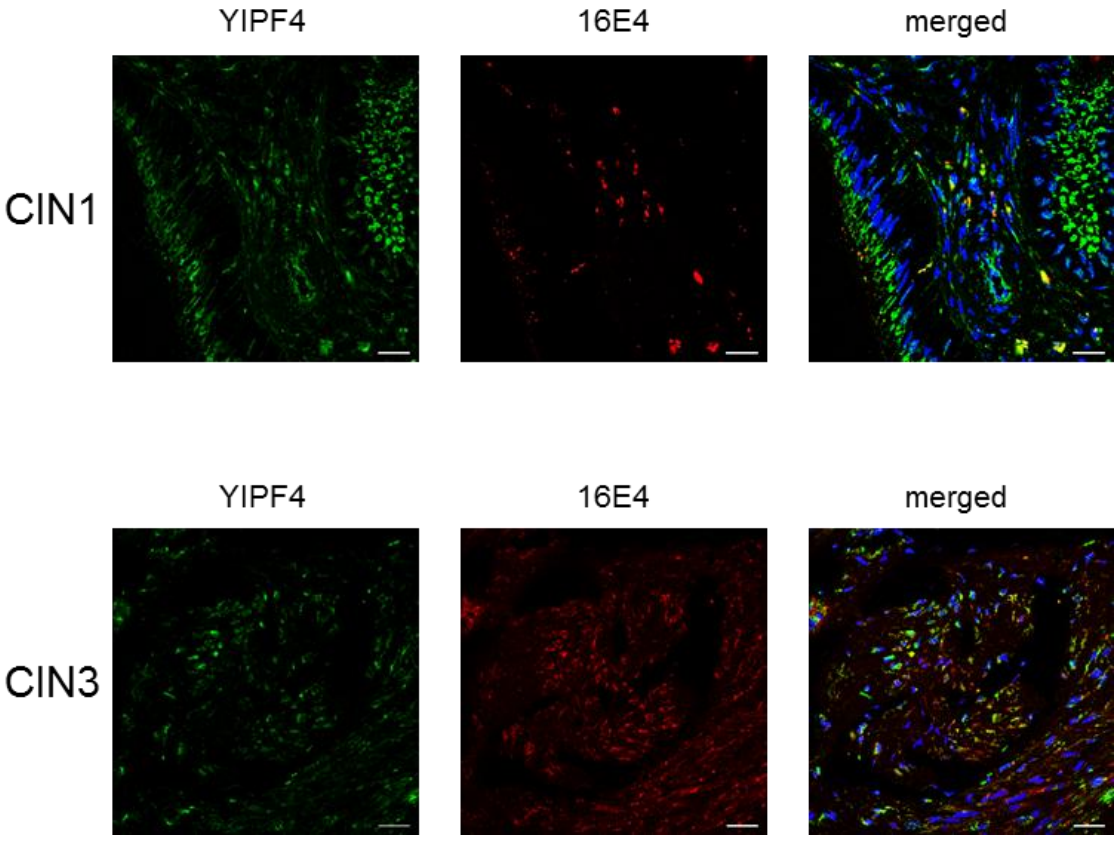

Figure 3.5 YIPF4 was expressed in clinical samples of cervical lesions. Pathological sections of HPV16 positive CIN grade 1 and 3 were stained with YIPF4 and 16E4 antibodies. Cell nuclei were visualised with DAPI (blue). Images were acquired on LSM700 confocal microscope. Scale bar = 20 µm

3.2.5. Presence of HPV18 genome rescued YIPF4 expression upon HFK differentiation

A complementary model system to the organotypic raft cultures to investigate differentiating cells is the methylcellulose (MC) HFK monolayer cell culture. HFK cell lines from all 3 donors were grown for 0 h and 48 h in MC medium and their lysates were analysed on Western blots (Figure 3.6A).

The cells were successfully differentiated after 48 h in MC medium, as implied by the decreased expression of the marker proteins cyclin A and HPV18 E7 compared to the 0 h time point.

The Western blots were probed with the YIPF4 antibody, and YIPF4 protein was detected in undifferentiated cells (Figure 3.6A, lanes 1, 3, 5, 7, 9) as before (Figure 3.3A). However, in contrast to what was observed in organotypic raft cultures of untransfected HFK cells (Figure 3.4A, middle panel), YIPF4 protein was no longer present in differentiated HPV18 negative HFK cells (Figure 3.6A, lane 2). The HFK HPV18 WT and E5 KO cell lines maintained YIPF4 protein levels upon differentiation (Figure 3.6A, lanes 4, 6, 8, 10) in accordance with the observation made in organotypic raft cultures (Figure 3.4A, lower panel).

The densitometry quantification partially supported this finding since the untransfected HFK cells showed a significant down-regulation of YIPF4 protein upon cell differentiation ($p \leq 0.05$) while the HFK HPV18 cell lines maintained YIPF4 protein levels upon differentiation (Figure 3.6B). In contrast, the YIPF4 protein level of differentiated HPV negative HFKs was not statistically significantly lower than in differentiated HPV18 positive HFK cell lines. There was, however, a clear trend towards increased YIPF4 protein in the differentiated HPV18 positive HFK cells. Note, that HFK HPV18 WT and E5 KO cells showed similar levels of YIPF4 upon differentiation. This implies that YIPF4 protein is normally down-regulated upon cell differentiation but the HPV context appears to rescue its expression (most likely independent of E5).

This investigation was extended to the examination of the YIPF4 transcript level. This was quantified relative to U6 by qPCR after 0 h and 72 h of MC-mediated differentiation. This investigation confirmed the significant down-regulation of YIPF4 in HPV negative HFKs upon differentiation (Figure 3.7A).

Comparison of these differentiated HPV negative HFKs and the differentiated HFK HPV18 WT (donors 1 and 2) and E5 KO (donor 1) cell lines showed a significantly reduced level of YIPF4 transcript ($p \leq 0.05$ and $p \leq 0.01$). This correlated with the trend towards down-regulation observed on protein level (Figure 3.6B). Notably, the HPV18 WT and E5 KO cell lines showed a similar phenotype implying that YIPF4 transcript levels was not necessarily dependent on E5. The YIPF4 transcript levels in HFK HPV18 E5 KO cell line of donor 2 was not significantly up-regulated compared to HPV negative cells, but followed the same trend (Figure 3.7A). The markedly decreased ($p \leq 0.01$) cyclin A (Figure 3.7B) and HPV18 E7 (Figure 3.7C) transcript levels in all HFK cell lines after 72 h growth in MC medium confirmed the advanced differentiation of the cells investigated here. Thus, the YIPF4 transcript levels were reduced in HPV-free HFK cell lines upon differentiation but they were rescued in the HPV18 positive cells lines most likely independently of E5.

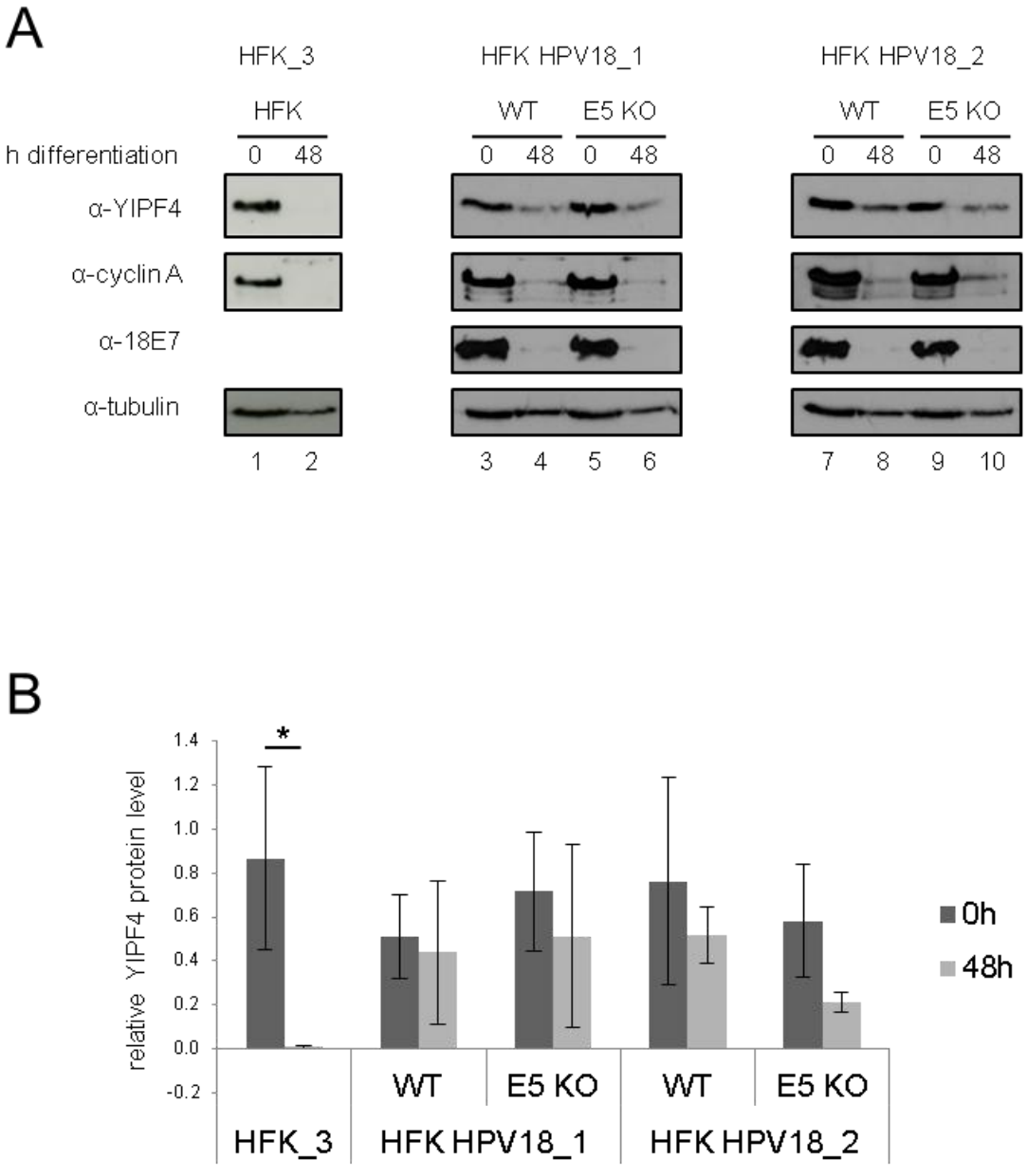

Figure 3.6 Quantitative approach to determine YIPF4 protein levels in differentiated HFK cell lines. A. HFK cell lines were grown in monolayers in MC medium for 0 h (control) and 48 h. Cells were lysed and total protein was separated by SDS-PAGE. YIPF4, differentiation marker HPV18 E7 and cyclin A and the loading control tubulin were detected on the Western blot with the respective antibodies. Representative blots are shown B. The relative YIPF4 protein levels are illustrated as the ratio of YIPF4 and tubulin protein band intensities as measured using ImageJ. Each bar represents the mean (± SDM) of three independent replicates. A one-way ANOVA was performed *$p \leq 0.05$

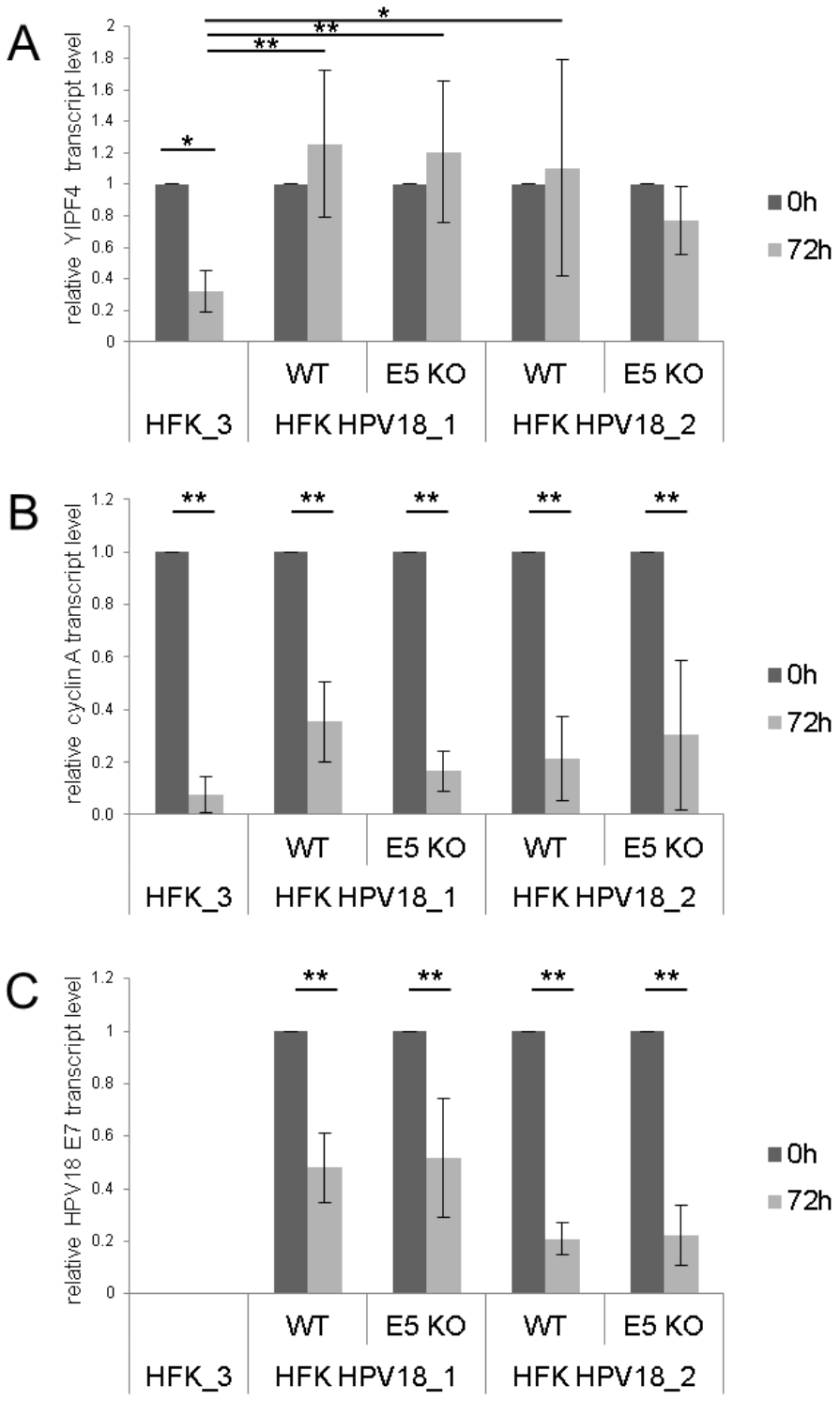

Figure 3.7 Effects of HFK cell line differentiation on YIPF4 transcript levels. HFK cell lines were grown in monolayer cell culture in MC medium. Total RNA was extracted at 0 h and 72 h time points. The YIPF4 (A), cyclin A (B) and HPV18 E7 (C) transcript levels were determined by qPCR and normalised to the housekeeping gene U6. The transcript levels of every cell line are expressed in relation to their 0 h time points (= undifferentiated cell control). According to expectations, no HPV18 E7 transcripts were detected in the HPV18 negative cell line HFK_3. Analysis of transcript levels was performed according to the $\Delta\Delta C_t$ method. Each bar represents the mean (± SDM) of at least three replicates. A one-way ANOVA was performed, however, only selected p-values are shown. ** $p \leq 0.01$

3.2.5.1. YIPF4 transcription could be regulated by HPV18 E2

It was established that in differentiated cells, YIPF4 expression was rescued in HFK cells carrying HPV18 genomes (3.2.5). This was achieved independently of E5 implying that its proposed interaction with YIPF4 is most likely not responsible for the rescue. It is more likely that E2 plays a role in the transcriptional regulation of YIPF4 in differentiated cells since the E2 binding motif (ACCNNNNNNGGT) (Hines et al., 1998) was identified eight times in the YIPF4 gene sequence (Figure 3.8A). However, the nucleotides 4 – 9 of the binding motif showed little conservation within the gene sequence according to the sequence logo compiled of the potential E2 binding sequences in the YIPF4 gene region (Figure 3.8).

It is also possible that YIPF4 transcription is regulated by cellular proteins that are involved in transcriptional regulation and interact with HPV18 E2 (Figure 3.8B).

A

potential E2BS (bp)	sequence at potential binding site
240 – 251	ACCGCGGCCGGT
3506 – 3517	ACCATGCCTGGT
12839 – 12850	ACCTTTTTTGGT
13906 – 13917	ACCTACACTGGT
18346 – 18357	ACCGAGGCGGGT
24109 – 24120	ACCCGGCCTGGT
27482 – 27493	ACCAAAATTGGT
28041 – 28052	ACCTGGATTGGT

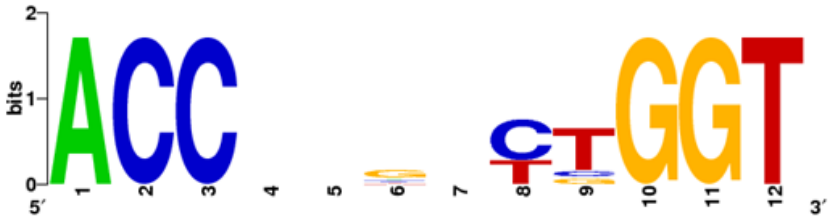

B

PV type	name and UniProt ID	references
HPV11,16,18	androgen receptor, P10275	(Wu et al., 2007a)
HPV8, 16, 18, BPV1	CCAAT/enhancer-binding protein alpha, P49715	(Hadaschik et al., 2003)
HPV18	CREB-binding protein, Q92793	(Lee et al., 2000)
HPV18	histone acetyltransferase KAT2B, Q92831	(Lee et al., 2002)
HPV11,16, 18	zinc finger protein PLAGL1, Q9UM63	(Wu et al., 2007b)
HPV18	transcription activator BRG1, P51532	(Cha and Seo, 2011)
HPV6, 11, 16, 18	SWI/SNF-related matrix-associated actin-dependent regulator of chromatin subfamily B member 1, Q12824	(Cha and Seo, 2011)
HPV18, BPV1	transcription initiation factor TFIID subunits 1 and 6, P21675 and P49848	(Carrillo et al., 2004)
HPV18, BPV1	TATA-box-binding protein, P20226	(Carrillo et al., 2004)

Figure 3.8 YIPF4 transcription could be regulated by HPV E2. A. The YIPF4 gene sequence (NCBI Reference Sequence: NT_022184.15|:11324845-11353545) was searched for the HPV E2 binding motif (ACCNNNNNNGGT) using the GeneQuest software. Potential E2 binding positions and their sequences are shown (table). The sequence logo describes the relative frequency of the bp (i.e. height of symbol) and the overall sequence conservation (height of stack) of the potential E2BS in the YIPF4 gene sequence. Sequence logo was created with WebLogo (http://weblogo.berkeley.edu/logo.cgi). B. Suggestive list of HPV18 E2 interaction partners that regulate transcription and therefore are candidates for YIPF4 transcriptional regulation in HPV18 genome transfected cells.

3.2.6. Topology of YIPF4

3.2.6.1. YIPF4 computational model comprised five TMDs

YIPF4 is a highly hydrophobic protein but there is little experimental evidence for its membrane association and topology. The 5 TMD configuration, summarised in Figure 3.9, was purely based on computational predictions with the SOSUI online tool. The orientation of the hydrophilic N-terminus towards the cytoplasm and the C-terminus towards the lumen correlated with observations made for YIPF1, YIPF2 and YIPF3 (Shakoori et al., 2003). The 5 intervening TMDs were compiled of one secondary and four primary α-helices of 23 and 21 amino acids, respectively (Figure 3.9A). A principally identical YIPF4 topology model was entered in the UniProt data base. It was based on several bioinformatics prediction tools (3.1.2). In this model all 5 TMD were of 21 amino acid length (Figure 3.9B). Thus, the analysis of the YIPF4 amino acid sequence with various bioinformatics prediction tools resulted in a 5 TMD topology model for YIPF4.

3.2.6.2. YIPF4 enriched in the membranous fraction

To experimentally evaluate the 5 TMD topology of YIPF4, first, the membrane protein nature of YIPF4 was investigated. For this, cells expressing endogenous as well as overexpressed, epitope tagged YIPF4 protein were partitioned into soluble and membranous protein fractions. The fractions were analysed by Western blot and the identity of the fractions confirmed with marker proteins (soluble fraction = GAPDH, membranous fraction = TfR and TGN46). Endogenous YIPF4 in BHK-21 cells was clearly confirmed as a membrane associated protein since it was detected in the membranous protein fraction (Figure 3.10A). The overexpression with two small epitope tags (N-terminal FLAG and C-terminal HA) (Figure 3.10B) and with the 27 kDa GFP tag (N-terminus) (Figure 3.10C) did not alter the properties of YIPF4 as a membrane protein because it remained in the fraction of membranous proteins. Notably, overexpressed YIPF4 formed potential dimers in accordance with previous observations (Figure 3.1).

A SOSUI

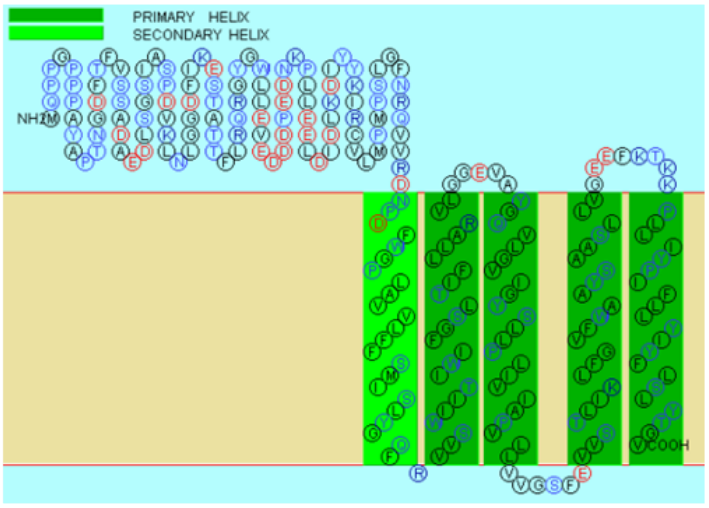

No.	N-terminal	trans-membrane region	C-terminal	helix type	length
1	112	NPDFWGPLAVVLFFSMISLYGQF	134	secondary	23
2	136	VVSWIITIWIFGSLTIFLLARVL	158	primary	23
3	164	YGQVLGVIGYSLLPLIVIAPVLL	186	primary	23
4	193	VVSTLIKLFGVFWAAYSAASLLV	215	primary	23
5	224	PLLIYPIFLLYIYFLSLYTGV	244	primary	21

B UniProt

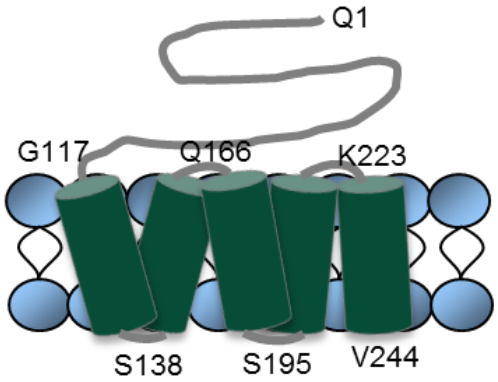

No.	N-terminal	trans-membrane region	C-terminal	length
1	114	DFWGPLAVVLFFSMISLYGQF	134	21
2	139	WIITIWIFGSLTIFLLARVLG	159	21
3	167	VLGVIGYSLLPLIVIAPVLLV	187	21
4	196	TLIKLFGVFWAAYSAASLLVG	216	21
5	224	PLLIYPIFLLYIYFLSLYTGV	244	21

Figure 3.9 Computationally predicted membrane topology of YIPF4. A. The YIPF4 amino acid sequence (NCBI Reference Sequence: NP_115688.1) was analysed with the online-tool SOSUI to predict its secondary structure. The software predicts 5 TMDs (upper panel). The protein regions predicted to span the membrane are indicated in the table below.'No.' = number of TMDs. Amino acids colour legend: black = hydrophobic, blue = polar, bold blue = positive charge, bold red = negative charge. B. Similar YIPF4 topology model based on the 5 potential TMDs published in UniProt (entry Q9BSR8, accessed Sept 2013). The table summarises the protein regions that form the TMDs.

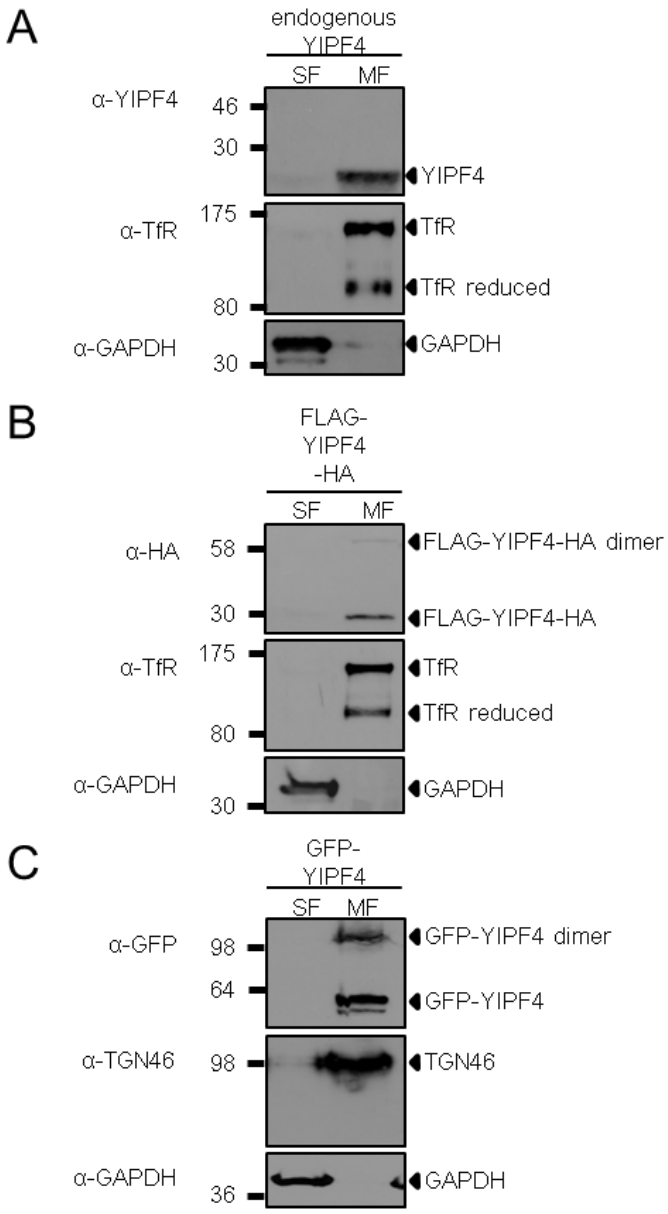

Figure 3.10 YIPF4 enriched in the membranous fraction in a subcellular fractionation experiment. Cells (A, B, C) were lysed by sonication and the membranous proteins separated from the soluble proteins by ultra-centrifugation. Proteins of both fractions were separated by SDS-PAGE and the Western blot probed for YIPF4 and a marker for soluble proteins (GAPDH) and for membrane proteins (TfR, TGN46). A. BHK-21 cells were subject to subcellular fractionation. Endogenous YIPF4 was detected on the corresponding Western blot with the YIPF4 antibody. B. Dual epitope tagged YIPF4 (FLAG-YIPF4-HA) was overexpressed in BHK-21 cells using the recombinant vaccinia virus VTF7-3. Cells underwent subcellular fractionation 24 h post-transfection/infection. FLAG-YIPF4-HA was detected on the resulting Western blot with an anti-HA antibody. C. A GFP-YIPF4 fusion protein was exogenously expressed in HEK293T cells which were harvested for subcellular fractionation 16 h post-transfection. On the corresponding Western blot, GFP-YIPF4 was detected by probing for its tag with a GFP antibody. SF = soluble fraction, MF = membranous fraction, marker in kDa.

3.2.6.3. Investigation of YIPF4 TMDs with the differential, detergent permeabilisation assay

3.2.6.3.1. Establishing the differential, detergent permeabilisation assay

Since there is no experimental evidence for the predicted 5 TMD nature of YIPF4, a differential, detergent permeabilisation assay was established to experimentally investigate this topology model. The assay is an immuno-cytochemistry approach that is based on the differential properties of two detergents: Triton X-100 permeabilises all cellular membranes while low concentrations of Digitonin selectively permeabilise the plasma membrane only (Figure 3.11A). The treatment of fixed cells with these detergents leads to different accesses for antibodies during the immuno-cytochemistry process.

To verify this assay, Huh7 cells were stained for the cytoplasmic protein tubulin and the Golgi lumen protein mannosidase II (Figure 3.11B) with Triton X-100 (Figure 3.11B, upper panel), Digitonin (Figure 3.11B, middle panel) and without detergent (Figure 3.11B, lower panel), respectively. The cytoplasmic tubulin could be detected in both, Triton X-100 and Digitonin permeabilised cells. In contrast, the Golgi luminal mannosidase II could only be detected in Triton X-100 permeabilised cells not under selective Digitonin permeabilisation. Cells stained without detergent showed little plasma membrane permeabilisation since some tubulin staining could be detected. However, the principle of the differential, detergent permeabilisation proved successful and could be employed to experimentally investigate the TMD model of YIPF4 (3.2.6.3.3).

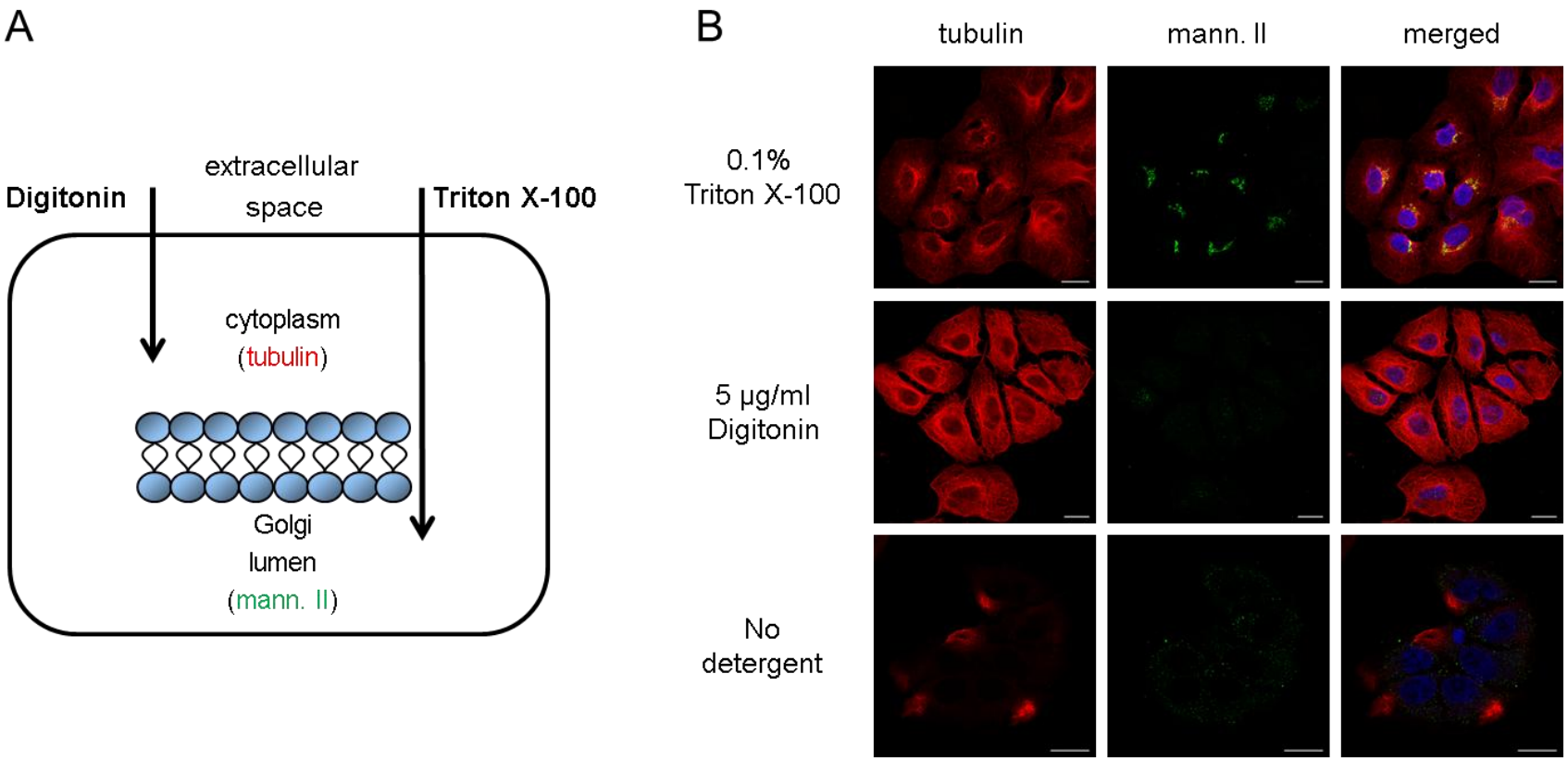

Figure 3.11Establishing a differential, detergent permeabilisation assay. A. Schematic representation of the differential, detergent permeabilisation assay. The detergent Triton X-100 permeabilises all cellular membranes while the detergent Digitonin selectively permeabilises the plasma membrane only. B. Huh7 cells were grown on cover slips, fixed and permeabilised with Triton X-100 (upper panel) or Digitonin (middle panel). No detergent was applied as negative control (lower panel). Cells were stained for tubulin (cytoplasma) and mannosidase II (Golgi lumen) with respective antibodies. DAPI (blue) was used to visualise the nuclei. Images were acquired with Zeiss LSM700 confocal microscope. mann. II = mannosidase II, Scale bar = 20 µm

3.2.6.3.2. Generation of FLAG-YIPF4-HA truncation mutants

YIPF4 truncation mutants were generated to enable the investigation of the TMD topology with the differential, detergent permeabilisation assay (3.2.6.3.3). The truncation mutants were designed to contain an N-terminal FLAG epitope tag (Figure 3.12A). The predicted TMDs entered in the UniProt database (Figure 3.9B) were serially truncated from the C-terminus and replaced with a HA epitope tag resulting in truncation mutants with two epitope tags. In the Del1-109 mutant the hydrophilic N-terminus was replaced with a FLAG epitope tag. The theoretical molecular weights of the truncated proteins were calculated with the 'Protein Molecular Weight Calculator'-online tool.

The truncations and epitope tags were introduced with specific primers in PCRs using the full-length YIPF4 nucleotide sequence as template. The PCR products were cloned into the destination vector pcDNA3.1(+). The correct sizes of the cloned inserts were confirmed by restriction digest (Figure 3.12B) and sequence analysis (data not shown).

All YIPF4 truncation mutants were successfully expressed with both tags (Figure 3.12C). The expression efficiency of truncation mutants FLAG-YIPF4-HA S138, FLAG-YIPF4-HA G117 and FLAG-YIPF4-HA Del1-109 (Figure 3.12C, lanes 5-7) was lower compared to the remaining truncation mutants because increased amounts of total protein were needed for detection. Overall, the sizes of the truncation mutants agree with the predicted molecular weight and are in relation to each other. The FLAG-YIPF4-HA Del1-109 mutant, however, was of smaller size than expected (compare to FLAG-YIPF5-HA S138), although the expression construct was error-free (Figure 3.12B). The truncation mutant FLAG-YIPF4-HA G117 (lane 6) appeared to express less FLAG epitope than HA epitope when comparing the band intensities on the corresponding Western blots although again, the expression construct was free from error.

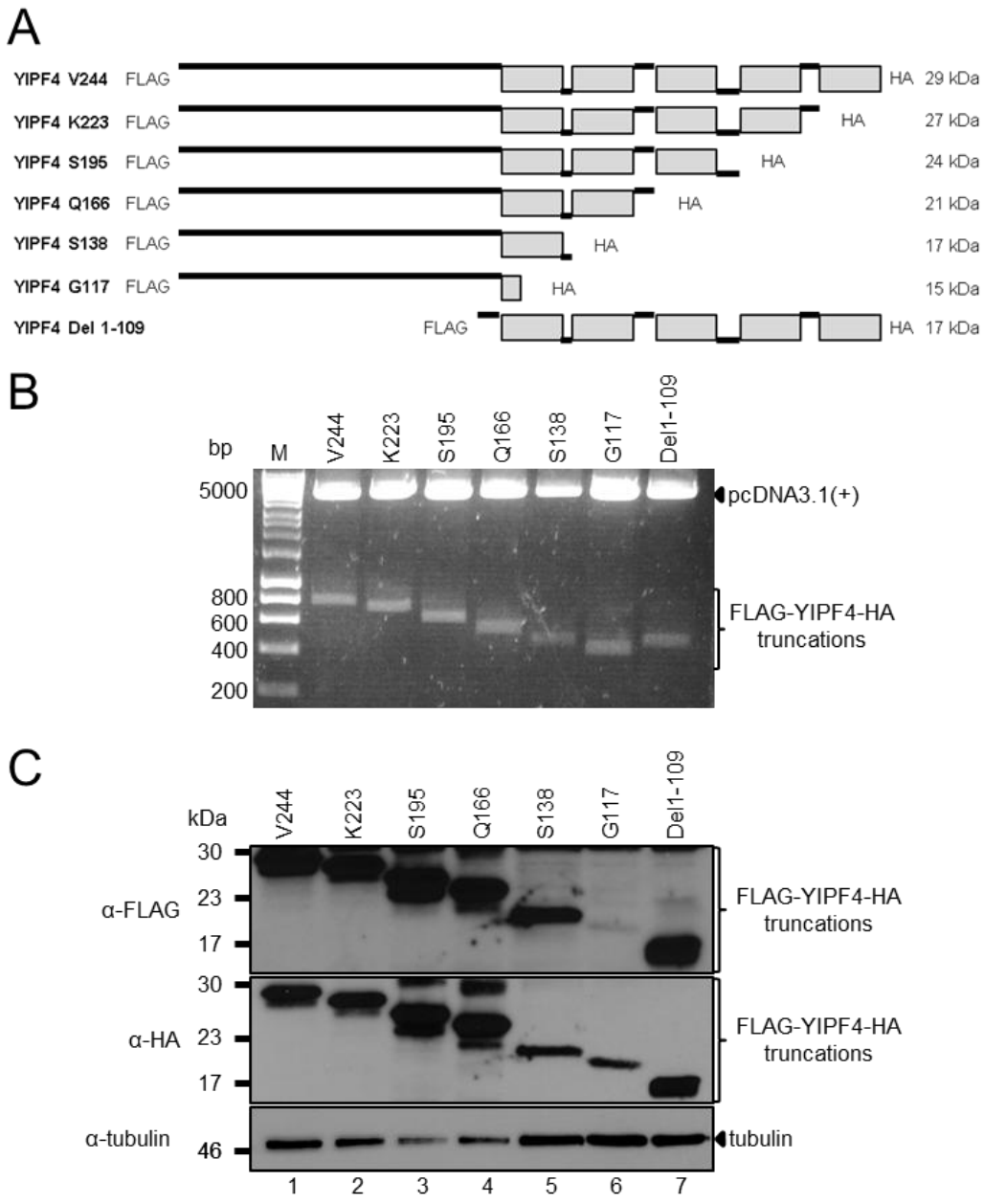

Figure 3.12 Generation of YIPF4 truncation mutants attaching an N-terminal FLAG and a C-terminal HA tag. A. Schematic representation of the YIPF4 truncations mutants with their N-terminal FLAG and C-terminal HA tags. The designated name for each truncation mutant is indicated on the left and consists of the one letter amino acid code and number of the final amino acid before truncation. The Del1-109 truncation mutants forms an exemption (Del = deletion of amino acids 1 to 109). Grey boxes represent potential TMD and black lines indicate luminal (subscript) and cytoplasmic (superscript) sites (based on UniProt entry Q9BSR8). The predicted molecular weights of the truncation mutants are indicated on the right. B. The FLAG and HA tags were added to the YIPF4 sequence with PCR primers which also truncated the full-length YIPF4. Truncated YIPF4 sequences were cloned into pcDNA3.1(+). Correct insert sizes were verified by restriction digests with BamHI and HindIII. C. FLAG-YIPF4-HA truncation mutants were exogenously expressed in BHK-21 cells using the vaccinia virus VTF7-3. Samples were separated by SDS-PAGE and the overexpressed YIPF4 detected with antibodies against both its tags.

3.2.6.3.3. The differential, detergent permeabilisation assay revealed that three TMDs were required for YIPF4 membrane association in cells

The full-length FLAG-YIPF4-HA and the truncation mutants were overexpressed in Huh7 cells and subject to the differential, detergent permeabilisation assay to investigate YIPF4 membrane topology. Most FLAG-YIPF4-HA mutants showed an ER-like and to some extend nuclear envelope distribution (Figure 3.13 - Figure 3.18). Due to insufficient expression level, the mutant FLAG-YIPF4-HA Del1-109 could not be analysed in this assay.

According to the computational topology model of YIPF4, the cytoplasmic N-terminus is followed by 5 TMDs and a luminal C-terminus (Figure 3.9) (Shakoori et al., 2003). The truncations of YIPF4 were designed from the C-terminus (Figure 3.12A). This left the N-termini of all truncation mutants (except Del1) exposed to the cytoplasm. In the differential, detergent permeabilisation assay, this meant that the N-terminal FLAG tags of all truncation mutants should be detectable in Triton X-100 and Digitonin permeabilised cells (Figure 3.13 - Figure 3.18). Indeed, the FLAG staining was observed for the full-length V244 (Figure 3.13B) as well as the K223 (Figure 3.14B), S195 (Figure 3.15B), Q166 (Figure 3.16B), S138 (Figure 3.17B) and G117 (Figure 3.18B) truncation mutants in Triton X-100 and Digitonin permeabilised cells. Thus, the cytoplasmic orientation of the hydrophilic N-terminus could be confirmed in accordance with the computational model (Figure 3.9) (Shakoori et al., 2003).

The Person correlation coefficient (PCC) of the FLAG and HA staining of every mutant was calculated with the PSC plug-in for ImageJ to determine the orientation of the (truncated) C-termini. In Digitonin permeabilised cells, a marked decrease of the PCC value compared to Triton X-100 treated cells indicated a luminal HA epitope/C-terminus. An equal PCC value between Digitonin and Triton X-100 permeabilised cell was indicative for a cytoplasmic HA tag/C-terminus. Non-permeabilised cells were stained as negative controls.

For the C-terminus, the computational topology model of YIPF4 predicts a luminal orientation (Figure 3.13A). This was tested with the full-length FLAG-YIPF4-HA V244 protein (Figure 3.13B). The PCC value in Digitonin

permeabilised cells (0.52) was clearly decreased compared to the PCC value in Triton X-100 permeabilised cells (0.92). This supported the exposure of the C-terminus to the luminal side of the organelle.

The K223 truncation mutant of YIPF4 is characterised by the truncation of the most C-terminal TMD (Figure 3.14A). According to the computational model, this removal places the truncated C-terminus to the cytoplasmic side of the organelle membrane. The examination of the K223 truncation mutant in the differential, detergent permeabilisation assay indeed resulted in similar PCC values (Digitonin = 0.79, Triton X-100 = 0.93) (Figure 3.14B). Together with the data from the full-length V244 protein (Figure 3.13), the existence of an outside-in orientated C-terminal TMD was verified.

A further potential TMD was truncated from the C-terminal side in the S195 truncation mutant (Figure 3.15A). Referring to the full-length YIPF4 protein this depicts a truncation of 2 C-terminal TMDs. The even number of truncated TMDs predicted a luminal orientation of the truncated C-terminus. The S195 showed a substantially decreased PCC value in Digitonin permeabilised cells (0.41) compared to Triton X-100 permeabilised cells (0.88) (Figure 3.15B). This confirmed the luminal orientation of the S195 residue as predicted from the computational model.

The data from the full-length V244 and the K223 and S195 truncation mutants thus far verified the presence of the two most C-terminal TMDs of YIPF4. The last TMD spans the membrane between amino acid residue 223 and 244 from the outside-in and the second to last TMD spans the membrane between amino acids 195 and 223 from the inside-out.

The Q166 truncation mutant was designed to truncate an additional TMD from the C-terminus (Figure 3.16A) which depicted an overall truncation of 3 TMDs referring to the full-length YIPF4 protein. The examination of the Q166 truncation mutant in the differential, detergent permeabilisation assay resulted in comparable PCC values in Digitonin (0.83) and Triton X-100 (0.91) permeabilised cells (Figure 3.16B). This was clearly indicative of a cytoplasmic

orientation of the Q166 amino acid residue. This also implied that the amino acids between position 166 and 195 span the membrane from the outside-in.

A further potential TMD was truncated in the S138 mutant which depicted a truncation of a total of 4 potential TMDs from the C-terminus referring to the full-length protein (Figure 3.17A). This even number implied that S138 faces the luminal side of the organelle like S195 and V244. The differential, detergent permeabilisation assay, however, revealed similar PCC values for Digitonin (0.76) and Triton X-100 (0.85) permeabilised cells (Figure 3.17B). This is indicative of a cytoplasmic orientation of the S138 amino acid. In contrast to the computation model, it is therefore to assume that the amino acids 138 – Q166 do not from a membrane spanning domain.

The final mutant investigated in this assay, G117, was developed by truncating all potential TMDs from the C-terminus. Thus, it consists only of the hydrophilic N-terminus of YIPF4 (Figure 3.18A). Logically, this was predicted to be localised in the cytoplasm. The differential, detergent permeabilisation assay indeed resulted in similar PCC values in Digitonin (0.81) and Triton X-100 (0.90) permeabilised cells (Figure 3.18B). However, due to the fact that S138 was aberrantly detected in the cytoplasm (Figure 3.17B), it is unlikely that a membrane spanning domain is formed between the cytosolic amino acids 117 and 138.

It was worthy of note that the cellular distribution of both S138 (Figure 3.17B, upper panel) and G117 (Figure 3.18B) differed from the ER-like distribution of the other truncation mutants. In Triton X-100 permeabilised cells, these truncation mutants depicted a wide distribution throughout the cell including the nucleus. But some examples of ER-like staining were also found (Figure A. 1).

In summary, the investigation of the full-length YIPF4 protein V244 and the truncation mutants K223, S195, Q166, S138 and G117 in the differential, detergent permeabilisation assay did not agree completely with the predicted 5 TMDs model of YIPF4. In this assay, only the amino acids between 166 - 195,

195 – 223 and 223 – 244 were confirmed to form TMDs. The amino acids between 117 – 138 and 138 – 166 did not span the membrane as predicted.

The analysis of the PCC values of two independent experiments supported this finding (Figure 3.19). It became obvious that only the PCC values of the full-length V244 and the truncation mutant S195 were significantly decreased in Digitonin permeabilised cells compared to Triton X-100 permeabilised cells ($p \leq 0.01$) implying their luminal orientation. The expected decrease of the PCC value of Digitonin permeabilised cells expressing the S138 mutant (Figure 3.19, highlighted in green) was not detected. The PCC values of the negative controls (= no detergent) showed similar PCC values as the Digitonin permeabilised cells. It was previously observed (Figure 3.11) that non-detergent treated cells exhibited some permeabilisation of the cell membrane. This could have been caused by the fixation of cells prior to staining.

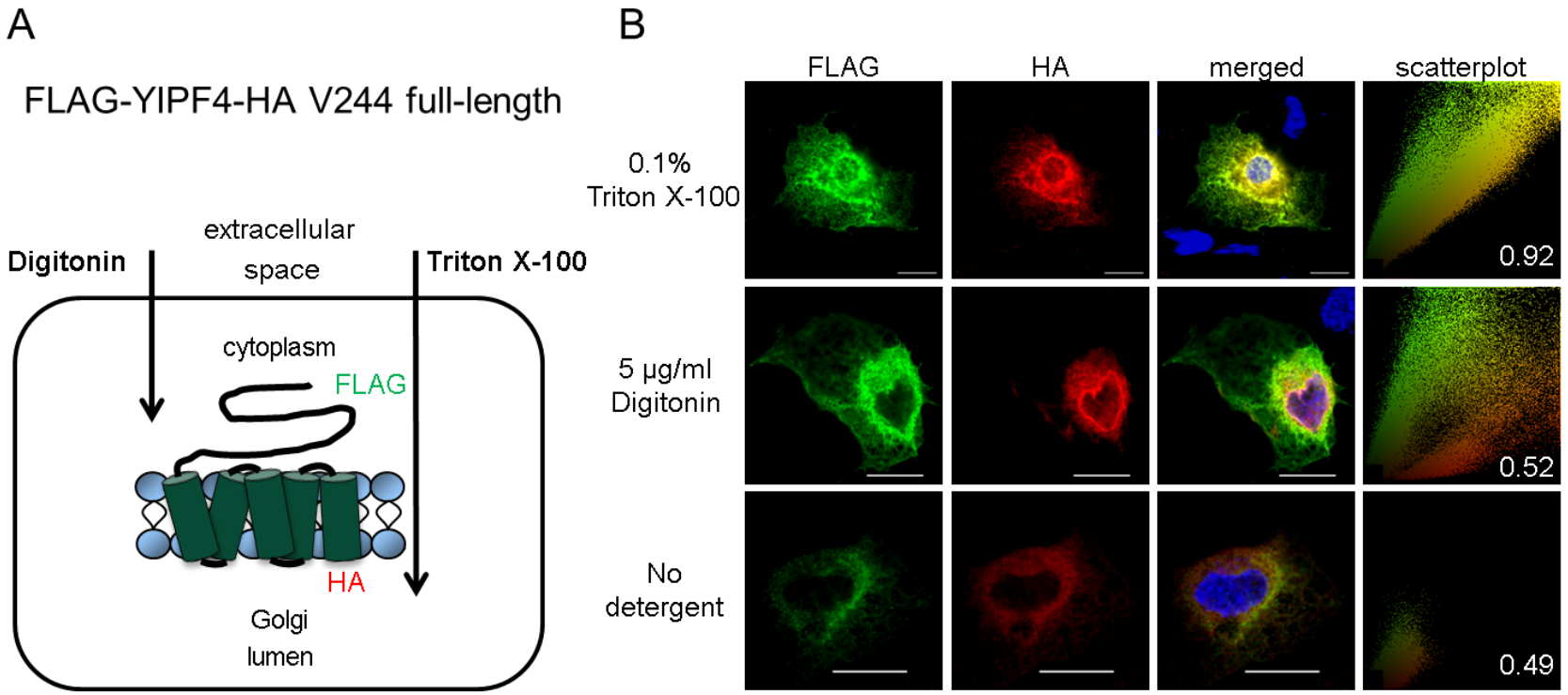

Figure 3.13 Examining the full-length FLAG-YIPF4-HA V244 protein in the differential, detergent permeabilisation assay. A. Schematic representation of the differential, detergent permeabilisation assay with overexpressed full-length FLAG-YIPF4-HA V244 in its predicted 5 TMD topology. B. Huh7 cells were grown on cover slips and transfected with full-length FLAG-YIPF4-HA V244. After 16 h, cells were fixed and differentially permeabilised with Triton X-100 (upper panel) and Digitonin (middle panel). No detergent was applied as negative control (lower panel). Cells were co-stained with FLAG and HA antibodies. DAPI (blue) was used to visualise the nuclei. Samples were viewed with a Zeiss LSM700 confocal microscope. The co-localisation of the FLAG and HA tag was determined using the PSC plug in for ImageJ which calculated the PCC value and generated the scatterplot. Representative images are shown. Scale bar = 20 µm

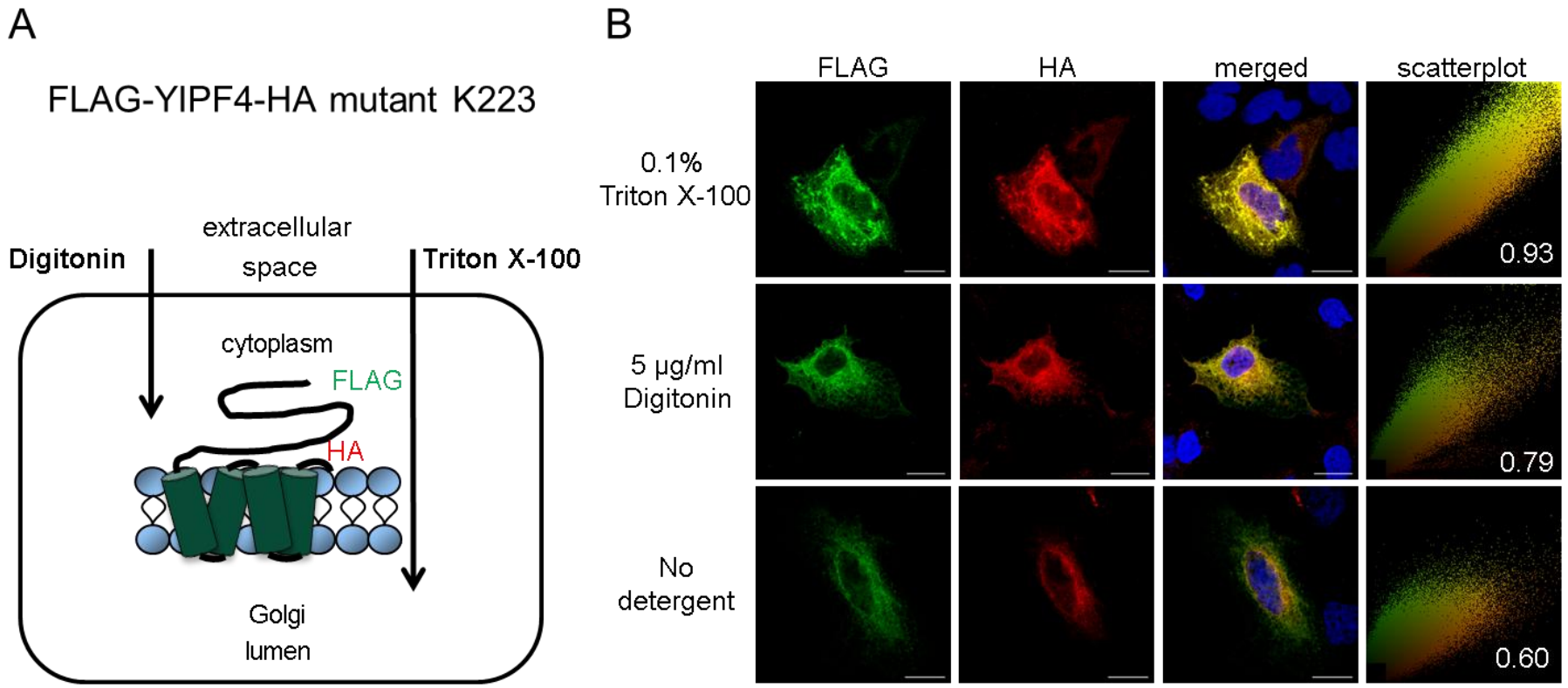

Figure 3.14 Examining the FLAG-YIPF4-HA K223 truncation mutant in the differential, detergent permeabilisation assay. A. Schematic representation of the FLAG-YIPF4-HA K223 truncation mutant in the differential, detergent permeabilisation assay. B. Huh7 cells were grown on cover slips and transfected with FLAG-YIPF4-HA K223. The assay was carried out as described in legend to Figure 3.13. Representative images are shown. Scale bar = 20 µm

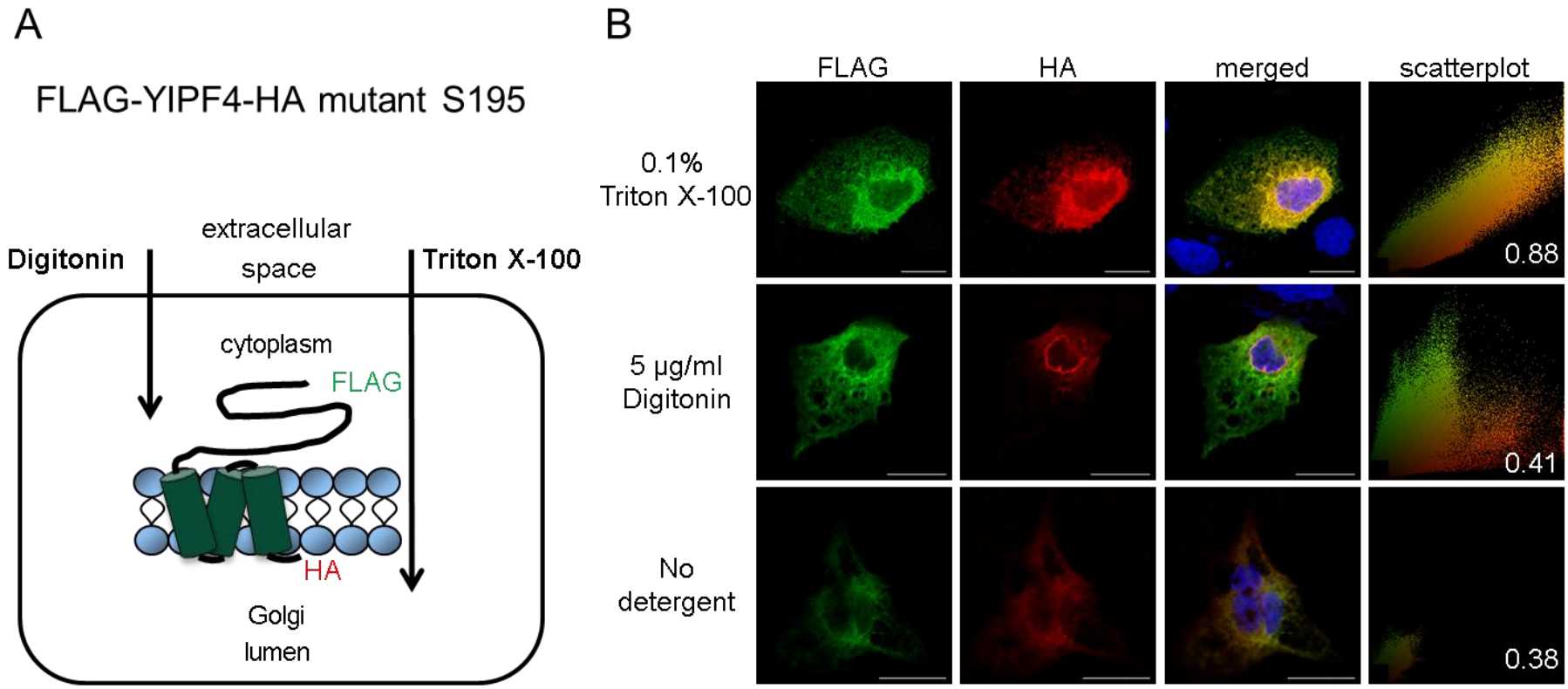

Figure 3.15 Examining the FLAG-YIPF4-HA S195 truncation mutant in the differential, detergent permeabilisation assay. A. Schematic representation of the FLAG-YIPF4-HA S195 truncation mutant in the differential, detergent permeabilisation assay. B. Huh7 cells were grown on cover slips and transfected with FLAG-YIPF4-HA S195. The assay was carried out as described in legend to Figure 3.13. Representative images are shown. Scale bar = 20 µm

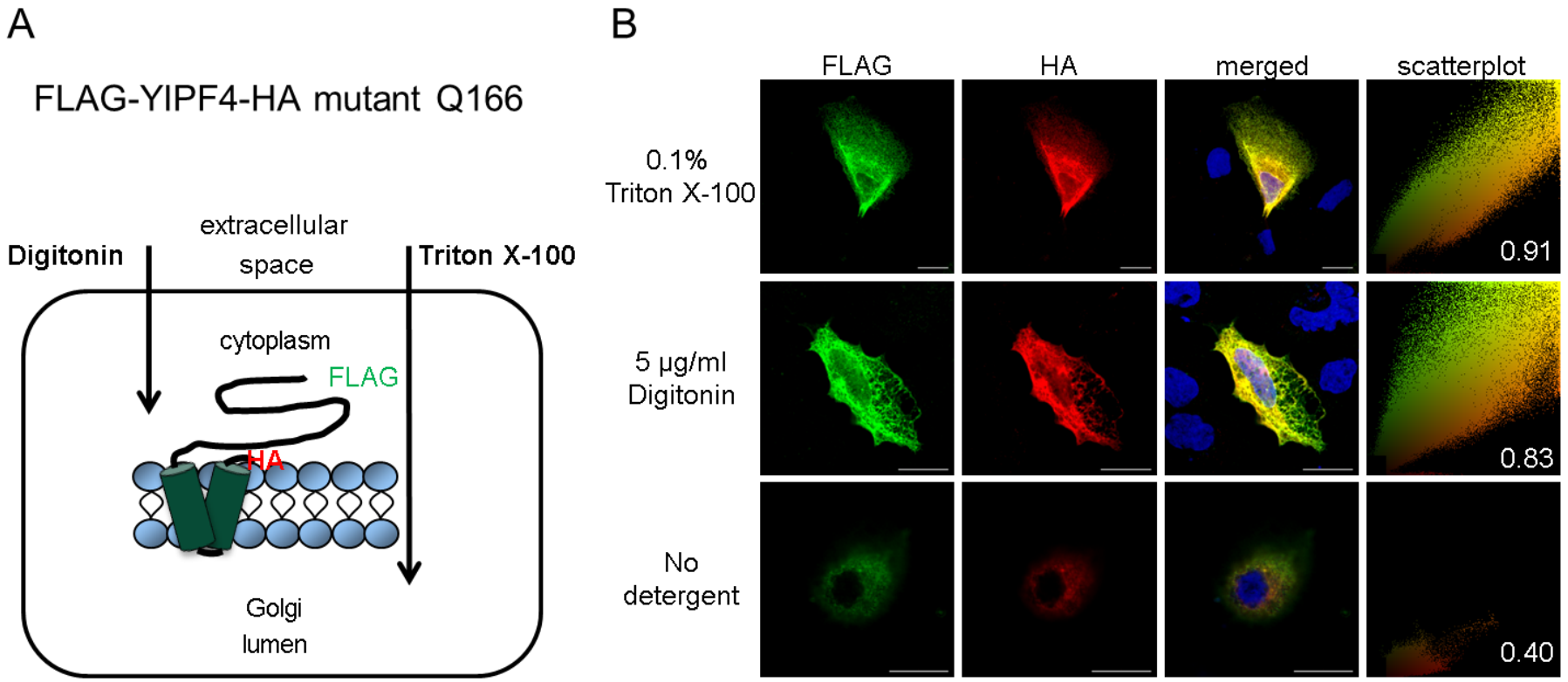

Figure 3.16 Examining the FLAG-YIPF4-HA Q166 truncation mutant in the differential, detergent permeabilisation assay. A. Schematic representation of the FLAG-YIPF4-HA Q166 truncation mutant in the differential, detergent permeabilisation assay. B. Huh7 cells were grown on cover slips and transfected with FLAG-YIPF4-HA Q166. The assay was carried out as described in legend to Figure 3.13. Representative images are shown. Scale bar = 20 µm

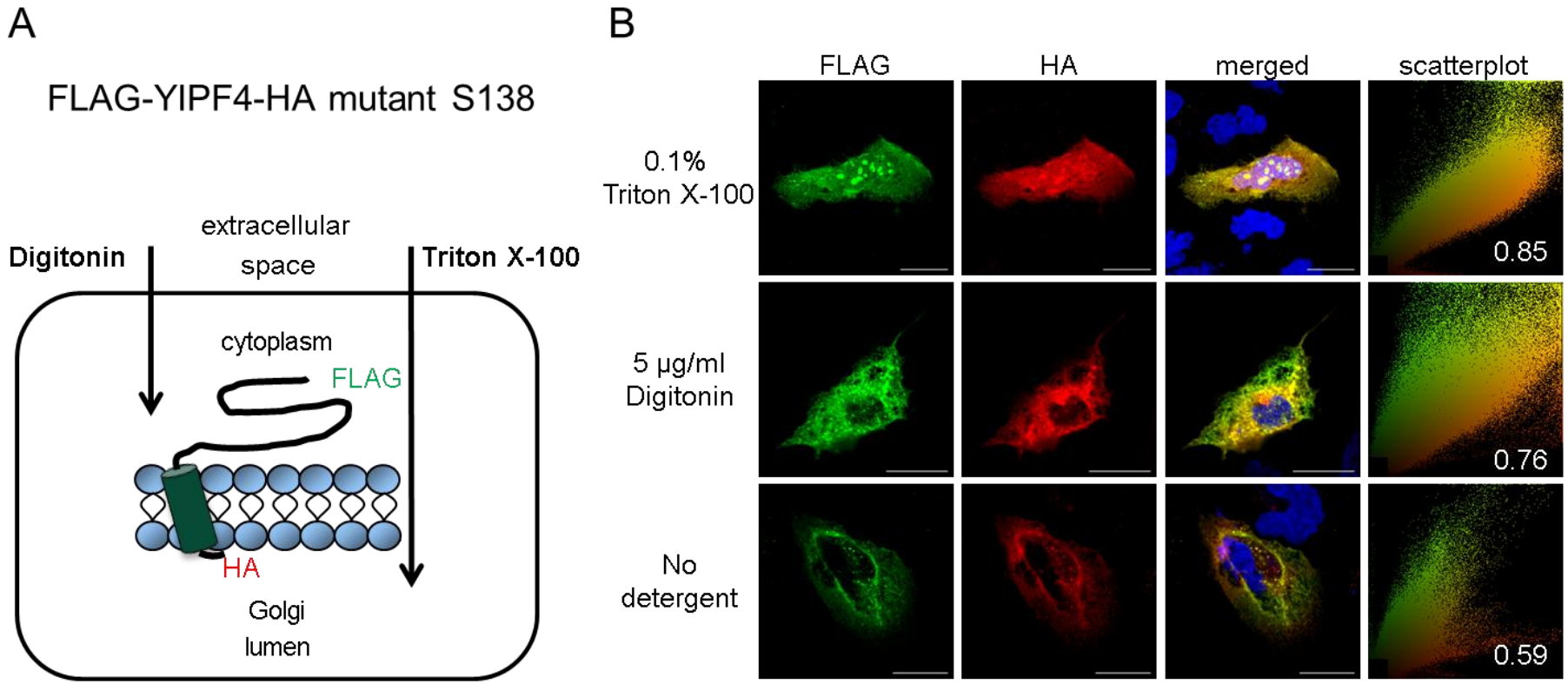

Figure 3.17 Examining the FLAG-YIPF4-HA S138 truncation mutant in the differential, detergent permeabilisation assay. A. Schematic representation of the FLAG-YIPF4-HA S138 truncation mutant in the differential, detergent permeabilisation assay. B. Huh7 cells were grown on cover slips and transfected with FLAG-YIPF4-HA S138. The assay was carried out as described in legend to Figure 3.13. Representative images are shown. Scale bar = 20 µm

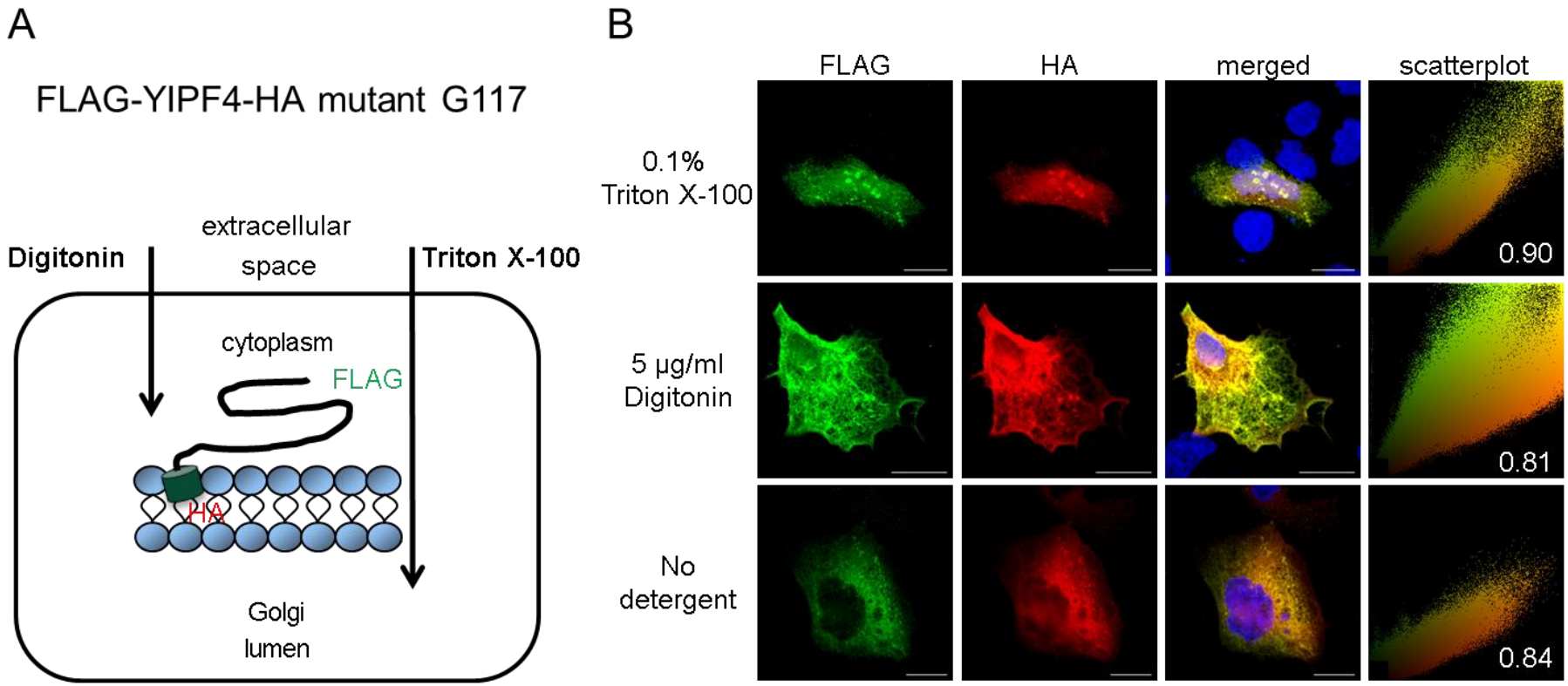

Figure 3.18 Examining the FLAG-YIPF4-HA G117 truncation mutant in the differential, detergent permeabilisation assay. A. Schematic representation of the FLAG-YIPF4-HA G177 truncation mutant in the differential, detergent permeabilisation assay. B. Huh7 cells were grown on cover slips and transfected with FLAG-YIPF4-HA G117. The assay was carried out as described in legend to Figure 3.13. Representative images are shown. Scale bar = 20 µm

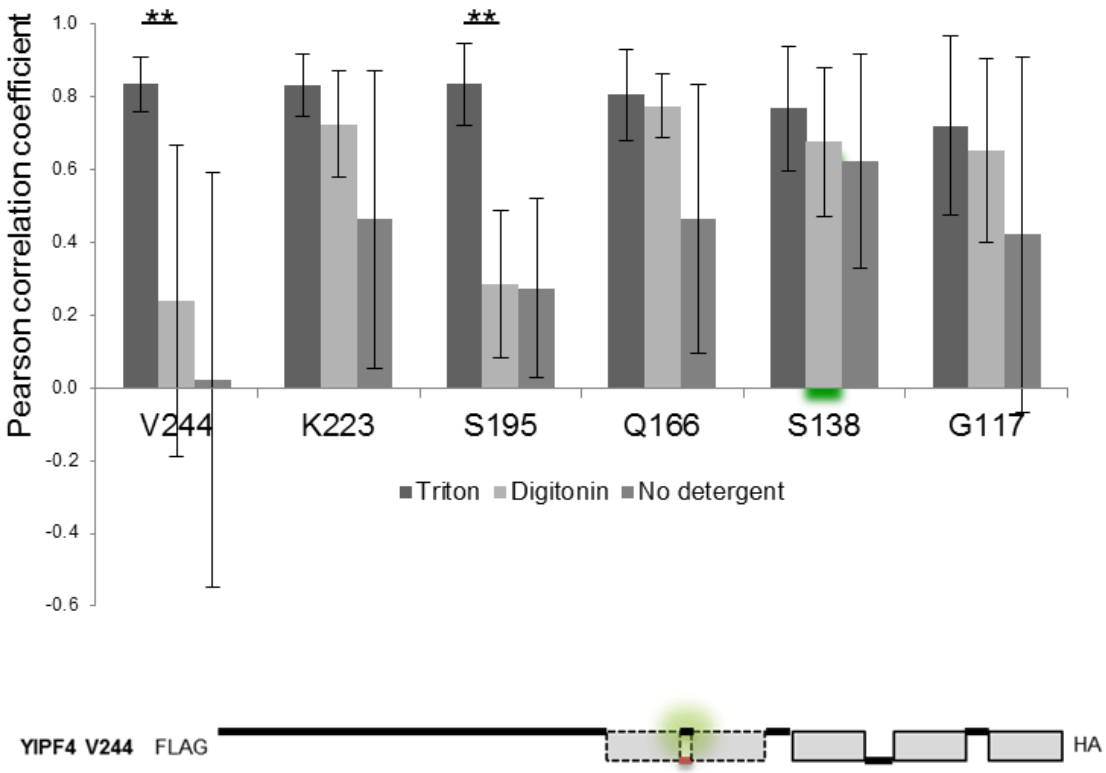

Figure 3.19 Summary of results from the differential, detergent permeabilisation assay. The bar chart compiles the PCC values of the YIPF4 truncation mutants in the differential, detergent permeabilisation assay. Each bar represents the mean PCC value (± SDM) of several cells of two independent repetitions. A one-way ANOVA was performed. **p ≤ 0.01, only selected p-values are shown. The schematic view of the full-length FLAG-YIPF4-HA indicates the position of where the data from the differential, detergent permeabilisation assay digresses from the computational 5 TMD model of YIPF4 (green shadow). The red subscript line describes the computationally predicted position of the hydrophilic linker while the black superscript line indicates the position of the hydrophilic linker according to the differential, detergent permeabilisation assay.Questionable TMDs are depicted with dashed grey boxes.

The findings from the differential, detergent permeabilisation assay implied that YIPF4 forms 3 TMDs only (Figure 3.20B) and questioned the predicted 5 TMD model of YIPF4 (Figure 3.20A). It was interesting to note that the 1st and 3rd TMDs of this proposed 3 TMD model of YIPF4 overlap with 2 of the predicted TMDs of the yeast homologue Yip1p (Figure 3.20C).

The YIPF4 full-length and truncation mutants were additionally examined in a subcellular fractionation experiment (Figure 3.21). BHK-21 cells overexpressing these proteins were fractioned into a soluble and membranous fraction. These were analysed on a Western blot where the fractions were successfully identified with the marker proteins tubulin (soluble fraction) and transferrin receptor (membranous fraction). Truncation mutants that form TMDs were expected to accumulate in the membranous fraction.
Indeed, the full-length V244 (Figure 3.21, lane 2) and K223 (Figure 3.21, lane 4) almost exclusively enriched in the membranous fraction as the amino acids 223 – 244 were shown to span the membrane from the outside-in in the differential detergent permeabilisation assay (Figure 3.13 and Figure 3.14). Also, the majority of the S195 (Figure 3.21, lane 6) and Q166 (Figure 3.21, lane 8) truncation mutants accumulated in the membranous fraction in accordance with the observation made in the differential, detergent permeabilisation assay (Figure 3.15 and Figure 3.16). It was very obvious that the S138 truncation mutant predominantly enriched in the soluble fraction (Figure 3.21, lane 9). This agrees with the fact that no anchoring TMD between amino acids 117 – 138 was found to be formed in the differential, detergent permeabilisation assay (Figure 3.17 and Figure 3.18). The G117 truncation mutants appeared to be equally distributed amongst the soluble and membranous fraction (Figure 3.21, lane 11, 12). A clearer enrichment in the soluble fraction would have been predicted concluding from the differential, detergent permeabilisation assay (Figure 3.18). The Del1-109 mutant was generated to lack the hydrophilic N-terminus of YIPF4. In accordance with this, the majority of Del1-109 protein accumulated in the membranous fraction (Figure 3.21, lane 14). Due to low expression levels when expressed transiently in Huh7 cells, it could not be investigated in the differential, detergent permeabilisation assay. However, its

enrichment in the membranous fraction agrees with the proposed model of YIPF4.

In general, the hydrophobic and hydrophilic properties of the truncation mutants mostly agree with the 3 TMD model of YIPF4 developed from the differential, detergent permeabilisation assay. They therefore depict first evidence towards the establishment of a new TMD model of YIPF4 as a representative for the YIP1 protein family.

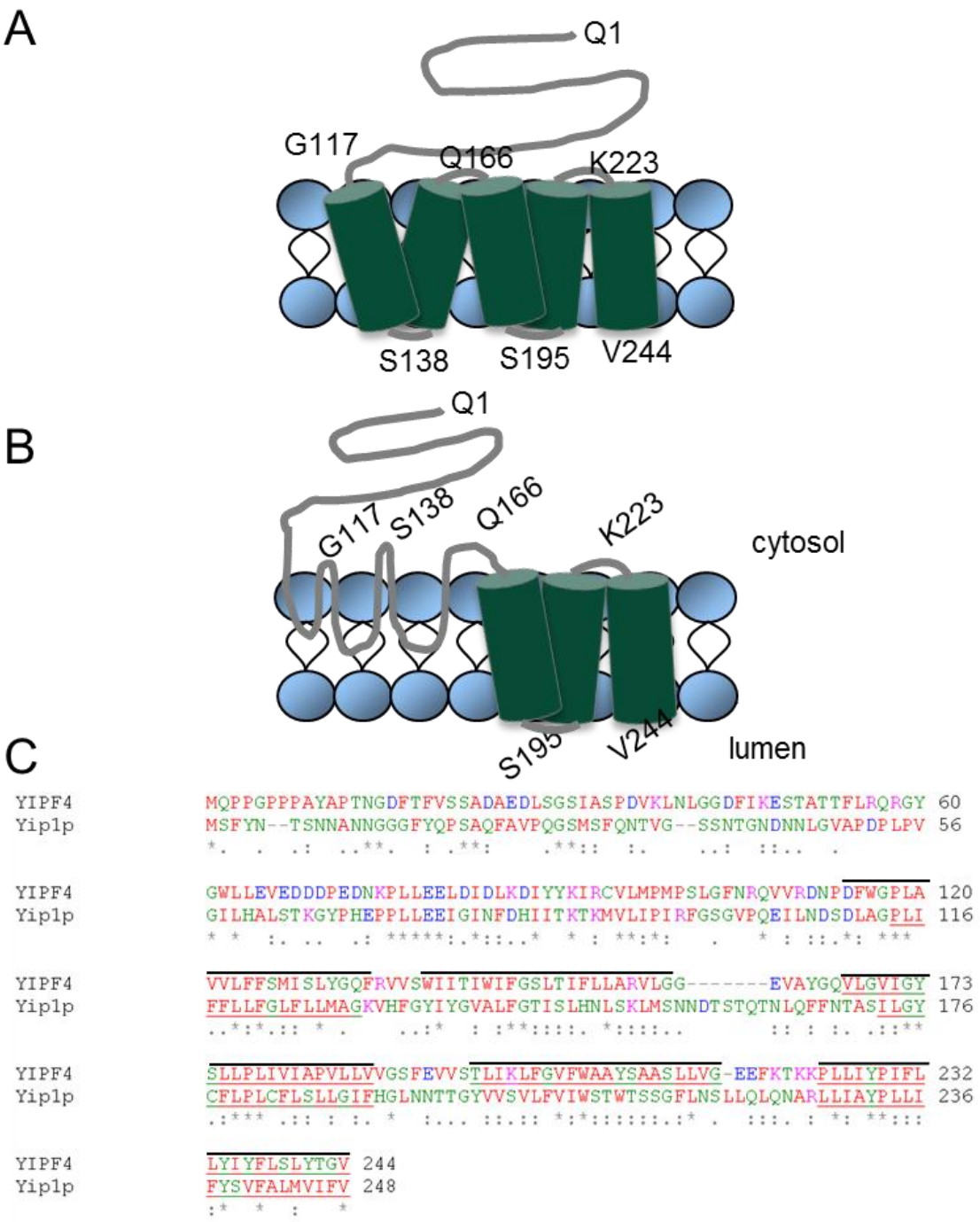

Figure 3.20 Juxtaposition of computational and evidence-based YIPF4 models. A. The 5 TMD model of YIPF4 is purely based on computational predictions. B. The 3 TMD model of YIPF4 was established with the data from the differential, detergent permeabilisation assay. C. Pairwise alignment with ClustalW2 of human YIPF4 and its yeast homologue Yip1p. Black lines = positions of YIPF4 TMD according to 5 TMD model (A), underlining in YIPF4 sequence = positions of 3 TMDs observed in differential, detergent permeabilisation assay (B), underlining in Yip1p sequence = predicted TMDs according to Yang et al., 1998, amino acid colour legend: red = small and hydrophobic (including aromatic without Y), blue = acidic, magenta = basic- without H, green = hydroxyl, sulfhydryl, amine including G; * = single, fully conserved residue, : = conservation between groups of strongly similar properties, . = conservation between groups of weakly similar properties

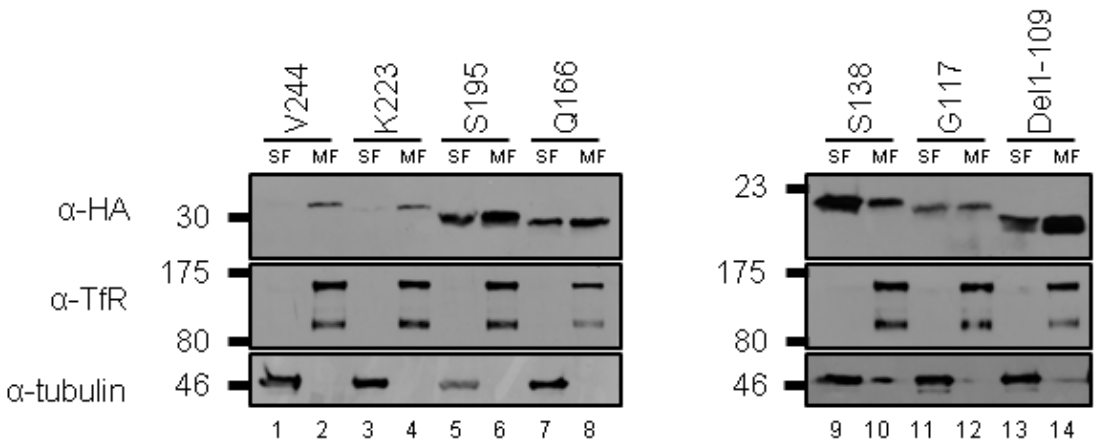

Figure 3.21 Membrane association of the FLAG-YIPF4-HA truncation mutants. FLAG-YIPF4-HA truncation mutants were expressed in BHK-21 cells using the VFT7-3 vaccinia virus. Cells were harvested 24 h post-transfection/infection and the soluble and membranous proteins were separated by ultra-centrifugation. On the Western blot, the FLAG-YIPF4-HA truncation mutants were detected with a HA antibody. TfR = marker for membranous fraction, tubulin = marker for soluble fraction. SF = soluble fraction, MF = membranous fraction, marker in kDa

3.3. Discussion

3.3.1. Expression profile of YIPF4

3.3.1.1. YIPF4 is expressed in various cell lines

To the best of our knowledge, this is the first confirmation of YIPF4 protein expression in a multitude of different cell lines (Figure 3.1 and Figure 3.3). So far, the only evidence for YIPF4 protein expression came from HeLa cells (Tanimoto et al., 2011). Its expression levels did not vary dramatically amongst the tested cell lines (Figure 3.1 and Figure 3.3).
No splicing variants could be detected by qPCR since the primers used did not span a potentially alternatively spliced region. Thus, the existence of multiple splicing variants as seen in a Northern blot approach (Shakoori et al., 2003) is theoretically possible. However, the presence of a single mRNA variant agrees with the Western blot detection of one clear band of the appropriate size for YIPF4. There is no hint of a different splicing form or major post-translational modifications as suggested by large-scale mass spectrometry observations (Hornbeck et al., 2004).

Endogenous YIPF4 exists as a monomer and only when overexpressed (Figure 3.1A, Figure 3.10B+C), it seems to form an additional potential dimer (approximately 58 kDa). The dimerisation could be mediated by a disulphide bond between their C94. However, since proteins were analysed by reducing SDS-PAGE, a hydrophobic interaction is more likely which could be caused by ‘flooding’ the cell with this protein. The potential dimer may therefore be an artefact of overexpression. However, YIPF4 is known to form large protein complexes of unknown composition with its paralogue YIPF3 (Tanimoto et al., 2011). These were not observed under the SDS-PAGE conditions used in this study. It is conceivable that endogenous YIPF4 self-associates within these complexes. A strong self-association was also observed for its paralogue YIPF6 in mice (Brandl et al., 2012). Although an endogenous YIPF4 dimer or protein complex could not be observed under the employed conditions, it cannot be excluded that endogenous YIPF4 self-associates to form dimer or higher order oligomers *in vivo*.

At the same time, a near loss of endogenous YIPF4 protein was observed in the myc-YIPF4 overexpressing cells (Figure 3.1A). It is conceivable that the overexpressed YIPF4 replaces endogenous YIPF4. A similar phenomenon was seen when overexpressing epitope tagged YIPF3 in HeLa cells (Tanimoto et al., 2011) which could be explained by the saturation of the cell with this protein.

The YIPF4 protein expression profile underlines the large-scale microarray data that described YIPF4 mRNA expression in a multitude of human tissues (MGC, 2004, Ohira et al., 2003, Ota et al., 2004) (summarised at http://biogps.org/). It also implies that YIPF4 is highly conserved amongst species since YIPF4 protein was detected in monkey and hamster kidney cell lines using the commercial antibody raised against the hydrophilic N-terminus of human YIPF4. Indeed, YIPF4 proteins of several animals have previously been identified and show a high grade of conservation when aligned to human YIPF4 (Figure A. 2). This study, however, reports first evidence of a potential hamster YIPF4 protein (Figure 3.1, lane 13). To validate its identity, mass spectroscopy identification or sequencing of its cDNA can be employed. Similar cross-reactivities of antibodies were previously observed for other mammalian YIP1 family members. An antibody raised against rat YIF1B cross-reacted with porcine YIF1B (Carrel et al., 2008) and an antibody raised against murine YIPF5 recognised YIPF5 in HeLa, Vero and normal rat kidney cells (Kano et al., 2009, Tang et al., 2001). It is therefore highly likely that the protein of approximately 27 kDa identified in the BHK-21 cell lysate with the antibody raised against human YIPF4 is indeed hamster YIPF4.

Despite the fact that the cellular role of YIPF4 is not understood yet, the expression of the protein in every cell line tested and its high grade of conservation suggest it might exert important housekeeping functions. Indeed, its paralogue YIPF5 has been proposed to function as a housekeeping gene because it is predicted to be transcribed from a characteristic TATA-box less promoter (Stolle et al., 2005). Further research is needed to determine the cellular functions of YIPF4 and further YIP1 family members.

3.3.1.2. YIPF4 is expressed in cells and sites relevant to HPV infection

Of great significance for the further course of this study was the validation of YIPF4 protein expression in cells that are theoretically susceptible and permissive to HPV infection (C33A, HaCaT, HFK) and cells that already carry a HPV genome (HPV16 = CaSki, SiHa; HPV18 = HeLa, HFK HPV18) (Figure 3.1 and Figure 3.3). Also, YIPF4 protein was clearly identified in clinical samples of HPV16 induced CIN1 and CIN3 lesions (Figure 3.5). But co-staining for more viral proteins is required to confirm the presence of YIPF4 in the same cells. Co-staining for its potential interaction partner 16E5 is currently not possible due to the lack of an effective E5 antibody. These findings nevertheless provide the crucial confirmation that YIPF4 is indeed expressed in sites relevant for HPV pathogenesis.

Above all, its expression in CaSki cells is an important evidence to justify the interaction of 16E5 with YIPF4 that was seen in Y2H system, LUMIER assay and TAP-MS (1.7). This is because, in contrast to SiHa cells, 16E5 protein expression could be confirmed by mass spectrometry in CaSki cells (Sahab et al., 2012).

3.3.1.3. YIPF4 might play a role in the productive phase of the HPV life-cycle

In undifferentiated HFKs, YIPF4 protein expression is not regulated differently in HPV18 negative and positive cells (Figure 3.3) suggesting that it might not be directly involved or needed for HPV genome maintenance.

We obtained some indication that in differentiated HFK HPV18 cells and thus in the productive phase of the HPV life-cycle, YIPF4 protein is slightly up-regulated or rescued compared to untransfected HFKs (Figure 3.6). This up-regulation was also confirmed on transcript level (Figure 3.7). This could imply a role for YIPF4 during genome amplification and/or virus assembly and/or release.

Notably, this effect was only seen in the MC differentiation model and not in the organotypic raft cultures (Figure 3.4). In the organotypic raft cultures YIPF4

protein was expressed in the basal, suprabasal and granular cell layers in untransfected HFKs to the same extend as in HFK HPV18 cells. Thus, there appears to be a discrepancy between these two *in vitro* models.

The differentiation of cells in organotypic raft cultures is induced by lifting the cell culture onto an air-liquid interface (Wilson and Laimins, 2005). This faithfully recapitulates epithelial cell differentiation allowing for generation of ample amounts of infectious virus stocks of HPV16 (McLaughlin-Drubin et al., 2004), HPV18 (Meyers et al., 1997), HPV31b (Ozbun and Meyers, 1997) and HPV45 (McLaughlin-Drubin et al., 2003). This system is therefore capable of supporting the entire HPV life-cycle although it is prone to variability.

The cell differentiation in MC cultures is induced by loss of contact to the culture dish (Wilson and Laimins, 2005). The use of a late p670 promoter luciferase reporter confirmed transcription of late HPV16 genes in this system (Bodily et al., 2013). A Northern blot approach revealed the transcription from the late HPV31 promoter p742 (Ruesch et al., 1998) and the expression of cellular differentiation markers involucrin and transglutaminase were demonstrated. However, no significant amounts of L1 protein could be observed. This establishes the fact that the monolayer MC cell differentiation model only allows limited completion of the HPV life-cycle.

The organotypic raft cultures are more faithful models for cell differentiation and the complete HPV life-cycle but protein and transcript expressions are harder to quantify than in MC cultures. The stratified nature of the raft cultures hardly allows the investigation of separated cell layers. In this study, the YIPF4 protein expression was attempted be quantified by fluorescence intensity profiles (Figure 3.4C) on a limited number of histological sections. This approach, however, does not correct for different cell numbers and positions in the section and it does not give the possibility to normalise to a reference protein.

On the contrary, the monolayer MC cell cultures are characterised by uniformity in cell differentiation. It is easily possible to extract ample amounts of protein and RNA. The determination of protein levels by densitometry analysis of Western blots (Figure 3.6B) and especially the evaluation of transcript levels by qPCR (Figure 3.7A) are more convincing methods for YIPF4 quantification.

In line with the more meaningful data obtained from the MC differentiation model, YIPF4 might be directly or indirectly up-regulated by HPV proteins or might play a role in the HPV life-cycle.

Since nothing is known about YIPF4 transcriptional regulation, the natural hypothesis would be to suspect the potential interaction with 16E5 as the cause for the rescue of YIPF4 mRNA and protein levels. Indeed, 16E5 was shown to up-regulate COX-2 expression by enhancing its promoter activity mainly as a result of EGF-R signalling pathway and NF-κB binding (Kim et al., 2009). Therefore, an indirect up-regulation of YIPF4 mRNA and protein by E5 is conceivable. 16E5 was also shown to have an effect on protein half-life when reducing the half-life of $p27^{Kip1}$ via the EGF-R pathway (Pedroza-Saavedra et al., 2010) and targeting CD1d for proteasomal degradation (Miura et al., 2010). Thus, an effect of 16E5 on YIPF4 half-life is feasible. However, the regulation of YIPF4 transcript and protein expression is likely to be independent of its proposed binding to E5 (3.2.5, 3.2.5.1).

Therefore, another hypothesis for the HPV controlled YIPF4 regulation emerges. The transcription of YIPF4 might be promoted by the HPV E2 protein (Figure 3.8) because it has well characterised functions in transcriptional regulation (McBride, 2013).

Transcriptional regulation by 16E2 was observed for a multitude of host genes in a microarray approach (Ramirez-Salazar et al., 2011). 16E2 was expressed from an adenoviral vector in C33A cells and the down-regulation of 1048 and up-regulation of 581 host genes was observed. However, YIPF4 or other immediate YIP1 family members were not amongst the regulated genes in this approach.

Also, functional and biochemical analysis confirmed an interaction of 18E2 with a variety of cellular proteins that regulate transcription (Figure 3.8B). It is conceivable that YIPF4 transcription is regulated by any of these proteins and a chromatin immuno-precipitation approach might help elucidating this.

Very interestingly, the YIPF4 gene region has eight potential E2BS (Figure 3.8A). The markedly increased YIPF4 transcription (Figure 3.7A) and thus the slightly increased protein levels (Figure 3.6B) could thus also be caused by

direct binding of the E2 protein to YIPF4 regulatory sequences. A direct transcriptional up-regulation by HPV E2 was indeed observed for several host genes. The expression of the host splicing protein SF2/ASF was activated by the binding of 16E2 to its regulatory sequence as shown by chromatin immuno-precipitation and electrophoretic mobility shift assay (Mole et al., 2009). Also, the activity of the interleukin-10 promoter was shown to be increased by binding of 16E2 protein (Bermúdez-Morales et al., 2011). A reporter gene assay revealed that increased matrix metalloproteinase-9 promoter activity is directly induced by the HPV8 E2 protein in a dose-dependent manner (Akgül et al., 2011).

However, E2 protein favours an A/T-rich spacer in the consensus DNA-binding site (Dell et al., 2003) which is only given in two (bp 12839-12850, 27482-27493, Figure 3.8A) of the eight potential E2BS in the YIPF4 gene region. In addition to that, E2 binding and transcriptional regulation of host genes was reported to be a rare event. A computational analysis identified 3388 potential E2BS in the human genome, however, only a minority was indeed accessible to 11E2 and cellular transcription was not affected for selected genes in SiHa, HaCaT and U-2 OS cells (Võsa et al., 2012).

Thus, the potential transcriptional regulation of YIPF4 by HPV E2 proteins needs to be investigated e.g. with chromatin immuno-precipitation and a reporter assay.

3.3.2. YIPF4 topology and cellular localisation

The investigation of YIPF4 topology with the differential, detergent permeabilisation assay was the first time experimental evidence has been generated for the complete membrane topology of a YIP1 family member (Figure 3.13 - Figure 3.19).

It confirmed the overall orientation of the N-terminus facing the cytoplasm and the C-terminus facing the organelle lumen which was previously determined by others for YIPF1, YIPF2 and YIPF3 (3.1.2) (Shakoori et al., 2003). However, it suggests the formation of 3 TMDs rather than the predicted 5 TMDs. Three TMDs were also proposed for its homologue in yeast, Yip1p, (Yang et al., 1998) but the positions of the TMDs do not agree entirely (Figure 3.20C).

The SOSUI model denotes the most N-terminal TMD (amino acids 112-134) as a secondary TM helix which is characterised by high hydrophilicity (Hirokawa et al., 1998). In the 3 TMD model established here, this region does not form a membrane spanning domain but it is assumed to at least partially reside in the membrane. This is supported by the cellular distribution of the S138 and G117 truncation mutants when overexpressed in Huh7 cells. In some cells, they show soluble-protein-like distribution throughout the cells, including the nucleus (Figure 3.17B and Figure 3.18B), and in others, their localisation appears ER-like which requires membrane association (Figure A. 1). A similar observation was made for GFP tagged truncation mutants of the YIP1 family member YIF1A (Jin et al., 2005). The truncation mutant consisting of the hydrophilic N-terminus only was diffuse throughout the cell while the truncation mutant comprising the hydrophobic C-terminus showed an ER-like staining pattern. Thus, the cellular localisations of the YIPF4 truncation mutants agree with observations made on YIF1A and the hydrophilic properties of a secondary TM helix according to the SOSUI computational prediction. This secondary TM helix has great potential of mediating protein-protein interactions (Hirokawa et al., 1998) or exerting other yet unknown functions of YIPF4.

There is, however, the possibility that the folding of YIPF4 is altered by the truncations made to the protein in this assay. More experimental evidence,

ideally a crystal structure, needs to be established to firmly validate the 3 TMD topology of YIPF4.

The membrane topology of its potential interaction partner 16E5 was investigated in a similar fashion determining its orientation in the membrane and partially confirming its 3 TMD model (Krawczyk et al., 2010). Thus, both YIPF4 and 16E5 are membrane proteins. Their interaction is therefore likely to be mediated by either their hydrophobic TMD or their hydrophilic, cytoplasm exposed termini. Also, both proteins are known to localise at the Golgi making their interaction probable (Figure 3.4B) (Schapiro et al., 2000, Tanimoto et al., 2011).

YIPF4 was shown to localise at the *trans*-Golgi network in SiHa cells (Figure 3.4B) which is in contrast to its firmly established localisation at the *cis*-Golgi in HeLa cells (Tanimoto et al., 2011). YIPF4 cellular localisation might differ between cell lines or the HPV18 proteins in HeLa cells and the HPV16 proteins in SiHa cells might induce slight alterations to its localisation. The staining with the *cis*-Golgi marker GM130 was not successful in this study (data not shown). Thus it cannot be excluded that YIPF4 also partially localises to the *cis*-Golgi in SiHa cells.

YIPF4 shows a distribution that resembles ER and sometimes nuclear envelope staining when overexpressed and epitope tagged in Huh7 cells (Figure 3.13 - Figure 3.18). The ER localisation of overexpressed, GFP tagged YIPF4 was also observed in an automated immuno-fluorescence approach (Simpson et al., 2000). So clearly, overexpression alters the subcellular localisation of this protein. A possible explanation for this ER and nuclear envelope distribution is that the protein cannot form complexes with its cellular binding partners e.g. YIPF3, and therefore accumulates in the ER (Tanimoto et al., 2011). This was observed for other members of the YIP1 family (Andrulis et al., 1998, Shakoori et al., 2003, Yang et al., 1998).
However, we could show that overexpression does not have an effect on the membrane association of YIPF4 (Figure 3.10) so the differential, detergent permeabilisation assay remains valid.

To further confirm that the integral membrane property of YIPF4 is not affected by its epitope tags, the subcellular fractionation into membranous and soluble proteins can be repeated under treatment of disrupted cells with high salt, high Urea, alkaline pH and detergent (Matern et al., 2000). YIPF4 as an integral membrane protein rather than a membrane associated protein is only expected to solubilise in the presence of detergent. Also, a phase separation assay is conceivable (Bordier, 1981) to firmly establish the integral membrane properties of YIPF4. These assays could also be employed on the FLAG-YIPF4-HA truncation mutants to further support the membrane association seen in the subcellular fractionation experiment (Figure 3.21).

The truncation mutant FLAG-YIPF4-HA Del1-109 could not be investigated in the differential, detergent permeabilisation assay since its expression was extremely low for unknown reasons. A similar unexplained low expression was observed with FLAG-YIPF4-HA S138 and G117 (Figure 3.12). Others observed that the overexpression efficiency of YIPF5, YIPF6 and YIF1B in HeLa cells was limited (Shakoori et al., 2003). Also, YIPF5 deletion mutants were not stable and even a single amino acid substitution in the predicted 3rd and 4th TMDs resulted in a highly unstable protein (Dykstra et al., 2013). This indicates that different parts of the YIP1 proteins mediate protein stability maybe due to correct folding. It is conceivable that the YIPF4 truncation mutants Del1-109, G117 and S138 are degraded because of folding into a less stable protein. Indeed, cell treatment with the proteasome inhibitor MG132 increased the overall GFP-YIPF4 S138, G117 and Del1-109 levels in Huh7 cells indicating that the truncation mutants are increasingly degraded by the proteasome (Figure A. 3). A correct folding of YIPF4 ‘truncation’ mutants might be achievable by replacing the ‘truncated’ sequence with repetitive sequences rather than deleting these completely.

In addition to the low expression efficiency, the FLAG-YIPF4-HA Del1-109 truncation mutant appears to be smaller than its predicted molecular weight (Figure 3.12C). This could be caused by formation of a condensed and not entirely denatured conformation on the Western blot due to its high hydrophobicity.

The FLAG-YIPF4-HA G117 truncation mutant showed another expression anomaly by apparently expressing less FLAG epitope than HA epitope although the sequence of the expression construct was confirmed. A possible explanation is that the FLAG epitope is less accessible to the FLAG antibody due to post-translational modification in this specific truncation mutant. A post-translational modification of the HA tag in FLAG-YIPF3-HA was reported to hamper the recognition with an HA antibody in HeLa cells (Tanimoto et al., 2011). However, the FLAG epitope could be detected in the differential detergent permeabilisation assay (Figure 3.6) ruling out a post-translational modification of the epitope.

Thus far, it was established that YIPF4 protein is widely expressed and is likely to play a role in HPV infected cells and tissue. Overexpression of YIPF4 causes artefacts like dimerisation and alteration of subcellular localisation. We proposed the first evidence-based 3 TMD topology of YIPF4 which might serve as a model for other YIP1 family members. Further investigations will address the confirmation and characterisation of the interaction of YIPF4 with E5 (Chapter 4) and the search for a potential role of the E5/YIPF4 complex (Chapter 5).

Chapter 4. Characterisation of the interaction between YIPF4 and E5

4.1. Introduction

HPV16 E5 protein is a small hydrophobic protein consisting of 83 amino acids, which arranges into 3 putative trans-membrane α-helices (Bubb et al., 1988, Wetherill et al., 2012a). The majority of 16E5 localises to the ER, the Golgi, the nuclear envelope and to a lesser extent the plasma membrane (Conrad et al., 1993, Hu and Ceresa, 2009, Oetke et al., 2000, Schapiro et al., 2000). This information is, however, purely derived from overexpression systems due to a lack of antibody detection reagents.

To date, no intrinsic enzymatic activity has been demonstrated for E5 so it is assumed that E5 exerts most its functions by interacting with proteins of the host cell. Recently purified 16E5 protein was identified as a viroporin consisting of a potential homo-hexamer (Wetherill et al., 2012a). The *in vitro* channel activity of E5 could be specifically blocked with a *de novo* designed small molecule inhibitor. This might be the first description of an intrinsic function of 16E5 proteins. With the cellular role of the viroporin formation yet to be determined the recognition of new cellular targets of E5 will provide a better understanding of its roles during the HPV life-cycle, host cell transformation and immune evasion.

The E5 proteins of the PVs share the presence of highly hydrophobic regions but their amino acid conservation is generally negligible (Bravo and Alonso, 2004). This implicates the absence of a conserved binding motif, although the highly hydrophilic C-terminus of the E5α family, whilst not conserved in amino acid sequence, is regarded as a main interaction mediator to host cell proteins as well as 4 di-leucine motifs in the 1st TMD of 16E5 (Regan and Laimins, 2008, Cortese et al., 2010).

For HPV E5, there are no points of reference from conserved binding motifs and homologies to proteins of other viruses that could assisted in the identification of host binding partners which is in contrast to the HPV E6 and E7 oncoproteins (1.5.6, 1.5.7). Therefore, the E5 interaction partners and their binding regions were mostly determined with a common set of assays combining Co-IPs and occasional observation of cellular localisation.

Co-IPs revealed that the HC of HLA-A2 binds to the 1st TMD of 16E5. Here, 2 of the 4 di-leucine motifs at positions 11/12 and 22/23 were found responsible for binding (Ashrafi et al., 2006b, Cortese et al., 2010). A direct co-localisation of the proteins in the host cell, however, was not shown.

The HLA HC and 16E5 are part of a ternary protein complex also including the chaperone calnexin (Gruener et al., 2007). Co-IPs with a codon adapted, mutant 16E5 which features a disrupted 1st TMD revealed that calnexin binds to the 1st TMD of 16E5. Immuno-fluorescence analysis was intended to show a co-localisation of GFP/AU1 tagged 16E5 and endogenous calnexin, but successful calnexin staining is debatable. The co-localisation with calnexin was, however, confirmed in keratinocytes with E5-AU1 expressed by retroviral transduction (Disbrow et al., 2003).

The binding region of 16E5 to the 16 kDa subunit of the vacuolar H^+ - ATPase (16K) is controversial. Co-IPs were performed with overexpressed untagged 16E5 truncation mutants and epitope tagged 16K in COS-7 cells (Adam et al., 2000). These identified amino acids 41 - 54 as the binding region with their hydrophobicity being crucial. The performance of similar Co-IPs, however, with *in vitro* translation of the proteins in microsomal membranes revealed amino acids 54 - 78 as the 16K binding region (Rodriguez et al., 2000). This discrepancy might be a result of the different experimental techniques used. The cellular co-localisation of the proteins was not shown in these studies.

Another 16E5 binding partner with identified binding region is the ER-localised protein Bap31 (Regan and Laimins, 2008). Its binding region was mapped to the 10 most C-terminal amino acids of 16E5 by performing Co-IPs with overexpressed, epitope tagged 16E5 truncation mutants and endogenous Bap31. The co-localisation of AU1 tagged 16E5 and endogenous Bap31 was confirmed in the HPV31 positive cell line CIN612.

The same 10 amino acids of 16E5 were found to be responsible for binding to KNβ3 (Krawczyk et al., 2008a). This is in accordance with the prediction of the hydrophilic C-terminus to be a mediator for interactions with host cell proteins. Co-IPs using endogenous KNβ3 and overexpressed, AU1 tagged 16E5 confirmed this. The overlapping localisation of AU1-16E5 and endogenous KNβ3 in COS-7 and primary human ectocervical cells was demonstrated by confocal microscopy.

This short list of cellular binding partners with located binding regions illustrates the common set of assays used to confirm new cellular targets for HPV E5 proteins. Due to lack of reliable antibodies to E5 and partly low expression efficiency, the analysis of overexpression systems is required. This implies performing Co-IPs with overexpressed and epitope tagged E5 and their respective mutants for determination of the binding region. Also, overlapping cellular localisations are determined referring to the overexpressed E5 protein. The advent of specific E5 antibodies would allow investigation of interactions with cellular proteins at physiological expression levels.

Due to the lack of conserved binding motifs, a newly found cellular target of one E5 protein needs reinvestigation for E5 proteins of other PV types. And indeed, the MHC HC was bound by the most C-terminal amino acids 32 - 44 of BPV4 E5 (Marchetti et al., 2005), which is in contrast to the N-terminal di-leucine binding site of 16E5. The binding to HLA HC was confirmed for the high-risk HPV83 E5 (Ashrafi et al., 2006a) but the binding region was not established. A functional association with HLA was also observed with the cutaneous HPV2a E5 (Cartin and Alonso, 2003), the low-risk HPV6b (Ashrafi et al., 2005) and BPV1 E5 (Ashrafi et al., 2002) but the direct binding to HC was not investigated. A clear difference in binding was seen with 16K where the glutamine residue at position 17 of BPV1 E5 was defined as mediator for 16K binding (Andresson et al., 1995). For 16E5, hydrophobic interactions were deemed responsible for binding to 16K (Adam et al., 2000). The binding to the low-risk HPV6 E5 was confirmed but the exact binding region could not be determined (Conrad et al., 1993). A similar observation was made with the low-risk HPV11 E5a where an

interaction was established but the binding region could not be determined (Chen et al., 1996d).
These findings illustrate that the poorly conserved E5 proteins can act on the same host cell targets but with completely independent mechanisms. Closer investigation of these differences might help to elucidate variations between high-risk, low-risk and cutaneous HPV types as well as their ungulate relatives.

The E5 proteins, however, do not act alone on the host cell but in the context of the other HPV proteins. Especially the three oncoproteins E5, E6 and E7 seem to complement the function of each other.
In this manner both 16E5 and 16E6 might modify vesicular trafficking of the host cell. HPV16 E6 was shown to target the cystic fibrosis trans-membrane regulator-associated ligand for degradation which could alter the exocytic and endocytic vesicular trafficking it is involved in (Jeong et al., 2007). Also, 16E5 modulates trafficking by rearranging the actin cytoskeleton (Thomsen et al., 2000) or impairing membrane fusion events (Suprynowicz et al., 2010).
In an assay with primary baby rat kidney cells, the cell proliferation and colony formation was significantly enhanced when 16E5 and 16E7 were co-expressed compared to cells expressing 16E7 only (Bouvard et al., 1994a). This indicates that they might collaborate to promote cell proliferation in favour of the HPV life-cycle *in vivo*. The same enhancement was observed for immortalisation of primary human keratinocytes by HPV when cells harbour an additional E5 gene in *cis* (Stöppler et al., 1996). The co-expression of 16E5 and 16E7 also promoted cell transformation as shown by the enhancement of anchorage-independent growth (Valle and Banks, 1995). This was reinforced with transgenic mouse models which express single HPV16 oncoproteins or a combination of those (Maufort et al., 2010). The development of tumours in 16E5/16E6 and 16E5/16E7 expressing mice, respectively, was greater than in mice expressing 16E6 and 16E7 individually. The complementary effects in cell transformation of the HPV oncoproteins was thus neatly proven from primary rodent cells to primary human cells to transgenic mouse models.

A novel interaction of 16E5 and YIPF4 was detected in a semi-automated Y2H screen against a HeLa cell and a human testis epithelial cell library (1.7). This

interaction was then reiterated in a LUMIER assay performed in HEK293 cells. The presence of YIPF4 in cell lines susceptible and permissive to HPV as well as in organotypic raft cultures and CIN1/3 samples was established in the previous Chapter (Chapter 3).

In this chapter, we sought to investigate the interaction of 16E5 with YIPF4 further using the well-established methods of Co-IP and detection of cellular co-localisation by confocal microscopy. Truncation mutants of both 16E5 and YIPF4 are used to locate the binding regions of the two proteins. Because of the occasional cooperation of 16E5 with 16E6 and 16E7, a possible interaction of YIPF4 with these oncoproteins is investigated. The conservation of this interaction is examined by screening E5 proteins of a representative panel of PV types for their binding to YIPF4.

4.2. Results

4.2.1. YIPF4 immuno-precipitated with 16E5

The binding of YIPF4 to 16E5 was examined by Co-IP to verify the interaction seen in the Y2H screen, LUMIER assay and TAP-MS (1.7). First, exogenous, epitope tagged proteins were used. GFP-16E5 and FLAG-YIPF4-HA as well as negative control proteins were expressed in HEK293T cells and the cell lysate subject to Co-IP using a GFP antibody (Figure 4.1A, schematic). The Western blots confirmed that FLAG-YIPF4-HA was bound specifically by GFP-16E5 (Figure 4.1A, lane 1). The epitope tag control proteins FLAG-Optineurin and HA-Optineurin were not pulled down by GFP-16E5 (lane 2, 3) eliminating the possibility that GFP-16E5 bound to the FLAG and/or HA epitope tag of FLAG-YIPF4-HA. It was ruled out that the GFP tag of GFP-16E5 mediates binding to FLAG-YIPF4-HA because free GFP did not interact with FLAG-YIPF4-HA (lane 4). The GFP antibody targeted to bind GFP-16E5 did not non-specifically bind FLAG-YIPF4-HA (lane 5) nor did the uncoupled beads (lane 6). Thus, 16E5 and YIPF4 interacted specifically in this Co-IP approach with overexpressed bait and prey proteins.

In order to verify this interaction with more physiological levels of protein, a Co-IP was performed with endogenous YIPF4 as bait (Figure 4.1B, schematic). However, due to the unavailability of a 16E5 antibody, the overexpressed GFP-16E5 fusion protein was used as prey. The Western blot confirmed that endogenous YIPF4 specifically bound to GFP-16E5 (Figure 4.1B, lane 1). Comparison with the overexpressed FLAG-YIPF4-HA and GFP-16E5 positive control (lane 2) showed a much weaker band for GFP-16E5 when bound to endogenous YIPF4 (lane 1). This might indicate that at physiological protein levels not all YIPF4 was bound by GFP-16E5. The negative control, GFP, was not pulled down by endogenous YIPF4 (lane 3), which underlines the specificity of the 16E5/YIPF4 interaction. Notably, endogenous YIPF4 non-specifically bound to the uncoupled beads (lane 4). This, however, does not affect the specificity of the 16E5/YIPF4 interaction seen.

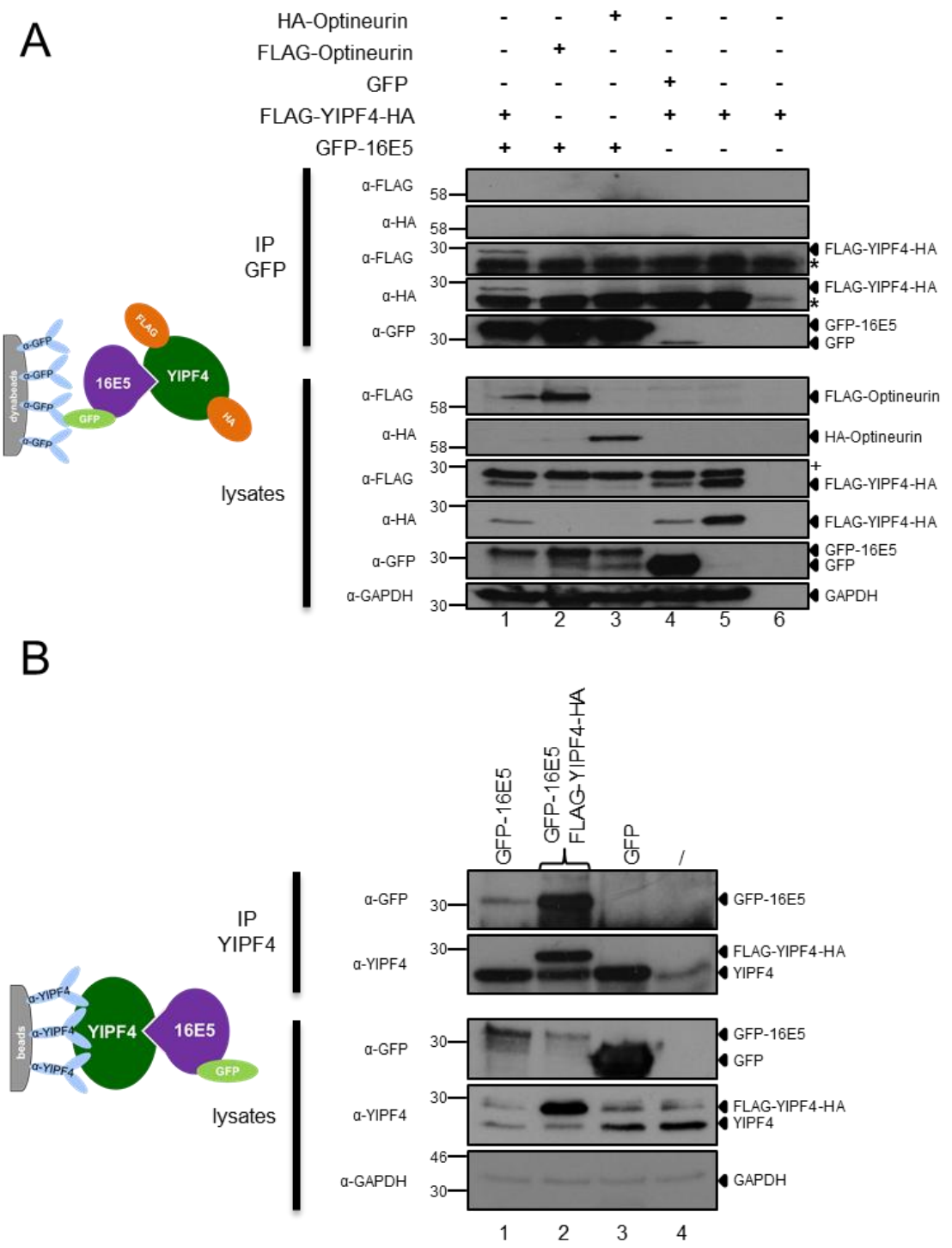

Figure 4.1 Co-IPs confirming the interaction of YIPF4 with 16E5. A. FLAG-YIPF4-HA and GFP-16E5 as well as negative control proteins (GFP, FLAG-Optineurin, HA-Optineurin) were overexpressed in HEK293T cells. Co-IPs were performed with a GFP antibody on dynabeads (schematic) and equal amounts of total proteins. Lane 6 holds the uncoupled beads control. ‘ * ‘ = GFP antibody light chain; ‘ + ‘ = unspecific band B. GFP-16E5, GFP (negative control) and FLAG-YIPF4-HA (positive control) were overexpressed in HEK293T cells. Co-IPs were performed with the YIPF4 antibody on dynabeads to pull down endogenous YIPF4 (schematic). Equal amounts of total protein were used. ’ / ‘ = cell lysate without overexpressed proteins incubated with uncoupled beads. Marker in kDa (A + B).

It was noted that co-transfected constructs expressed less efficiently than single transfected constructs. This became obvious by comparing the relative amount of FLAG-YIPF4-HA when co-expressed with GFP-16E5 and GFP, respectively (Figure 4.1A, lane 1 and 4), to the amount when overexpressed alone (Figure 4.1A, lane 5). Its expression was clearly less in co-expressing cells. Co-transfection also affected the GFP-16E5 expression since its protein amount was dramatically decreased when co-expressed with FLAG-YIPF4-HA (Figure 4.1B, lane 1 and 2). In addition, expression of GFP-16E5 but not GFP seemed to reduce the amount of endogenous YIPF4 (Figure 4.1B, lane 1 and 3). However, these varying amounts of protein did not inhibit binding of bait and prey in these Co-IP experiments.

4.2.2. YIPF4 bound to the 2nd TMD of 16E5

Thus far, the interaction of 16E5 and YIPF4 was clearly confirmed by Y2H screen, LUMIER assay (1.7) and Co-IP (Figure 4.1). The site of 16E5 responsible for binding to YIPF4 was determined by Co-IP using 16E5 truncation mutants.

HPV16 E5 is proposed to have 3 TMDs (Figure 4.2A) which were used as a basis to generate 5 truncation mutants (Figure 4.2B) (Ashrafi et al., 2006b). The TMDs and their linker sequences were sequentially truncated from the C-terminus. Only the Del1 mutant was designed to lack the most N-terminal TMD. All truncation mutants and the full-length 16E5 T83 protein were created with a GFP tag at the N-terminus. The theoretical molecular weights of these proteins were calculated with the ‘Protein Molecular Weight Calculator’-online tool.

Co-IPs were performed with the full-length FLAG-YIPF4-HA as bait and the GFP fusion proteins of 16E5 truncation mutants as prey (Figure 4.2C, schematic). Clear binding to YIPF4 was observed for the full-length GFP-16E5 T83 (lane 1) as well as R79 (lane 2) and A54 (lane 3) (Figure 4.2C). In contrast, the V36 (lane 4) and R30 (lane 5) truncation mutants showed strikingly reduced binding to YIPF4 while the Del1 truncation mutant (lane 6) was recognisably bound by YIPF4. This suggests that YIPF4 predominantly binds to amino acids 37 - 54 of 16E5. These amino acids form the 2nd TMD of 16E5 including the linker to the 3rd TMD.

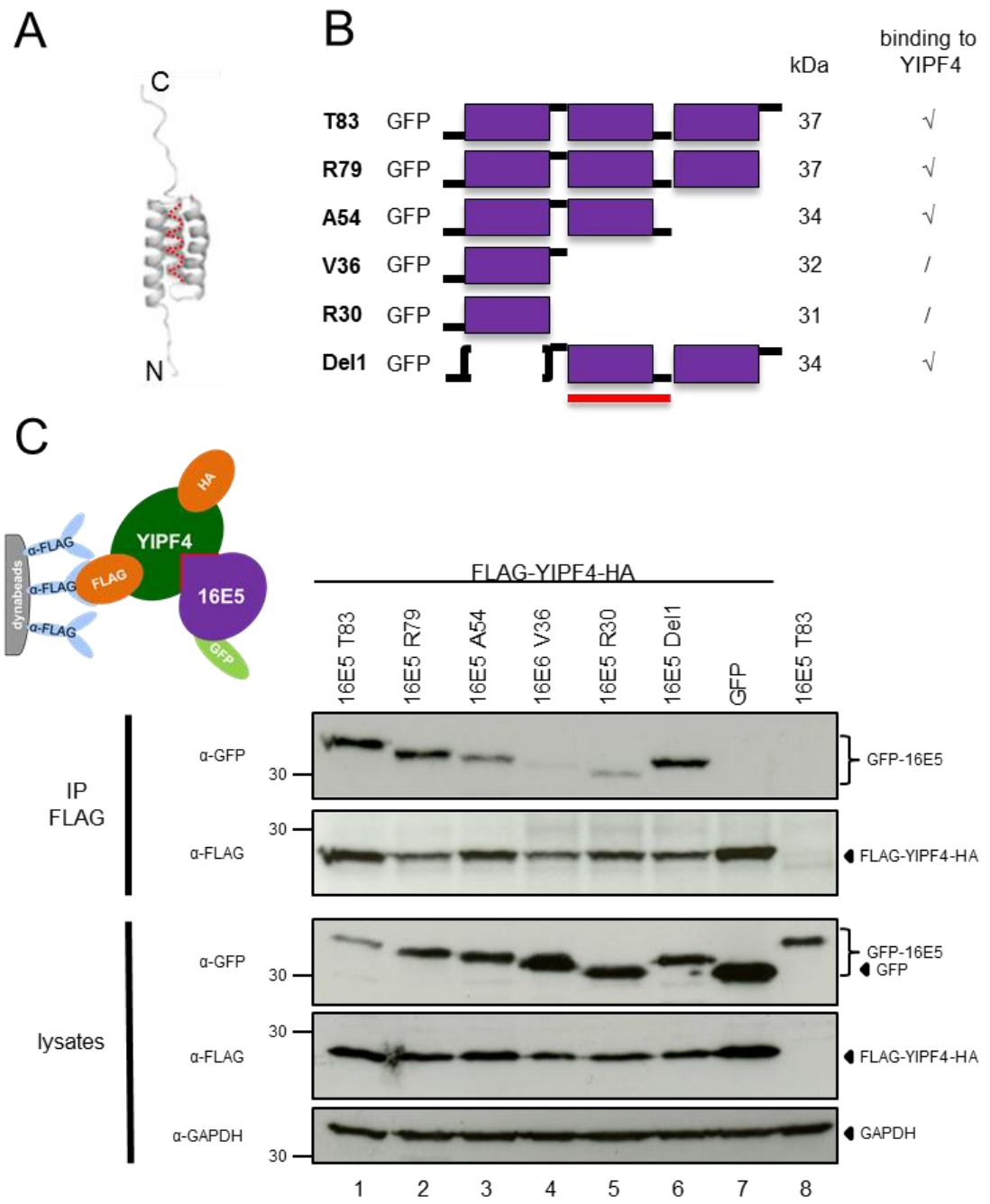

Figure 4.2 Mapping of 16E5 binding sites to FLAG-YIPF4-HA. A. Model of 16E5 as a monomer with 3 TMDs. Adapted from Wetherill et al., 2012a. B. Schematic representation of 16E5 truncation mutants as GFP fusion proteins. The designated name for each truncation mutant is indicated on the left and consists of the one letter amino acid code and number of the final amino acid before truncation (counting the amino acids of 16E5 only). The Del1 truncation mutant forms an exemption (Del1 = deletion of 1st TMD). Boxes represent TMDs and black lines indicate luminal (subscript) and cytoplasmic (superscript) sites ' √ ' = mutant bound to YIPF4; ' / ' = mutant bound very little to YIPF4. C. Co-IPs of GFP-16E5 truncation mutants with FLAG-YIPF4-HA. GFP-16E5 truncation mutants were co-expressed alongside FLAG-YIPF4-HA in HEK293T cells (including GFP as negative control). The Co-IPs were performed with equal amounts of total protein using dynabeads and FLAG antibody (schematic). Representative blot is shown. Marker in kDa. Red highlights (A, B, C) indicate binding site of YIPF4.

To investigate the cellular localisation of full-length GFP-16E5, the truncation mutants and FLAG-YIPF4-HA, the proteins were overexpressed in Huh7 cells. After fixation, the cells were stained with a FLAG antibody, imaged and the PCC values between the GFP fusion proteins and FLAG-YIPF4-HA were determined using the PSC plug-in for ImageJ (Figure 4.3).

Both, the full-length GFP-16E5 T83 and FLAG-YIPF4-HA showed an ER-like cellular distribution and a reasonable co-localisation (PCC value = 0.66) (Figure 4.3). However, in other cells of the same sample, FLAG-YIPF4-HA showed a Golgi-like cellular distribution which exhibited reduced co-localisation with the ER-like localised GFP-16E5 T83 (0.17).

This Golgi-like localisation of YIPF4 was observed when co-expressed with the GFP-16E5 truncation mutants. The GFP-16E5 truncation mutants did not visibly alter their ER-like localisation with decreasing protein length. As expected from the deviating cellular distribution, the PCC values revealed that a co-localisation with FLAG-YIPF4-HA was virtually absent for the GFP-16E5 R79 (PCC value = 0.10), A54 (0.24) and Del1 (0.22) truncation mutants. Only GFP-16E5 V36 (0.50) and R30 (0.59) showed a reasonable co-localisation with FLAG-YIPF4-HA. Thus, against expectations, the GFP-16E5 truncation mutants that bound to FLAG-YIPF4-HA (Figure 4.2C) did not co-localise with it but the non-binding GFP-16E5 V36 and R30 truncation mutants exhibited increased co-localisation with FLAG-YIPF4-HA.

The PCC values of two independent experiments were analysed to statistically evaluate this finding (Figure 4.4). Indeed, the localisation of the full-length GFP-16E5 T83 coincided to some extent with the mixed cell populations of ER- and Golgi-like localised FLAG-YIPF4-HA (PCC value = 0.43 ± 0.27). The GFP-16E5 truncation mutants R79 (0.08 ± 0.13), A54 (0.18 ± 0.08) and Del1 (0.23 ± 0.15) did not co-localise markedly with FLAG-YIPF4-HA, although their binding was confirmed by Co-IP (Figure 4.2C). The GFP-16E5 V36 (0.50 ± 0.06) and R30 (0.53 ± 0.09) truncation mutants showed increased co-localisation with FLAG-YIPF4-HA although binding of these proteins was strikingly weak (Figure 4.2C).

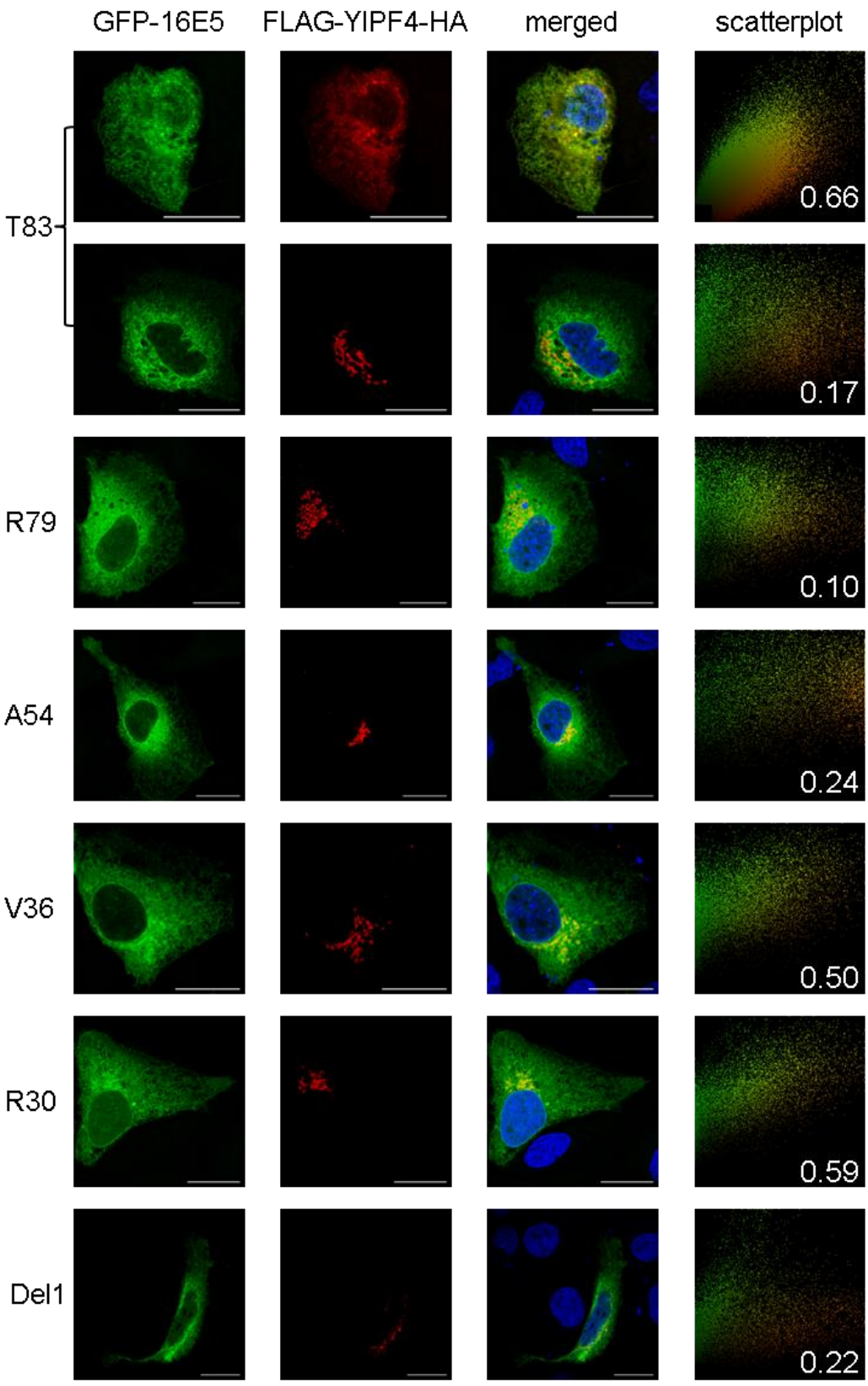

Figure 4.3 Determination of the cellular localisations of GFP16-E5 truncation mutants and FLAG-YIPF4-HA. Huh7 cells overexpressing GFP fusions of 16E5 truncation mutants and FLAG-YIPF4-HA were stained with FLAG antibody. Cell nuclei were labelled with DAPI (blue). Images were acquired with Zeiss LSM700 confocal microscope and analysed for co-localisation of GFP-16E5 and FLAG-YIPF4-HA with the PSC tool. The scatterplots illustrate the PCC values. Representative images are shown. Scale bars = 20 µm

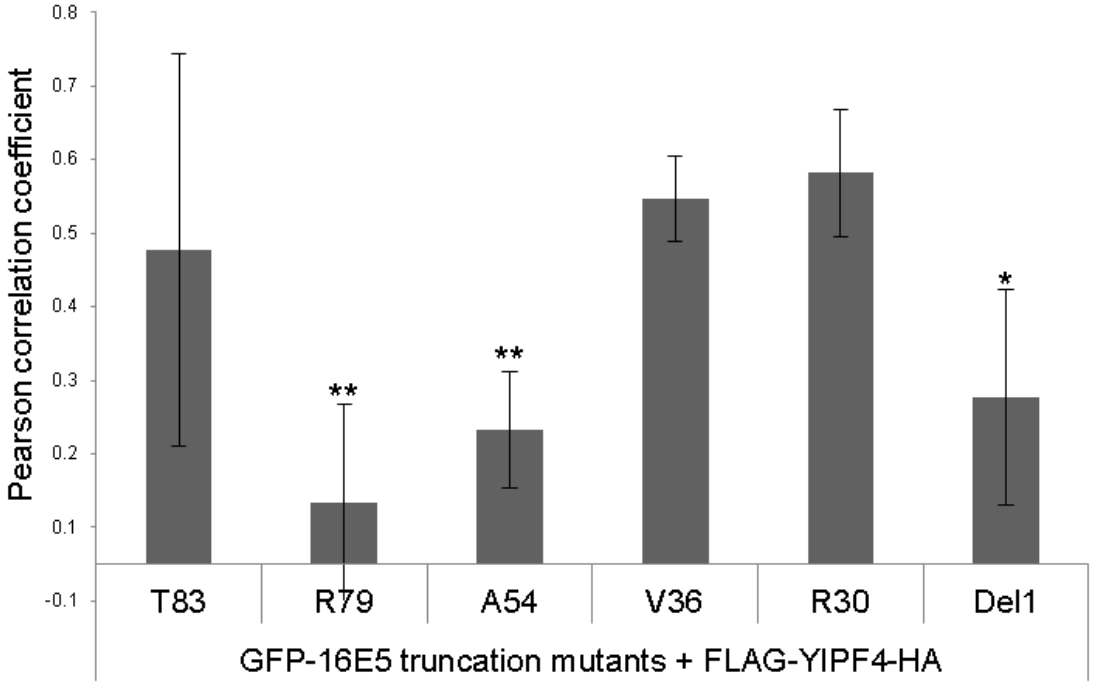

Figure 4.4 PCC values of GFP-16E5 truncation mutants and FLAG-YIPF4-HA. Each bar represents the mean PCC value (± SDM) of several cells (n ≥ 10 cells/sample) of two independent experiments (except one experiment only for GFP-16E5 Del1). A one-way ANOVA was performed. *p ≤ 0.05, **p ≤ 0.01

The co-localisation experiment was performed with overexpressed FLAG-YIPF4-HA and GFP-16E5 truncation mutants in the Huh7 liver carcinoma cell line (Figure 4.3). It was observed that overexpression of YIPF4 leads to an alteration of its cellular distribution (3.3.2). It was investigated whether a co-localisation of the interacting proteins can be observed in a more physiologically relevant expression system. For this, the HPV16 positive cell line SiHa was used to examine the co-localisation of endogenous YIPF4 with the full-length GFP-16E5 and its truncation mutants.

The full-length GFP-16E5 and the truncation mutants were exogenously expressed in SiHa cells. The cells were fixed, stained for endogenous YIPF4 and imaged. All GFP-16E5 constructs showed an ER-like distribution while endogenous YIPF4 clearly exhibited its previously observed Golgi staining pattern (Figure 4.5 and Figure 3.4B).

As to expect from the cellular distribution, the localisation of GFP-16E5 did not markedly overlap with the endogenous YIPF4 protein (PCC value = 0.09). Also, the GFP-16E5 truncation mutants that were shown to bind to FLAG-YIPF4-HA (Figure 4.2C), did not co-localise with the endogenous protein (R79 = 0.10; A54 = 0.05; Del1 = -0.05). Only the GFP-16E5 V36 and R30 truncation mutants showed a marked increase in the level of co-localisation with endogenous YIPF4 (V36 = 0.63; R30 = 0.68) despite the finding that their binding was recognisably reduced (Figure 4.2C).

Repetition of this experiment confirmed the conflicting absence of co-localisation of endogenous YIPF4 with its binding partners GFP-16E5 truncation mutants R79 (PCC value = 0.02 ± 012), A54 (0.14 ± 0.18) and Del1 (-0.01 ± 0.1) and the full-length T83 (-0.04 ± 0.17)(Figure 4.6). A significant increase in co-localisation of endogenous YIPF4 with the non-binding truncation mutants V36 (0.54 ± 0.11) and R30 (0.56 ± 0.08) was observed ($p \leq 0.01$).

Thus, the paradox findings from the overexpression system in Huh7 cells (Figure 4.3 and Figure 4.4) agree with the observations made in the more physiological relevant expression system (Figure 4.5 and Figure 4.6). According to these, YIPF4 did not localise to the same cellular compartment as its GFP-16E5 interaction partners but shares localisation with the non-binding GFP-16E5 truncation mutants V36 and R30.

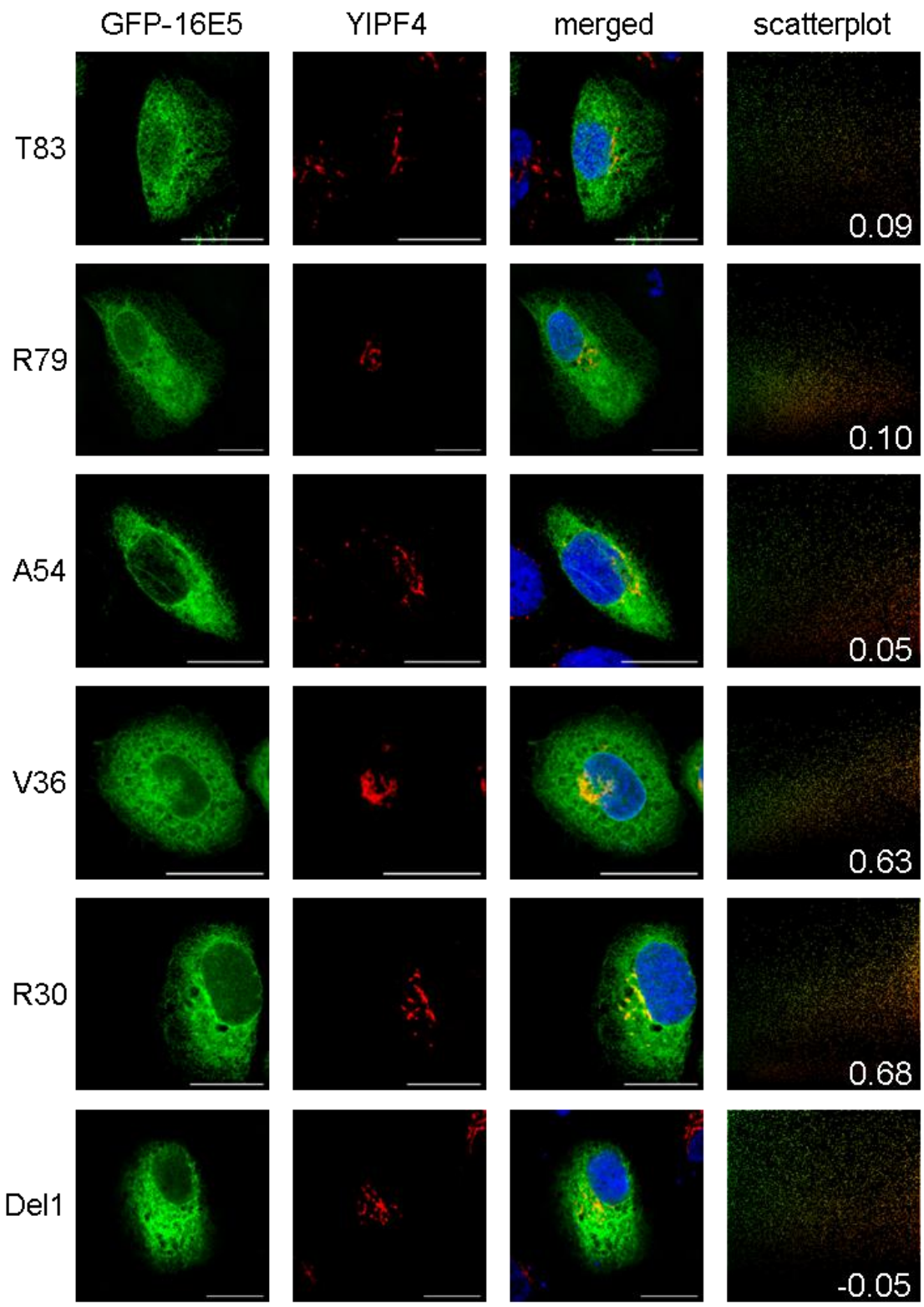

Figure 4.5 Cellular localisation of 16E5 mutants and endogenous YIPF4. SiHa cells overexpressing GFP tagged 16E5 truncations mutants were stained with the YIPF4 antibody. Cell nuclei were labelled with DAPI (blue). Images were acquired with Zeiss LSM700 confocal microscope and analysed for co-localisation of GFP-16E5 and YIPF4 using the PSC tool. The scatterplots illustrate the PCC values. Representative images are shown. Scale bars = 20 µm

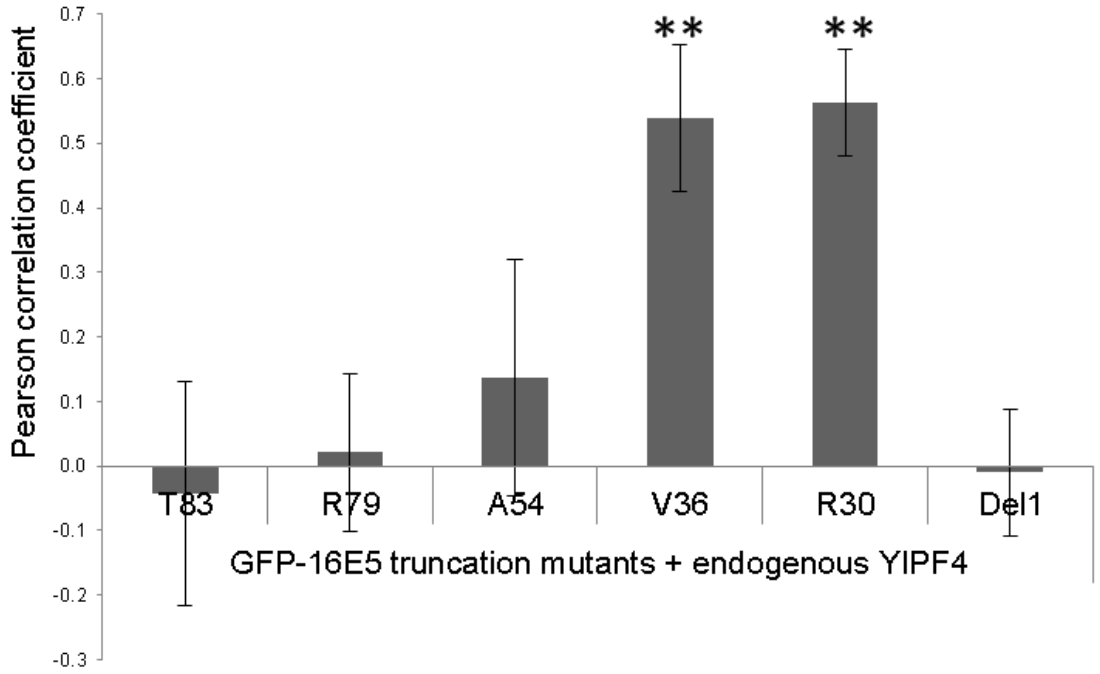

Figure 4.6 PCC values of GFP-16E5 truncation mutants and endogenous YIPF4. Each bar represents the mean PCC value (± SDM) of several cells (n ≥ 8 cells/sample) of two independent experiments. A one-way ANOVA was performed **p ≤ 0.01

4.2.3. The amino acids 118 - 138 and the cellular localisation of YIPF4 were crucial for 16E5 binding

There is no information on binding domains of YIPF4 to other proteins. Therefore, the binding region to 16E5 was investigated with YIPF4 truncation mutants in a Co-IP approach. The FLAG-YIPF4-HA truncation mutants (Figure 4.7B) were used as bait and are shown based on the novel 3 TMD model of YIPF4 (Figure 4.7A) previously established (3.2.6). GFP-16E5 served as prey. Proteins were overexpressed in HEK293T cells.

The expression levels of the FLAG-YIPF4-HA truncation mutants varied as seen before (Figure 3.12). The K223, S138, Q166 and G117 truncation mutants (Figure 4.7C, lane 2, 3, 4, 6) showed reasonable expression but S138 and the full-length V244 expressed very little (Figure 4.7C, lane 1, 5). No expression was detectable for the Del1-109 mutant and therefore its binding to GFP-16E5 could not be examined.

The Co-IPs revealed that FLAG-YIPF4-HA V244, K223, S195 and Q166 were clearly bound by GFP-16E5 (Figure 4.7C, lanes 1, 2, 3, 4). A faint band corresponding to GFP-16E5 could be observed in the Co-IP with the S138 truncation mutant (Figure 4.7C, lane 5). Given the weak expression of this bait protein, the detection of a little amount of prey was rated as protein binding. The G117 truncation mutant was no longer bound by GFP-16E5 (Figure 4.7C, lane 6). Negative controls confirmed that the GFP tag of 16E5 did not bind to FLAG-YIPF4-HA (Figure 4.7C, lane 8) nor did GFP-16E5 non-specifically bind to the antibody coupled beads (Figure 4.7C, lane 9). Therefore, this Co-IP approach mapped the binding region of 16E5 to amino acids 118 - 138 of YIPF4.

The cellular localisation of the YIPF4 truncation mutants in relation to 16E5 was determined in SiHa cells. The YIPF4 truncation mutants were expressed as GFP fusion proteins alongside Cherry-FLAG tagged 16E5.
Notably, expressed as a GFP fusion protein, most YIPF4 truncation mutants showed an ER-like cellular distribution (Figure 4.8). Only the G117 truncation mutant was distributed throughout the cell including the nucleus. Also, the Cherry-FLAG-16E5 protein exhibited an ER-like distribution pattern.
The co-localisation was determined with the PSC plug-in for ImageJ. In accordance with the ER-like cellular localisation, the full-length GFP-YIPF4 V244 depicted co-localisation with Cherry-FLAG-16E5 (PCC value = 0.85). The YIPF4 truncation mutants that bound to 16E5 in the Co-IP assay were clearly co-localising (K223 = 0.84; S195 = 0.80; Q166 = 0.84; S138 = 0.65). The G117 truncation mutants that did not bind 16E5 displayed reduced co-localisation (G117 = 0.43) as its cellular localisation was not limited to the ER but distributed throughout the cell. Expression as a GFP fusion protein allowed the detection of the Del1-109 truncation mutants that could not be investigated for 16E5 binding in the Co-IP assay (Figure 4.7C). It clearly co-localised with Cherry-FLAG-16E5 (Del1-109 = 0.89) (Figure 4.8).

The statistical analysis of several cells revealed that the YIPF4 truncation mutants that are bound by 16E5 indeed co-localised (PCC value for V244 = 0.77 ± 0.12; K223 = 0.82 ± 0.10; S195 = 0.83 ± 0.06; Q166 = 0.82 ± 0.05; S138 = 0.70 ± 0.10) (Figure 4.9). Also, the GFP-YIPF4 Del1-109 truncation mutant

which could not be analysed in the Co-IP assay co-localised with Cherry-FLAG-16E5 (Del1-109 = 0.82 ± 0.12). This might indicate that 16E5 is able to bind to this truncation mutant. It would agree with the fact that Del1-109 contains the identified binding region of amino acids 118 - 138. The co-localisation of the G117 truncation mutant with 16E5 was significantly reduced (0.38 ± 0.13; $p \leq 0.01$). The conjoined reduced co-localisation and loss of binding raises the possibility that the co-localisation plays an important role for the interaction of 16E5 to YIPF4.

Overall the findings so far confirm that YIPF4 is indeed a new cellular target of 16E5. It binds YIPF4 at amino acids 118 - 138 when they are co-localised (Figure 4.9). YIPF4 binds to the 2nd TMD of 16E5 but significant co-localisation was not detected in this experiment (4.2.2).

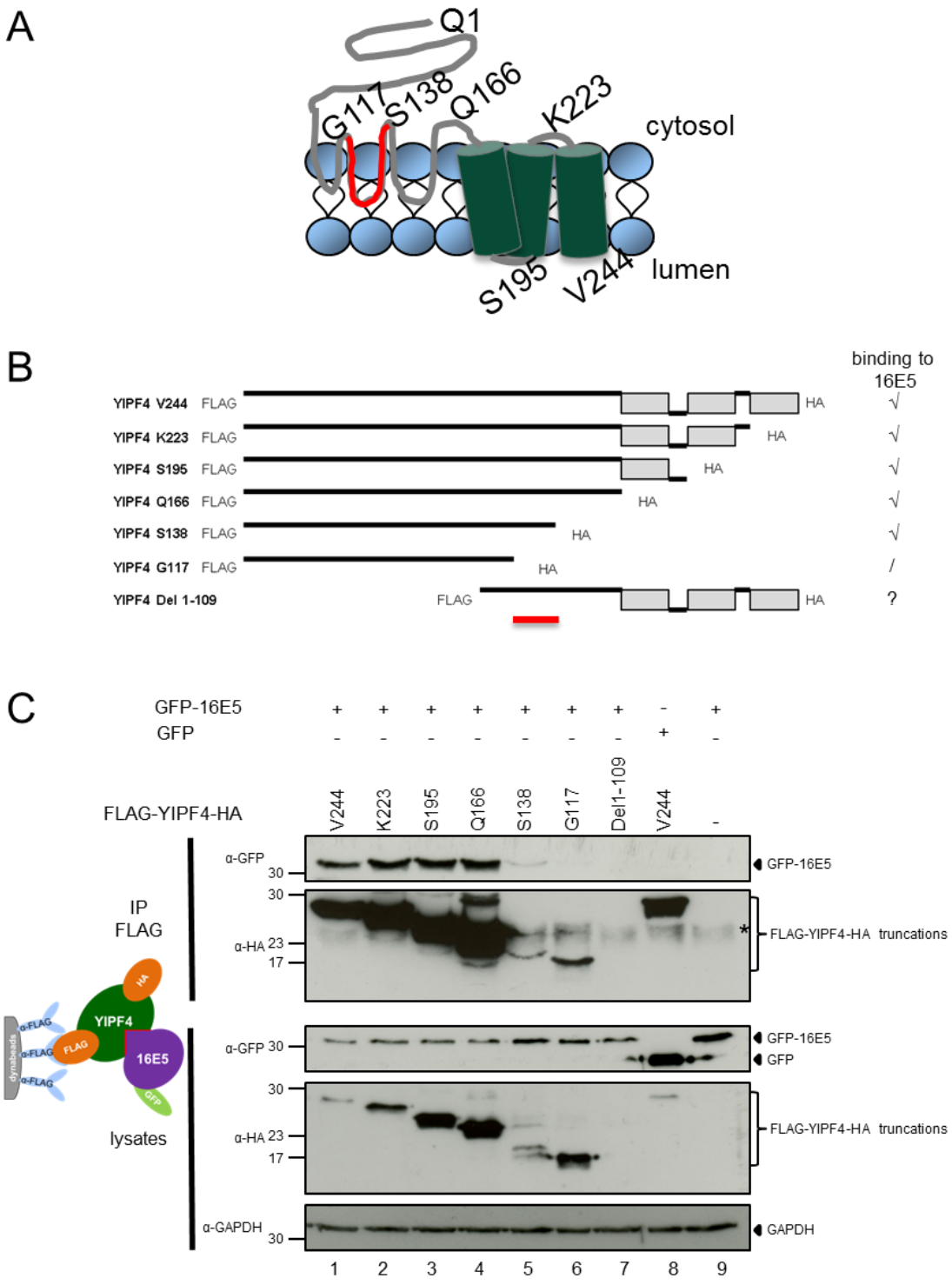

Figure 4.7 Mapping of YIPF4 binding sites to 16E5. A. YIPF4 topology model according to the differential, detergent permeabilisation assay (3.2.6.3.3). B. Schematic representation of FLAG-YIPF4-HA truncation mutants based on the 3 TMD model of YIPF4. ' √ ' = truncation mutant bound to YIPF4; ' / ' = truncation mutant did not bind to YIPF4; ' ? ' = truncation mutant was not investigated. C. Co-IP of FLAG-YIPF4-HA truncation mutants with GFP-16E5. Epitope tagged 16E5 and YIPF4 truncation mutants were overexpressed in HEK293T cells. The Co-IPs were performed with equal amounts of total protein with FLAG antibody on dynabeads (schematic). A representative blot is shown. Marker in kDa. * = antibody light chain. Red highlights (A, B, C) indicate binding region.

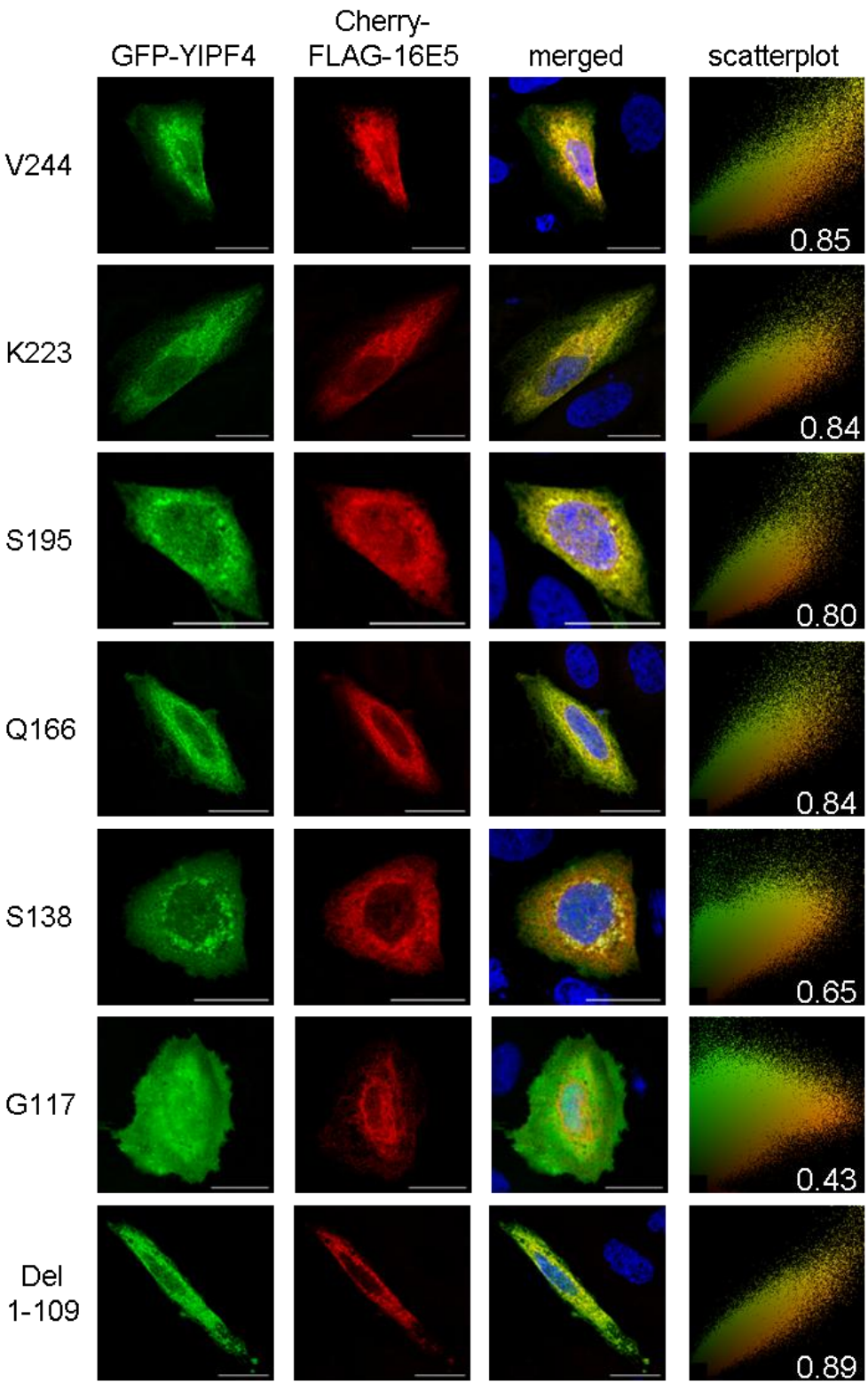

Figure 4.8 Cellular localisation of GFP-YIPF4 truncation mutants and Cherry-FLAG-16E5. SiHa cells overexpressing GFP fusion proteins of YIPF4 truncation mutants and Cherry-FLAG-16E5 were fixed and imaged using a Zeiss LSM700 confocal microscope. Images were analysed for co-localisation of GFP-YIPF4 truncation mutants and Cherry-FLAG-16E5 using the PSC tool. The scatterplots illustrate the PCC values. Representative images are shown. Cell nuclei were labelled with DAPI (blue). Scale bars = 20 µm

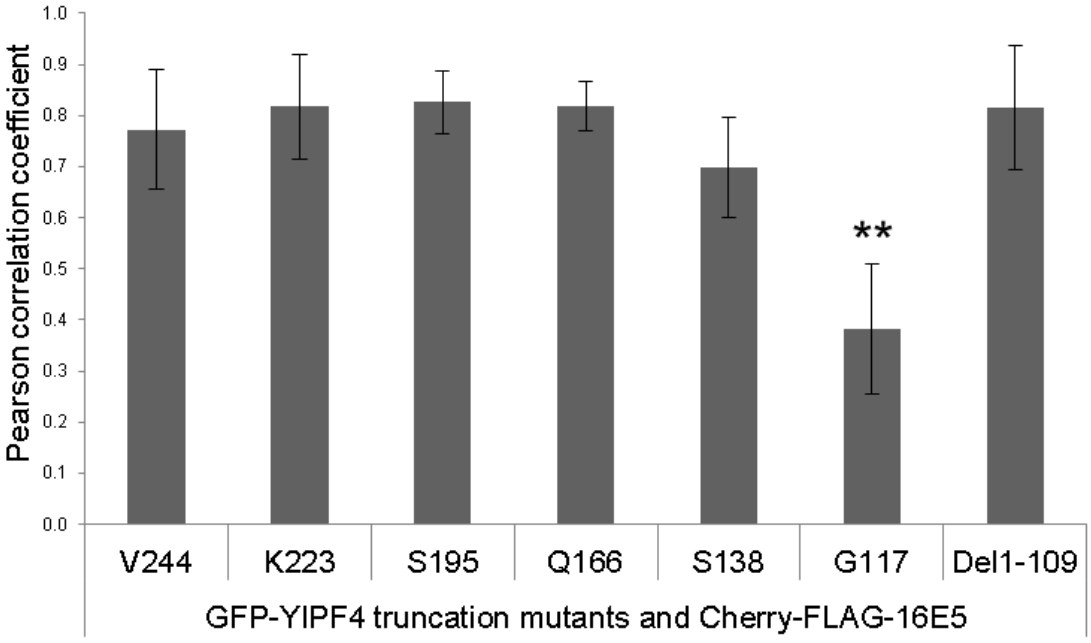

Figure 4.10 PCC values of GFP-YIPF4 truncation mutants and Cherry-FLAG-16E5. Each bar represents the mean PCC value (± SDM) of several cells (n ≥ 5). A one-way ANOVA was performed ** $p \leq 0.01$

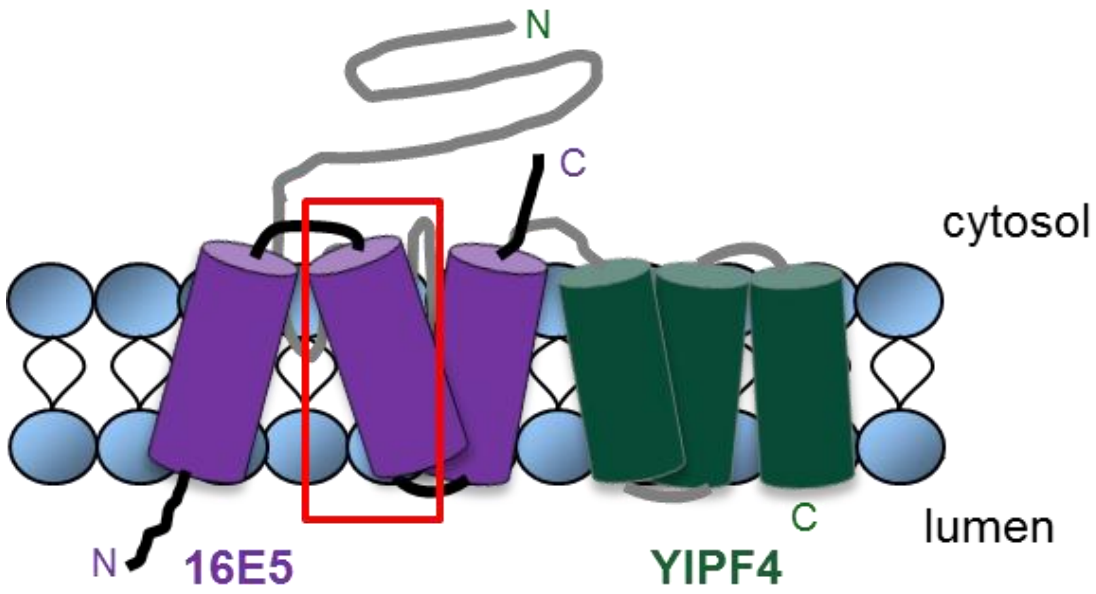

Figure 4.9 Preliminary model of 16E5 and YIPF4 interaction. The model shows the potential interaction of 16E5 with YIPF4 according to the binding sites mapped by Co-IP with their respective truncation mutants. HPV16 E5 binds with its 2nd TMD to amino acids 118 - 138 of YIPF4. This binding region is indicated by a red box.

4.2.4. YIPF4 did not interact with 16E6 and 16E7 and did not co-localise with all three HPV16 oncoproteins

The three HPV oncoproteins E5, E6 and E7 complement each other in their manipulation of cellular processes (4.1). It is therefore possible that not only 16E5 interacts with YIPF4 but also the other two oncoproteins of HPV16, E6 and E7.

The interaction of the HPV16 oncoproteins with YIPF4 was investigated by Co-IP using overexpressed FLAG-YIPF4-HA as bait and GFP fusion proteins of 16E5 (positive control), 16E6 and 16E7 as prey (Figure 4.11, schematic). The Western blot clearly confirmed the interaction of GFP-16E5 with FLAG-YIPF4-HA (Figure 4.11, lane 1). Interestingly, the GFP fusion proteins of 16E6 (lane 2) and 16E7 (lane 3) were not bound by FLAG-YIPF4-HA. The negative control, GFP (lane 4), also did not show any binding as expected. 16E5 was therefore the only HPV16 oncoprotein that bound YIPF4.

To examine the cellular localisation, the GFP fusion proteins of 16E5, 16E6 and 16E7 were expressed in SiHa cells which were fixed and stained for endogenous YIPF4 and the *trans*-Golgi network marker TGN46 (Figure 4.12A). Imaging of the samples confirmed the previously observed ER-like staining pattern of GFP-16E5. GFP-16E6 localised throughout the cell and GFP-16E7 was mainly localised in the nucleus but some cytoplasmic staining was detectable. The endogenous YIPF4 protein co-localised with the *trans*-Golgi network marker TGN46 in all samples.
The PCC values between the GFP-fusion proteins and endogenous YIPF4 were determined with the PSC plug-in for ImageJ. The PCC value indicated that GFP-16E5 and endogenous YIPF4 did not co-localise in SiHa cells (PCC value = 0.00) although an interaction was convincingly established. This was in accordance with the fact that GFP-16E5 appeared to be localised at the ER and YIPF4 clearly localised at the *trans*-Golgi network. The same observation was true for 16E6 (0.17) and 16E7 (0.17) where no notable co-localisation with YIPF4 was observed.

The analysis was conducted with several cells (Figure 4.12B). The paradox absence of co-localisation of GFP-16E5 with YIPF4 was confirmed (PCC value = -0.04 ± 0.2). There was no significant difference to the PCC values of GFP-16E6 (0.16 ± 0.1) and GFP-16E7 (0.09 ± 0.1) implying that these also did not markedly co-localise with endogenous YIPF4.

Thus, the interaction of YIPF4 was clearly confined to the 16E5 oncoprotein although their co-localisation could not be observed. The 16E6 and 16E7 oncoproteins neither bound nor co-localised with YIPF4.

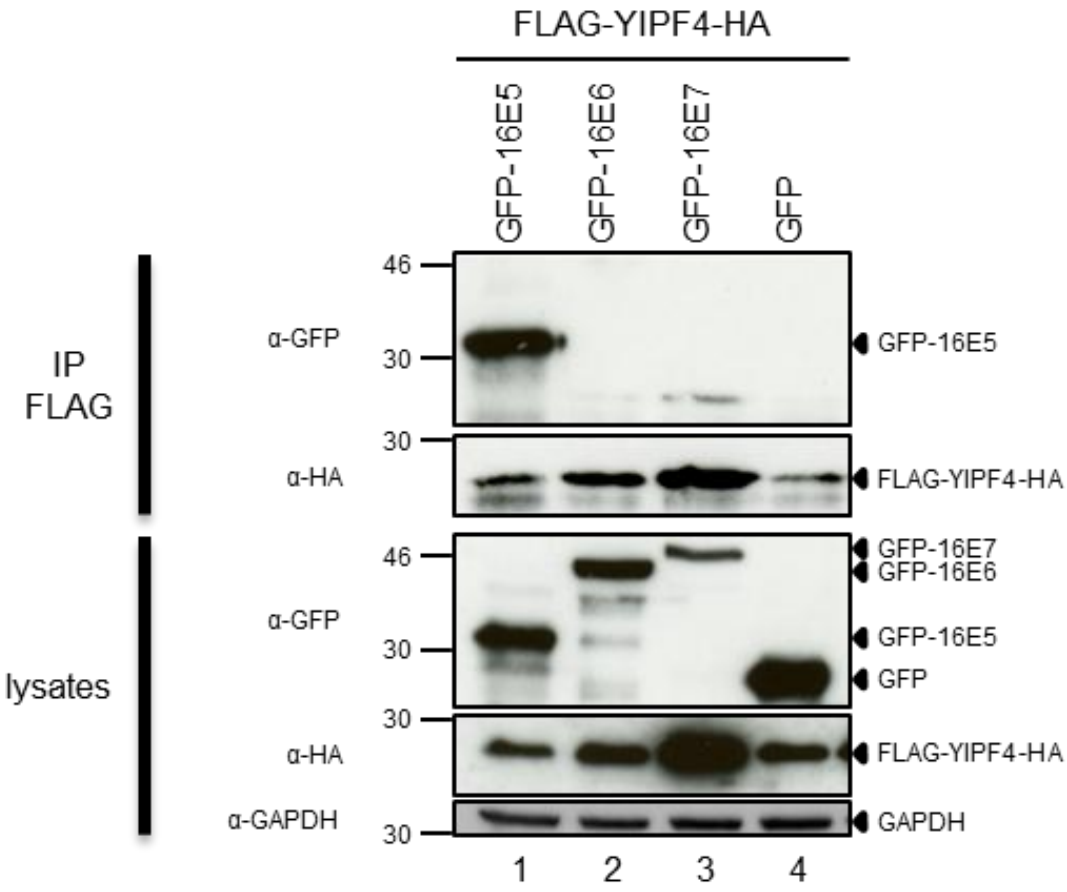

Figure 4.11 Co-IPs with FLAG-YIPF4-HA and the HPV16 oncoproteins E5, E6 and E7. GFP (negative control) and GFP fusion proteins of 16E5, 16E6 and 16E7 were co-expressed with FLAG-YIPF4-HA in HEK293T cells. The cells were lysed and equal amounts of total protein used for Co-IP with a FLAG antibody on dynabeads (schematic). The eluates were analysed on a Western blot by probing for the epitope tags of the exogenously expressed bait and prey proteins. Marker in kDa.

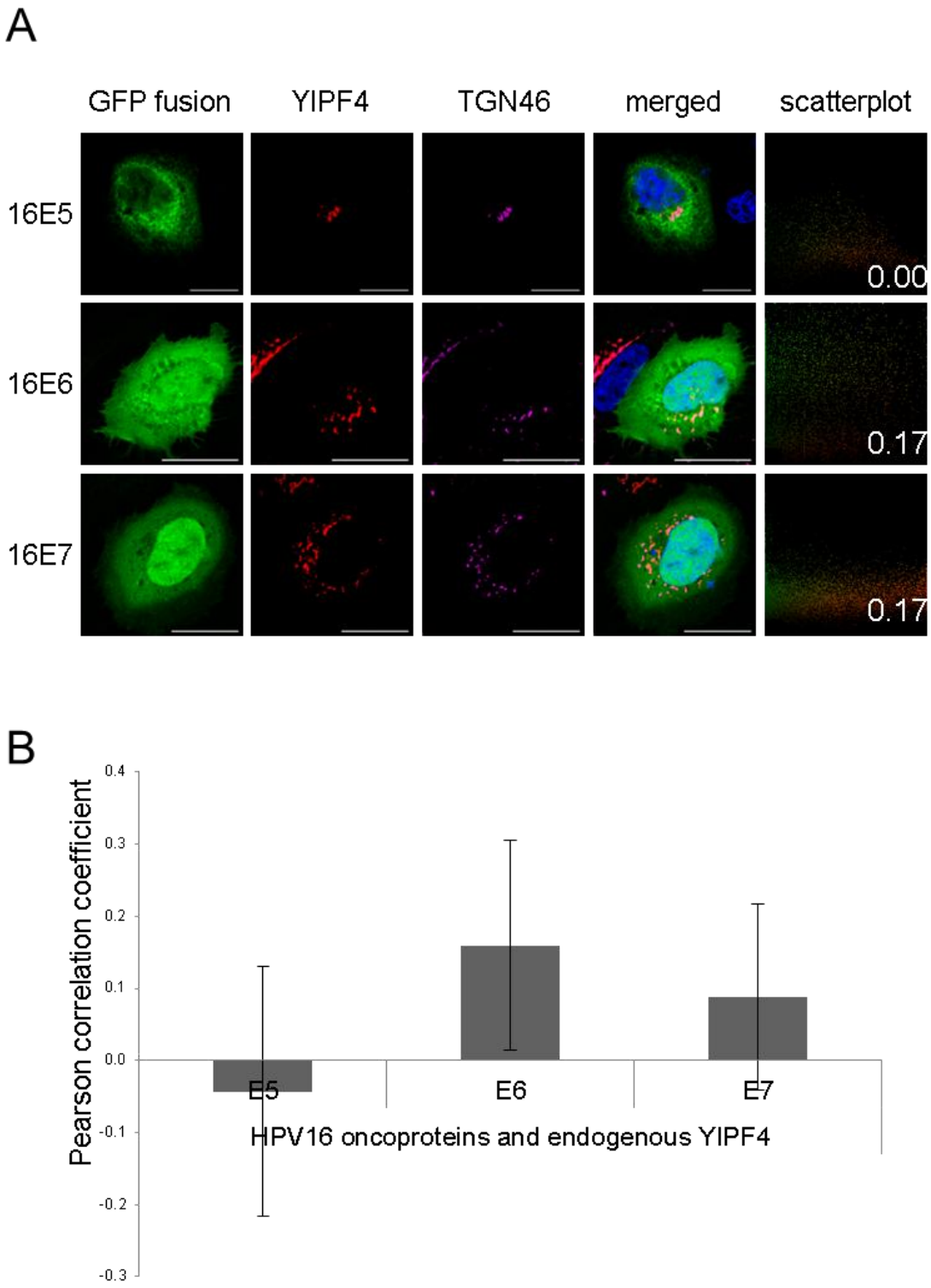

Figure 4.12 Identification of cellular localisation of endogenous YIPF4 and the HPV16 oncoproteins E5, E6 and E7. A. SiHa cells were transfected with GFP fusion-proteins of 16E5, 16E6 and 16E7. Cells were fixed and stained with the YIPF4 antibody and the *trans*-Golgi marker protein TGN46. Cells were imaged on Zeiss LSM700 confocal microscope. Cell nuclei were labelled with DAPI (blue). Representative images are shown. Scale bars = 20 µm B. The PCC values of the GFP fusion proteins and endogenous YIPF4 were determined using the PSC plug-in for ImageJ. Each bar represents the mean (± SDM) of several cells (n ≥ 8 cells/sample) of two independent experiments (except for one experiment for 16E7). A one-way ANOVA was performed and no significant differences could be detected.

4.2.5. YIPF4 bound to E5 proteins from various HPV and BPV types

The E5 proteins of HPV and BPV types are not conserved regarding amino acid identity. Nevertheless, they share some binding partners within the host cell. It is therefore possible that E5 proteins from PV types other than HPV16 also interact with YIPF4.

Co-IPs were performed with representative E5 proteins from the clinically most relevant α-PVs (cutaneous HPV2a, low-risk HPV 6b, 11, high-risk HPV16, 18, 31) and the ungulate BPV1 of the δ-PVs. Overexpressed FLAG-YIPF4-HA was used as bait and GFP fusion E5 proteins as prey (Figure 4.13A). All GFP-E5 fusion proteins were expressed successfully alongside FLAG-YIPF4-HA in HEK293T cells showing slight differences in their expression efficiency.

The E5 protein from the cutaneous HPV2a was clearly bound by YIPF4 (Figure 4.13A, lane1). Also, the E5 proteins from low-risk HPV6b and 11 were pulled down by YIPF4 (lane 2, 3). In addition to the established interaction with 16E5 (lane 4), YIPF4 formed complexes with further high-risk E5 proteins from HPV 18 and 31 (lane 5, 6). Interestingly, the ungulate BPV1 E5 protein was also bound by YIPF4. This indicates that the interaction with YIPF4 is widely conserved amongst PV E5 proteins.

The high-risk and low-risk HPV oncoproteins E6 and E7 have some conserved binding regions which mediate the interaction to the same proteins but with different affinity. The affinities of the various E5 proteins to YIPF4 were estimated by densitometry from the Co-IP Western blot (Figure 4.13A). The ratios of the respective band intensities of E5 to YIPF4 from the IP Western blots were divided by the same ratio of the lysate blots (Figure 4.13B). This provided an estimate of the amount of E5 protein bound by the YIPF4 bait which served as surrogate for the binding affinity.

The analysis of three repetitions of Co-IPs revealed some differences between the mean relative binding affinities to YIPF4 (2aE5 = 0.68 ± 0.28; 6bE5a = 1.10 ± 1.13; 11E5a = 1.40 ± 0.45; 16E5 = 1.37 ± 0.40; 18E5 = 1.02 ± 0.31; 31E5 = 1.37 ± 2.10; BPV1E5 = 0.89 ± 1.21). However, the differences were not significant and it is therefore to assume that the approximated binding affinity of the tested E5 proteins to YIPF4 does not vary markedly.

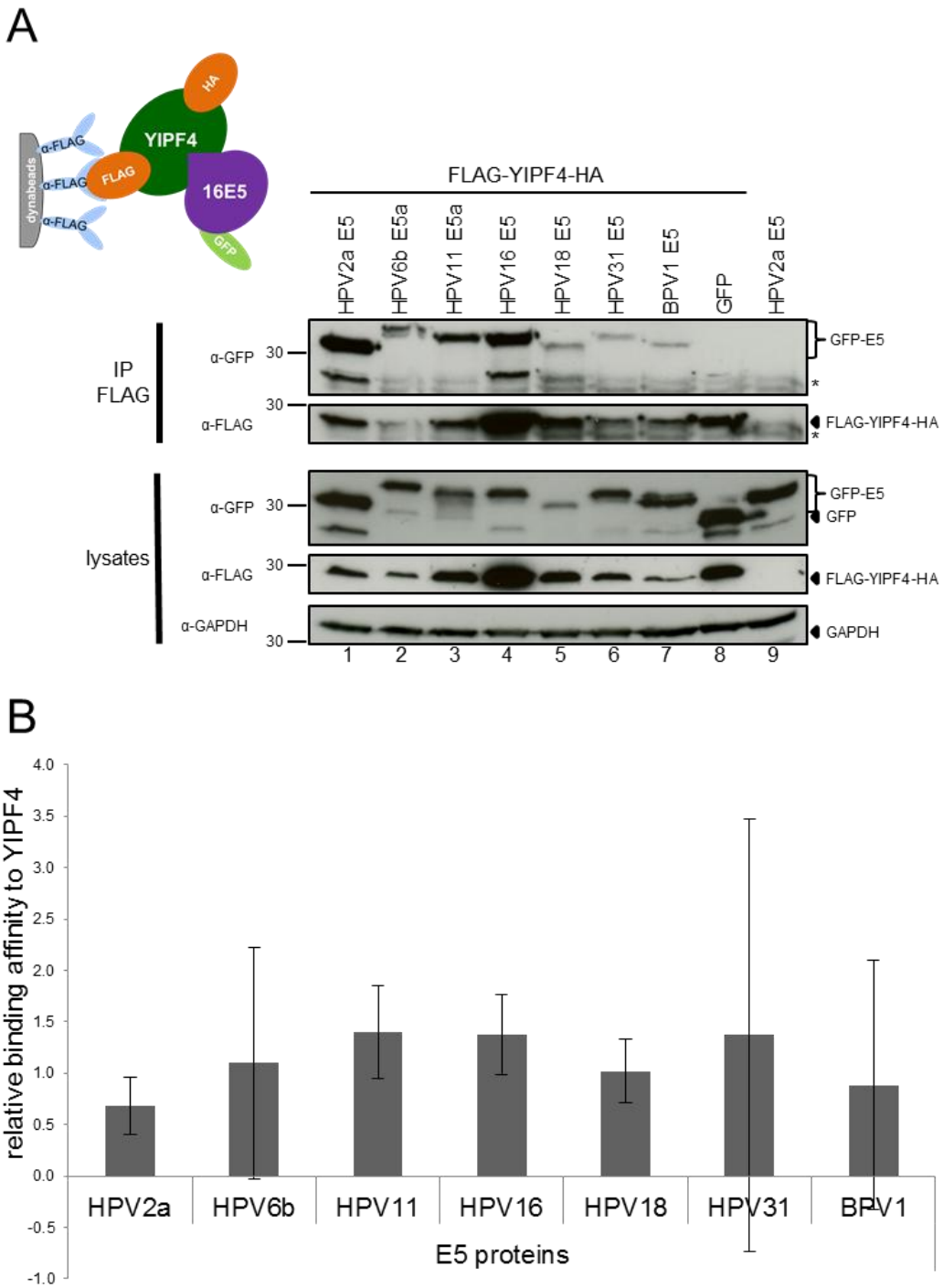

Figure 4.13 Interaction of YIPF4 with E5 proteins from a representative panel of PV types. A. Co-IPs of FLAG-YIPF4-HA and GFP-E5 fusion proteins of HPV types (cutaneous = 2a, low-risk = 6b, 11, high-risk = 16, 18, 31) and BPV1. GFP-E5 fusion proteins (and negative control GFP) were overexpressed alongside FLAG-YIPF4-HA in HEK293T cells. The Co-IPs were performed with equal amounts of total protein and a FLAG antibody on dynabeads (schematic). Representative Western blot is shown. Marker in kDa. ‘ * ‘ = antibody light chain. B. Densitometry analysis of three sets of Co-IPs. The mean relative binding affinities (±SDM) of E5 and YIPF4 are shown and were determined as follows: (IP blot(E5 band intensity/YIPF4 band intensity)) / (lysate blot(E5 band intensity/YIPF4 band intensity)). A one-way ANOVA was performed and no significant differences were detected.

The cellular localisation of GFP-E5 fusion proteins in relation to endogenous YIPF4 was investigated in SiHa cells (Figure 4.14A). As expected, endogenous YIPF4 localised at the *trans*-Golgi network since it visibly co-localised with the *trans*-Golgi network marker TGN46. The GFP-E5 fusion proteins exhibited an ER-like distribution pattern within the cells. The PCC values of GFP-E5 proteins and endogenous YIPF4 were determined using the PSC plug-in for ImageJ.

In accordance with the co-localisation pattern observed before (Figure 4.5 and Figure 4.11), there is no marked co-localisation detectable between YIPF4 and any of the GFP-E5 proteins investigated (PCC value of 2E5 = 0.40; 6bE5a = -0.02; 11E5a = 0.29; 16E5 = -0-32; 18E5 = 0.11; 31E5 = -0.12; BPV1E5 = 0.21).

The analysis of several cells per sample revealed differences in the mean PCC values (Figure 4.15). The HPV2 E5 protein showed some co-localisation with endogenous YIPF4 (PCC value = 0.46 ± 0.27) while 16E5 did not co-localise with YIPF4 (-0.03 ± 0.20). In this small sample set, however, these differences were not significant. All GFP-E5 proteins therefore showed little or no co-localisation with endogenous YIPF4 in this experiment.

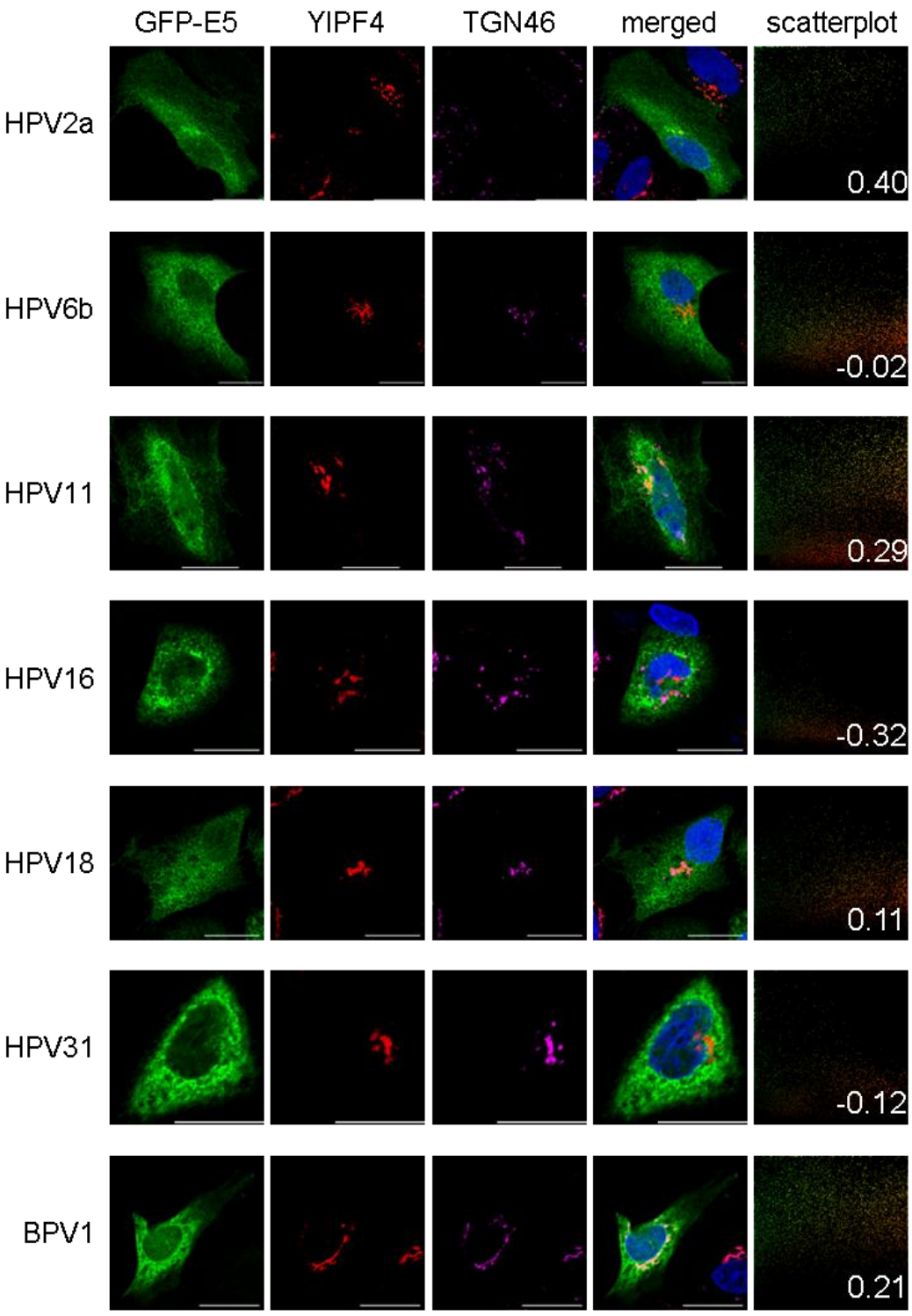

Figure 4.14 Cellular localisation of endogenous YIPF4 and GFP-E5 fusion proteins of a representative panel of PV types. GFP-E5 fusion proteins of HPV types (2a, 6b, 11, 16, 18, 31) and BPV1 were expressed in SiHa cells. Cells were fixed and stained with antibodies against YIPF4 and the *trans*-Golgi network marker protein TGN46. Cell nuclei were labelled with DAPI (blue). Images were acquired with Zeiss LSM700 confocal microscope. The PCC values of GFP-E5 fusion proteins and YIPF4 were determined with the PSC plug-in for ImageJ. The scatterplots illustrate the PCC values. Representative images are shown. Scale bars = 20 µm

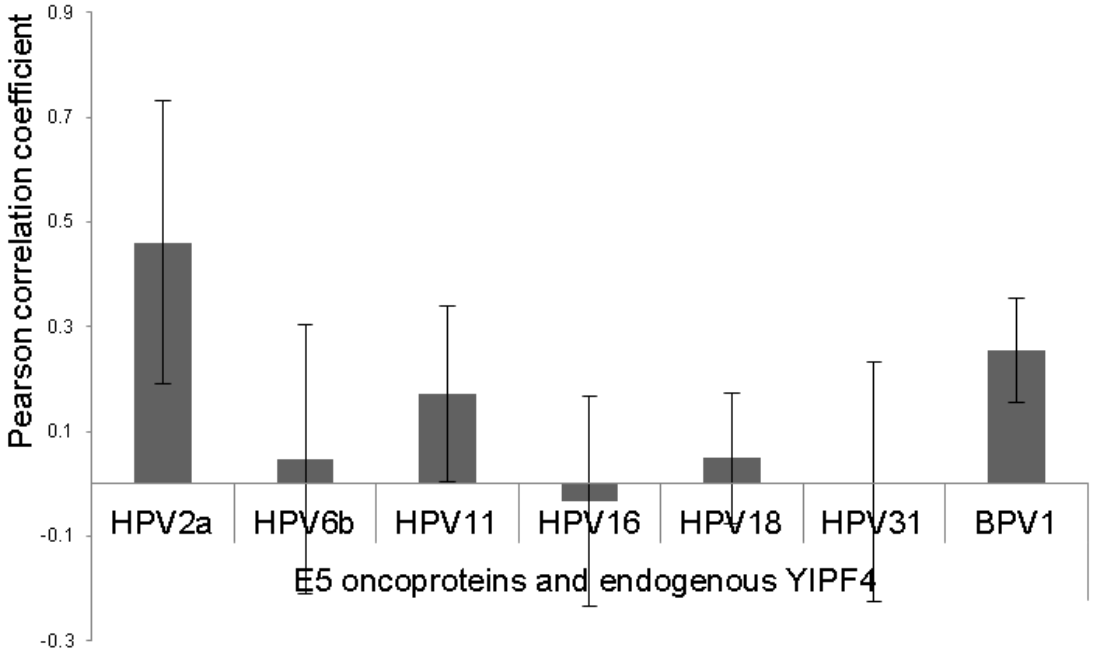

Figure 4.15 PCC values of E5 oncoproteins of a representative panel of PV types and endogenous YIPF4. Each bar represents the mean PCC value (± SDM) of several cells/sample (n ≥ 5). A one-way ANOVA was performed and no significant differences were detected.

4.3. Discussion

4.3.1. YIPF4 is confirmed as a novel 16E5 interaction partner

The Co-IPs undertaken in this study firmly established YIPF4 as a novel interaction partner for 16E5. The use of a number of appropriate negative controls insured that the interaction was not mediated by epitope tags or non-specific binding by antibodies or beads but by true interaction of the two proteins (Figure 4.1A). We could therefore validate the results from the Y2H screen, LUMIER assay and TAP-MS analysis that preliminarily identified YIPF4 as a novel 16E5 binding partner (1.7).

The Co-IP approach indeed verified the 16E5/YIPF4 interaction but it could not reveal whether 16E5 directly binds YIPF4 or whether the interaction is mediated by another unknown protein. The support for a direct interaction comes from the Y2H screen. By nature it requires a direct interaction of bait and prey so that the fused DBD and the activation domain of GAL4, respectively, are united to promote transcription of the reporter gene. It is therefore likely that the binding of 16E5 and YIPF4 is of direct nature. A fluorescence resonance energy transfer (FRET) assay in mammalian cells could be conducted to support this finding.
Interestingly, many of the cellular targets of 16E5 have been determined by Co-IP (4.1), so an interrogation of the direct nature of their binding might be appropriate in some cases.

It is possible that 16E5 and YIPF4 are part of a bigger protein complex. This could include YIPF3, the only known binding partner of YIPF4 to date (Tanimoto et al., 2011). Indeed, TAP-MS analysis suggests that 16E5, 18E5 and 6bE5 interact with YIPF3 (Rozenblatt-Rosen et al., 2012). A further YIP1 family member, YIF1B, interacted with 18E5 and 6bE5 in the same TAP-MS analysis but more research is needed to investigate the expression of YIPF3 and YIF1B in keratinocytes and to determine whether these interactions are part of or independent of the E5/YIPF4 complex. It is also conceivable that other known 16E5 interacting proteins form part of the potential bigger protein complex.

Thus, further experiments need to be carried out to determine the exact stoichiometry and composition of the E5/YIPF4 protein complex.

It was noted that 16E5 bound less efficiently to endogenous YIPF4 than to overexpressed YIPF4 (Figure 4.1B). This phenomenon was observed by others with the 16K subunit of the vacuolar H^+ - ATPase. A Co-IP with overexpressed and epitope tagged 16K and 16E5 in COS-7 cells showed that the majority (62%) of total 16K bound to 16E5 (Suprynowicz et al., 2010). A similar Co-IP but with endogenous 16K and stably expressing 16E5 in HFK cells revealed that only a minor portion of the endogenous 16K (5%) interacted with 16E5. Consequently, 16E5 bound dramatically less endogenous 16K than would have been predicted by the overexpression system. It is likely that the overall amount of (overexpressed) protein in this assay plays a crucial role and might explain the decreased binding of 16E5 to endogenous YIPF4. Also, a shared binding region with other 16E5 interaction partners might be the cause of this (see 4.3.2).

Ideally, the Co-IP would be repeated with endogenous 16E5 to circumvent the artificially high proteins levels. The most appropriate cell line for this experiment would be CaSki. These cells are known to express YIPF4 (Figure 3.1) and were shown to express 16E5 by protein mass spectrometry (Sahab et al., 2012). Unfortunately, despite several attempts over more than two decades (Adam et al., 2000, Chang et al., 2001, Chen and Mounts, 1989, Hwang et al., 1995, Kell et al., 1994, Sahab et al., 2012), there is no specific antibody available to 16E5 that would allow this experiment to date. The advent of purification systems for near native 16E5 (Wetherill et al., 2012a, Yang et al., 2003a) should however facilitate the development of such an antibody and therefore permit Co-IPs with endogenous 16E5.

This study has also shown that the simultaneous overexpression of two proteins dramatically reduced the total amount of each individual protein (Figure 4.1). This was confirmed with various different constructs to a greater or lesser degree (Figure A. 4). The co-expression of Cherry-FLAG-16E5 and GFP-YIPF4 formed an exception (Figure 4.8). The decrease in protein levels of co-

expressing proteins might be explainable by the competition for cellular transcriptional and translational resources. To exclude a potential impact on the Co-IP results, the expression efficiency of individual proteins can be adjusted by co-transfecting empty vectors.

A fast turnover of the 16E5/YIPF4 complex could also be the reason for the decrease of both protein levels when co-expressed. This would also justify the decrease in endogenous YIPF4 in GFP-16E5 expressing cells (Figure 4.1B). The rapid turnover of this protein complex could depict its function in HPV infected host cells. A possible mechanism is the reciprocal interference with stabilising binding partners. Indeed, the YIP1 family member YIPF5 is known to stabilise another member of this family, YIF1A (Yoshida et al., 2008). The only known binding partner of YIPF4, YIPF3, however, was shown not to be required for YIPF4 protein stability (Tanimoto et al., 2011) but other yet unknown interacting proteins could play this role. A comparison of the 16E5 and YIPF4 half-lives individually and as a protein complex should be conducted to investigate this possibility (see 5.3.2).

In contrast to this, this decrease of endogenous YIPF4 was not observed in HFK cells stably transfected with the HPV18 WT genome (Figure 3.3). The comparison with the HFK HPV18 E5 KO cell lines showed no alteration of the YIPF4 protein level. In this experimental system, 18E5 is expressed at physiological levels without an epitope tag and in context of the remaining HPV proteins. It is therefore to be regarded as the more authentic model for the E5/YIPF4 protein complex and would thus argue for no acceleration of E5/YIPF4 turnover. However, 18E5 may have a different effect on YIPF4 than 16E5.

Whether the decrease of protein levels observed here is an experimental artefact of protein overexpression or whether it is a clue towards E5/YIPF4 protein complex functionality remains to be elucidated.

4.3.2. 16E5 binds with its 2nd TMD to amino acids 118 - 138 of YIPF4 requiring correct cellular localisation

The 2nd TMD including the linker sequence to the 3rd TMD of 16E5 was identified as the binding site of YIPF4 in Co-IP experiments with 16E5 truncation mutants (Figure 4.2). The interaction with the mutants V36 and R30, which lack this region, was not completely abrogated. This suggests that there might be other sites of 16E5 that mediate weak binding to YIPF4. A similar observation was made with Bap31, which was shown to bind to the 10 most C-terminal amino acids of 16E5 (Regan and Laimins, 2008). A Co-IP with a deletion mutant deficient of those 10 amino acids still bound Bap31 at low levels. The potential additional binding sites were not investigated further. Other examples are the YIPF4 homologues in yeast, Yip1p and Yif1p. They interact with the Ypt35 GTPase via the N-termini but truncation mutants consisting of the C-termini only still show weak interaction with Ypt35 GTPase in a binding assay (Vollert and Uetz, 2004). Generation of extra point or deletion mutants of 16E5 could help to define the exact amino acids responsible for binding to YIPF4 in this case.

The 2nd TMD of 16E5 is also the putative binding site to 16K according to Adam and colleagues (Adam et al., 2000). It is therefore conceivable that 16K and YIPF4 compete for it. A potential support for this hypothesis is the observation that only a minority of endogenous 16K interacts with 16E5 in HFK cells (Suprynowicz et al., 2010). The expression of YIPF4 was confirmed in this cell type (Figure 3.3) so it is possible that YIPF4 displaces 16K from the 16E5 binding site and vice versa. And indeed, as mentioned before (4.3.1) endogenous YIPF4 shows reduced binding to 16E5 in HEK293T cells (Figure 4.1B) meaning a competition for the 16E5 binding site is theoretically possible. The hypothesis could be tested by re-performing the Co-IPs from cells depleted of YIPF4 and 16K by RNA interference, respectively. The binding capacity of 16E5 to the one protein should increase when the other is knocked down if this hypothesis holds true.

In addition to mediating binding to host cell proteins, the 2nd TMD is proposed to play a significant role for self-interaction and thus formation of the homo-hexameric viroporin (Wetherill, 2012, Wetherill et al., 2012a, Yang et al., 2003a). *In silico* modelling predicts the threonine at position 40 to form a hydrogen bond with the threonine at position 38 of the adjacent 16E5 monomer. The binding of YIPF4 could therefore disrupt the viroporin confirmation. HPV16 E5 might thus exist in several oligomerisation states within the host cell. The E5 protein of BPV1 is known to function in two oligomeric states within the cell. It interacts with the PDGF-β receptor as a dimer (Nilson et al., 1995), whereas it binds 16K as a monomer (Gieswein et al., 2003). The binding of YIPF4 and other interaction partner could therefore determine the oligomeric state of 16E5 within the cell, which might all exert distinct functions.

The Co-IP experiments with YIPF4 truncation mutants mapped the 16E5 binding regions to amino acids 118 - 138 (Figure 4.7C). But the reverse speculations about the competition of 16E5 with other proteins for binding to this region are not possible. The only firmly established binding partner of YIPF4 is YIPF3 (Tanimoto et al., 2011) but their binding regions were not investigated. A suggestion can be derived from other YIP1 family members, YIPF1 and YIPF6. In Y2H experiments it was observed that all their TMD mediated the binding (Shakoori et al., 2003). The N-terminal cytoplasmic region was not necessary. The C-terminus of the yeast homologue Yip1p was also shown to be important for function, especially its final 18 amino acids (Chen et al., 2004). If interaction via the C-terminal half is conserved between YIP1 family members, 16E5 binding could abrogate the interaction with YIPF3. Further experiments are needed to determine the cellular binding partners of YIPF4 (5.2.3) and the consequence of 16E5 binding for their interaction.

A clue about the actual mode of interaction of 16E5 to this site of YIPF4 came from the analysis of co-localisation. It revealed that the non-binding YIPF4 truncation mutant G117 no longer co-localises with 16E5 (Figure 4.9). The G117 mutant only contains the highly hydrophilic N-terminus of YIPF4 and it clearly shows a more dispersed cellular distribution (Figure 4.8) although exceptions have been observed (Figure A. 1). It is conceivable that this mainly

soluble truncation mutant is inaccessible for binding to the 2nd TMD of 16E5. The binding of the remaining YIPF4 truncation mutants might be facilitated by their closer membrane association which mediates the access to the 2nd TMD of 16E5.

This can be supported by the properties of the S138 truncation mutant. It was shown to be partially soluble but a fraction of the protein remained associated with the membrane (Figure 3.21 and Figure A. 1). In the binding assay with 16E5, only a small fraction was bound to GFP-16E5 (Figure 4.7). It is intriguing to speculate that only the membrane-associated fraction of S138 interacts with 16E5. This could theoretically be investigated by performing the Co-IP with GFP-16E5 again, however, with the soluble and membranous fraction of S138 expressing cells. It could show that GFP-16E5 only binds to S138 from the membranous fraction. Overall, the membrane association and hence the cellular localisation seem to contribute to the binding of YIPF4 by 16E5.

The requirement of co-localisation was also observed for binding to the HLA class I HC (Cortese et al., 2010). The di-leucine motifs at position 11/12 and 22/23 of 16E5 were found to mediate direct binding to the HC, but the remaining two di-leucine motifs at positions 16/17 and 27/28 were necessary for the correct localisation of the protein. Only the presence of all four di-leucine motifs allowed the exertion of the function of the 16E5/HLA HC complex.

It remains to be elucidated which amino acids are required for the appropriate function of the 16E5/YIPF4 complex and a more extensive investigation with further point and deletion mutants could help to determine these.

In theory, the 16E5/YIPF4 interaction could be mediated by a disulphide bond since both proteins carry cysteine residues. However, the cysteine residues of 16E5 are not located in the 2nd TMD but in the 1st (C18, C20, C24, C26) and 3rd (C59). The cysteine residue of YIPF4 is localised at position 94. This would mean that the G117 truncation mutant should still be able to form the disulphide bond. But as established (Figure 4.7), this mutant no longer binds to 16E5. Also, the binding buffer used for the Co-IPs contained the reducing agent DTT, which abrogates any disulphide bonds within the cell lysate. The formation of disulphide bonds between 16E5 and YIPF4 is therefore unlikely.

Notably, 16E5 and YIPF4 are oriented in an anti-parallel fashion within the membranes. The C-terminus of 16E5 and the N-terminus of YIPF4 face the cytoplasm. This anti-parallel orientation is also taken by BPV1 E5 and the PDGF-β receptor. It allows the aspartic acid at position 33 of 16E5 and the lysine at position 499 of PDGFR to get into close proximity and form a salt bridge that stabilises the complex (DiMaio and Petti, 2013, Meyer et al., 1994, Surti et al., 1998). Whether the orientation of 16E5 and YIPF4 favours the formation of a complex remains to be elucidated. *In silico* modelling as conducted for the 16E5 homo-hexamer (Wetherill, 2012) could help identify important residues for the formation of the 16E5/YIPF4 complex. These could be taken as point of reference for further mutational analysis of this complex.

4.3.3. The absence of co-localisation of E5 and YIPF4 might be an artefact of the overexpression system

In this study the binding of E5 to YIPF4 was firmly established by Co-IP. Surprisingly, examination of the PCC values showed that these interacting proteins did not co-localise within the cell (Figure 4.6, Figure 4.11, Figure 4.15). The determination of the PCC value was recently successfully applied to establish a co-localisation of YIF1A with the *cis*-Golgi protein GM130 and ERGIC53 (Kuijpers et al., 2013). In contrast to expectation, the localisation overlapped more when 16E5 truncation mutants no longer bound to YIPF4 (Figure 4.4 and Figure 4.6).

It is conceivable that E5 and YIPF4 partially co-localise within the cell to an extent that is not detectable by the immuno-fluorescence approach with PCC analysis used in this study. This is extremely likely considering that YIPF4 homologues cycle between the ER and Golgi within the cell (1.8). YIPF4 could be located at the Golgi at steady state and only a small portion of the cellular YIPF4 pool cycle between ER and Golgi and co-localise with E5. This agrees with the observation that not the whole endogenous YIPF4 pool seems to interact with 16E5 (Figure 4.1). This minor co-localisation might be detectable by nycodenz gradient centrifugation (Yoshida et al., 2008). But further research is needed to investigate this hypothesis.

Another explanation is likely to be found in the overexpression system used in this study. Due to the unavailability of a specific E5 antibody (4.3.1), the E5 proteins had to be overexpressed with an epitope tag. The expression of 16E5 with a small epitope tag (FLAG and HA, respectively) was vanishingly low and thus an immuno-fluorescent detection not possible (data not shown). Only a fluorescent tag, namely eGFP (Figure 4.3, Figure 4.5, Figure 4.12, Figure 4.14) and mCherry (Figure 4.8) allowed sufficient expression of the E5 proteins. These tags (27 kDa) are, however, three times the size of 16E5 (9 kDa) and more than five times of BPV1 E5 (5 kDa). This could have an effect on their cellular distribution (see below).

This does not appear to be the case for GFP-16E6 and GFP-16E7 (Figure 4.12). GFP-16E6 was clearly distributed throughout the cell as seen with HA tagged E6 (Guccione et al., 2002). The majority of GFP-16E7 was detected in the nucleus in accordance with the HA tagged 16E7 investigated by others (Guccione et al., 2002). Some GFP-16E7 localised to the cytoplasm but this was also observed for endogenous E7 of CaSki cells in subcellular fractionation experiments (Smotkin and Wettstein, 1987).

Due to the lack of a 16E5 antibody, the GFP fusion protein was frequently used in PV E5 research. It retains its function of binding to 16K, as determined by Co-IP (Figure A. 5), which serves as a surrogate for a conserved biological activity.
Its localisation was directly compared with the localisation of 16E5 with the much smaller BPV E2 hinge epitope in HeLa cells and their localisation appeared identical (Auvinen et al., 2004). A similar comparison with AU1 tagged codon adapted 16E5 also found no marked differences caused by the epitope tags (Gruener et al., 2007).
In our hands GFP-16E5 does not localise to the *trans*-Golgi network because its expression does not overlap with YIPF4 and hence the *trans*-Golgi network marker TGN46 (Figure 4.12 and Figure 4.14). When GFP-16E5 was expressed in HaCaT cells (Lewis et al., 2008) and HeLa cells (Auvinen et al., 2004) by others it co-localised with 58K, another *trans*-Golgi network marker. A co-localisation with a further *trans*-Golgi network marker, golgin-97, and the *cis*-Golgi marker GM130 was, however, not observed (Auvinen et al., 2004). This study also disproved the co-localisation of GFP-16E5 with the early endosome marker EEA-1, the late endosome marker Rab7 and the lysosome marker LAMP-1.
A codon adapted 16E5 with a FLAG epitope tag expressed in HaCaT cell, however, co-localised with EEA-1 and LAMP-2 (Lewis et al., 2008). But the localisation of codon adapted and WT 16E5 diverged markedly in this study, which might explain this discrepancy.
GFP-16E5 expression in HaCaT cells did not show significant co-localisation with the ER marker protein calnexin (Lewis et al., 2008). But others observed GFP-16E5 localisation in the ER (Ashrafi et al., 2006b). In our hands, although staining with an ER marker was not successful (data not shown), GFP-16E5

conveys the impression of ER-like distribution as well. Others also detected 16E5 with a RNGS epitope tag predominantly in the ER (Conrad et al., 1993). Besides, the same RNGS-16E5 was detected in the Golgi and the nuclear membrane. A T7 tagged 16E5 was seen to form perinuclear aggregates (Gieswein et al., 2003) while Hu and colleagues detected HA tagged 16E5 at the plasma membrane (Hu and Ceresa, 2009).
Concluding from this, the cellular localisation of 16E5 appears to depend on several factors. These might include the epitope tag, the overexpression system, and the cell line and codon usage of the 16E5 protein.
It is conceivable that the use of a different expression system for 16E5 might have confirmed a co-localisation with its binding partner YIPF4.

The same observation was made for the GFP-16E5 truncation mutants. In our hands, the GFP-16E5 truncation mutants mainly showed an ER-like distribution in Huh7 and SiHa cells (Figure 4.3 and Figure 4.5). But the V36 and R30 truncation mutants localised slightly more at the Golgi since its co-localisation with YIPF4 increased. The same full-length and truncation mutants expressed by others in HaCaT cells, however, showed consistent overlapping localisation with the Golgi marker BODIPY-TR-ceramide (Ashrafi et al., 2006b). No variation of cellular localisation was detected with decreasing lengths of the mutants as in this study. Others used a T7 tagged deletion mutant of the 3rd TMD (equivalent to the A54 used in this study), which showed a more dispersed localisation compared to the full-length construct (Gieswein et al., 2003). But all the truncation mutants remained endomembrane proteins. This was confirmed with HA tagged truncation mutants, which were all associated with membranes in an *in vitro* translation assay (Rodriguez et al., 2000).
These examples indicate that the exact cellular localisation of the 16E5 truncation mutants is as controversial as for the full-length protein and possibly depends on similar factors.
As long as no suitable antibody is available to 16E5 it could be tried to insert a small epitope tag into the viral genome. This would allow the detection of 16E5 at near physiological levels and might even lead the way to the expression of E5 truncation mutants in the HPV genome context. However, unpublished

attempts at this suggest that insertion of epitope sequences may adversely affect genome splicing (Lamonis Laimins, personal communication).

A co-localisation of 16E5 and YIPF4 was only seen when both proteins were overexpressed with a fluorescent tag (Figure 4.9). The expression of YIPF4 with a N-terminal GFP tag is likely to retain its function since this was observed for its orthologue in yeast, Yip1p (Chen and Collins, 2005a, Heidtman et al., 2003). The fluorescent tags of E5 and YIPF4 allow more efficient expression of both proteins. With this they form an exception because simultaneous expression of these proteins with differing epitope tags or endogenous YIPF4 lead to the decrease of expression efficiency (discussed in 4.3.1). The increased amount of YIPF4 in the cell was shown to lead to its accumulation in the ER rather than its natural localisation at the Golgi (discussed in 3.3.2). The expression of YIPF5 as a GFP fusion protein also altered its cellular localisation from the ERGIC to the ER and the ER exit sites (Kano et al., 2009) maybe due to similar accumulation of the protein. For this reason, GFP-YIPF4 shows significant co-localisation with the ER-like localised Cherry-FLAG-16E5. It is therefore conceivable, that the co-localisation observed here might be an artefact of the overexpression of fluorescently tagged E5 and YIPF4. This stresses the urgent need for a specific and fully functional 16E5 antibody. Only when both interaction partners are investigated at endogenous level in the same cell can their co-localisation be determined conclusively.

4.3.4. YIPF4 interacts with 16E5 but not with 16E6, 16E7

YIPF4 was found to interact with only one of the three HPV16 oncoproteins, namely E5. 16E6 and 16E7 were not bound by YIPF4 emphasising the specificity of its interaction with 16E5 (Figure 4.11). This allows speculations about the functions of this protein complex which may play a complementary role to the functions of 16E6 and 16E7.

Indeed, 16E5 in combination with 16E7 was shown to mediate cell proliferation, colony formation and development of tumours in transgenic mice (4.1). This leaves room for some involvement of the 16E5/YIPF4 complex in host cell transformation. However, since YIPF4 does not directly interact with the main transforming proteins 16E6 and 16E7, host cell transformation is unlikely to be the primary role of the 16E5/YIPF4 complex.

The 16E7 protein induces alkalisation of cellular compartments via the Na^+/H^+ exchanger (Reshkin et al., 2000). HPV16 E5 contributes to this by binding to 16K (Straight et al., 1995) or maybe by disruption of endosome trafficking (Thomsen et al., 2000, Suprynowicz et al., 2010). Thus, the 16E5/YIPF4 complex might play a role in the alkalisation of cellular compartments.

The oncoproteins were also shown to jointly mediate HLA class I down-regulation from the cell surface (1.3.7). Induction of 16E7 expression reduced HLA class I at the cell surface (Bottley et al., 2008) and the same was observed for 16E5 (Ashrafi et al., 2005). This might be associated with the modulation of intracellular trafficking that could be altered by 16E6 effects on cystic fibrosis trans-membrane regulator-associated ligand (Jeong et al., 2007) and 16E5 impact on the actin cytoskeleton (Thomsen et al., 2000) or endosome fusion (Suprynowicz et al., 2010).

Thus, because the HPV oncoproteins achieve the same effect by different mechanisms, it is indeed possible that the 16E5/YIPF4 complex plays a complementary role to 16E6 and 16E7 functions. However, further investigations are needed identify the function of the E5/YIPF4 complex.

4.3.5. YIPF4 interacts with E5 proteins from various PV types

In this study we showed that YIPF4 interacts with E5 proteins from a representative panel of PV types with equal affinity (Figure 4.13).
There are four families (α, β, γ, δ) of HPV E5 proteins according to phylogenetic analysis (1.6) (Bravo and Alonso, 2004). We successfully tested E5 proteins from three of these families for its interaction with YIPF4: E5α = HPV16, 18, 31; E5β= HPV2a and E5γ = HPV6b, 11. TAP-MS analysis using IMR-90 normal human diploid fibroblasts transfected with E5 ORFs from different HPV types confirmed YIPF4 as a potential interaction partner of HPV16, HPV18 and HPV6b E5 protein, respectively (Rozenblatt-Rosen et al., 2012). It is likely that YIPF4 also interacts with further members of these E5α, -β, -γ families.

The ungulate E5 proteins were not included into this phylogenetic classification. But the prototypic BPV1 E5 clearly bound to the human YIPF4. The YIPF4 protein is highly conserved amongst different species so in all probability, the bovine YIPF4 will bind to the BPV1 E5 protein as well. The alignment of the bovine YIPF4 amino acid sequence with the human version revealed that the E5 binding region of amino acids 118 - 138 is identical between the two proteins (Figure A. 2). It is also completely conserved for the YIPF4 protein of rhesus macaque, house mouse, brown rat, grey wolf, chicken and zebrafish and highly identical to *Caenorhabditis elegans*. This could mean that E5 proteins from other PV types might interact with their respective YIPF4 protein.

In contrast to this, the HPV E5 proteins of the four families and their relatives from other animal PV types are hardly conserved regarding amino acid sequences. They do not have conserved binding domains (4.1) and might thus not share the same interaction mode with YIPF4. This was seen for the interaction of HPV16 E5 and BPV1 E5 with 16K. It is most likely mediated by hydrophobic interactions of 16E5 to the 4^{th} TMD of 16K (Adam et al., 2000). But for BPV the interaction of glutamine 17 of E5 with a glutamic acid 143 in the 4^{th} TMD of 16K is mediating the binding (Andresson et al., 1995). Thus, the binding sites to YIPF4 have to be determined individually with truncation and point mutants of the respective E5 proteins.

The E5/YIPF4 complex must play a significant role for virus infection since it appears to be conserved amongst PVs. Concluding from the properties of 16E5, it could play a role in host cell transformation, viral life-cycle and immune evasion.

The role in cell transformation could be complementary to the functions of E6 and E7 proteins as described (4.3.4). It is also noteworthy that YIPF4 interacts with the E5 protein of BPV1. In this PV type E5 constitutes the main oncoproteins (Surti et al., 1998, Schlegel et al., 1986) which would make a contribution of the E5/YIPF4 complex to host cell transformation plausible. On the contrary, the binding affinity to the low-risk, high-risk and cutaneous E5 proteins was equally strong implying that a role in the viral life-cycle or immune evasion is more likely.

E5 functions in the viral life-cycle and contributes to evasion from the host immune system (1.6.2 and 1.6.3). Some of these functions might be mediated by the modification of intracellular trafficking of e.g. HLA class I and II and CD1d. Concluding from the homologues of YIPF4 in yeast and mammals, YIPF4 is also likely to play a role in intracellular trafficking events (1.8). It is therefore conceivable that the E5/YIPF4 complex exerts an important function in the viral life-cycle or immune evasion by modulation of intracellular trafficking. Notably, YIPF4 expression was rescued upon HFK differentiation by presence of the HPV18 WT and E5 KO genomes (Figure 3.7 and Figure 3.8). YIPF4 might therefore play a further, E5 independent role in the HPV life-cycle.

In summary, YIPF4 was established as a novel interaction partner of 16E5. The binding regions were identified as the 2nd TMD of 16E5 and amino acids 118 - 138 of YIPF4 requiring correct cellular localisation. The other HPV16 oncoproteins E6 and E7 do not interact with YIPF4. Most importantly the interaction was conserved for E5 proteins from a representative panel of PV types. It is likely that the E5/YIPF4 complex plays an important role for the virus other than transformation of the host cell. The investigation of its function is the subject of the next chapter.

Chapter 5. Investigation of the function of the 16E5/YIPF4 complex

5.1. Introduction

The interaction with YIPF4 is highly conserved amongst a representative panel of PV E5 proteins (Chapter 4). It is equally conserved for cutaneous, low-risk and high-risk HPV types as well as BPV1 and therefore the E5/YIPF4 protein complex is unlikely to play a role in host cell transformation. A contribution to the viral life-cycle or viral immune evasion is considered more probable. The cellular functions of YIPF4 have not been investigated yet but referring to its homologues in yeast and mammals it is likely to play a role in cellular trafficking (1.8). E5 also mediates some of its cellular roles by the modification of endocytic and exocytic trafficking (Figure 1.7). The modulation of HLA/MHC class I exocytic trafficking has been shown to be common to PVs E5 proteins (Ashrafi et al., 2006a).

In a flow cytometry approach, untagged E5 was shown to reduce the HLA class I cell surface levels of stably expressing HaCaT and NIH3T3 cells by approximately 50% compared to control cells (Ashrafi et al., 2005). The same effect was seen in primary bovine PalF cells that were transformed with a retrovirus expressing 16E5. Also, transient expression of a GFP-16E5 fusion protein in HEK293T cells resulted in a down-regulation of 35% (Gruener et al., 2007).
This down-regulation was found to be specific for certain HLA class I types. HPV16 E5 can reduce HLA class I types A and B but not C and E on the cell surface (Ashrafi et al., 2006b, Ashrafi et al., 2005, Campo et al., 2010). When treated with IFN-β, HPV E5 expressing cells can overcome the reduced HLA class I cell surface exposure (Ashrafi et al., 2005).

Crucially, it was confirmed that 16E5 reduces HLA class I by blocking its trafficking to the cells surface. Immuno-cytochemistry with the Golgi-marker

golgin showed that HLA class I is retained in the Golgi (Ashrafi et al., 2005). The expression level of the HLA HC and TAP were not affected. A decrease of total HLA class I protein or inhibition of complex assembly therefore do not qualify as an explanation for this phenomenon.

The exact mechanism for the retention of HLA class I in the Golgi is controversial. Cortese and colleagues employed point mutants in Co-IP assays to confirm a direct interaction of two di-leucine motifs in the 1st TMD of 16E5 with the HLA HC (Cortese et al., 2010). They propose this interaction as the reason for the Golgi-retention (Ashrafi et al., 2006b, Cortese et al., 2010). Gruener and colleagues, however, reason that the formation of a ternary complex of 16E5 and HLA class I HC with calnexin causes the retention (Gruener et al., 2007). Another possible mechanism could be the interaction of 16E5 with the ER resident chaperone Bap31 (Regan and Laimins, 2008). An involvement in this process, however, still needs investigation.

The 16E5 mediated down-regulation of HLA class I molecules from the cell surface was indeed shown to contribute to viral immune evasion. The exogenous co-expression of the HLA-A2 type and 16E5 in mouse mastocytoma cells not only show the expected down-regulation of cell surface HLA-A2 but also the consequential reduced recognition by CD8+ T cells (Campo et al., 2010). This successful evasion from the host immune surveillance was confirmed with patient samples that exhibited only rare CD8+ T cell response to 16E5 (Liu et al., 2007).

The down-regulation of HLA/MHC class I molecules by E5 proteins is conserved amongst three different phylogenetic families (Bravo and Alonso, 2004). The E5α proteins are represented by 16E5 (Ashrafi et al., 2005), but also the E5β proteins of HPV2a and HPV83 (Ashrafi et al., 2006a, Cartin and Alonso, 2003) and the E5γ protein of HPV6b (Ashrafi et al., 2005) down-regulate cell surface HLA class I molecules. The only tested E5 proteins from the ungulate BPV1 and BPV4 also decreased MHC class I at the cell surface (Araibi et al., 2004, Araibi et al., 2006, Ashrafi et al., 2002, Marchetti et al., 2002). However, the E5 proteins employ different mechanisms to achieve the same goal. The ungulate E5 proteins e.g. down-regulate total MHC class I

molecule levels on transcriptional level and also promote its degradation in addition to preventing its trafficking to the cell surface (Marchetti et al., 2005). Despite employing multiple complementary techniques to down-regulate HLA/MHC class I from the cell surface, all investigated E5 proteins universally perturb HLA/MHC trafficking. It is indeed very striking that YIPF4 is likely to be involved in secretory trafficking as well. But more importantly, it is known to interact with the same phylogenetic E5 proteins families that consistently inhibit HLA/MHC class I trafficking (Chapter 4).

The aim of this chapter is therefore to establish a potential involvement of YIPF4 in the E5 mediated down-regulation of HLA class I molecules from the cell surface. First, the effect of transiently expressed E5 on the surface levels of HLA class I molecules is sought to be verified by flow cytometry. A knock down of endogenous YIPF4 is achieved by utilisation of specific siRNA. The effect of the YIPF4 depletion of the cell surface HLA class I expression is examined by flow cytometry. Because of the clinical significance of HPV16 it is the focus of these investigations.

5.2. Results

5.2.1. GFP-16E5 did not have an effect on cell surface HLA class I molecules

5.2.1.1. GFP-16E5 did not down-regulate endogenous HLA class I molecules in SiHa cells

A GFP-16E5 fusion protein was previously shown to down-regulate HLA class I molecules from the surface of HEK293T cells using an antibody against HLA-A, B and C (Gruener et al., 2007). In order to establish the potential involvement of YIPF4 in this process, this effect of E5 needed to be verified first.
SiHa cells were transiently transfected with GFP-16E5 and free GFP as a negative control. A GFP fusion protein of human cytomegalovirus (HCMV) US6 was used as a positive control. US6 is known to reliably down-regulate HLA class I from the cell surface by preventing peptide loading and consequently correct assembly of the HLA class I complex (Ahn et al., 1997, Hewitt et al., 2001, Kyritsis et al., 2001).

The SiHa cells were stained 16h post-transfection with the W6/32 antibody that recognises the HLA class I types A, B and C and analysed by flow cytometry. Propidium iodide (PI) was used to evaluate cell viability. The gates for live (PI negative) and successfully stained cells were established by analysing untransfected cell populations that were not stained with W6/32 and either untreated or treated with PI (data not shown). From 500 000 collected single cells, only the live and GFP positive cells were analysed for HLA class I cell surface levels (Figure 5.1).

Prior to analysing the HLA class I cell surface expression level, the cell count revealed a significantly lower expression efficiency of the GFP-16E5 fusion protein ($p \leq 0.01$) (Figure 5.1A). In the seven cell populations investigated, the mean percentage of GFP-16E5 positive cells was 4% (± 1.1) in contrast to 20% (± 4.3) of free GFP expressing cells and 22% (± 4.3) of GFP-US6 expressing cells. Due to the high number of collected single cells, an average of 14893 (±

4921) live, GFP-16E5 positive cells per replica were analysed despite the low expression efficiency. This was sufficient for meaningful statistical analysis.

When observing the HLA class I cell surface expression, the negative control, free GFP expressing cells, was regarded as base value. The histogram of the positive control, GFP-US6 expressing cells, showed a clear shift towards the lower fluorescence indicative of successful cell surface down-regulation of HLA class I (Figure 5.1B). This signified that this fluorescence-activated cell sorting (FACS)-based assay for determination of cell surface HLA class I levels was producing reliable results. However, very surprisingly, the histogram of the GFP-16E5 expressing cells showed a minute shift towards increased fluorescence which would imply an up-regulation of HLA class I to the cell surface.

This experiment was repeated a total of seven times (Figure 5.1C) to draw statistically supported conclusions. Compared to the GFP expressing cell population, only the GFP-US6 expressing cells showed a statistically significant down-regulation of surface HLA class I molecules of 23% (± 8.8) ($p \leq 0.01$). GFP-16E5 expressing cells up-regulated HLA class I molecules by 9.1% (± 19.5), however, this was not statistically significant. These observations contradict the 16E5 mediated down-regulation of HLA class I that was observed before (Ashrafi et al., 2005, Gruener et al., 2007).

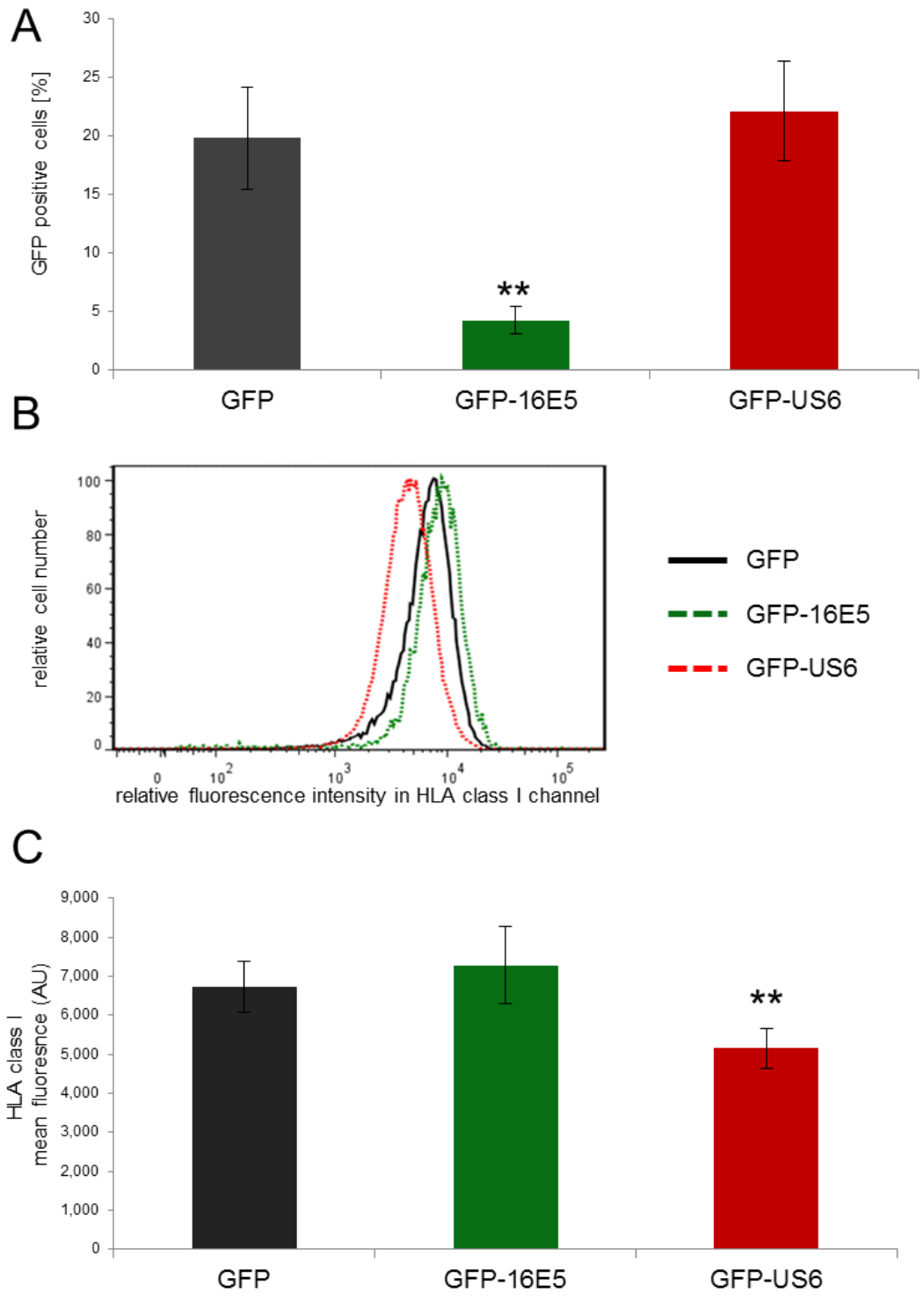

Figure 5.1 HLA class I cell surface regulation by 16E5. SiHa cells were transfected with GFP-16E5 as well as the negative control GFP and the positive control GFP-US6. Cells were harvested 16 h post-transfection and stained with W6/32 and Alexa Fluor® 647 goat anti-mouse IgG antibody. A flow cytometer was used to collect 500 000 single cells and analyse the live (PI negative) and GFP positive cells for their cell surface HLA class I levels. A. Relative expression efficiency of GFP and GFP fusion proteins in the live cell population. B. Histograms of a representative flow cytometry experiment are shown C. Results of seven independent experiments are depicted in the bar chart. Each bar represents the mean fluorescence in the HLA class I channel (± SDM). A one-way ANOVA was performed (A. and C.) **$p \leq 0.01$

5.2.1.2. GFP-16E5 did not down-regulate exogenously expressed HLA-A2 in SiHa cells

Contrary to expectations, GFP-16E5 did not cause cell surface down-regulation of the endogenous HLA class I molecules in SiHa cells (5.2.1.1). HPV16 E5 is also known to specifically down-regulate exogenously expressed HLA-A2 from the cell surface (Campo et al., 2010). Since SiHa cells do not express this HLA class I type (Schoell et al., 1999), we sought to verify the 16E5 induced down-regulation of exogenously expressed HLA-A2 in SiHa cells.

SiHa cell were transfected with GFP-16E5 and untagged HLA-A2 in a ratio of 1:2 to ensure that every cell expressing GFP-16E5 was also expressing HLA-A2. GFP was co-expressed with HLA-A2 in the same 1:2 ratio to make up the base value. A third cell population was transfected with free GFP only to serve as a HLA class I expression control. The HCMV US6 protein does not effectively down-regulate the HLA-A2 type (Dugan and Hewitt, 2009) and could therefore not be used as a positive control in this assay.

Cells were stained for HLA-A2 16h post-transfection with the specific antibody BB7.2. The gates for live (PI negative) and successfully stained cells were established as before (5.2.1.1). From 500 000 collected live cells only the GFP positive cells were analysed for HLA-A2 cell surface expression (Figure 5.2).
The expression efficiencies were similar to those observed earlier (Figure 5.1A). With only 3% (± 1.4) the transfection efficiency for GFP-16E5 was markedly lower compared to GFP (15% ± 2.3 and 16% ± 3.3, respectively) ($p \leq 0.01$). Despite this, an average of 9014 (± 2384) GFP-16E5 positive cells were analysed per sample which was sufficient for meaningful statistical analysis.

The histogram of GFP expressing cells which served as a HLA-A2 expression control formed a peak at low intensity in the HLA-A2 fluorescent channel (Figure 5.2B). This was regarded as a false positive signal. The GFP and HLA-A2 expressing cells had a peak around the same fluorescent intensity that probably accounts for GFP expressing cells that were not successfully co-transfected with HLA-A2. A second peak was recorded at a ~ 2 log higher fluorescent

intensity. This cell population effectively co-expressed GFP and HLA-A2 and were regarded as base value. GFP-16E5 and HLA-A2 transfected cells exhibited a minor peak only for HLA-A2 untransfected cells. The peak at higher HLA-A2 fluorescence accounting for co-transfected cells almost coincided with the same peak for GFP and HLA-A2 expressing cells. However, it was remotely shifted towards greater fluorescence intensity. This means that GFP-16E5 expression slightly promoted HLA-A2 cell surface levels which is in contrast to what was observed by others (Campo et al., 2010).

A total of six repetitions of the experiment and subsequent statistical analysis confirmed the phenomenon observed. Only cells that confidently expressed HLA-A2 were considered for the analysis (Figure 5.2B, dashed box). The HLA-A2 recognition of the BB7.2 antibody was significantly increased by 760% in GFP and HLA-A2 expressing cells compared to the HLA-A2 expression control cells ($p \leq 0.01$) (Figure 5.2C). This confirmed not only that SiHa cells are HLA-A2 negative but also that expression of exogenously expressed HLA-A2 was successful. Grounded on the base value, GFP-16E5 expressing cells exhibited a significant up-regulation of cell surface HLA-A2 by 29.7% (± 21.8) ($p \leq 0.01$). This confirmed the observation made in the histogram (Figure 5.2B) but is in contrast to published findings (Campo et al., 2010).

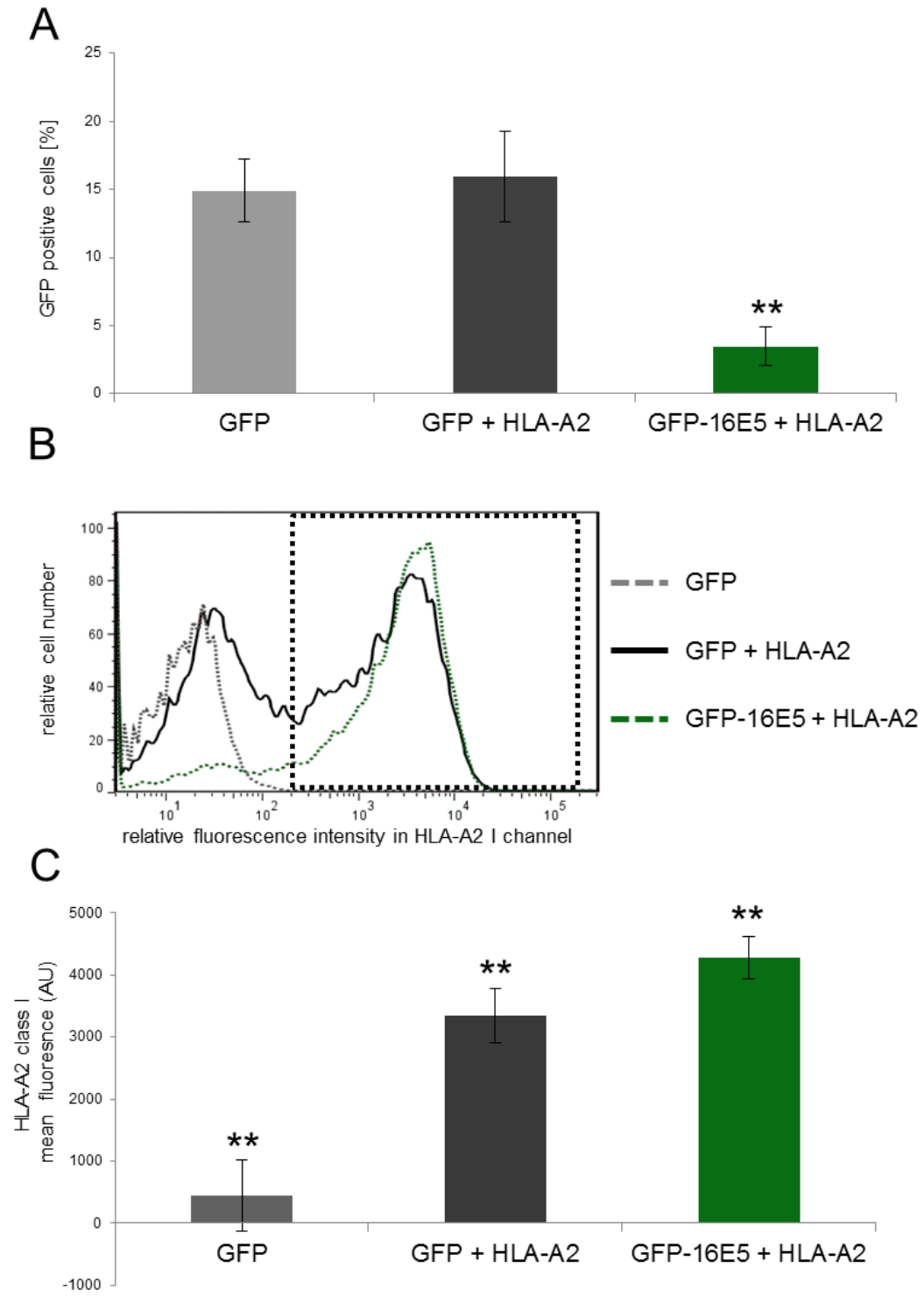

Figure 5.2 Cell surface regulation of HLA-A2 by 16E5. SiHa cells were transfected with GFP-16E5 + HLA-A2 as well as the negative controls GFP and GFP + HLA-A2. Cells were stained with BB7.2 and Alexa Fluor® 647 goat anti-mouse IgG antibody for HLA-A2 16 h post-transfection. A flow cytometer was used to collect 500 000 live (PI negative) cells and analyse the GFP positive cells for their HLA-A2 cell surface levels. A. Relative expression efficiency of GFP-16E5 and GFP, respectively, in live cells. B. Histograms from a representative flow cytometry experiment are shown. The mean fluorescence in the indicated box was used for comparative analysis. C. The data from six independent experiments are summarised in the bar chart. Each bar represents the mean fluorescence of the HLA-A2 channel (± SDM). A one-way ANOVA was performed (A. + C.) **$p \leq 0.01$

5.2.2. YIPF4 was not involved in HLA class I cell surface regulation

5.2.2.1. Determination of YIPF4 half-life

The 16E5 induced down-regulation of cell surface HLA class I molecules could not be verified (5.2.1.1, 5.2.1.2) and thus the investigation of the involvement of YIPF4 in this process was not possible. However, due to the localisation of YIPF4 at the Golgi and its potential role in intracellular trafficking (Figure 1.7) we sought to investigate whether YIPF4 may play a role in HLA class I secretory trafficking. This was tested by siRNA mediated knock down of YIPF4 and subsequent observation of the effect on HLA class I cell surface level.

To achieve efficient knock down, the half-life of endogenous YIPF4 needed to be determined. For this, U-2 OS cells were incubated with the translation elongation inhibitor cycloheximide for up to 72 h. Several time points were taken and the YIPF4 protein levels monitored on a Western blot (Figure 5.3A). For 30 h of translational inhibition, YIPF4 protein levels appeared to be constant. Only after 48 h a marked decrease in YIPF4 protein levels could be observed and an almost complete absence at 72 h. The YIPF4 half-life therefore ranged between 30 h and 48h.

The densitometry analysis of this Western blot allowed a closer examination of the YIPF4 half-life (Figure 5.3B). The YIPF4 protein levels were determined in relation to the loading control actin and plotted as a scatter graph. A fitted linear trend line ($R^2 = 0.838$) enabled the calculation of the YIPF4 half-life according to its equation ($y = -0.0109x + 0.8641$). The YIPF4 half-life emerged to be ~ 44 h.

A

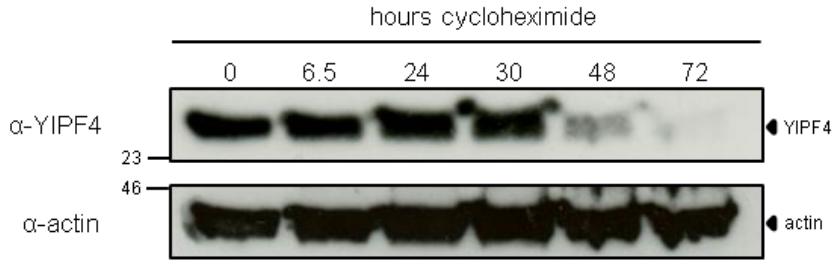

B

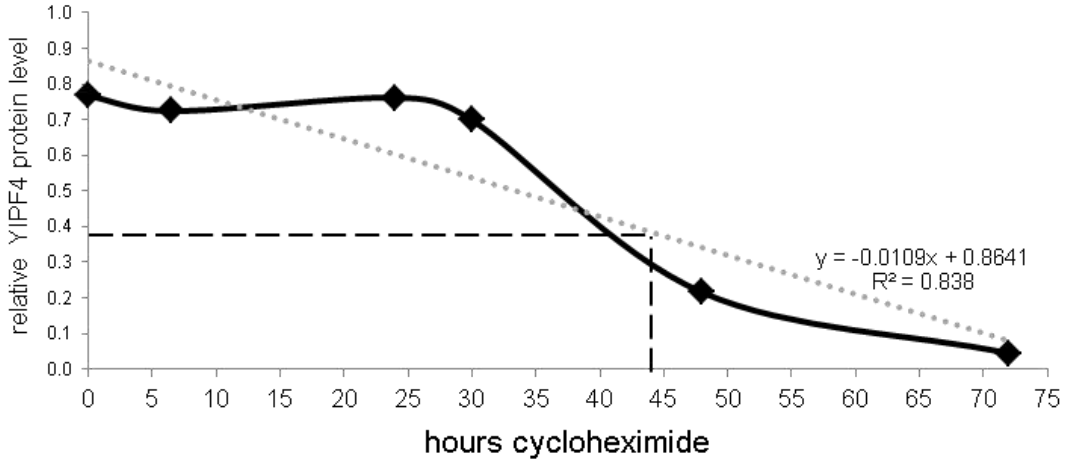

Figure 5.3 Determination of YIPF4 half-life. A. The half-life of YIPF4 was determined in U-2 OS cells by incubation with 100 µg/ml cycloheximide. The YIPF4 expression level was monitored on a Western blot at several time points. B. Densitometry analysis of YIPF4 expression levels relative to the loading control actin. A linear trendline (dotted line) was fitted that allowed approximate determination of the YIPF4 half-life ≈ 44 h (dashed line).

5.2.2.2. YIPF4 was successfully knocked down with specific siRNA

The knock down of YIPF4 was mediated with siRNA. Four specific commercial siRNAs were tested. Here, only data for the effective siRNA4 are presented.

The 21-nucleotide siRNA4 completely aligned to bp 503 - 523 of the YIPF4 mRNA (Figure 5.4A) which forms part of the hydrophilic N-terminus in the protein. A BLASTN search confirmed that these 21 nucleotides did not align with transcripts of other human genes (data not shown) thus reducing the probability of off target effects.

SiHa cells were transfected with 300 ng siRNA4 and incubated for up to 72 h while taking several time points. The YIPF4 protein level was monitored on a Western blot (Figure 5.4B). A reduction of YIPF4 protein level was detected 16 h post-transfection and a near absence of YIPF4 after 40 h.

Densitometry analysis revealed a 97% knock down of YIPF4 40 h post-transfection (Figure 5.4C). This was a more efficient knock down than expected based on the data from the cycloheximide experiment (5.2.2.1).

A

```
YIPF4          1 aatcccagcgccgctgtcactgttatggtcctgtcagggtgccggcgtcg     50
siRNA4         1 ---------------------------------------------------     0

                 ..........................................................

YIPF4        501 ggaagaattggacattgatctaaaggatatttactacaaaatccgatgtg    550
                   ||||||||||||||||||||
siRNA4         1 --aagaattggacattgatctaa--------------------------     21

                ...........................................................

YIPF4       1951 ttttgttttacagcaaaaaaaaaaaaaaaaaa   1982
siRNA4        22 --------------------------------     21
```

B

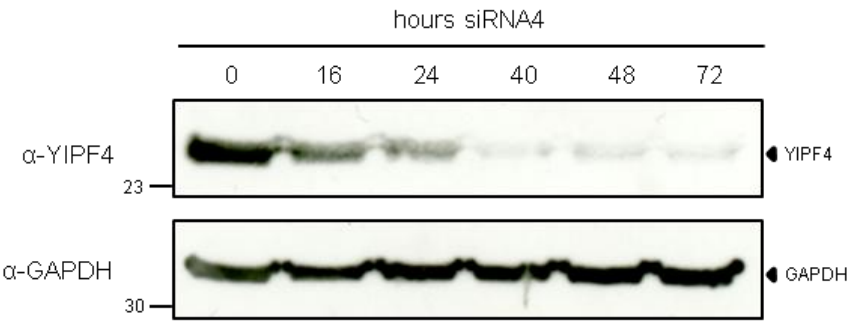

C

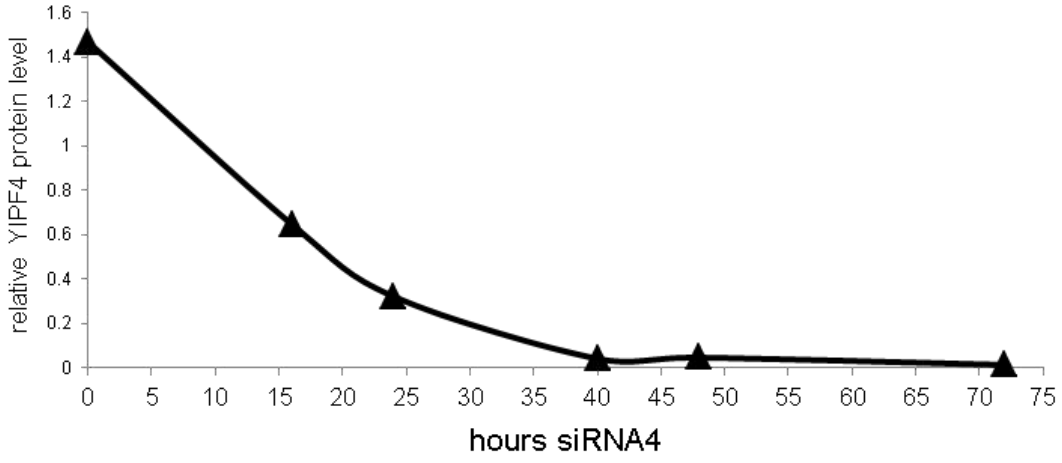

Figure 5.4 Knock down of YIPF4 with specific siRNA. A. The sequence of the 21nt siRNA4 was aligned to the mRNA sequence of YIPF4 (NCBI Ref. NM_032312.3). The overlapping sequences are shown as well as the beginning and end of the YIPF4 mRNA sequence. B. SiHa cells were transfected with 300 ng of siRNA. The YIPF4 protein levels were monitored at several time points on a Western blot. C. The protein levels of YIPF4 were determined relative to GAPDH by densitometry analysis of the Western blot (B).

5.2.2.3. siRNA mediated knock down of YIPF4 did not affect cell surface HLA class I expression

The effect of YIPF4 on HLA class I trafficking was examined by comparing the HLA class I cell surface levels in siRNA4 (Figure 5.4) transfected cells with untransfected cells. The untransfected cells served as the base value. A commercial negative control siRNA (siRNA NC) was included to exclude possible nonspecific effects caused by transfection with siRNA.

The SiHa cells that were transfected with siRNA4 and siRNA NC, respectively, were incubated for 40 h to guarantee sufficient knock down (5.2.2.2). Aliquots of three samples sets were analysed by Western blot for YIPF4 protein levels (Figure 5.5) to verify the flow cytometry data (Figure 5.6). Compared to untransfected cells, the YIPF4 protein levels in siRNA4 transfected cells were obviously decreased. The siRNA NC appeared to elevate the YIPF4 protein levels in sample sets 2 and 3. The densitometry analysis confirmed a relative knock down of YIPF4 in sample set 1 (80%), set 2 (50%) and set 3 (40%) (Figure 5.5B). The surprising up-regulation of YIPF4 protein levels by siRNA NC could be described for sample set 2 (30%) and set 3 (100%). The reason for the up-regulation of YIPF4 protein levels by the siRNA NC was not investigated further.

The HLA class I molecules of the remaining cells were stained with W6/32. PI was used as a viability marker and the respective gate was established using untransfected, PI negative cells (data not shown). The 100 000 collected live cells were analysed for their HLA class I cell surface expression (Figure 5.6). The histogram of untransfected cells was used as the base value (Figure 5.6A). According to expectations, the histogram of the siRNA NC cell population almost overlapped with the untransfected cells. Only a minor shift towards decreased fluorescence intensity was observed. Thus, the siRNA NC did not non-specifically alter HLA class I cell surface levels. Interestingly, the histogram of cells transfected with YIPF4-specififc siRNA4 also overlapped with the untransfected cells. Therefore, YIPF4 appeared not to be involved in HLA class I cell surface regulation.

These observations were statistically supported by evaluating the data from the three sample sets (Figure 5.6B). Cells transfected with YIPF4-specififc siRNA4 showed an average HLA class I cells surface down-regulation of 6.1% (± 19.4). This, however, was not significantly different from the untransfected control cells. The same was true for the siRNA NC transfected cells that showed an average down-regulation of 15.9% (± 6.1). Concluding from this, YIPF4 does not play a role in HLA class I cell surface regulation.

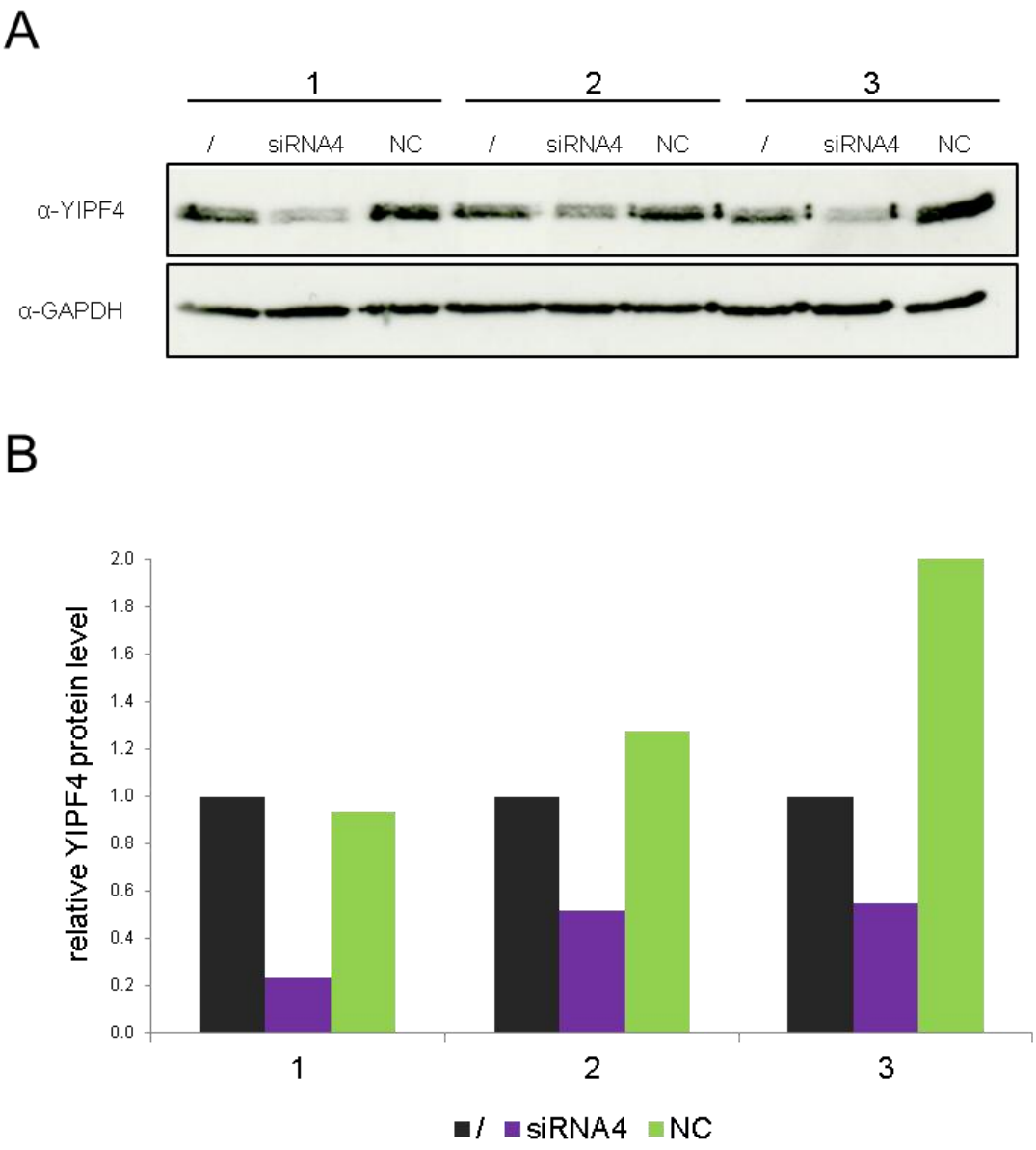

Figure 5.5 Verification of the knock down of YIPF4 in the SiHa cells analysed for HLA class I surface expression. A. An aliquot of the samples analysed by FACS (Figure 5.6) was lysed and the YIPF4 protein levels were observed on a Western blot. B. The protein levels of YIPF4 were determined by densitometry relative to the loading control GAPDH. YIPF4 was knocked down between 80%, 50% and 40%, respectively. The numbers 1, 2 and 3 indicate the number of the experimental repetition. ‘ / ‘ = untransfected cells; ‘ NC ‘ = siRNA NC

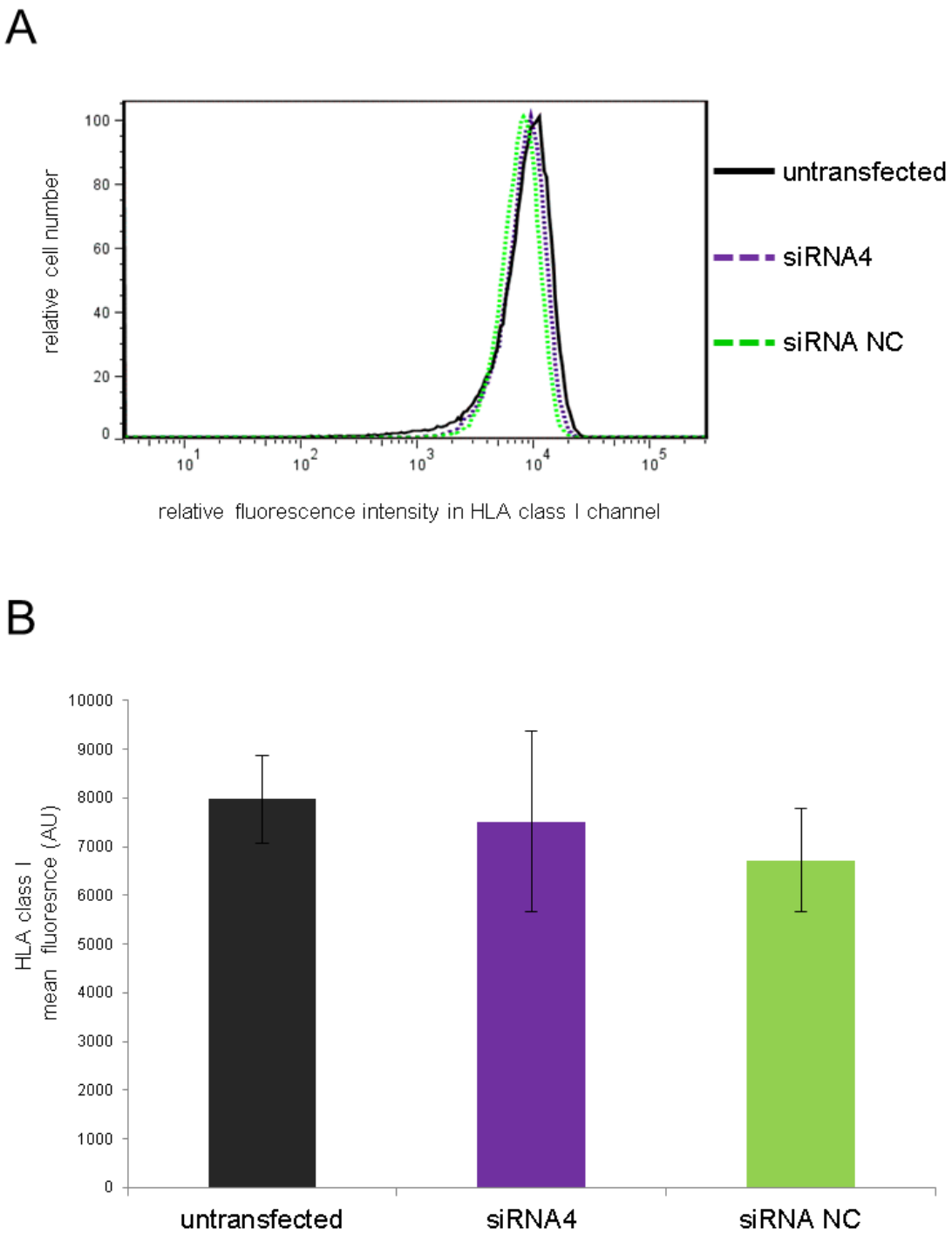

Figure 5.6 HLA class I cell surface expression in SiHa cells upon siRNA mediated knock down of YIPF4. SiHa cells were transfected with 300 ng of specific siRNA4. Forty hours post-transfection cells were stained with W6/32 and Alexa Fluor® 647 goat anti-mouse IgG antibody. A flow cytometer was used to analyse 100 000 live (PI negative) cells for their HLA class I cell surface expression. A. Histograms of a representative experiment are shown B. The data from three independent experiments were analysed. A one-way ANOVA revealed no significant differences between the samples. Each bar represents the mean fluorescence (± SDM) of the HLA class I channel.

5.2.3. Determination of the YIPF4 interactome

In our hands, the 16E5 induced down-regulation of HLA class I could not be verified (5.2.1.1, 5.2.1.2). In addition, our data do not support a role for YIPF4 in HLA class I cell surface expression (5.2.2.3). To eventually establish the role of the E5/YIPF4 complex within the cell, we sought to determine the cellular role of YIPF4. This should greatly facilitate the investigation of the E5/YIPF4 complex. YIPF3 is the only known interaction partner of YIPF4 within the cell (Tanimoto et al., 2011) and its role is equally unclear. Therefore, we set out to determine the interactome of YIPF4 to be able to identify biological processes it might be involved in. This was achieved by immuno-precipitating YIPF4 and identifying binding partners by mass spectrometry analysis.

The GFP-YIPF4 fusion protein and GFP, respectively, were expressed in HEK293T cells (Figure 5.7). Cells were harvested and lysed 20 h post-transfection and the expression of the exogenous proteins confirmed on a Western blot (Figure 5.7, upper blot). Note that the GFP-YIPF4 fusion protein showed lower expression efficiency than free GFP. The same amount of total protein from these lysates was subject to IP with a GFP binding protein based on *Camelidae* HC antibodies coupled to magnetic beads. After o/n incubation and two washing steps, an aliquot of the eluates was successfully analysed on a Western blot for the presence of GFP and GFP-YIPF4 (Figure 5.7, lower blot). Again, GFP-YIPF4 was present to a lesser extent than free GFP. The eluates were trypsin digested and separately analysed by nano-LC ESI-MS/MS for their composition. The potential binding partners of YIPF4 were identified by label free quantification (LFQ) relative to GFP interacting proteins (performed at CECAD, Cologne, Germany)

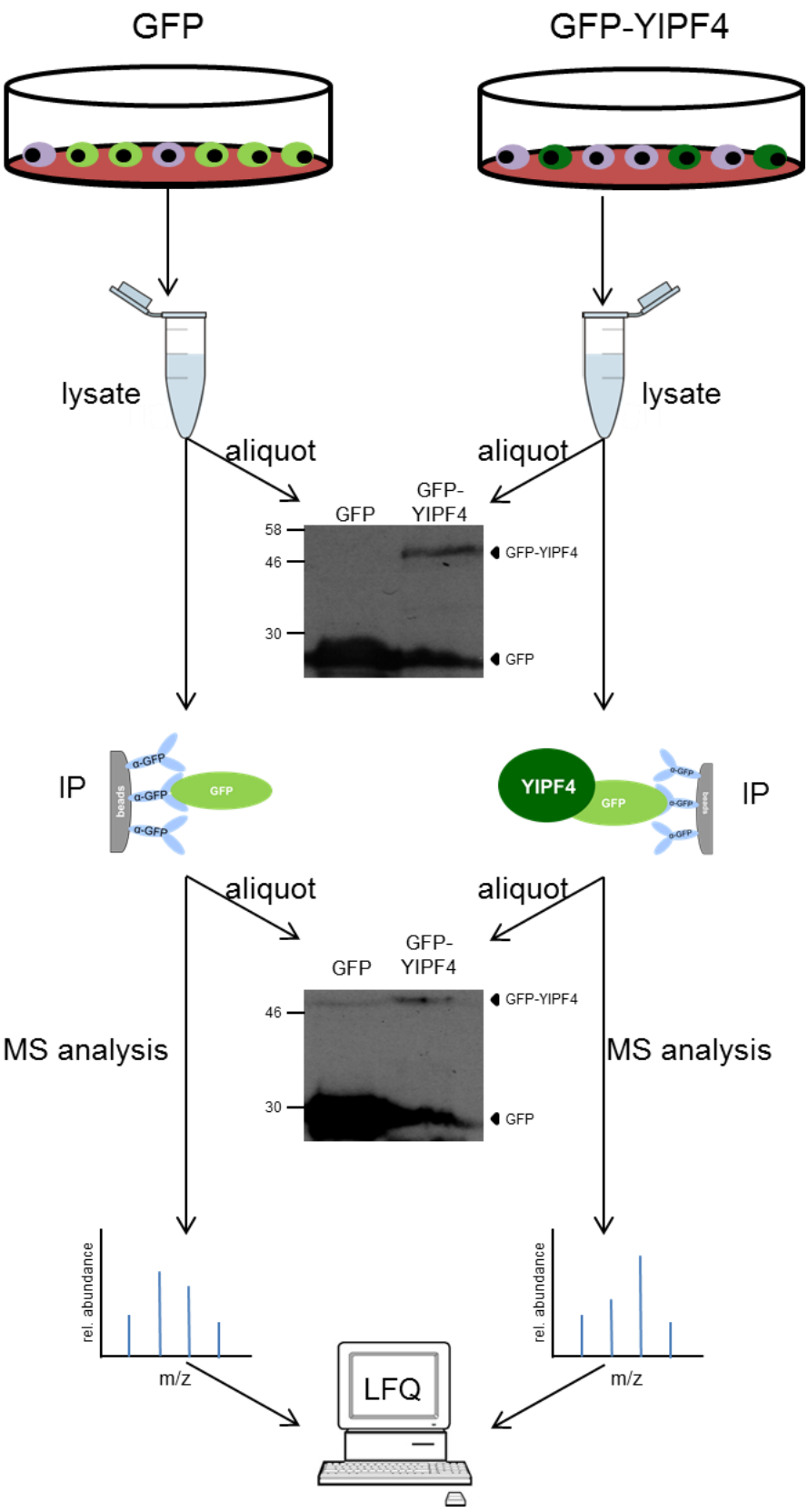

Figure 5.7 Schematic of the procedure to determine cellular binding partners of YIPF4 by nano-LC ESI-MS/MS. For detailed description refer to main text (5.2.3).

5.2.3.1. Classification of YIPF4 binding proteins

The LFQ resulted in a list of 1114 identified proteins for both samples (data not shown). The following criteria were applied to narrow down the identified proteins to increase confidence in potential YIPF4 binding partners: Only proteins that were identified by > 2 unique peptides were considered when these were enriched by ≥ 1.5 fold in the GFP-YIPF4 sample. In addition to that, the unique peptides accounting for the enrichment needed to be ≥ 1/3 of the overall peptide count of the protein. These criteria narrowed down the list to 105 potential YIPF4 binding partners (Table 5.1, Table A. 7, Table A. 8). These were categorised according to their molecular function (Figure 5.8) and biological processes (Figure 5.9) with the PANTHER classification system (Mi et al., 2013). Note that the PANTHER classification system did not recognise the UniProt IDs for pinin, probable ATP-dependent RNA helicase and histone deacetylase complex subunit, thus, the analysis was based on a list of 102 potential YIPF4 binding partners.

The annotation of the protein list according to the molecular function revealed that a majority of potential YIPF4 interaction partners (45%) were involved in binding (Figure 5.8A). Most of these bound to nucleic acid (86%) of which 62% constitute RNA (data not shown). A quarter of potential YIPF4 interaction partner exerted catalytic activity (25.4%) (Figure 5.8A) with almost half of them being involved in RNA splicing (45.7%) (Figure 5.8B). The third largest class of YIPF4 binders served as structural molecules (18.3%) (Figure 5.8A) predominantly by constituting ribosomes (90.3%) (Figure 5.8B). It was striking that many of these proteins are localised in the cell nucleus (Table A. 7) which deviates from the Golgi localisation of endogenous YIPF4.

The classification of the potential YIPF4 interaction partners according to their biological function revealed a great involvement in metabolic processes (45.1%) (Figure 5.9A) which were classified as primary metabolic processes (100%) (Figure 5.9B). Very interestingly for the HPV context, 12% of potential YIPF4 interaction partners played a role in cellular processes (Figure 5.9A) and predominantly the cell cycle (43.3%) (Figure 5.9B). A minority of binding

partners were classified as transport proteins (5.4%) (Figure 5.9A) of which 46.7% mediate protein transport and 13.3% vesicle transport (Figure 5.9B). This was in accordance with the suspected function of YIPF4 (5.1). Although no effect on the HLA class I cell surface regulation was observed (5.2.2.3), 3.8% of potential YIPF4 interaction partners were involved in immune response to IFN-γ (Figure 5.9A).

Concluding from this annotation of potential YIPF4 binding partners, YIPF4 appeared to play a role in the metabolism of the cell which includes RNA binding, splicing and translation. However, as mentioned before, the majority of these proteins were localised in the nucleus (Table A. 7) and should therefore not be accessible to the Golgi-localised YIPF4 within the living cell (see 5.3.3.1). Table 5.1 summarises the more confident potential YIPF4 binding partners that are not confined to the nucleus (discussed in 5.3.3.1).

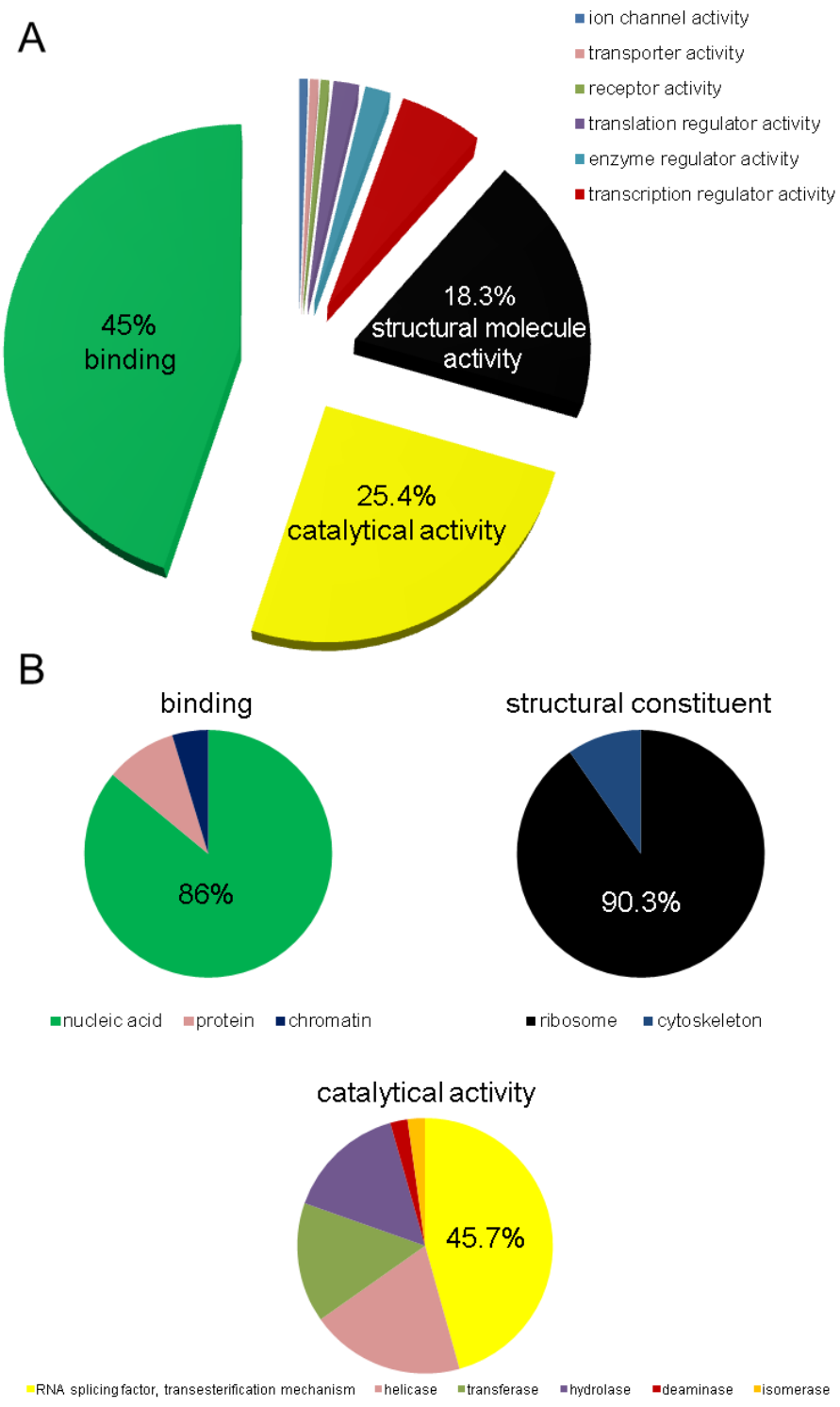

Figure 5.8 Analysis of the molecular functions of the potential cellular binding partners of YIPF4. The LFQ by mass spectrometry returned 105 cellular proteins as probable binding partner of YIPF4. The UniProt IDs were used to analyse the molecular functions of the proteins using the PANTHER classification system. Three protein IDs were not recognised by PANTHER. A. Pie chart showing the categories of molecular functions represented by the probable YIPF4 binding partners. The three largest categories were examined further B. The pie charts represent the proteins from the three largest categories (A) and show their further composition.

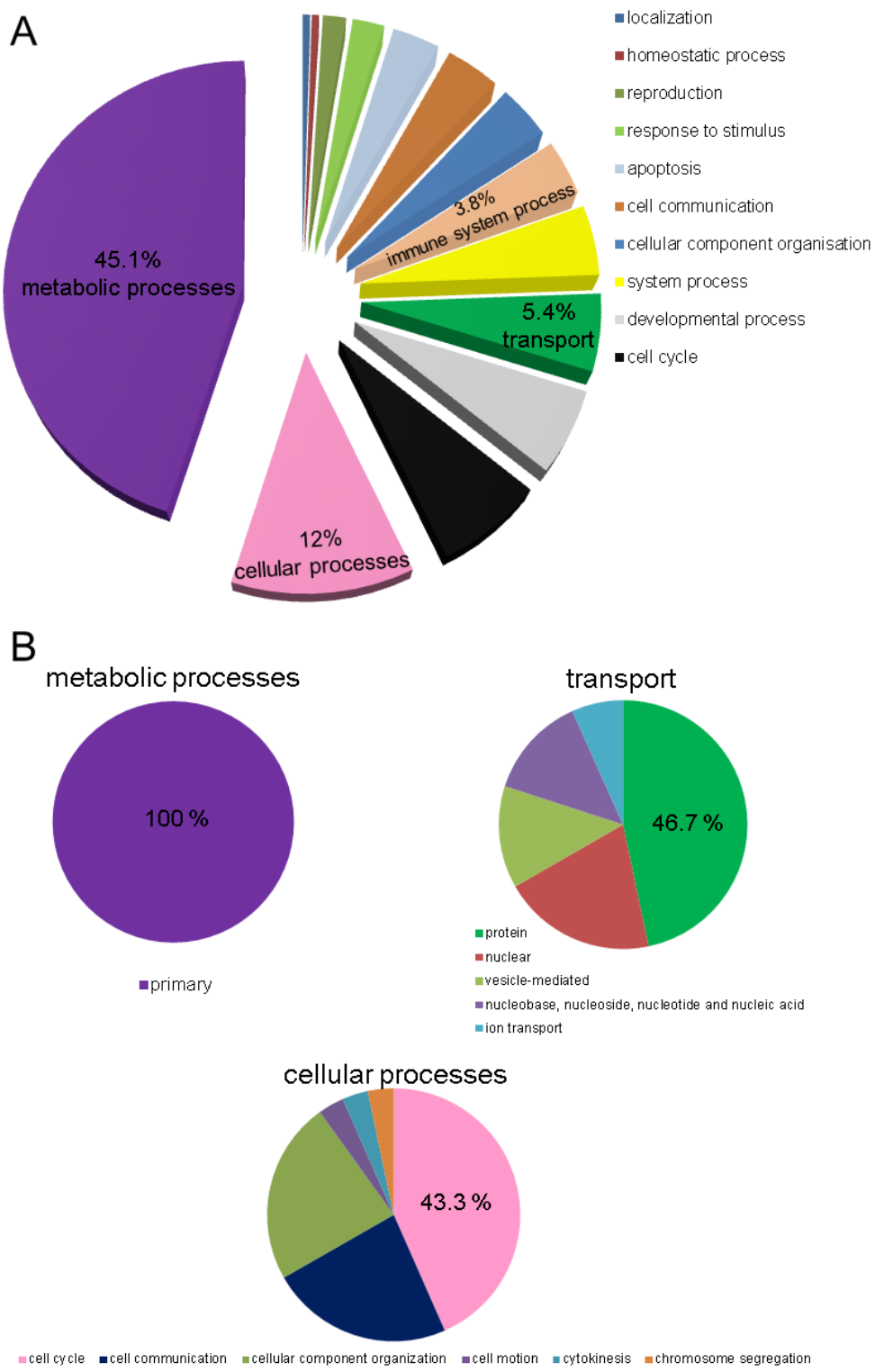

Figure 5.9 The potential YIPF4 binding partners are involved in a variety of biological processes. The 102 probable cellular interaction partners of YIPF4 were categorised according to the biological processes they are involved in using the PANTHER classification system. A. Pie chart showing the categories of biological processes represented by the probable YIPF4 binding partners. The two largest and the 'transport' category were examined further B. The pie charts represent the proteins from the 'metabolic processes', 'transport' and cellular processes' category (A) and show their further composition.

Table 5.1 Potential YIPF4 binding partners determined with the LFQ approach. Proteins were annotated with the PANTHER classification system. Information about the cellular localisation was derived from the UniProt database.

gene ID	gene name	enrichment factor	cellular localisation	PANTHER family/subfamily	GO molecular function	GO biological process	PANTHER protein class	pathway
P02765	alpha-2-HS-glycoprotein	36.84	secreted	α-2-HS- glycoprotein (FETUIN-A) (PTHR13814:SF6)	protein binding, cysteine-type endopeptidase inhibitor activity	immune system, proteolysis, mesoderm/skeletal system development	extracellular matrix glycoprotein, cysteine protease inhibitor	n/n
P62258	14-3-3 protein epsilon	13.82	cytoplasm	14-3-3 protein epsilon (PTHR18860:SF10)	n/n	cell cycle, signal transduction	chaperone	EGF-R/FGF signalling
Q9NYF8	Bcl-2-associated transcription factor 1	7.55	cytoplasm, nucleus	BCL-2-associated transcription factor 1 (PTHR15268:SF4)	transcription factor activity	induction of apoptosis, regulation of transcription from RNA polymerase II promoter	transcription factor	n/n
P63244	guanine nucleotide-binding protein subunit beta-2-like 1	6.29	cell membrane, cytoplasm, perinuclear region, dendrite	n/n (PTHR19868:SF0)	n/n	protein targeting, signal transduction	n/n	n/n

gene ID	gene name	enrichment factor	cellular localisation	PANTHER family/subfamily	GO molecular function	GO biological process	PANTHER protein class	pathway
P05023	sodium/potassium-transporting ATPase subunit alpha-1	4.93	cell membrane; multi-pass membrane protein.	n/n (PTHR24093:SF58)	hydrolase activity, cation trans-membrane transporter activity, ion channel activity	cation transport, cellular calcium ion homeostasis	cation transporter, ion channel, hydrolase	n/n
P13797	plastin-3	3.86	cytoplasm	plastin (PTHR19961:SF8)	structural constituent of cytoskeleton, actin binding	cellular component morphogenesis	non-motor actin binding protein	n/n
P06737	glycogen phosphorylase, liver form	3.71	cytoplasm, plasma membrane	n/n (PTHR11468:SF0)	phosphorylase activity	glycogen metabolic process	phos-phorylase	Hetero-trimeric G-protein signalling, Gi alpha and Gs alpha mediated pathway-, phosphorylase a/b
Q71U36	tubulin alpha-1A chain	3.21	cytoplasm	tubulin alpha chain (PTHR11588:SF10)	structural constituent of cytoskeleton	intracellular protein transport, mitosis, cell motion, chromosome segregation, cellular component morphogenesis	tubulin	gonadotropin releasing hormone receptor pathway

gene ID	gene name	enrichment factor	cellular localisation	PANTHER family/subfamily	GO molecular function	GO biological process	PANTHER protein class	pathway
P50990	T-complex protein 1 subunit theta	2.78	cytoplasm, centrosome	chaperonin containing T-complex protein 1, theta subunit, TCPQ (PTHR11353:SF19)	n/n	protein folding	chaperonin	n/n
O60884	dnaJ homolog subfamily A member 2	1.79	membrane, lipid-anchor	n/n (PTHR24076:SF45)	n/n	immune system process, protein folding, response to stress	chaperone	n/n
P60709	actin, cytoplasmic 1	1.75	cytoplasm	n/n (PTHR11937:SF120)	structural constituent of cytoskeleton	intracellular protein transport, exocytosis, endocytosis, mitosis, cytokinesis, cellular component morphogenesis	actin and actin related protein	Alzheimer and Huntington disease-presenilin, cytoskeletal regulation by Rho GTPase, nicotinic acetylcholine receptor, cadherin cytokine and integrin signalling, inflammation mediated by chemokine

gene ID	gene name	enrichment factor	cellular localisation	PANTHER family/subfamily	GO molecular function	GO biological process	PANTHER protein class	pathway
P53621	coatomer subunit alpha	1.61	cytoplasm, Golgi membrane; peripheral membrane protein; COPI-coated vesicle membrane	coatomer alpha subunit (PTHR19876:SF1)	n/n	intracellular protein transport, endocytosis, exocytosis	vesicle coat protein	n/n

‘gene ID’ indicates the UniProt database ID; ‘enrichment factor’ indicates the enrichment of the respective protein in the GFP-YIPF4 sample compared to the GFP control sample. n/n = not named; GO = gene ontology

5.3. Discussion

5.3.1. GFP-16E5 does not (down-)regulate cell surface HLA class I molecules

5.3.1.1. GFP-16E5 does not down-regulate endogenous HLA class I molecules in SiHa cells

In this study, the 16E5 mediated down-regulation of HLA class I cell surface levels could not be verified (Figure 5.1). With the utilisation of a suitable positive control it was excluded that the lack of effect was evoked by an inadequate assay. This result is surprising because this effect of 16E5 is established in the literature and was shown in various cell lines using different techniques to exogenously express 16E5 (Ashrafi et al., 2006b, Ashrafi et al., 2005, Campo et al., 2010). Indeed, Gruener and colleagues used an N-terminal GFP fusion protein of 16E5 comparable to the one used in this study to successfully generate this effect in HEK293T cells (Gruener et al., 2007).

Further investigations are needed to determine the reason for this discrepancy. The functional activity of the GFP-16E5 fusion protein could be explored by determining its ability to interact with the HLA HC or calnexin. However, its binding to the 16K subunit of the vacuolar H^+ - ATPase was successfully shown (Figure A. 5). In addition, the similar GFP-16E5 fusion construct used by Gruener and colleagues interacted with HLA HC and calnexin in a ternary complex (Gruener et al., 2007). Thus, the large GFP tag at the N-terminus of 16E5 does not cause the abrogation of binding to HLA HC and calnexin via the 1^{st} TMD. The ability to down-regulate HLA class I from the cell surface was directly compared between GFP tagged and HA tagged 16E5 with no major difference being observed (Gruener et al., 2007).

The expression of calnexin was shown to be necessary for the E5 induced down-regulation of HLA class I from the cell surface (Gruener et al., 2007). The study here used SiHa cells, which express 4.8 fold less calnexin compared to HaCaT cells (Ahn et al., 2005). It is therefore conceivable, that the lack of down-regulation observed is caused by insufficient amounts of calnexin in those cells.

The SiHa cell line contains 1 or 2 integrated copies of the HPV16 genome and was derived from a cervical SCC (Pater and Pater, 1985). This implies that the cells successfully evaded the patient's immune system. Due to the way the HPV16 genome is integrated, SiHa cells do not express the 16E5 protein (Pater and Pater, 1985, Sahab et al., 2012). The immune evasion must have been at least partially mediated by another HPV protein. Indeed, siRNA mediated knock down of 16E7 in SiHa and CaSki cells significantly up-regulated HLA class I cell surface levels by 50% - 70% (Bottley et al., 2008, Li et al., 2006). This means that the 16E7 oncoprotein is also capable of inducing down-regulation of HLA class I molecules. It appears to achieve this effect with multiple strategies.

It was shown that 16E7 represses HLA class I promoter activity (Georgopoulos et al., 2000, Li et al., 2006, Li et al., 2009). HPV16 E7 binds to a GGTCA motif upstream of the transcription initiation site to induce the repression (Li et al., 2009). A complementary mechanism is the interaction with histone deacetylase 1 (Li et al., 2006) which is most likely mediated by its C-terminal amino acid residues at position 78, 80 and 88 (Heller et al., 2011). The deacetylation of the chromatin around the HLA class I promoter in CaSki cells was shown to prevent transcription from this promoter (Li et al., 2006). The inaccessibility of the promoter not only prevents the constitutive expression of the HLA class I gene but also its inducible expression (Li et al., 2006). The HLA class I promoter can no longer be accessed by the transcription factor NF-κB which is induced by specific cytokines. In addition to that, NF-κB is sequestered in the cytoplasm to prevent induction of transcription. Therefore, in contrast to 16E5, 16E7 down-regulates HLA class I on a transcriptional level.

An additional mechanism of 11E7 mediated cell surface down-regulation of HLA class I is the direct binding to TAP-1 (Vambutas et al., 2001). The interaction inhibits the transport of peptides from the cytoplasm into the ER lumen. This eventually prevents the correct assembly of the HLA class I molecule and its expression on the cell surface. A previously established loss of TAP-1 protein in HPV infected cells (Cromme et al., 1994, Vambutas et al., 2000) was revised (Vambutas et al., 2001).

It is theoretically conceivable that the down-regulation of HLA class I by 16E7 in SiHa cells is exhaustive. This might explain the inability of GFP-16E5 to achieve further down-regulation (Figure 5.1). However, the HCMV US6 protein could mediate a further reduction of HLA class I cell surface expression by 23% (± 8.8) (Figure 5.1C). US6 deprives TAP from its energy source to prevent the correct assembly and cell surface presentation of HLA class I (Ahn et al., 1997, Dugan and Hewitt, 2008, Hewitt et al., 2001, Kyritsis et al., 2001). This shows that the HLA class I down-regulation in SiHa cells is not exhaustive and that it should therefore be possible to achieve the HLA class I cell surface down-regulation by exogenously expressing 16E5.

Preliminary experiments with exogenous GFP-16E5 in HEK293T and Huh7 cells also did not induce a down-regulation of HLA class I molecules from the cell surface (data not shown). The inability of GFP-16E5 to down-regulate HLA class I cell surface levels is therefore not obscured by the 16E7 protein or insufficient amounts of calnexin in SiHa cells but is cell line independent.

An interesting observation was made when overexpressing 16E7 in U-2 OS cells (Bottley et al., 2008). The cell surface levels of HLA class I were decreasing over time with the first effect being recorded after 24 h. The same research group observed the up-regulation of HLA class I 72 h post-transfection with 16E7 specific siRNA. Thus, at least for 16E7, there appears to be a certain amount of time (~24h) required to be able to observe the HLA class I down-regulation. Gruener and colleagues expressed the GFP-16E5 fusion protein 20h prior to analysis by FACS (Gruener et al., 2007). However, due to high cytotoxicity of GFP-16E5, the transfected cells had to be analysed 16h post-transfection in this study. The detrimental effect of exogenous 16E5 for cell viability was previously observed (Auvinen et al., 2004). It is theoretically possible that a greater effect on HLA class I cell surface expression becomes obvious with increasing duration of expression. This effect was observed for GFP-US6 which showed a more pronounced decrease of cell surface HLA class I levels 48 h post-transfection (data not shown).

To circumvent the high cytotoxicity of GFP-16E5, the GFP fusions of other PV E5 proteins (4.2.5: HPV2a, 6b, 11, 18, 31, BPV1 E5) can be investigated in this FACS-based assay since the effect on HLA/MHC class I is conserved amongst these E5 proteins (5.1). It is also conceivable to compare HLA class I cell surface levels in HFK HPV18 WT and E5 KO cell lines (3.2.2).

5.3.1.2. GFP-16E5 does not down-regulate exogenous HLA-A2 class I molecules in SiHa cells

As discussed above, the approach to verify the down-regulation of HLA class I with the W6/32 antibody in SiHa cells was not successful (5.3.1.1). The W6/32 antibody recognises HLA-A, B and C types. It is theoretically possible that 16E5 induces the down-regulation of one type in this experiment but the effect is masked by the remaining, unaffected HLA class I molecules. It was therefore logical to investigate the effect of GFP-16E5 on one specific HLA class I type.

The HLA-A2 type was previously confirmed to be down-regulated by 16E5 (Campo et al., 2010). This research group used a heterologous system where HA tagged 16E5 and untagged HLA-A2 HC were stably expressed in mouse mastocytoma cells. The down-regulation mediated by HA-16E5 was successfully demonstrated by FACS-based analysis.

The experimental system employed in this study used transient overexpression of GFP-16E5 and untagged HLA-A2 in SiHa cells. Very importantly, exogenous HLA-A2 was expressed from a HCMV immediate-early promoter in these cells. HPV16 E7 only affects endogenous HLA class I promoters (Georgopoulos et al., 2000, Li et al., 2006, Li et al., 2009) so a potential exhaustive down-regulation of HLA-A2 by the endogenous 16E7 protein of SiHa cells could be confidently excluded (5.3.1.1).

A similar expression system was applied to investigate the effect of GFP-US6 on this HLA type resulting in the understanding that an effective down-regulation is not achieved (Dugan and Hewitt, 2009). HCMV US6 could therefore not be employed as a positive control in this assay. However, the increased recognition of the exogenous HLA-A2 by BB7.2 confirmed that the overexpression was successful (Figure 5.2). Possible positive controls for the

down-regulation could be the HCMV proteins US2 and US11 which are known to target HLA-A2 for degradation (Gewurz et al., 2001, Schust et al., 1998).

Despite the previously confirmed down-regulation of HLA-A2 by 16E5 (Campo et al., 2010) and the verification of the assay (Dugan and Hewitt, 2009), in our hands, GFP-16E5 caused an up-regulation of HLA-A2 cell surface levels (Figure 5.2). Compared to the GFP and GFP + HLA-A2 controls, the GFP-16E5 + HLA-A2 samples had very few GFP-16 positive cells that did not express HLA-A2. It is possible that this is indicative of an over-expression artefact. It is conceivable that the expression of HLA-A2 is augmented by co-expression with GFP-16E5 compared to GFP. Indeed, Campo and colleagues specifically assessed the HA-16E5 and HLA-A2 expression levels by Western blot to exclude any variations in the overall amount of HLA-A2. An increase in total HLA-A2 could be responsible for the cell surface up-regulation seen in our GFP-16E5 + HLA-A2 cell populations. In contrast, it was previously observed that the transient co-expression of proteins leads to a decrease of the amounts of both proteins (4.3.1 and Figure A. 4). An aliquot of the cell populations investigated by FACS could be analysed for the total amount of HLA-A2 protein by Western blot to investigate the effect further.

In this assay (5.2.1.2), the cell populations were investigated by FACS only 16h post-transfection due to the high cytotoxicity of the GFP-16E5 overexpression (5.3.1.1). To avoid cytotoxic effects of exogenous GFP-16E5, the HFK HPV18 WT and E5 KO cell lines (3.2.2) might be used in this assay. This requires previous determination of their HLA-A2 cell surface expression. If these cells are HLA-A2 negative, exogenous HLA-A2 has to be introduced to be able to perform this assay.

5.3.2. YIPF4 is not involved in HLA class I cell surface regulation

To the best of your knowledge, this is the first study that determined the half-life of the YIPF4 protein or indeed any protein from the YIP1 family. This was achieved by incubation of U-2 OS cells, which are known to express endogenous YIPF4 (Figure 3.1), with the translational elongation inhibitor cycloheximide. After ~ 44h, half of the YIPF4 protein was degraded. HeLa cells expressing exogenous YIPF4 were previously treated with cycloheximide, but

only for 120 min to determine its natural cellular localisation (Shakoori et al., 2003). GFP-16E5 has a half-life of ~2 h (Dr Andrew Macdonald - personal communication) so it would be very interesting to observe whether the interaction with the much shorter lived E5 proteins has an effect on the YIPF4 half-life. The premature degradation of YIPF4 could contribute to the function of the E5/YIPF4 complex. An Initial experiment observing the half-life of YIPF4 in GFP-16E5 expressing cells did not succeed (data not shown). Alternatively, the incubation of HFK HPV18 WT and E5 KO cells with cycloheximide would allow a comparison of the YIPF4 half-life with and without the E5 interaction.

In this study, YIPF4 protein levels were successfully knocked down with commercial siRNA (Figure 5.4). Previously, commercial shRNA constructs with a GFP reporter gene were employed but a knock down was neither achieved on transcript nor on protein level (data not shown). The GFP reporter gene would have offered the advantage of cell sorting. This way only cells successfully transfected with the shRNA could have been analysed. The siRNA approach did not allow for such discrimination between transfected and untransfected cells. However, the analysis of YIPF4 protein levels in the transfected cell population confirmed an overall successful knock down (Figure 5.5).
The initial application of siRNA4 showed a ~97% knock down of YIPF4 after 40 h in SiHa cells (Figure 5.4). According to the half-life of YIPF4 (~44h) determined in U-2 OS cells (Figure 5.3), this knock down appears too efficient. It is possible that the half-life varies in different cell lines. Later applications in SiHa cells, however, showed an average down-regulation of 60% (Figure 5.5) which is in agreement with the YIPF4 half-life of ~ 44h.

A siRNA mediated knock down of YIPF4 was achieved previously (Tanimoto et al., 2011). Their siRNA targeted a different sequence (bp 589 – 607) of the hydrophilic N-terminus than the siRNA4 used in this study (bp 503 - 523) (Figure 5.4A). With their siRNA, a knock down of ~ 80% was accomplished (Tanimoto et al., 2011). Notably, the YIPF4 specific siRNA also significantly reduced the levels of YIPF3 within the cell. It was not conclusively established whether this was due to cross reaction of the siRNA or instability of the YIPF3 protein due to lack of its binding partner YIPF4. The cross reactivity of the

siRNA4 used in this study with YIPF3 or any other YIP1 family protein was not directly investigated. But in the BLASTN search, the siRNA4 sequence exclusively aligned to the YIPF4 sequence which makes an off target effect on other cellular proteins unlikely (5.2.2.2).
Surprisingly, the siRNA NC increased the amount of YIPF4 within the cells of sample set 2 and 3 (Figure 5.5). The elevated amount of YIPF4 within the cells did not have a significant effect on the HLA class I cell surface levels (Figure 5.6). How the siRNA NC increased the YIPF4 protein levels was not investigated further.

The almost complete depletion of YIPF4 in HeLa cells caused the fragmentation of the Golgi (Tanimoto et al., 2011). This phenotype was not examined in this study but could easily be achieved by immuno-fluorescent staining with the *trans*-Golgi network marker TGN46.
This fragmentation of the Golgi, however, does not affect its functions in protein transport and post-translational modification (Tanimoto et al., 2011). This was also acknowledged in this study because the knock down of YIPF4 did not appear to prevent the trafficking of HLA class I molecules to the cell surface (Figure 5.6). However, further experiments are needed to confirm this observation. It is still possible that the knock down of YIPF4 is compensated for by other members of the YIP1 protein family or by un-related proteins with redundant functions. YIPF4 might also be responsible for the trafficking of certain HLA class I types only. In this case the effect could have been concealed by the usage of the W6/32 antibody which recognises a wide variety of HLA class I types. It is also conceivable that YIPF4 regulates the trafficking of HLA class I types that are not endogenously expressed in SiHa cells, like HLA-A2 (Schoell et al., 1999). In these cases the experiment here would depict a false negative result.

Future experiments could target the issue of a potential concealed effect of YIPF4 in HLA class I trafficking. An investigation of the involvement of YIPF4 in other E5 affected trafficking pathways like HLA class II (Zhang et al., 2003), CD1d (Miura et al., 2010), EGF-R (Straight et al., 1993) or caveolin-1 and ganglioside GM1 (Suprynowicz et al., 2008) might be worthwhile.

5.3.3. Determination of cellular binding partners of YIPF4

The analysis of single pathways to determine the role of YIPF4 not only in the E5/YIPF4 complex but also in its natural cellular environment is not efficient. We therefore employed a strategy that aimed to identify all cellular binding partners of YIPF4. To the best of your knowledge, this is the first holistic approach to understand the function of YIPF4 as a representative for other members of the YIP1 family.

The IP of exogenously expressed GFP-YIPF4 fusion protein with the GFP-TRAP® system was chosen to determine the YIPF4 interactome (Figure 5.7). The utilisation of GFP fusion proteins for this sort of application is routinely performed because of several advantages (Trinkle-Mulcahy et al., 2008). The GFP *Camelidae* HC antibody used for the IP binds with very high affinity to the GFP tag. It is therefore very much suitable for this application and outperformed a monoclonal GFP antibody in a direct comparison. Furthermore, stable isotope labelling with amino acids in cell culture (SILAC) and photobleaching experiments revealed that free GFP does not show great interaction with cellular proteins. Thus, despite its size, it is unproblematic to use as a protein tag for pull down.
In addition, the GFP-YIPF4 fusion protein achieved higher expression levels than FLAG-YIPF4-HA (data not shown) which were meant to ensure proper identification by mass spectrometry. Compared to free GFP expression, however, the GFP-YIPF4 fusion protein expressed markedly less (Figure 5.7). This is in accordance with the observation made with the GFP-16E5 fusion protein which expressed significantly lower than free GFP (Figure 5.1A). The GFP-US6 fusion protein, however, expressed to similar extends than free GFP (Figure 5.1A). Why certain GFP-fusion proteins express less efficiently than free GFP was not established.

The use of endogenous YIPF4 for this experiment was not considered to produce more informative results than the overexpression system. As mentioned above, the GFP *Camelidae* HC antibody binds with high affinity and specificity and is widely used for proteomics analysis. The affinity and especially

the specificity of the YIPF4 antibody is less well characterised and would have added uncertainty to the results obtained. Co-IP experiments with endogenous YIPF4 revealed non-specific binding of YIPF4 to the bead matrix (Figure 4.1B). This would have complicated the identification of specific interaction partners.

Magnetic beads were chosen for this experiment. In a comparison with sepharose/agarose beads by SILAC, they showed the least non-specific binding of nuclear proteins (Trinkle-Mulcahy et al., 2008). The exclusion of nuclear proteins was aspired to reduce the amount of contaminants. An interaction of YIPF4 with nuclear proteins is unlikely, because it was firmly established to reside at the Golgi (Figure 3.4) (Tanimoto et al., 2011). Despite the choice of magnetic dynabeads, the majority of proteins identified localised to the nucleus (5.2.3.1 and Table A. 7). This was clearly in contrast to expectations and does not agree with the cellular localisation of YIPF4. The LFQ approach (Figure 5.7) was repeated with the cytoplasmic fraction of cells (data not shown) to eliminate these possible contaminants. This additional handling step during the fractionation procedure, however, introduced great sample-to-sample variations (see below) that made a confident analysis impossible.
Another feasible approach to eliminate these possible contaminants is the modification of the IP. In this study, the IP was performed o/n but an incubation for 30 min was shown to be sufficient to precipitate the desired proteins and minimise the level of contaminants (Trinkle-Mulcahy et al., 2008). Also, the stringency of washed could be modified to achieve this purpose.

The LFQ approach was employed in this study to confidently identify YIPF4 cellular binding partners. Indeed, the peptide sequence coverage by LFQ is significantly better than by chemically labelled samples (Patel et al., 2009). However, in LFQ, in contrast to label-based methods, the samples are treated and analysed separately. As mentioned above, this can induce great variations between the samples. For this reason, it is highly recommended to perform multiple technical and biological replicas to allow the statistical evaluation of potential binding partners (ten Have et al., 2011). In this study, the LFQ was performed for one GFP-YIPF4 and one GFP control sample and can therefore be regarded as a preliminary determination of the YIPF4 interactome.

5.3.3.1. Classification of YIPF4 binding proteins

The list of proteins from the preliminary YIPF4 interactome was filtered under certain criteria to increase the confidence in the identified proteins (5.2.3.1). This resulted in a list of 102 proteins that was annotated with the PANTHER classification system (Mi et al., 2013) (Table 5.1, Table A. 7, Table A. 8).

Surprisingly, the only previously known interaction partner of YIPF4, YIPF3 (Tanimoto et al., 2011), was not amongst these proteins. The experiment was carried out in HEK293T cells, but until now, YIPF3 expression was only confirmed in HeLa cells, normal rat kidney cells, rat liver Golgi membranes (Tanimoto et al., 2011) and nucleated hematopoietic cells (Prost et al., 2002). However, it is likely that its expression is similarly conserved as for YIPF4 (Figure 3.1).
The interaction sites of YIPF4 and YIPF3 were never mapped, so it possible that the GFP tag of the YIPF4 fusion protein sterically hinders the binding. The analysis of the eluate on the Western blot (Figure 5.7) with a specific YIPF3 antibody (Tanimoto et al., 2011) might help to elucidate this issue.
Also, no other YIP1 family proteins were identified in the eluate which is against expectations (1.8). The additional components in the YIPF4/YIPF3 protein complexes (520 kDa, 450 kDa, 260 kDa, 220 kDa) (Tanimoto et al., 2011) could therefore be un-related proteins.

Endogenous YIPF4 was also not amongst the proposed YIPF4 binding partners. This implies that it does not bind to exogenous YIPF4 protein. It is in accordance with the fact that endogenous YIPF4 does not form dimers while exogenously expressed YIPF4 self-associates (Figure 3.1 and Figure 3.10).
The overexpression of myc-YIPF4 rigorously decreased the amounts of endogenous YIPF4 (Figure 3.1). So, the down-regulation of endogenous YIPF4 in GFP-YIPF4 expressing cells might also be the reason for not detecting it amongst the YIPF4 binding partners.
As mentioned above (5.2.3.1, 5.3.3), a great proportion of proteins identified in the eluate (Figure 5.7) are nuclear proteins (Table A. 7), which are likely to be contaminants. Certain groups of proteins are known to ‘reliably’ interact with the

bead matrix in this type of experiment (Boulon et al., 2010, Trinkle-Mulcahy et al., 2008). This ‘bead proteome’ mainly consists of structural and motility proteins, histones, DEAD box helicases, heterogeneous nuclear ribonucleoproteins proteins, eukaryotic elongation/initiation factors, heat shock proteins and ribosomal proteins. And indeed, the list of potential YIPF4 binding partners comprises many of these proteins (Table A. 8). It is therefore possible that these are part of the bead proteome and thus contaminants of this sample. Concluding from this, YIPF4 would not be mainly involved in the metabolic processes including RNA binding, splicing and translation or perform structural molecule activity by binding to ribosomes (Figure 5.8).
The repetition of the experiment with sufficient technical and biological samples will help to distinguish between bead proteome and YIPF4 interactome. In addition to that, the list of protein IDs can be screened against the protein frequency library (Boulon et al., 2010) which evaluates the likelihood of any identified protein to be a contaminant based on a huge database of similar experiments.

In this preliminary approach (Figure 5.7), a number of interesting proteins were identified amongst the potential YIPF4 binding partners that were not obviously part of the bead proteome (Table 5.1). These could either interact with YIPF4 directly or be part of the protein complexes (520kDa, 450kDa, 260kDa, 220 kDa) identified for YIPF4 (Tanimoto et al., 2011).

The protein with the highest enrichment factor (36.84) was α-2-HS-glycoprotein (also fetuin-A) which is secreted from the cell and plays a role in the metabolism, central nervous system, cardiovascular system and bone metabolism and mineralisation (Mori et al., 2011). It is intriguing to speculate that the exocytosis of α-2-HS-glycoprotein is mediated by YIPF4. However, α-2-HS-glycoprotein is predominantly synthesised in the liver and maybe osteoblasts so the expression in the kidney cell line (HEK293T) used for the LFQ experiment might be an artefact of cell culture. A similar observation was made with the glycogen phosphorylase that is enriched by 3.71 fold in the GFP-YIPF4 sample. It is an enzyme of the carbohydrate metabolism in the liver (Ekstrom et al., 2002). Why these proteins are expressed in the HEK293T cell

line used for this experiment and whether the interaction with YIPF4 is genuine remains to be determined.

The protein 14-3-3ε was enriched in the GFP-YIPF4 sample by 13.82 fold. It is one of the seven members of the highly conserved 14-3-3 protein family (Freeman and Morrison, 2011). These proteins bind specifically to phosphoserines/phosphothreonines of their target proteins and alter their conformation, cellular binding partners and cellular localisation. 14-3-3 proteins have been shown to play roles in protein trafficking, regulation of the cell cycle, proliferation and apoptosis. Interestingly, the 14-3-3σ and 14-3-3ζ proteins play roles in carcinogenesis and 14-3-3ζ was shown to interact with the E6 oncoprotein of high-risk HPV types (Boon and Banks, 2013). It can be speculated that E5 exerts its oncogenic properties in a 16E5/YIPF4/14-3-3ε complex formation. Notably, the 14-3-3 proteins predominantly bind to phosphorylated proteins and large scale mass spectrometry analyses indeed suggest that the tyrosines at positions 10 and 60 of YIPF4 are phosphorylated (Hornbeck et al., 2004). Since the 14-3-3 protein family preferentially binds phosphoserines and phosphothreonines, the interaction with 14-3-3ε is therefore likely to be indirect and mediated by another protein within the complex.

The Bcl-2-associated transcription factor 1 is enriched by 7.55 fold in the GFP-YIPF4 sample. It is an interesting candidate for a YIPF4 binding partner when this is in complex with E5. 16E5 was shown to co-localise with the anti-apoptotic protein Bcl-2 in cellular membranes (Auvinen et al., 2004), but whether a functional 16E5/Bcl-2 protein complex is formed remains to be investigated.

The guanine nucleotide-binding protein subunit β-2-like 1 is part of a myriad of signalling complexes within the cell (Gibson, 2012) and is enriched by 6.29 fold in the GFP-YIPF4 sample in this analysis. However, it also forms part of the ribosome complex and is therefore at risk of being part of the bead proteome (Boulon et al., 2010, Trinkle-Mulcahy et al., 2008).

A very interesting binding candidate for YIPF4 is the Na^+/K^+-transporting ATPase subunit α-1 which is enriched by 4.93 fold. This is the catalytic subunit of an enzyme that hydrolyses ATP to promote the exchange of Na^+ and K^+ ions across the plasma membrane (Blanco, 2005). It is indeed intriguing to speculate that in HPV infected cells, YIPF4 interacts with the viroporin 16E5 instead of/in addition to the Na^+/K^+-transporting ATPase to manage cellular ion flux in favour of the virus.

The DnaJ homolog subfamily A member 2 (also called cell cycle progression restoration gene 3 protein) was enriched in the GFP-YIPF4 sample by 1.78 fold. It is known to positively regulate cell proliferation (Edwards et al., 1997) and is therefore a conceivable YIPF4 binding candidate in the E5/YIPF4 complex to promote cell transformation upon HPV infection. However, DnaJ homolog subfamily A member 2 also serves as a chaperone for heat shock cognate 70 (Terada and Mori, 2000) which was identified as potential bead proteome (Table A. 8). It is therefore likely that DnaJ homolog subfamily A member 2 is part of the bead proteome rather than a genuine YIPF4 interacting protein.

With regard to other YIP1 family members, the coatomer subunit α (enrichment factor 1.61), tubulin α-1A chain (3.21), actin (1.75), plastin-3 (3.86) and T-complex protein 1 subunit θ (2.78) could be involved in YIPF4 mediated cellular trafficking processes. The coatomer subunit α is part of the COPI complex that mediates retrograde vesicle trafficking of the early exocytic pathway (Langer et al., 2008). The paralogues of YIPF4 in mammals, YIF1A and YIF1B, are thought to be involved in COPI-dependent trafficking (1.8.3.5 and 1.8.3.6) making coatomer subunit α a likely YIPF4 binding partner. The first precise model of cellular trafficking by a YIP1 family member was established for YIF1B (Al Awabdh et al., 2012). YIF1B facilitates the formation of a complex that moves the serotonin receptor $5\text{-}HT_{1A}R$ through the cell on the tubulin cytoskeleton (Figure 1.11). Here we identified the cytoskeleton components tubulin α-1A chain and actin as a potential part of a YIPF4 protein complex as well as the actin associated protein plastin-3 (Oprea et al., 2008) and the T-complex protein 1 subunit θ that might play a key role in actin and tubulin

folding (Kubota et al., 1994). It is therefore conceivable that YIPF4 mediates intracellular trafficking in a similar fashion to its paralogue YIF1B.

The confirmation of these and other proteins from the preliminary interactome list (Table 5.1, Table A. 7, Table A. 8) as YIPF4 binding partners needs to be addressed to elucidate the cellular roles of YIPF4. This will enable the identification of the function of the E5/YIPF4 complex during PV infection.

Chapter 6. Summary and conclusion

The work in this thesis was based on observations made in a Y2H screen, LUMIER assay and TAP-MS analysis which suggested YIPF4 as a novel cellular interaction partner of 16E5. The YIPF4 protein was subject to intense investigation to confirm it as a likely *in vivo* binding partner of PV E5 proteins.

This study demonstrated the expression of YIPF4 protein in a variety of human, monkey and hamster established cell lines and cell lines derived from primary human keratinocytes. To the best of our knowledge, we provided the first indication of a YIPF4 protein in hamster cells. Due to its ubiquitous expression and high conservation, YIPF4 might be a housekeeping protein.

It was observed that endogenous YIPF4 localises to the *trans*-Golgi but a partial localisation to the *cis*-Golgi, as published in the literature, is not excluded. The overexpression of epitope tagged YIPF4 caused dimerisation and accumulation in the ER and perinuclear region.

In this study experimental evidence for a 3 TMD topology model of YIPF4 was provided which refuted the existing computational model suggesting 5 TMDs. This depicts the first experiment-based topology model for any of the YIP1 family members and might thus serve as a representative for this protein family.

Notably, YIPF4 was found to be expressed in cells susceptible and permissive to HPV infection and in cells carrying HPV16 and HPV18 genomes. The presence in HPV18 positive organotypic raft culture and HPV16 positive CIN1 and CIN3 pathological specimens was confirmed. These findings imply that YIPF4 could indeed be an *in vivo* binding partner of E5 proteins.

YIPF4 protein levels were shown to decrease when HFKs differentiate but the expression was rescued in differentiating HPV18 positive HFKs. This effect was independent of 18E5. It is therefore conceivable that YIPF4 is required for the

productive stage of the viral life-cycle. The expression might be regulated by 18E2 because several potential E2BS were identified in the YIPF4 ORF.

Co-IP experiments confirmed that not only overexpressed but also endogenous YIPF4 interacts with the E5 oncoprotein of HPV16, which is in agreement with the observations made in the Y2H screen and LUMIER assay. This interaction was mediated by the 2nd TMD of 16E5 and amino acids 118 – 138 of YIPF4. The other HPV16 oncoproteins E6 and E7 did not interact with YIPF4, which stresses the specificity of this interaction with the E5 protein.

A major finding was that E5 proteins representing the HPV E5 families E5α, E5β, E5γ and the ungulate BPV1 E5 all interact with human YIPF4. The interaction is thus likely to be conserved for E5 proteins of further high-risk, low-risk and cutaneous HPV types and maybe other animal PV types. This implies that the E5/YIPF4 complex plays an important role for the virus presumably during the life-cycle or immune evasion. A co-localisation between the E5 proteins and YIPF4 was not observed but this is likely to be an artefact of the overexpression of epitope tagged E5 employed due to lack of specific detection reagents for 16E5.

It is established in the literature that E5 proteins down-regulate the cell surface expression of HLA/MHC class I molecules to aid viral immune evasion. Also YIPF4 is likely to modify exocytic and endocytic cellular trafficking concluding from other YIP1 family members. Thus, an involvement of the 16E5/YIPF4 complex in trafficking of HLA class I molecules was investigated with the unexpected finding that neither expression of 16E5 nor knock down of YIPF4 abrogated cell surface expression of HLA class I specifically including the HLA-A2 type. According to these findings, the 16E5/YIPF4 complex is not involved in regulation of HLA class I cell surface expression to mediate viral immune evasion.

In conclusion, the interaction of E5 proteins with the YIP1 family protein YIPF4 is highly likely to be crucial for the virus since it is conserved amongst a representative panel of PV E5 proteins. The E5/YIPF4 complex might alter the trafficking of cellular proteins to promote the viral life-cycle or immune evasion. Further research is needed to identify this role and a first approach was made to determine the YIPF4 cellular interactome. The establishment of the functions of YIPF4 within the cell will facilitate the determination of the role of the E5/YIPF4 complex. Exploiting the interaction of E5 and YIPF4 as a drug target could help to combat the broad spectrum of PV related diseases.

Appendix

Table A. 1 Sub-cloning E5 genes from various PV types and truncation mutants of 16E5. Restriction enzymes are indicated and their recognition sites are highlighted by underlining in the forward and reverse primer sequences. The pcDNA-Neo-HA-HPV16E5 plasmids encoding for the 16E5 truncation mutants were kindly provided by Prof M. Saveria Campo, University of Glasgow, UK.

name and isolate denotation	template	destination vector	fwd primer 5' – 3'	rev primer 5' - 3'	ann. temp	elon. time
peGFP-C2-HPV16E5 c.o.	pBABE-puro-FLAG-HPV16E5 c.o.	peGFP-C2	EcoRI ATATATGAATTCACAAATCTGGATACTGCATCCACAACACTGCTGG	BamHI AATTGGATCCTTATGTAATCAGAAAGCGTGCATGTGTATGGATCAG	65°C	3 sec
pmCherry-C2-FLAG-HPV16E5	pSG5-FLAG-HPV16E5	pmCherry-C2	EcoRI ATATATGAATTCGCGGCCATGGATTACAAGGATGACGACGATAAGATAACAAATCTGGATACT	BamHI AATTGGATCCTTATGTAATCAGAAAGCGTGCATGTGTATGGAT	65°C	3 sec
peGFP-C2-HPV2aE5 (isolate CN-HB1)	n/doc.	peGFP-C2	EcoRI ATATATGAATTCTACCCTGTTGTGTATAAGGGATCTGAGGGAACATATCCTGTGG	BamHI AATTGGATCCTTAGGTGTGGTTTAACAAACGGACATAAAACATCAACAATAAAAAGGCGA	54°C	3 sec
peGFP-C2-HPV6bE5a	n/doc.	peGFP-C2	EcoRI ATATATGAATTCGAAGTGGTGCCTGTACAAATAGCTGCAGGAACAACCAGCACATTCATACTGCC	BamHI AATTGGATCCTCACTGCTGTGTGGTCACAATATAGTAGTGGATATACAGTGCGGGACAGT	54°C	3 sec
peGFP-C2-HPV11E5a (isolate GUMC-AJ-Lung)	n/doc.	peGFP-C2	EcoRI ATATATGAATTCGAGGTAGTGCTGTACAAATTGCTGCAGCAAAC	BamHI AATTGGATCCTTATTGTTGCGTTTGCACAATGTATATGTGTATATAAAAGGCAGGAAAATAGCA	54°C	3 sec
peGFP-C2-HPV18E5 (isolate CU16)	n/doc.	peGFP-C2	EcoRI ATATATGAATTCTTATCACTTATTTTTTTATTTTGCTTTTGTGTATGCATGTATGTGTGCTGCC	BamHI AATTGGATCCTTACTGTAAAGACAATATAGCATGTATATGCAATAGTAACATGGGGCAATAAAAA	54°C	3 sec

name and isolate denotation	template	destination vector	fwd primer 5' – 3'	rev primer 5' - 3'	ann. temp	elon. time
peGFP-C1-HPV31E5	n/doc	peGFP-C1	EcoRI ATATTTGAATTCAATTGAACTAAATATTTCTACAGTAAGCATTGTGCTATGC	BamHI AATTGGATCCTTACTGTTGACTTAAAAAAGATGCATGTGTATG	65°C	3 sec
peGFP-C1-BPV1E5	pcDNA3.1 BPV1E5	peGFP-C1	EcoRI ATATTTGAATTCACCAAATCTATGGTTTCTATTGTTCTTGGGACTAGTTGCTGC	BamHI AATTGGATCCTTAAAAGGGCAGACCTGTACAGGAGCACTC	65°C	3 sec
peGFP-C1-HPV16E5R79	pcDNA-Neo-HA-HPV16E5R79	peGFP-C1	EcoRI ATATTTGAATTCAACAAATC T TGATACTGC A TCCACAACA T TACTGGCGT G C	BamHI AATTGGATCCTTATGTAATT A AAAATTATG C ATGTGTATG	65°C	3 sec
peGFP-C1-HPV16E5A54	pcDNA-Neo-HA-HPV16E5A54	peGFP-C1	EcoRI ATATTTGAATTCAACAAATCTTGATACTGCATCCACAACATTACTGGCGTGC	BamHI AATTGGATCCTTATGTAATCAGAAAGCGTGCATGTGTATGGAT	65°C	3 sec
peGFP-C1-HPV16E5V36	pcDNA-Neo-HA-HPV16E5V36	peGFP-C1	EcoRI ATATTTGAATTCAACAAATCTTGATACTGCATCCACAACATTACTGGCGTGC	BamHI AATTGGATCCTTAAGACAAAAGCAGCGGACG	65°C	3 sec
peGFP-C1-HPV16E5R30	pcDNA-Neo-HA-HPV16E5R30	peGFP-C1	EcoRI ATATTTGAATTCAACAAATCTTGATACTGCATCCACAACATTACTGGCGTGC	BamHI AATTGGATCCTTATGTAATCAGAAAGCGTGCATGTGTATGGAT	65°C	3 sec
peGFP-C1-HPV16E5Del1	pcDNA-Neo-HA-HPV16E5Del1	peGFP-C1	EcoRI ATATTTGAATTCACCGCTGCTTTTGTCTGTGTC	BamHI AATTGGATCCTTATGTAATCAGAAAGCGTGCATGTGTATGGAT	65°C	3 sec

c.o. = codon optimised, n/doc. = not documented, ann. temp = annealing temperature, elon. time = elongation time

Table A. 2 Sub-cloning YIPF4 to attach an N-terminal GFP tag and an N-terminal FLAG and C-terminal HA tag, respectively. Also, generation of six YIPF4 truncation mutants with the afore-mentioned tags. Restriction enzymes are indicated and their recognition sites are highlighted by underlining in the forward and reverse primer sequences. The pCR-myc-YIPF4 plasmid was kindly provided by Prof Jürgen Haas, University of Edinburgh, UK.

name	template	destination vector	fwd primer 5' – 3'	rev primer 5' - 3'	ann. temp	elon. time
peGFP-C1-YIPF4 V244	pCR-myc-YIPF4	peGFP-C1	HindIII ATATATAAGCTTCGCAGCCTCCGGGCCCG	BamHI AATTGGATCCTTACACACCAGTATATAACGAC	53°C	7 sec
peGFP-C1-YIPF4 K223	pCR-myc-YIPF4	peGFP-C1	HindIII ATATATAAGCTTCGCAGCCTCCGGGCCCG	BamHI AATTGGATCCTTACTTTTTGGTCTTGAATTCTTCACCC	53°C	7 sec
peGFP-C1-YIPF4 S195	pCR-myc-YIPF4	peGFP-C1	HindIII ATATATAAGCTTCGCAGCCTCCGGGCCCG	BamHI AATTGGATCCTTAAGACACCACTTCAAATGATCCAACC	53°C	7 sec
peGFP-C1-YIPF4 Q166	pCR-myc-YIPF4	peGFP-C1	HindIII ATATATAAGCTTCGCAGCCTCCGGGCCCG	BamHI AATTGGATCCTTATTGGCCATATGCAACTTCTCCACC	53°C	7 sec
peGFP-C1-YIPF4 S138	pCR-myc-YIPF4	peGFP-C1	HindIII ATATATAAGCTTCGCAGCCTCCGGGCCCG	BamHI AATTGGATCCTTATGAGACCACCCTAAACTGTCC	53°C	7 sec
peGFP-C1-YIPF4 G117	pCR-myc-YIPF4	peGFP-C1	HindIII ATATATAAGCTTCGCAGCCTCCGGGCCCG	BamHI AATTGGATCCTTAACCCCAAAAGTCAGGATTGTC	53°C	7 sec
peGFP-C1-YIPF4 Del1-109	pCR-myc-YIPF4	peGFP-C1	HindIII ATATATAAGCTTCGAGAGACAATCCTGACTTTTGGGG	BamHI AATTGGATCCTTACACACCAGTATATAACGAC	53°C	7 sec
pcDNA3.1+ FLAG-YIPF4-HA V244	pCR-myc-YIPF4	pcDNA3.1+	HindIII ATATATAAGCTTGCGGCCATG*GATTACAAGGATGACGACGATAAG*CAGCCTCCGGGCCCGCCCCCG	BamHI AATTGGATCCTTA*AGCGTAGTCTGGGACGTCGTATGGGTA*CACACCAGTATATAACGACAAAAAATAAATG	53°C	7 sec
pcDNA3.1+ FLAG-YIPF4-HA K223	pCR-myc-YIPF4	pcDNA3.1+	HindIII ATATATAAGCTTGCGGCCATG*GATTACAAGGATGACGACGATAAG*CAGCCTCCGGGCCCGCCCCCG	BamHI AATTGGATCCTTA*AGCGTAGTCTGGGACGTCGTATGGGTA*CTTTTTGGTCTTGAATTCTTCACCC	53°C	7 sec

name	template	destination vector	fwd primer 5' – 3'	rev primer 5' - 3'	ann. temp	elon. time
pcDNA3.1+ FLAG-YIPF4-HA S195	pCR-myc-YIPF4	pcDNA3.1+	HindIII ATATATAAGCTTGCGGCCATG*GATTACAAGGATGACGACGATAAG*CAGCCTCCGGGCCCGCCCCCG	BamHI AATTGGATCCTTA*AGCGTAGTCTGGGACGTCGTATGGGTA*AGACACCACTTCAAATGATCCAACC	53°C	7 sec
pcDNA3.1+ FLAG-YIPF4-HA Q166	pCR-myc-YIPF4	pcDNA3.1+	HindIII ATATATAAGCTTGCGGCCATG*GATTACAAGGATGACGACGATAAG*CAGCCTCCGGGCCCGCCCCCG	BamHI AATTGGATCCTTA*AGCGTAGTCTGGGACGTCGTATGGGTA*TTGGCCATATGCAACTTCTCCACC	53°C	7 sec
pcDNA3.1+ FLAG-YIPF4-HA S138	pCR-myc-YIPF4	pcDNA3.1+	HindIII ATATATAAGCTTGCGGCCATG*GATTACAAGGATGACGACGATAAG*CAGCCTCCGGGCCCGCCCCCG	BamHI AATTGGATCCTTA*AGCGTAGTCTGGGACGTCGTATGGGTA*TGAGACCACCCTAAACTGTCC	53°C	7 sec
pcDNA3.1+ FLAG-YIPF4-HA G117	pCR-myc-YIPF4	pcDNA3.1+	HindIII ATATATAAGCTTGCGGCCATG*GATTACAAGGATGACGACGATAAG*CAGCCTCCGGGCCCGCCCCCG	BamHI AATTGGATCCTTA*AGCGTAGTCTGGGACGTCGTATGGGTA*ACCCCAAAAGTCAGGATTGTCTCTC	53°C	7 sec
pcDNA3.1+ FLAG-YIPF4-HA Del1-109	pCR-myc-YIPF4	pcDNA3.1+	HindIII ATATATAAGCTTGCGGCCATG*GATTACAAGGATGACGACGATAAG*AGAGACAATCCTGACTTTTGGGG	BamHI AATTGGATCCTTA*AGCGTAGTCTGGGACGTCGTATGGGTA*CACACCAGTATATAACGACAAAAAATAAATG	53°C	7 sec

ann. temp = annealing temperature, elon. time = elongation time

Table A. 3 YIPF4 protein sequences of different species. The NCBI reference IDs for the YIPF4 proteins are indicated.

protein accession	gene	organism
NP_115688.1	YIPF4	*H. sapiens*
XP_001106365.1	YIPF4	*M. mulatta*
XP_532925.1	YIPF4	*C. lupus*
XP_002691265.1	YIPF4	*B. taurus*
NP_080693.2	Yipf4	*M. musculus*
NP_001009712.1	Yipf4	*R. norvegicus*
NP_001026229.1	YIPF4	*G. gallus*
NP_998056.1	yipf4	*D. rerio*
NP_001123056.1	CELE_Y60A3A.19	*C. elegans*

Table A. 4 Primary antibodies used for detection of proteins on Western blots and by immuno-chemistry.

antibody	manufacturer	description	immunogen	size of target	dilution WB	dilution ICC/IHC
α-beta tubulin	EnoGene, USA	mouse monoclonal	recombinant β-tubulin protein from bacteria	50 kDa	1:1000	1:250
α-E4 (HPV16, 18, 31)	Kindly provided by Dr Sally Roberts, University of Birmingham, UK	mouse monoclonal	not known	n/a	n/a	1:100
α-FLAG	Sigma, USA	mouse monoclonal	synthetic peptide DYKDDDDK	n/a	1:5000	n/a
α-FLAG	EnoGene, USA	rabbit polyclonal	synthetic peptide DYKDDDDK	n/a	1:5000	1:500
α-GAPDH	Abcam, UK	mouse monoclonal	rabbit muscle GAPDH	36 kDa	1:20 000	n/a
α-GFP	Santa Cruz Biotech-technology, USA	mouse monoclonal	full-length GFP of *Aequorea victoria* origin	37 kDa	1:1000	n/a

antibody	manufacturer	description	immunogen	size of target	dilution WB	dilution ICC/IHC
α-HA	Sigma, USA	mouse monoclonal	amino acids 98-106 of human Influenza virus hemagglutinin	n/a	1:5000	1:500
α-HPV18 E7	Abcam, UK	mouse monoclonal	recombinant full-length HPV18 E7 protein	12 kDa	1:250	n/a
α-Lamin B1	Calbiochem, UK	mouse monoclonal	nuclear matrix from the human cervical cancer cell line ME-180	68 kDa	1:1000	n/a
α-mannosidase II	AbD serotec, USA	rabbit polyclonal	human mannosidase II	135 kDa	n/a	1:250
α-TGN46	kindly provided by Dr Sreenivasan Ponnambalam, University of Leeds, UK	sheep	(Towler et al., 2000)	46 kDa	1:250	1:250
α-Transferrin receptor (TfR)	Invitrogen, USA	mouse monoclonal	amino acids 3-28 of human TfR	95 kDa	1:2500	n/a
α-YIPF4	Sigma, USA	rabbit polyclonal	amino acids 12 - 105 of human YIPF4	27.1 kDa	1:250	1:250

WB = Western blot, ICC = immuno-cytochemistry, IHC = immuno-histochemistry, α- = anti, n/a = not applicable

Table A. 5 Secondary antibodies conjugated with horseradish peroxidase used for Western blot analysis

antibody	manufacturer	produced in	dilution
α-mouse IgG (whole molecule) – peroxidase	Sigma, USA	goat	1:5000
α-rabbit IgG (whole molecule) – peroxidase	Sigma, USA	goat	1:5000
α-sheep IgG (whole molecule) – peroxidase	Sigma, USA	donkey	1:5000

Table A. 6 Secondary antibodies conjugated with Alexa dyes used for immuno-histochemistry and immuno-cytochemistry

antibody	manufacturer	dilution
Alexa Fluor® 488 Goat Anti-Rabbit IgG	Invitrogen, USA	1:500
Alexa Fluor® 594 Goat Anti-Mouse IgG	Invitrogen, USA	1:500
Alexa Fluor® 488 Chicken Anti-Mouse IgG	Invitrogen, USA	1:500
Alexa Fluor® 594 Chicken Anti-Rabbit IgG	Invitrogen, USA	1:500
Alexa Fluor® 633 Goat Anti-Mouse IgG	Invitrogen, USA	1:500
Alexa Fluor® 633 Goat Anti-Rabbit IgG	Invitrogen, USA	1:500
Alexa Fluor® 633 Donkey Anti-Sheep IgG	Invitrogen, USA	1:500

6.1. Macro for PSC plug-in for ImageJ

```
rename ("image");
run("Split Channels");
run("Merge Channels...", "red=[C3-image] green=[C2-image] blue=*None* gray=*None*
create");
run("RGB Color");
run("Select All");
run("PSC Colocalization ", "please=25");
selectWindow("ImageJ selection mask (rectangular)");
close();
selectWindow("Composite (RGB)");
close();
selectWindow("Composite");
close();
selectWindow("C1-image");
close();
String.copy Results();
```

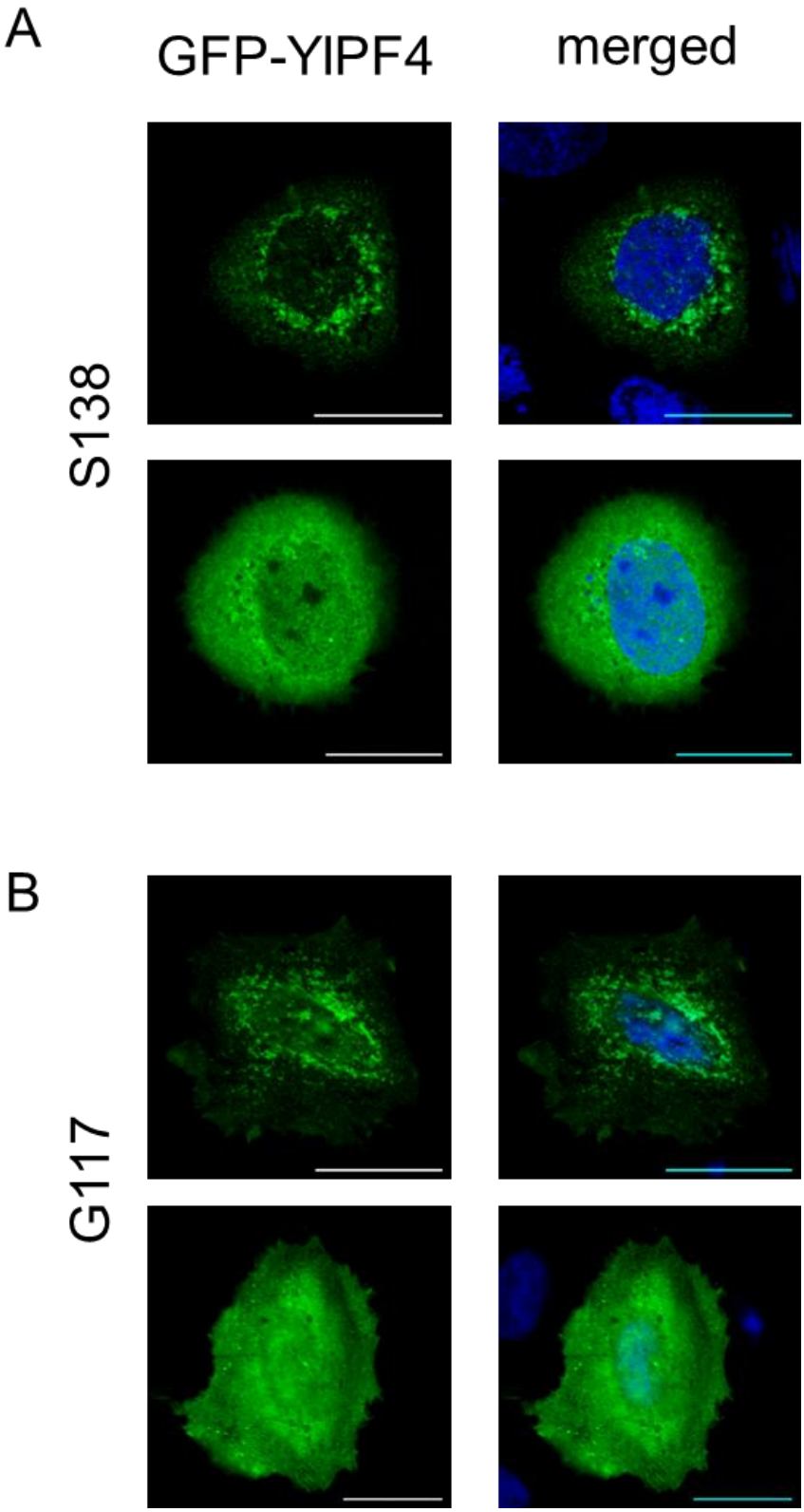

Figure A. 1 Different subcellular localisations of the GFP-YIPF4 truncation mutants S138 and G117. SiHA cells were transfected with GFP fusion proteins of the YIPF4 truncation mutants S138 (A) and G117 (B). Cells were fixed and imaged with Zeiss LSM 700 confocal microscope. Upper panels show ER-like localisation and lower panels show distribution throughout the cell. Nuclei were stained with DAPI (blue). Scale bar = 20 µm

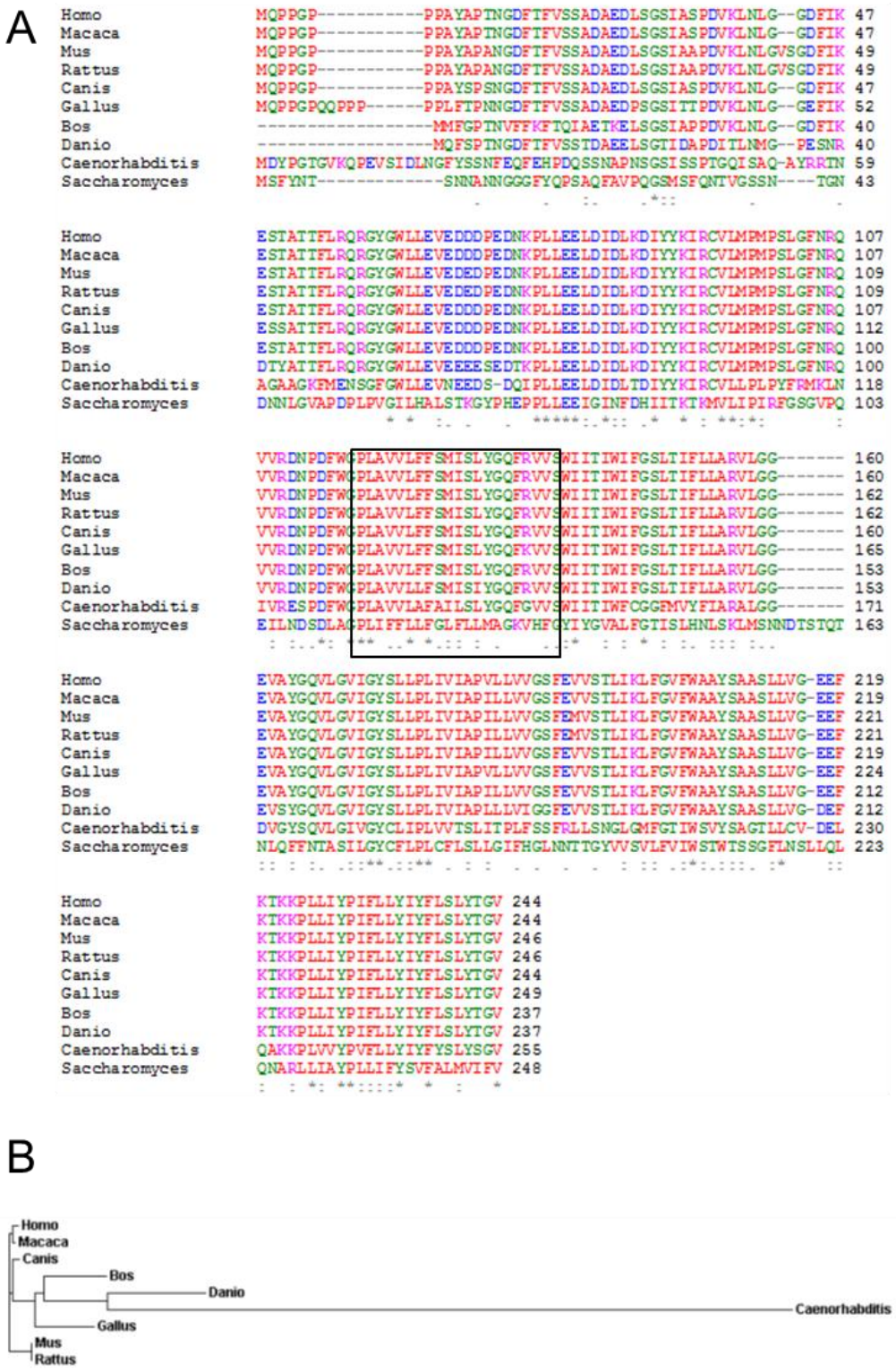

Figure A. 2 Multiple alignment and phylogeny of YIPF4 proteins from various species. A. Multiple alignment with ClustalW2 of YIPF4 proteins of various species. Black box indicates the potentially conserved binding region of 16E5. red = small and hydrophobic (including aromatic without Y), blue = acidic, magenta = basic- without H, green = hydroxyl, sulfhydryl, amine including G, * = single, fully conserved residue, : = conservation between groups of strongly similar properties, . = conservation between groups of weakly similar properties B. Phylogenetic tree showing the relationships of species based on their YIPF4 proteins.

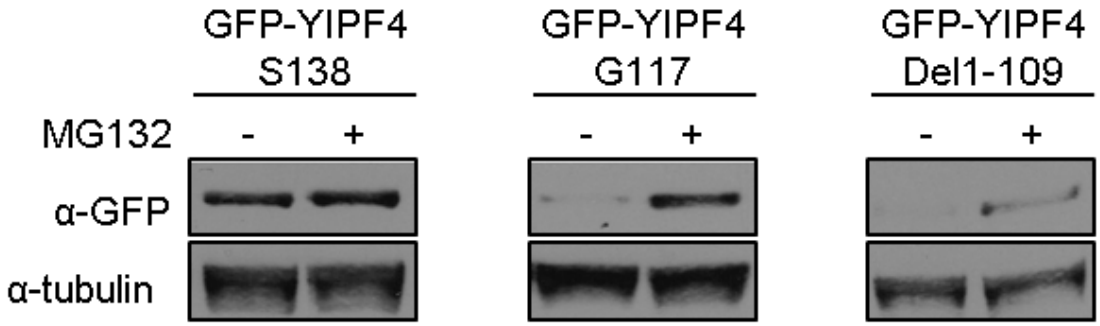

Figure A. 3 MG132 treatment of cells transfected with GFP-YIPF4 truncation mutants. Plasmids encoding the GFP tagged YIPF4 truncation mutants S138, G117 and Del1-109 were transfected into Huh7 cells. Sixteen hours post-transfection, cells were treated with the proteasome inhibitor MG132 (10 μM) for 6 h. Cells were lysed and analysed on a Western blot probing for the GFP tag.

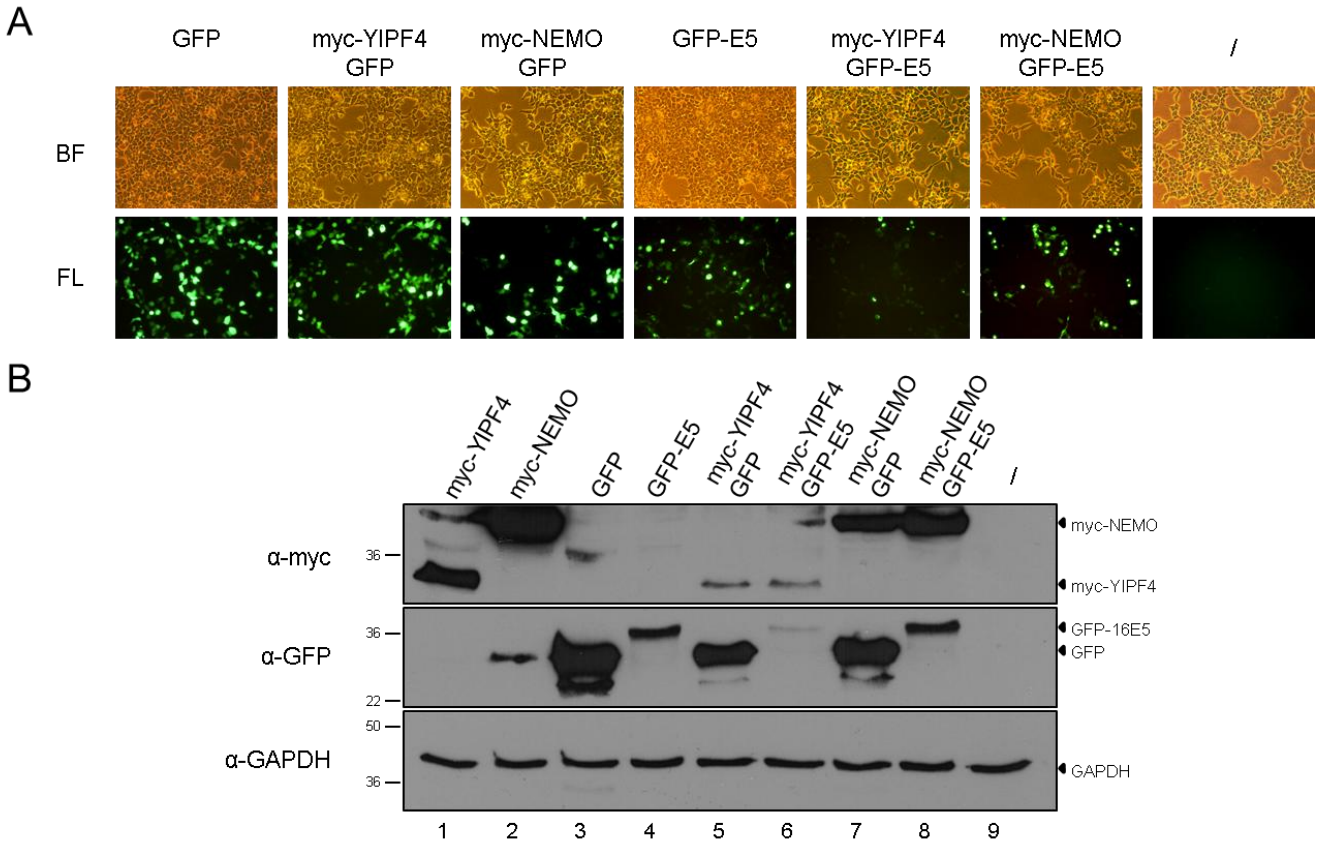

Figure A. 4 Effects of co-transfections in HEK293 cells. A. HEK293 cells were co-transfected with different plasmids using PEI. GFP and GFP-16E5 expression were non-quantitatively analysed by observation with an epifluorescence microscope (Nikon Eclipse TS 100). GFP-E5 expression is drastically reduced when co-transfected with myc-YIPF4. BF = bright field, FL = fluorescence B. The same HEK293 cells were lysed and a Western blot performed using antibodies against their GFP and myc tags. A general reduction in expression levels was seen in co-transfected samples, however, this effect is extreme in myc-YIPF4 and GFP-E5 co-expressing sample (lane 6). The GFP detected in lane 2 is overflow from lane 3. ‘ / ‘ = lysate of untransfected HEK293 cells.

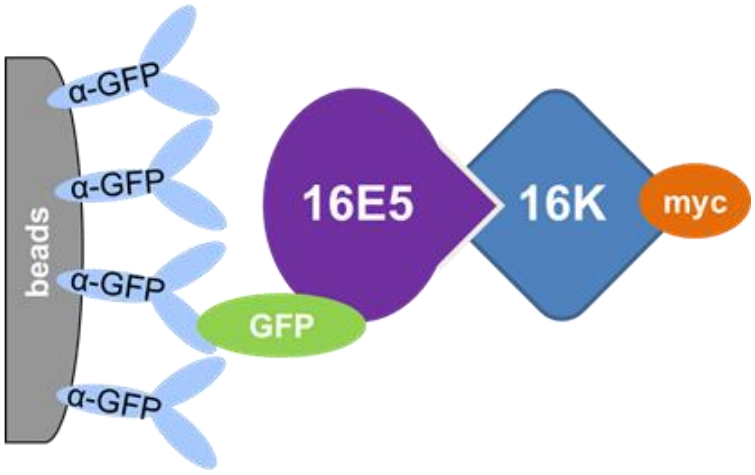

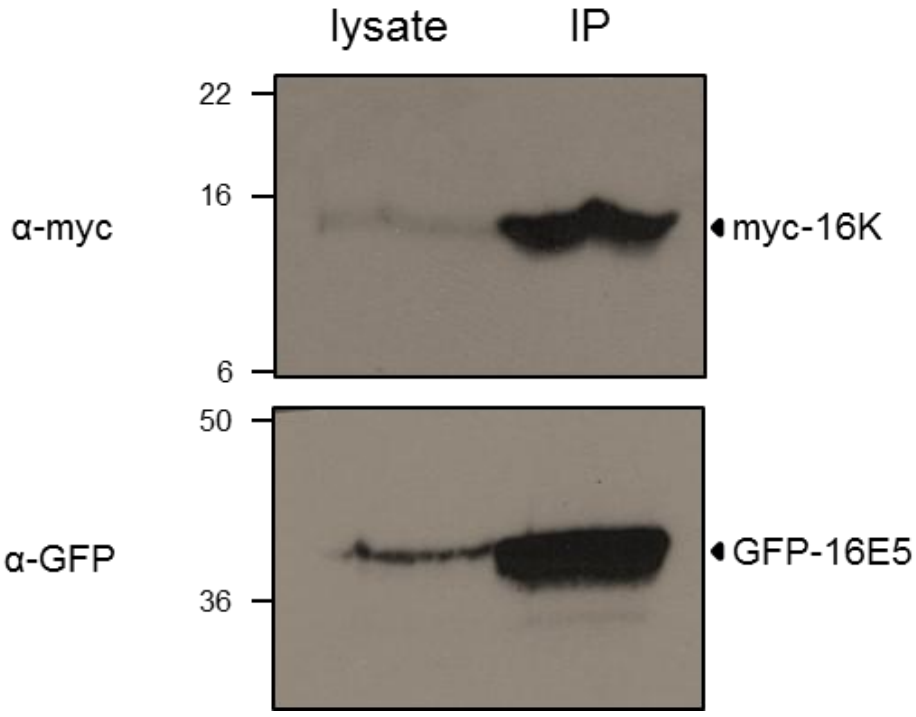

Figure A. 5 GFP-16E5 interacts with the 16K subunit of the vacuolar H^+ - ATPase. The GFP-16E5 fusion protein and the myc epitope tagged 16K were expressed in HEK293T cells. Cells were lysed 24 h post-transfection and cell lysate adjusted to equal concentrations. The Co-IP was performed with GFP *Camelidae* HC antibody coupled to magnetic beads (schematic). Eluates were analysed on a Western blot which was probed for the protein tags with GFP and myc antibodies. Marker in kDa.

Table A. 7 List of YIPF4 potential interaction partners with nuclear and mitochondrial localisation. The protein annotations originate from the PANTHER classification system. Details about cellular localisations were derived from the UniProt database.

gene ID	gene name	enrichment factor	cellular localisation	PANTHER family/subfamily	GO molecular function	GO biological process	PANTHER protein class	pathway
P62306	small nuclear ribonucleoprotein F	48.23	nucleus	n/n(PTHR11021:SF0)	RNA splicing factor activity, transesterification mechanism, mRNA binding	nuclear mRNA splicing, via spliceosome	mRNA splicing factor	n/n
P31943	hetero-geneous nuclear ribonucleoprotein H	47.09	nucleus, nucleoplasm	RNA-binding protein 12 (PTHR13976:SF5)	structural constituent of ribosome	nuclear mRNA splicing, via spliceosome	ribosomal protein	n/n
Q07955	serine/arginine-rich splicing factor 1	40.68	nucleus speckle, cytoplasm, shuttles between nucleus and cytoplasm	splicing factor, arginine/serine-rich1 (PTHR10548:SF10)	RNA splicing factor activity, transesterification mechanism, mRNA binding	nuclear mRNA splicing, via spliceosome	mRNA splicing factor	n/n
O75533	splicing factor 3B subunit 1	40.51	nucleus speckle	n/n (PTHR12097:SF0)	RNA splicing factor activity, transesterification mechanism, mRNA binding	nuclear mRNA splicing, via spliceosome	mRNA splicing factor	n/n
P84090	enhancer of rudimentary homolog	32.41	nucleus	n/n (PTHR12373:SF0)	transcription factor activity	regulation of transcription from RNA polymerase II promoter	transcription factor	n/n
Q9Y3B4	pre-mRNA branch site protein p14	20.74	nucleus	n/n (PTHR22630:SF0)	RNA splicing factor activity, transesterification mechanism, mRNA binding	nuclear mRNA splicing, via spliceosome	mRNA splicing factor	n/n
Q8IXT5	RNA-binding protein 12B	18.64	n/n	SWAN-related (PTHR13976:SF6)	structural constituent of ribosome	nuclear mRNA splicing, via spliceosome	ribosomal protein	n/n
P35637	RNA-binding protein FUS	17.47	nucleus	TATA-binding protein associated factor 2N (PTHR23238:SF5)	RNA splicing factor activity, transesterification mechanism, transcription factor activity, mRNA binding	neurological system, nuclear mRNA splicing, via spliceosome	transcription factor, DNA-binding factor, mRNA splicing factor	n/n

gene ID	gene name	enrichment factor	cellular localisation	PANTHER family/subfamily	GO molecular function	GO biological process	PANTHER protein class	pathway
O15042	U2 snRNP-associated SURP motif-containing protein	16.92	nucleus	n/n (PTHR23140:SF0)	mRNA binding	mRNA processing	mRNA processing factor	n/n
Q9UQ35	serine/arginine repetitive matrix protein 2	16.74	nucleus speckle	n/n (PTHR32093:SF0)	n/n	n/n	n/n	n/n
P08621	U1 small nuclear ribonucleoprotein 70 kDa	15.97	nucleus, nucleus speckle	n/n (PTHR13952:SF3)	RNA splicing factor activity, transesterification mechanism, mRNA binding	nuclear mRNA splicing, via spliceosome	mRNA splicing factor	n/n
Q9NZI8	insulin-like growth factor 2 mRNA-binding protein 1	15.3	nucleus, cytoplasm, lamellipodium, dendrite, dendritic spine	Insulin-like growth factor 2 mRNA-binding protein 3 (PTHR10288:SF92)	RNA splicing factor activity, transesterification mechanism, mRNA binding, protein binding	neurological system, intracellular/nuclear protein transport, induction of apoptosis, signal transduction, transcription from RNA polymerase II promoter, nuclear mRNA splicing, via spliceosome, protein metabolism	mRNA splicing factor, ribonucleoprotein, enzyme modulator	n/n
Q92804	TATA-binding protein-associated factor 2N	13.52	nucleus, cytoplasm, shuttles from the nucleus to the cytoplasm	TATA-binding protein associated factor 2N (PTHR23238:SF5)	RNA splicing factor activity, transesterification mechanism, transcription factor activity, mRNA binding	neurological system, nuclear mRNA splicing, via spliceosome	transcription factor, DNA-binding protein, mRNA splicing factor	n/n
Q6UX04	peptidyl-prolyl cis-trans isomerase CWC27 homolog	12.29	nucleus speckle	peptidyl-prolyl cis-trans isomerase SDCCAG10 (PTHR11071:SF33)	isomerase activity	immune system, intracellular/nuclear protein transport, protein folding	isomerase	n/n
Q15459	splicing factor 3A subunit 1	11.02	nucleus	n/n (PTHR15316:SF1)	RNA splicing factor activity, transesterification mechanism, mRNA binding	nuclear mRNA splicing, via spliceosome	mRNA splicing factor	n/n

gene ID	gene name	enrichment factor	cellular localisation	PANTHER family/subfamily	GO molecular function	GO biological process	PANTHER protein class	pathway
P09874	poly [ADP-ribose] polymerase 1	10.81	nucleus, nucleolus, localises at sites of DNA damage	n/n (PTHR15447:SF4)	transferase activity, transferring glycosyl groups	immune system, DNA repair, protein amino acid ADP-ribosylation, response to stress	glycosyltransferase	FAS signalling->Poly (ADP-ribose) polymerase
Q96PK6	RNA-binding protein 14	9.48	nucleus, nucleolus	n/n (PTHR24011:SF59)	RNA splicing factor activity, transesterification mechanism, DNA replication origin binding, ssDNA binding, transcription factor activity, poly(A) RNA binding	cell cycle, signal transduction, DNA replication, transcription from RNA polymerase II promoter, nuclear mRNA splicing, via spliceosome, mRNA polyadenylation, protein metabolism, ectoderm/nervous system development	transcription factor, DNA-binding protein, mRNA polyadenylation factor, mRNA splicing factor, ribonucleoprotein	n/n
Q8IWX8	calcium homeostasis ER protein	8.79	cytoplasm, perinuclear region, ER	n/n (PTHR12323:SF0)	RNA binding	nuclear mRNA splicing, via spliceosome	RNA binding protein	n/n
Q14978	nucleolar and coiled-body phosphoprotein 1	8.42	nucleus, nucleolus, shuttles between nucleus to cytoplasm	n/n (PTHR23216:SF0)	n/n	n/n	n/n	n/n
Q15059	bromodomain-containing protein 3	7.89	nucleus	Bromodomain-containing protein 3 (PTHR22880:SF20)	acetyltransferase activity, nucleic acid/chromatin binding,	transcription from RNA polymerase II promoter, establishment or maintenance of chromatin architecture	acetyltransferase, chromatin/chromatin-binding protein	n/n
Q6P2Q9	pre-mRNA-processing-splicing factor 8	7.47	nucleus speckle	n/n (PTHR11140:SF0)	RNA splicing factor activity, transesterification mechanism, mRNA binding	nuclear mRNA splicing, via spliceosome	mRNA splicing factor	n/n

gene ID	gene name	enrichment factor	cellular localisation	PANTHER family/subfamily	GO molecular function	GO biological process	PANTHER protein class	pathway
Q15233	non-POU domain-containing octamer-binding protein	7.21	nucleus, nucleolus	NONO protein (PTHR23189:SF15)	RNA splicing factor activity, transesterification mechanism, mRNA binding	spermatogenesis, regulation of transcription from RNA polymerase II promoter, nuclear mRNA splicing, via spliceosome	mRNA splicing factor	n/n
Q9UKV3	apoptotic chromatin condensation inducer in the nucleus	6.01	nucleus, nucleus speckle, nucleoplasm	n/n (PTHR14127:SF0)	nucleic acid/chromatin binding	apoptosis	chromatin/chromatin-binding protein	n/n
P23246	splicing factor, proline- and glutamine-rich	5.97	nucleus matrix, cytoplasm	PTB-associated splicing factor (PTHR23189:SF13)	RNA splicing factor activity, transesterification mechanism, mRNA binding	spermatogenesis, regulation of transcription from RNA polymerase II promoter	mRNA splicing factor	n/n
Q9HCG8	pre-mRNA-splicing factor CWC22 homolog	5.68	nucleus	cell cycle control protein CWF22 (PTHR18034:SF3)	nuclease activity, nucleic acid binding	nuclear mRNA splicing, via spliceosome, translation	nuclease	n/n
Q66PJ3	ADP-ribosylation factor-like protein 6-interacting protein 4	5.6	nucleus	n/n (PTHR13595:SF0)	n/n	n/n	n/n	n/n
Q9UHX1	poly(U)-binding-splicing factor PUF60	5.43	nucleus	n/n (PTHR24011:SF51)	RNA splicing factor activity, transesterification mechanism, DNA replication origin binding, ssDNA binding, transcription factor activity, poly(A) RNA binding	cell cycle, DNA replication, transcription from RNA polymerase II promoter, nuclear mRNA splicing, via spliceosome, mRNA polyadenylation, protein metabolism, ectoderm/nervous system development	transcription factor, DNA-binding protein, mRNA polyadenylation factor, mRNA splicing factor, ribonucleoprotein	n/n
P17480	nucleolar transcription factor 1	4.75	nucleus, nucleolus	SWI/SNF-related (PTHR13711:SF13)	transcription factor activity, chromatin/receptor binding	intracellular signalling cascade, regulation of transcription from RNA polymerase II promoter, establishment or maintenance of chromatin architecture	HMG box transcription factor, signalling molecule, chromatin/chromatin-binding protein	general transcription by RNA polymerase I->UBF1

gene ID	gene name	enrichment factor	cellular localisation	PANTHER family/subfamily	GO molecular function	GO biological process	PANTHER protein class	pathway
P22626	heterogeneous nuclear ribonucleoproteins A2/B1	4.57	nucleus, nucleoplasm, cytoplasm	n/n (PTHR24012:SF14)	RNA splicing factor activity, transesterification mechanism, structural constituent of ribosome, poly(A) RNA binding	neurological system, cell cycle, DNA replication, nuclear mRNA splicing, via spliceosome, mRNA polyadenylation, rRNA metabolism, protein metabolism, ectoderm/nervous system development	mRNA polyadenylation factor, mRNA splicing factor, ribonucleoprotein, ribosomal protein	n/n
P46087	putative ribosomal RNA methyltransferase NOP2	4.46	nucleus, nucleolus	nucleolar protein NOL1/NOP2 (yeast) (PTHR22807:SF11)	methyltransferase activity, nucleic acid binding	rRNA metabolism	methyltransferase, nucleic acid binding	n/n
Q9Y383	putative RNA-binding protein Luc7-like 2	4.34	nucleus speckle, nucleus, nucleoplasm	RNA-binding protein LUC7 (PTHR12375:SF15)	n/n	n/n	n/n	n/n
O14646	chromodomain-helicase-DNA-binding protein 1	4.11	nucleus, cytoplasm	Chromodomain-helicase-DNA-binding protein 1 (PTHR10799:SF206)	DNA helicase activity, nucleic acid binding	DNA repair, DNA recombination, regulation of transcription from RNA polymerase II promoter, establishment or maintenance of chromatin architecture	DNA helicase	n/n
Q9UJV9	probable ATP-dependent RNA helicase DDX41	4.11	nucleus	n/n (PTHR24031:SF20)	RNA helicase activity, translation factor activity, nucleic acid binding	nucleobase, nucleoside, nucleotide/nucleic acid metabolism, translation	RNA helicase	n/n
Q9BUJ2	heterogeneous nuclear ribonucleoprotein U-like protein 1	3.91	nucleus	E1B-55 kDA-associated protein 5 (PTHR12381:SF10)	RNA binding	n/n	RNA binding protein	n/n
P25440	bromodomain-containing protein 2	3.89	nucleus	bromodomain-containing protein (PTHR22880:SF18)	acetyltransferase activity, nucleic acid/chromatin binding	transcription from RNA polymerase II promoter, establishment or maintenance of chromatin architecture	acetyltransferase, chromatin/chromatin-binding protein	n/n

gene ID	gene name	enrichment factor	cellular localisation	PANTHER family/subfamily	GO molecular function	GO biological process	PANTHER protein class	pathway
Q9NW13	RNA-binding protein 28	3.81	nucleus, nucleolus	predicted protein (PTHR24012:SF49)	RNA splicing factor activity, transesterification mechanism, structural constituent of ribosome, poly(A) RNA binding	neurological system, cell cycle, DNA replication, nuclear mRNA splicing, via spliceosome, mRNA polyadenylation, rRNA metabolism, protein metabolism, ectoderm/nervous system development	mRNA polyadenylation factor, mRNA splicing factor, ribonucleoprotein, ribosomal protein	n/n
Q8IYB3	serine/arginine repetitive matrix protein 1	3.31	nucleus matrix, nucleus speckle	n/n (PTHR23148:SF0)	mRNA binding	mRNA processing	mRNA processing factor	n/n
Q9UKJ3	G patch domain-containing protein 8	3.31	n/n	n/n PTHR17614:SF10)	n/n	n/n	n/n	n/n
P18583	protein SON	3.08	nucleus speckle	n/n (PTHR12813:SF2)	n/n	n/n	n/n	n/n
Q12906	interleukin enhancer-binding factor 3	2.92	nucleus, nucleolus, cytoplasm	Interleukin enhancer-binding factor 3 (PTHR10910:SF34)	hydrolase activity, deaminase activity, DNA/mRNA/protein binding, kinase activator/regulator activity	spermatogenesis, response to IFN-γ, neurological system, nucleobase, nucleoside, nucleotide/nucleic acid transport, apoptosis, cell cycle, purine base metabolism, mRNA processing, protein metabolism, anterior/posterior axis specification, response to stimulus, RNA localisation	DNA-binding protein, mRNA processing factor, deaminase, kinase activator, defense/immunity protein	n/n
Q9BQG0	myb-binding protein 1A	2.92	cytoplasm, nucleus, shuttles between nucleus and cytoplasm	DNA polymerase V (PTHR13213:SF2)	DNA-directed DNA polymerase activity, transcription factor activity	cell cycle, DNA replication, transcription from RNA polymerase II promoter, mRNA transcription	transcription factor, DNA-directed DNA polymerase	n/n

gene ID	gene name	enrichment factor	cellular localisation	PANTHER family/subfamily	GO molecular function	GO biological process	PANTHER protein class	pathway
O75947	ATP synthase subunit d, mitochondrial	2.8	mitochondrion inner membrane	n/n PTHR12700:SF6)	n/n	n/n	n/n	n/n
P38159	RNA-binding motif protein, X chromosome	2.78	nucleus	n/n (PTHR24012:SF93)	RNA splicing factor activity, transesterification mechanism, structural constituent of ribosome, poly(A) RNA binding	neurological system, cell cycle, DNA replication, nuclear mRNA splicing, via spliceosome, mRNA polyadenylation, rRNA metabolism, protein metabolism, ectoderm/nervous system development	mRNA polyadenylation factor, mRNA splicing factor, ribonucleoprotein, ribosomal protein	n/n
Q92499	ATP-dependent RNA helicase DDX1	2.77	nucleus, cytoplasm, cytoplasmic granule	n/n (PTHR24031:SF61)	RNA helicase activity, translation factor activity, nucleic acid binding	nucleobase, nucleoside, nucleotide/nucleic acid metabolism, translation	RNA helicase	n/n
Q9NRR4	ribonuclease 3	2.72	nucleus, nucleolus	ribonuclease 3 (PTHR11207:SF0)	endoribonuclease activity, nucleic acid binding	rRNA metabolism	endoribonuclease, nuclease	n/n
P61978	heterogeneous nuclear ribonucleoprotein K	2.67	cytoplasm, nucleus	heterologenous nuclear ribonucleoprotein K (PTHR10288:SF38)	RNA splicing factor activity, transesterification mechanism, mRNA binding, protein binding	neurological system, intracellular/nuclear protein transport, induction of apoptosis, signal transduction, transcription from RNA polymerase II promoter, nuclear mRNA splicing, via spliceosome, protein metabolism	mRNA splicing factor, ribonucleoprotein, enzyme modulator	n/n
Q9Y3Y2	chromatin target of PRMT1 protein	2.65	nucleus	RNA and export factor binding protein (PTHR19965:SF8)	RNA binding	nucleobase, nucleoside, nucleotide/nucleic acid transport, transcription from RNA polymerase II promoter	RNA binding protein	n/n
Q9Y2W1	thyroid hormone receptor-associated protein 3	2.65	nucleus	thyroid hormone receptor associated protein 3 (PTHR15268:SF7)	receptor activity, transcription factor activity, DNA polymerase processivity factor activity	induction of apoptosis, cell cycle, DNA replication, regulation of/initiation of transcription from RNA polymerase II promoter	transcription factor, receptor, DNA polymerase processivity factor	n/n

gene ID	gene name	enrichment factor	cellular localisation	PANTHER family/subfamily	GO molecular function	GO biological process	PANTHER protein class	pathway
P17844	probable ATP-dependent RNA helicase DDX5	2.63	nucleus, nucleolus	N/N (PTHR24031:SF0)	RNA helicase activity, translation factor activity, nucleic acid binding	nucleobase, nucleoside, nucleotide/nucleic acid metabolism, translation	RNA helicase	n/n
P38919	eukaryotic initiation factor 4A-III	2.55	nucleus, nucleus speckle, cytoplasm	n/n (PTHR24031:SF57)	RNA helicase activity, translation factor activity, nucleic acid binding, translation initiation factor activity	nucleobase, nucleoside, nucleotide/nucleic acid metabolism, translation	RNA helicase, translation initiation factor, helicase	n/n
Q99590	protein SCAF11	2.54	nucleus	n/n (PTHR15242:SF0)	n/n	nuclear mRNA splicing, via spliceosome	n/n	n/n
Q08211	ATP-dependent RNA helicase A	2.53	nucleus, nucleolus, cytoplasm	n/n (PTHR18934:SF68)	RNA helicase activity, nucleic acid binding	nuclear mRNA splicing, via spliceosome	RNA helicase	n/n
P19338	nucleolin	2.5	nucleus, nucleolus, cytoplasm	n/n (PTHR24012:SF1)	RNA splicing factor activity, transesterification mechanism, structural constituent of ribosome, poly(A) RNA binding	neurological system, cell cycle, DNA replication, nuclear mRNA splicing, via spliceosome, mRNA polyadenylation, rRNA metabolism, protein metabolism, ectoderm/nervous system development	mRNA polyadenylation factor, mRNA splicing factor, ribonucleoprotein, ribosomal protein	n/n
Q15393	splicing factor 3B subunit 3	2.39	nucleus	splicing factor 3B subunit 3 (PTHR10644:SF1)	RNA splicing factor activity, transesterification mechanism, damaged DNA binding, poly(A) RNA binding	DNA repair, nuclear mRNA splicing, via spliceosome, mRNA polyadenylation	damaged DNA-binding protein, mRNA polyadenylation factor, mRNA splicing factor	n/n
O75643	U5 small nuclear ribonucleoprotein 200 kDa helicase	2.14	nucleus	U520 (PTHR11752:SF7)	DNA/RNA helicase activity, hydrolase activity, RNA splicing factor activity, transesterification mechanism, mRNA binding	meiosis, nuclear mRNA splicing, via spliceosome	DNA/RNA helicase, mRNA splicing factor, hydrolase	n/n
Q15029	116 kDa U5 small nuclear ribonucleoprotein component	2.07	nucleus	116 kDA U5 small nuclear ribonuclein component (PTHR23115:SF5)	GTPase activity, RNA binding, translation factor activity, nucleic acid/protein binding, translation initiation/elongation factor activity	mRNA processing, translation	ribonucleoprotein, translation initiation/elongation factor, hydrolase, G-protein	n/n

gene ID	gene name	enrichment factor	cellular localisation	PANTHER family/subfamily	GO molecular function	GO biological process	PANTHER protein class	pathway
P22087	rRNA 2'-O-methyltransferase fibrillarin	1.98	nucleus, nucleolus.	rRNA 2'-O-methyltransferase fibrillarin (PTHR10335:SF0)	methyltransferase activity	rRNA metabolism	methyltransferase	n/n
Q9Y3I0	tRNA-splicing ligase RtcB homolog	1.94	cytoplasm	n/n (PTHR11118:SF0)	n/n	n/n	n/n	DNA replication->RFC
Q9UHB7	AF4/FMR2 family member 4	1.86	nucleus	AF4/FMR2 family member 1 (PTHR10528:SF6)	transcription factor activity	signal transduction, regulation of transcription from RNA polymerase II promoter	transcription factor	n/n
Q14690	Protein RRP5 homolog	1.82	nucleus, nucleolus	n/n (PTHR23270:SF1)	n/n	n/n	n/n	n/n
P12956	X-ray repair cross-complementing protein 6	1.77	nucleus, chromosome	KU P70 DNA helicase (PTHR12604:SF2)	DNA helicase activity, nucleic acid binding	immune system, DNA repair/recombination	DNA helicase	n/n
Q9GZR7	ATP-dependent RNA helicase DDX24	1.76	cytoplasm, nucleolus	n/n (PTHR24031:SF91)	RNA helicase activity, translation factor activity, nucleic acid binding	nucleobase, nucleoside, nucleotide/nucleic acid metabolism, translation	RNA helicase	n/n
Q96HR8	H/ACA ribonucleoprotein complex non-core subunit NAF1	1.63	nucleus, cytoplasm, shuttles between cytoplasm and nucleus	n/n (PTHR31991:SF0)	n/n	n/n	n/n	n/n

‘gene ID’ indicates the UniProt database ID; ‘enrichment factor’ indicates the enrichment of the protein in the GFP-YIPF4 sample compared to the GFP control sample. n/n = not named; GO = gene ontology

Table A. 8 Potential bead proteome of the LFQ experiment. The PANTHER classification system was used to annotate the proteins whereby the information about the cellular localisation was derived from the UniProt database.

gene ID	gene name	enrichment factor	cellular localisation	PANTHER family/subfamily	GO molecular function	GO biological process	PANTHER protein class	pathway
P62917	60S ribosomal protein L8	122.58	cytoplasm	60S ribosomal protein L8 (PTHR13691:SF4)	structural constituent of ribosome, nucleic acid binding	fatty acid metabolism, translation	ribosomal protein	n/n
P62424	60S ribosomal protein L7a	60.71	cytoplasm	60S ribosomal protein L7A (PTHR23105:SF1)	structural constituent of ribosome, nucleic acid binding	rRNA metabolism, translation	ribosomal protein	n/n
Q07020	60S ribosomal protein L18	57.79	cytoplasm	60S ribosomal protein L18 (PTHR10934:SF0)	structural constituent of ribosome, nucleic acid binding	translation	ribosomal protein	n/n
P40429	60S ribosomal protein L13a	20.01	cytoplasm	60S ribosomal protein L13A (PTHR11545:SF3)	structural constituent of ribosome, nucleic acid binding	translation	ribosomal protein	n/n
P18621	60S ribosomal protein L17	18.67	cytoplasm	n/n (PTHR11593:SF3)	n/n	protein metabolism	n/n	n/n
P46777	60S ribosomal protein L5	15.97	nucleus, cytoplasm	n/n (PTHR23410:SF3)	structural constituent of ribosome, nucleic acid binding	translation	ribosomal protein	n/n
P46777	60S ribosomal protein L5	15.97	cytoplasm, nucleus, nucleolus	n/n (PTHR23410:SF3)	structural constituent of ribosome, nucleic acid binding	translation	ribosomal protein	n/n
P05388	60S acidic ribosomal protein P0	15.28	nucleus, cytoplasm	n/n (PTHR21141:SF7)	structural constituent of ribosome, nucleic acid binding	translation	ribosomal protein	n/n
P39023	60S ribosomal protein L3	14.99	cytoplasm, nucleus, nucleolus	60S ribosomal protein L3 (PTHR11363:SF0)	structural constituent of ribosome, nucleic acid binding	translation	ribosomal protein	n/n
P39023	60S ribosomal protein L3	14.99	cytoplasm, nucleus, nucleolus	60S ribosomal protein L3 (PTHR11363:SF0)	structural constituent of ribosome, nucleic acid binding	translation	ribosomal protein	n/n
Q02878	60S ribosomal protein L6	13.3	cytoplasm	60S ribosomal protein L6 (PTHR10715:SF0)	structural constituent of ribosome, nucleic acid binding	translation	ribosomal protein	n/n
P62910	60S ribosomal protein L32	11.7	cytoplasm	60S ribosomal protein L32 (PTHR23413:SF1)	structural constituent of ribosome, nucleic acid binding	translation	ribosomal protein	n/n

gene ID	gene name	enrichment factor	cellular localisation	PANTHER family/subfamily	GO molecular function	GO biological process	PANTHER protein class	pathway
P18124	60S ribosomal protein L7	11.4	cytoplasm	n/n (PTHR11524:SF5)	structural constituent of ribosome, nucleic acid binding	translation	ribosomal protein	n/n
P11142	heat shock cognate 71 kDa protein	8.34	cytoplasm, melanosome, nucleus, nucleolus	heat shock protein 70 (PTHR19375:SF1)	n/n	immune system, protein folding/complex assembly, response to stress	Hsp70 family chaperone	Parkinson disease, apoptosis signalling
P15880	40S ribosomal protein S2	6.86	nucleus, cytoplasm	n/n (PTHR13718:SF17)	structural constituent of ribosome, nucleic acid binding	translation	ribosomal protein	n/n
P62979	40S ribosomal protein S27a	6.68	Ubiquitin: cytoplasm, nucleus	ubiquitin (PTHR10666:SF2)	structural constituent of ribosome, nucleic acid binding	proteolysis	ribosomal protein	n/n
P62753	40S ribosomal protein S6	5.91	cytoplasm, nucleolus	n/n (PTHR11502:SF3)	structural constituent of ribosome, nucleic acid binding	translation	ribosomal protein	n/n
P61247	40S ribosomal protein S3a	4.58	cytoplasm, nucleus	40S ribosomal protein S3A (PTHR11830:SF0)	structural constituent of ribosome, nucleic acid binding	translation	ribosomal protein	n/n
P36578	60S ribosomal protein L4	4.36	cytoplasm, nucleolus	n/n (PTHR19431:SF0)	n/n	translation	n/n	n/n
P13639	elongation factor 2	4.01	cytoplasm	translation elongation factor G (PTHR23115:SF13)	GTPase activity, translation factor activity, nucleic acid/protein binding, translation initiation/elongation factor activity	translation	translation initiation/elongation factor, hydrolase, G-protein	n/n
P62750	60S ribosomal protein L23a	3.97	cytoplasm, nucleus	n/n (PTHR11620:SF2)	structural constituent of ribosome, nucleic acid binding	translation	ribosomal protein, nuclease	n/n
P62701	40S ribosomal protein S4, X isoform	2.97	cytoplasm	n/n (PTHR11581:SF0)	structural constituent of ribosome, nucleic acid binding	translation	ribosomal protein	n/n
P62829	60S ribosomal protein L23	2.56	cytoplasm, nucleolus	60S ribosomal protein L23 (PTHR11761:SF4)	structural constituent of ribosome, nucleic acid binding	translation	ribosomal protein	n/n
P18077	60S ribosomal protein L35a	2.34	cytoplasm	60S ribosomal protein L35A (PTHR10902:SF0)	structural constituent of ribosome, nucleic acid binding	translation	ribosomal protein	n/n

gene ID	gene name	enrichment factor	cellular localisation	PANTHER family/subfamily	GO molecular function	GO biological process	PANTHER protein class	pathway
P62241	40S ribosomal protein S8	2.08	cytoplasm	40S ribosomal protein S8 (PTHR10394:SF1)	structural constituent of ribosome, nucleic acid binding	translation	ribosomal protein	n/n
P62249	40S ribosomal protein S16	1.89	cytoplasm	n/n (PTHR21569:SF0)	structural constituent of ribosome, RNA binding	translation	ribonucleoprotein, ribosomal protein	n/n
Q02543	60S ribosomal protein L18a	1.85	cytoplasm	60S ribosomal protein L18A (PTHR10052:SF1)	structural constituent of ribosome, nucleic acid binding	translation	ribosomal protein	n/n
P10809	60 kDa heat shock protein, mitochondrial	1.83	mitochondrion matrix	chaperonin-60kDa (PTHR11353:SF9)	n/n	protein folding and complex assembly	chaperonin	n/n
P30050	60S ribosomal protein L12	1.67	cytoplasm	60S ribosomal protein L12 (PTHR11661:SF2)	structural constituent of ribosome, nucleic acid binding	translation	ribosomal protein	n/n

‘gene ID’ indicates the UniProt database ID; ‘enrichment factor’ indicates the enrichment of the respective protein in the GFP-YIPF4 sample compared to the GFP control sample. n/n = not named; GO = gene ontology

Bibliography

ABRAMSON, A. L., STEINBERG, B. M. & WINKLER, B. 1987. Laryngeal papillomatosis - clinical, histopathologic and molecular studies. *Laryngoscope,* 97**,** 678-685.

ADAM, J. L., BRIGGS, M. W. & MCCANCE, D. J. 2000. A mutagenic analysis of the E5 protein of human papillomavirus type 16 reveals that E5 binding to the vacuolar H+-ATPase is not sufficient for biological activity, using mammalian and yeast expression systems. *Virology,* 272**,** 315-325.

AHN, K., GRUHLER, A., GALOCHA, B., JONES, T. R., WIERTZ, E., PLOEGH, H. L., PETERSON, P. A., YANG, Y. & FRUH, K. 1997. The ER-luminal domain of the HCMV glycoprotein US6 inhibits peptide translocation by TAP. *Immunity,* 6**,** 613-621.

AHN, W. S., SEO, M. J., BAE, S. M., LEE, J. M., NAMKOONG, S. E., KIM, C. K. & KIM, Y. W. 2005. Cellular process classification of human papillomavirus-16-positive SiHa cervical carcinoma cell using gene ontology. *International Journal of Gynecological Cancer,* 15**,** 94-106.

AKGÜL, B., GARCIA-ESCUDERO, R., EKECHI, C., STEGER, G., NAVSARIA, H., PFISTER, H. & STOREY, A. 2011. The E2 protein of human papillomavirus type 8 increases the expression of matrix metalloproteinase-9 in human keratinocytes and organotypic skin cultures. *Medical Microbiology and Immunology,* 200**,** 127-135.

AKHTER, H., HAYASHIDA, Y., YOSHIDA, Y., OHKUMA, S., YAMAMOTO, H. & NAKAMURA, N. 2007. Characterization of ArfGAP1 and FinGER7/FinGER8 interaction by quantitative yeast two-hybrid analysis. *Journal of the Juzen Medical Society* 116**,** 137-142.

AL AWABDH, S., MISEREY-LENKEI, S., BOUCEBA, T., MASSON, J., KANO, F., MARINACH-PATRICE, C., HAMON, M., EMERIT, M. B. & DARMON, M. 2012. A New Vesicular Scaffolding Complex Mediates the G-Protein-Coupled 5-HT1A Receptor Targeting to Neuronal Dendrites. *Journal of Neuroscience,* 32**,** 14227-14241.

ALBERS, M., KRANZ, H., KOBER, I., KAISER, C., KLINK, M., SUCKOW, J., KERN, R. & KOEGL, M. 2005. Automated yeast two-hybrid screening for nuclear receptor-interacting proteins. *Molecular & Cellular Proteomics,* 4**,** 205-213.

AMADOR-MOLINA, A., HERNÁNDEZ-VALENCIA, J., LAMOYI, E., CONTRERAS-PAREDES, A. & LIZANO, M. 2013. Role of Innate Immunity against Human Papillomavirus (HPV) Infections and Effect of Adjuvants in Promoting Specific Immune Response. *Viruses,* 5**,** 2624-2642.

AMMERMANN, I., BRUCKNER, M., MATTHES, F., IFTNER, T. & STUBENRAUCH, F. 2008. Inhibition of Transcription and DNA Replication by the Papillomavirus E8∧E2C Protein Is Mediated by Interaction with Corepressor Molecules. *Journal of Virology,* 82**,** 5127-5136.

ANDRESSON, T., SPARKOWSKI, J., GOLDSTEIN, D. J. & SCHLEGEL, R. 1995. Vacuolar H+-ATPase Mutants Transform Cells and Define a Binding Site for the Papillomavirus E5 Oncoprotein. *Journal of Biological Chemistry,* 270**,** 6830-6837.

ANDROPHY, E. J., HUBBERT, N. L., SCHILLER, J. T. & LOWY, D. R. 1987a. Identification of the HPV-16 E6 protein from transformed mouse cells and human cervical-carcinoma cell-lines *Embo Journal,* 6**,** 989-992.

ANDROPHY, E. J., LOWY, D. R. & SCHILLER, J. T. 1987b. Bovine papillomavirus E2 trans-activating gene product binds to specific sites in papillomavirus DNA. *Nature,* 325**,** 70-73.

ANDRULIS, E. D., NEIMAN, A. M., ZAPPULLA, D. C. & STERNGLANZ, R. 1998. Perinuclear localization of chromatin facilitates transcriptional silencing. *Nature,* 394**,** 592-595.

ANSARI, T., BRIMER, N. & VANDE POL, S. B. 2012. Peptide Interactions Stabilize and Restructure Human Papillomavirus Type 16 E6 To Interact with p53. *Journal of Virology,* 86**,** 11386-11391.

ANTSON, A. A., BURNS, J. E., MOROZ, O. V., SCOTT, D. J., SANDERS, C. M., BRONSTEIN, I. B., DODSON, G. G., WILSON, K. S. & MALTLAND, N. J. 2000. Structure of the intact transactivation domain of the human papillomavirus E2 protein. *Nature,* 403**,** 805-809.

ARAIBI, E. H., MARCHETTI, B., ASHRAFI, G. H. & CAMPO, M. S. 2004. Downregulation of major histocompatibility complex class I in bovine papillomas. *Journal of General Virology,* 85**,** 2809-2814.

ARAIBI, E. H., MARCHETTI, B., DORNAN, E. S., ASHRAFI, G. H., DOBROMYLSKYJ, M., ELLIS, S. A. & CAMPO, M. S. 2006. The E5 oncoprotein of BPV-4 does not interfere with the biosynthetic pathway of non-classical MHC class I. *Virology,* 353**,** 174-183.

ARBEIT, J. M., HOWLEY, P. M. & HANAHAN, D. 1996. Chronic estrogen-induced cervical and vaginal squamous carcinogenesis in human papillomavirus type 16 transgenic mice. *Proceedings of the National Academy of Sciences of the United States of America,* 93**,** 2930-2935.

ASHRAFI, G. H., BROWN, D. R., FIFE, K. H. & CAMPO, M. S. 2006a. Down-regulation of MHC class I is a property common to papillomavirus E5 proteins. *Virus Research,* 120**,** 208-211.

ASHRAFI, G. H., HAGHSHENAS, M., MARCHETTI, B. & CAMPO, M. S. 2006b. E5 protein of human papillomavirus 16 downregulates HLA class I and interacts with the heavy chain via its first hydrophobic domain. *International Journal of Cancer,* 119**,** 2105-2112.

ASHRAFI, G. H., HAGHSHENAS, M. R., MARCHETTI, B., O'BRIEN, P. M. & CAMPO, M. S. 2005. E5 protein of human papillomavirus type 16 selectively downregulates surface HLA class I. *International Journal of Cancer,* 113**,** 276-283.

ASHRAFI, G. H., PITTS, J. D., FACCINI, A., MCLEAN, P., O'BRIEN, V., FINBOW, M. E. & CAMPO, M. S. 2000. Binding of bovine papillomavirus type 4 E8 to ductin (16K proteolipid), down-regulation of gap junction intercellular communication and full cell transformation are independent events. *Journal of General Virology,* 81**,** 689-694.

ASHRAFI, G. H., TSIRIMONAKI, E., MARCHETTI, B., O'BRIEN, P. M., SIBBET, G. J., ANDREW, L. & CAMPO, M. S. 2002. Down-regulation of MHC class I by bovine papillomavirus E5 oncoproteins. *Oncogene,* 21**,** 248-259.

AUVINEN, E., ALONSO, A. & AUVINEN, P. 2004. Human papillomavirus type 16 E5 protein colocalizes with the antiapoptotic Bcl-2 protein. *Archives of Virology,* 149**,** 1745-1759.

BADARACCO, G., VENUTI, A., SEDATI, A. & MARCANTE, M. L. 2002. HPV16 and HPV18 in genital tumors: Significantly different levels of viral integration and correlation to tumor invasiveness. *Journal of Medical Virology,* 67**,** 574-582.

BALL, S. L. R., WINDER, D. M., VAUGHAN, K., HANNA, N., LEVY, J., STERLING, J. C., STANLEY, M. A. & GOON, P. K. C. 2011. Analyses of Human Papillomavirus Genotypes and Viral Loads in Anogenital Warts. *Journal of Medical Virology,* 83**,** 1345-1350.

BANERJEE, N. S., WANG, H.-K., BROKER, T. R. & CHOW, L. T. 2011. Human Papillomavirus (HPV) E7 Induces Prolonged G(2) following S Phase Reentry in Differentiated Human Keratinocytes. *Journal of Biological Chemistry,* 286**,** 15473-15482.

BARBOSA, M. S., EDMONDS, C., FISHER, C., SCHILLER, J. T., LOWY, D. R. & VOUSDEN, K. H. 1990. The region of the HPV E7 oncoprotein homologous to adenovirus E1A and SV40 large T-antigen contains separate domains for RB binding and casein kinase-II phosphorylation *Embo Journal,* 9**,** 153-160.

BARBOSA, M. S., LOWY, D. R. & SCHILLER, J. T. 1989. Ppaillomavirus polypeptide-E6 and polypeptide-E7 are zinc-binding proteins *Journal of Virology,* 63**,** 1404-1407.

BARNARD, P. & MCMILLAN, N. A. J. 1999. The human papillomavirus E7 oncoprotein abrogates signaling mediated by interferon-alpha. *Virology,* 259**,** 305-313.

BARROWMAN, J., WANG, W., ZHANG, Y. Y. & FERRO-NOVICK, S. 2003. The Yip1p-Yif1p complex is required for the fusion competence of endoplasmic reticulum-derived vesicles. *Journal of Biological Chemistry,* 278**,** 19878-19884.

BASTIEN, N. & MCBRIDE, A. A. 2000. Interaction of the Papillomavirus E2 Protein with Mitotic Chromosomes. *Virology,* 270**,** 124-134.

BEGLIN, M., MELAR-NEW, M. & LAIMINS, L. 2009. Human Papillomaviruses and the Interferon Response. *Journal of Interferon and Cytokine Research,* 29**,** 629-635.

BELLEUDI, F., LEONE, L., PURPURA, V., CANNELLA, F., SCROFANI, C. & TORRISI, M. R. 2011. HPV16 E5 affects the KGFR/FGFR2b-mediated epithelial growth through alteration of the receptor expression, signaling and endocytic traffic. *Oncogene,* 30**,** 4963-4976.

BERGANT, M. & BANKS, L. 2013. SNX17 Facilitates Infection with Diverse Papillomavirus Types. *Journal of Virology,* 87**,** 1270-1273.

BERGANT MARUSIC, M., MENCIN, N., LIČEN, M., BANKS, L. & GRM, H. Š. 2010. Modification of Human Papillomavirus Minor Capsid Protein L2 by Sumoylation. *Journal of Virology,* 84**,** 11585-11589.

BERGANT MARUSIC, M., OZBUN, M. A., CAMPOS, S. K., MYERS, M. P. & BANKS, L. 2012. Human papillomavirus L2 facilitates viral escape from late endosomes via sorting nexin 17. *Traffic (Copenhagen, Denmark),* 13**,** 455-67.

BERGMAN, P., USTAV, M., SEDMAN, J., MORENOLOPEZ, J., VENNSTROM, B. & PETTERSSON, U. 1988. The E5 gene of bovine papillomavirus type-1 is sufficient for complete oncogenic transformation of mouse fibroblasts *Oncogene,* 2**,** 453-459.

BERGVALL, M., MELENDY, T. & ARCHAMBAULT, J. 2013. The E1 proteins. *Virology,* 445**,** 35-56.

BERMÚDEZ-MORALES, V. H., PERALTA-ZARAGOZA, O., ALCOCER-GONZÁLEZ, J. M., MORENO, J. & MADRID-MARINA, V. 2011. IL-10 expression is regulated by HPV E2 protein in cervical cancer cells. *Molecular Medicine Reports,* 4**,** 369-375.

BERNARD, B. A., BAILLY, C., LENOIR, M. C., DARMON, M., THIERRY, F. & YANIV, M. 1989. The human papillomavirus type 18 (HPV18) E2 gene product is a repressor of the HPV18 regulatory region in human keratinocytes. *Journal of Virology,* 63**,** 4317-4324.

BERNARD, H.-U. 2013. Regulatory elements in the viral genome. *Virology,* 445**,** 197-204.

BERNARD, H.-U., BURK, R. D., CHEN, Z., VAN DOORSLAER, K., HAUSEN, H. Z. & DE VILLIERS, E.-M. 2010. Classification of papillomaviruses (PVs) based on 189 PV types and proposal of taxonomic amendments. *Virology,* 401**,** 70-79.

BIAN, X.-L., ROSAS-ACOSTA, G., WU, Y.-C. & WILSON, V. G. 2007. Nuclear Import of Bovine Papillomavirus Type 1 E1 Protein Is Mediated by Multiple Alpha Importins and Is Negatively Regulated by Phosphorylation near a Nuclear Localization Signal. *Journal of Virology,* 81**,** 2899-2908.

BIAN, X.-L. & WILSON, V. G. 2010. Common importin alpha specificity for papillomavirus E2 proteins. *Virus Research,* 150**,** 135-137.

BIBLE, J. M., MANT, C., BEST, J. M., KELL, B., STARKEY, W. G., RAJU, K. S., SEED, P., BISWAS, C., MUIR, P., BANATVALA, J. E. & CASON, J. 2000. Cervical lesions are associated with human papillomavirus type 16 intratypic variants that have high transcriptional activity and increased usage of common mammalian codons. *Journal of General Virology,* 81**,** 1517-1527.

BIENKOWSKA-HABA, M., WILLIAMS, C., KIM, S. M., GARCEA, R. L. & SAPP, M. 2012. Cyclophilins Facilitate Dissociation of the Human Papillomavirus Type 16 Capsid Protein L1 from the L2/DNA Complex following Virus Entry. *Journal of Virology,* 86**,** 9875-9887.

BIRD, G., O'DONNELL, M., MOROIANU, J. & GARCEA, R. L. 2008. Possible Role for Cellular Karyopherins in Regulating Polyomavirus and Papillomavirus Capsid Assembly. *Journal of Virology,* 82**,** 9848-9857.

BLANCO, G. 2005. Na,K-ATPase Subunit Heterogeneity as a Mechanism for Tissue-Specific Ion Regulation. *Seminars in Nephrology,* 25**,** 292-303.

BODILY, J. M., HENNIGAN, C., WROBEL, G. A. & RODRIGUEZ, C. M. 2013. Regulation of the human papillomavirus type 16 late promoter by E7 and the cell cycle. *Virology,* 443**,** 11-19.

BOON, S. S. & BANKS, L. 2013. High-Risk Human Papillomavirus E6 Oncoproteins Interact with 14-3-3 zeta in a PDZ Binding Motif-Dependent Manner. *Journal of Virology,* 87**,** 1586-1595.

BORDEAUX, J., FORTE, S., HARDING, E., DARSHAN, M. S., KLUCEVSEK, K. & MOROIANU, J. 2006. The L2 Minor Capsid Protein of Low-Risk Human Papillomavirus Type 11 Interacts with Host Nuclear Import Receptors and Viral DNA. *Journal of Virology,* 80**,** 8259-8262.

BORDIER, C. 1981. Phase-separation of the integral membrane-proteins in Tiron X-114 solution *Journal of Biological Chemistry,* 256**,** 1604-1607.

BORGOGNA, C., ZAVATTARO, E., DE ANDREA, M., GRIFFIN, H. M., DELL'OSTE, V., AZZIMONTI, B., LANDINI, M. M., PEH, W. L., PFISTER, H., DOORBAR, J., LANDOLFO, S. & GARIGLIO, M. 2012. Characterization of beta papillomavirus E4 expression in tumours from Epidermodysplasia Verruciformis patients and in experimental models. *Virology,* 423**,** 195-204.

BORZACCHIELLO, G., IOVANE, G., MARCANTE, M. L., POGGIALI, F., ROPERTO, F., ROPERTO, S. & VENUTI, A. 2003. Presence of bovine papillomavirus type 2 DNA and expression of the viral oncoprotein E5 in naturally occurring urinary bladder tumours in cows. *Journal of General Virology,* 84**,** 2921-2926.

BORZACCHIELLO, G., RUSSO, V., GENTILE, F., ROPERTO, F., VENUTI, A., NITSCH, L., CAMPO, M. S. & ROPERTO, S. 2006. Bovine papillomavirus E5 oncoprotein binds to the activated form of the platelet-derived growth factor beta receptor in naturally occurring bovine urinary bladder tumours. *Oncogene,* 25**,** 1251-1260.

BOSCH, F. X., TSU, V., VORSTERS, A., VAN DAMME, P. & KANE, M. A. 2012. Reframing Cervical Cancer Prevention. Expanding the Field Towards Prevention of Human Papillomavirus Infections and Related Diseases. *Vaccine,* 30**,** F1-F11.

BOTTLEY, G., WATHERSTON, O. G., HIEW, Y. L., NORRILD, B., COOK, G. P. & BLAIR, G. E. 2008. High-risk human papillomavirus E7 expression reduces cell-surface MHC class I molecules and increases susceptibility to natural killer cells. *Oncogene,* 27**,** 1794-1799.

BOULON, S., AHMAD, Y., TRINKLE-MULCAHY, L., VERHEGGEN, C., COBLEY, A., GREGOR, P., BERTRAND, E., WHITEHORN, M. & LAMOND, A. I. 2010. Establishment of a Protein Frequency Library and Its Application in the Reliable Identification of Specific Protein Interaction Partners. *Molecular & Cellular Proteomics,* 9**,** 861-879.

BOUSARGHIN, L., TOUZE, A., SIZARET, P. Y. & COURSAGET, P. 2003. Human papillomavirus types 16, 31, and 58 use different endocytosis pathways to enter cells. *Journal of Virology,* 77**,** 3846-3850.

BOUVARD, V., BAAN, R., STRAIF, K., GROSSE, Y., SECRETAN, B., EL GHISSASSI, F., BENBRAHIM-TALLAA, L., GUHA, N., FREEMAN, C., GALICHET, L., COGLIANO, V. & WO, W. H. O. I. A. R. C. M. 2009. A review of human carcinogens-Part B: biological agents. *Lancet Oncology,* 10**,** 321-322.

BOUVARD, V., MATLASHEWSKI, G., GU, Z. M., STOREY, A. & BANKS, L. 1994a. The human papillomavirus type-16 E5 gene cooperates with the E7 gene to stimulate proliferation of primary-cells and increases viral gene-expression. *Virology,* 203**,** 73-80.

BOUVARD, V., STOREY, A., PIM, D. & BANKS, L. 1994b. Characterization of the human papillomavirus E2 protein: Evidence of trans-activation and trans-repression in cervical keratinocytes. *Embo Journal,* 13**,** 5451-5459.

BOYER, S. N., WAZER, D. E. & BAND, V. 1996. E7 protein of human papilloma virus-16 induces degradation of retinoblastoma protein through the ubiquitin-proteasome pathway. *Cancer Research,* 56**,** 4620-4624.

BRANDL, K., TOMISATO, W., LI, X., NEPPL, C., PIRIE, E., FALK, W., XIA, Y., MORESCO, E. M. Y., BACCALA, R., THEOFILOPOULOS, A. N., SCHNABL, B. & BEUTLER, B. 2012. Yip1 domain family, member 6 (Yipf6) mutation induces spontaneous intestinal inflammation in mice. *Proceedings of the National Academy of Sciences,* 109**,** 12650-12655.

BRAVO, I. G. & ALONSO, A. 2004. Mucosal human papillomaviruses encode four different E5 proteins whose chemistry and phylogeny correlate with malignant or benign growth. *Journal of Virology,* 78**,** 13613-13626.

BRAVO, I. G. & ALONSO, A. 2007. Phylogeny and evolution of papillomaviruses based on the E1 and E2 proteins. *Virus Genes,* 34**,** 249-262.

BRAVO, I. G., CRUSIUS, K. & ALONSO, A. 2005. The E5 protein of the human papillomavirus type 16 modulates composition and dynamics of membrane lipids in keratinocytes. *Archives of Virology,* 150**,** 231-246.

BREUZA, L., HALBEISEN, R., JENO, P., OTTE, S., BARLOWE, C., HONG, W. J. & HAURI, H. P. 2004. Proteomics of endoplasmic reticulum-golgi intermediate compartment (ERGIC) membranes from brefeldin A-treated HepG2 cells identifies ERGIC-32, a new cycling protein that interacts with human Erv46. *Journal of Biological Chemistry,* 279**,** 47242-47253.

BRIMER, N., LYONS, C. & VANDE POL, S. B. 2007. Association of E6AP (UBE3A) with human papillomavirus type 11 E6 protein. *Virology,* 358**,** 303-310.

BRONNIMANN, M. P., CHAPMAN, J. A., PARK, C. K. & CAMPOS, S. K. 2013. A Transmembrane Domain and GxxxG Motifs within L2 Are Essential for Papillomavirus Infection. *Journal of Virology,* 87**,** 464-473.

BROWN, D. R., KITCHIN, D., QADADRI, B., NEPTUNE, N., BATTEIGER, T. & ERMEL, A. 2006. The human papillomavirus type 11 E1^E4 protein is a transglutaminase 3 substrate and induces abnormalities of the cornified cell envelope. *Virology,* 345**,** 290-298.

BUBB, V., MCCANCE, D. J. & SCHLEGEL, R. 1988. DNA-sequence of the HPV-16 E5 ORF and the structural conservation of its encoded protein. *Virology,* 163**,** 243-246.

BUCK, C. B., CHENG, N., THOMPSON, C. D., LOWY, D. R., STEVEN, A. C., SCHILLER, J. T. & TRUS, B. L. 2008. Arrangement of L2 within the papillomavirus capsid. *Journal of Virology,* 82**,** 5190-5197.

BUCK, C. B., DAY, P. M. & TRUS, B. L. 2013. The papillomavirus major capsid protein L1. *Virology,* 445**,** 169-174.

BUCK, C. B., THOMPSON, C. D., PANG, Y. Y. S., LOWY, D. R. & SCHILLER, J. T. 2005. Maturation of papillomavirus capsids. *Journal of Virology,* 79**,** 2839-2846.

BURKHARDT, A., DIMAIO, D. & SCHLEGEL, R. 1987. Genetic and biochemical definition of the bovine papillomavirus E5 transforming protein *Embo Journal,* 6**,** 2381-2385.

BURKHARDT, A., WILLINGHAM, M., GAY, C., JEANG, K. T. & SCHLEGEL, R. 1989. The E5-oncoprotein of bovine papillomavirus is oriented asymmetrically in Golgi and plasma-membranes *Virology,* 170**,** 334-339.

BURNETT, S., STROM, A. C., JAREBORG, N., ALDERBORN, A., DILLNER, J., MORENO-LOPEZ, J., PETTERSON, U. & KIESSLING, U. 1990. Induction of bovine papillomavirus E2 gene expression and early region transcription by cell growth arrest: Correlation with viral DNA amplification and evidence for differential promoter induction. *Journal of Virology,* 64**,** 5529-5541.

CALÇADA, E. O., FELLI, I. C., HOŠEK, T. & PIERATTELLI, R. 2013. The Heterogeneous Structural Behavior of E7 from HPV16 Revealed by NMR Spectroscopy. *ChemBioChem,* 14**,** 1876-1882.

CALERO, M., CHEN, C. Z., ZHU, W. Y., WINAND, N., HAVAS, K. A., GILBERT, P. M., BURD, C. G. & COLLINS, R. N. 2003. Dual prenylation is required for Rab protein localization and function. *Molecular Biology of the Cell,* 14**,** 1852-1867.

CALERO, M. & COLLINS, R. N. 2002. Saccharomyces cerevisiae Pra1p/Yip3p Interacts with Yip1p and Rab Proteins. *Biochemical and Biophysical Research Communications,* 290**,** 676-681.

CALERO, M., WHITTAKER, G. R. & COLLINS, R. N. 2001. Yop1p, the yeast homolog of the polyposis locus protein 1, interacts with Yip1p and negatively regulates cell growth. *Journal of Biological Chemistry,* 276**,** 12100-12112.

CALERO, M., WINAND, N. J. & COLLINS, R. N. 2002. Identification of the novel proteins Yip4p and Yip5p as Rab GTPase interacting factors. *Febs Letters,* 515**,** 89-98.

CAMPO, M. S., GRAHAM, S. V., CORTESE, M. S., ASHRAFI, G. H., ARAIBI, E. H., DORNAN, E. S., MINERS, K., NUNES, C. & MAN, S. 2010. HPV-16 E5 down-regulates expression of surface HLA class I by CD8 T cells. *Virology,* 407**,** 137-142.

CAMPOS, S. K. & OZBUN, M. A. 2009. Two Highly Conserved Cysteine Residues in HPV16 L2 Form an Intramolecular Disulfide Bond and Are Critical for Infectivity in Human Keratinocytes. *Plos One,* 4.

CARDOSO, J. C. & CALONJE, E. 2003. Cutaneous manifestations of human papillomaviruses: a review. *Acta dermatovenerologica Alpina, Panonica, et Adriatica,* 20**,** 145-54.

CARR, E. A., THEON, A. P., MADEWELL, B. R., HITCHCOCK, M. E., SCHLEGEL, R. & SCHILLER, J. T. 2001. Expression of a transforming gene (E5) of bovine papillomavirus in sarcoids obtained from horses. *American Journal of Veterinary Research,* 62**,** 1212-1217.

CARREL, D., MASSON, J., AL AWABDH, S., CAPRA, C. B., LENKEI, Z., HAMON, M., EMERIT, M. B. & DARMON, M. 2008. Targeting of the 5-HT1A serotonin receptor to neuronal dendrites is mediated by Yif1B. *Journal of Neuroscience,* 28**,** 8063-8073.

CARRILLO, E., GARRIDO, E. & GARIGLIO, P. 2004. Specific in vitro interaction between papillomavirus E2 proteins and TBP-associated factors. *Intervirology,* 47**,** 342-349.

CARTER, J. J., KOUTSKY, L. A., HUGHES, J. P., LEE, S. K., KUYPERS, J., KIVIAT, N. & GALLOWAY, D. A. 2000. Comparison of Human Papillomavirus Types 16, 18, and 6 Capsid Antibody Responses Following Incident Infection. *Journal of Infectious Diseases,* 181**,** 1911-1919.

CARTIN, W. & ALONSO, A. 2003. The human papillomavirus HPV2a E5 protein localizes to the Golgi apparatus and modulates signal transduction. *Virology,* 314**,** 572-579.

CASTELLSAGUÉ, X., BRUNI, L., BROTONS, M., BARRIONUEVO, L., SERRANO, B., MUÑOZ, J., BOSCH, F. & DE SANJOSÉ, S. 2013. ICO Information Centre on HPV and Cervical Cancer (HPV Information Centre). Human Papillomavirus and Related Diseases in United Kingdom. PREHDICT edition. Summary Report 2013.

CASTELLSAGUE, X., DRUDIS, T., PAZ CANADAS, M., GONCE, A., ROS, R., PEREZ, J. M., JESUS QUINTANA, M., MUNOZ, J., ALBERO, G., DE SANJOSE, S. & XAVIER BOSCH, F. 2009. Human Papillomavirus (HPV) infection in pregnant women and mother-to-child transmission of genital HPV genotypes: a prospective study in Spain. *Bmc Infectious Diseases,* 9.

CHA, S. & SEO, T. 2011. hSNF5 Is Required for Human Papillomavirus E2-Driven Transcriptional Activation and DNA Replication. *Intervirology,* 54**,** 66-77.

CHANG, J. L., TSAO, Y. P., LIU, D. W., HUANG, S. J., LEE, W. H. & CHEN, S. L. 2001. The expression of HPV-16 E5 protein in squamous neoplastic changes in the uterine cervix. *Journal of Biomedical Science,* 8**,** 206-213.

CHATTOPADHYAY, S., ROBERTS, P. M. & PEARCE, D. A. 2003. The yeast model for Batten disease: a role for Btn2p in the trafficking of the Golgi-associated vesicular targeting protein, Yif1p. *Biochemical and Biophysical Research Communications,* 302**,** 534-538.

CHATURVEDI, A. K., ENGELS, E. A., PFEIFFER, R. M., HERNANDEZ, B. Y., XIAO, W., KIM, E., JIANG, B., GOODMAN, M. T., SIBUG-SABER, M., COZEN, W., LIU, L., LYNCH, C. F., WENTZENSEN, N., JORDAN, R. C., ALTEKRUSE, S., ANDERSON, W. F., ROSENBERG, P. S. & GILLISON, M. L. 2011. Human Papillomavirus and Rising Oropharyngeal Cancer Incidence in the United States. *Journal of Clinical Oncology,* 29**,** 4294-4301.

CHAUX, A. & CUBILLA, A. L. 2012. Advances in the pathology of penile carcinomas. *Human Pathology,* 43**,** 771-789.

CHEN, C. Z., CALERO, M., DEREGIS, C. J., HEIDTMAN, M., BARLOWE, C. & COLLINS, R. N. 2004. Genetic analysis of yeast Yip1p function reveals a requirement for golgi-localized Rab proteins and Rab-guanine nucleotide dissociation inhibitor. *Genetics,* 168**,** 1827-1841.

CHEN, C. Z. & COLLINS, R. N. 2005a. Analysis and properties of the yeast YIP1 family of Ypt-interacting proteins. *Gtpases Regulating Membrane Targeting and Fusion,* 403**,** 333-339.

CHEN, C. Z. & COLLINS, R. N. 2005b. Insights into biological functions across species: examining the role of Rab proteins in YIP1 family function. *Biochemical Society Transactions,* 33**,** 614-618.

CHEN, S. L., HSIEH, T. B., TSAO, Y. P., HAN, C. P. & YANG, Y. F. 1996a. Coincidental expression of E5a and c-jun in human papillomavirus type 6/11-infected condylomata. *Journal of General Virology,* 77**,** 1145-1149.

CHEN, S. L., HUANG, C. H., TSAI, T. C., LU, K. Y. & TSAO, Y. P. 1996b. The regulation mechanism of c-jun and junB by human papillomavirus type 16 E5 oncoprotein. *Archives of Virology,* 141**,** 791-800.

CHEN, S. L., LIN, S. T., TSAI, T. C., HSIAO, W. C. & TSAO, Y. P. 2007. ErbB4 (JM-b/CYT-1)-induced expression and phosphorylation of c-Jun is abrogated by human papillomavirus type 16 E5 protein. *Oncogene,* 26**,** 42-53.

CHEN, S. L., LIN, Y. K., LI, L. Y., TSAO, Y. P., LO, H. Y., WANG, W. B. & TSAI, T. C. 1996c. E5 proteins of human papillomavirus types 11 and 16 transactivate the c-fos promoter through the NF1 binding element. *Journal of Virology,* 70**,** 8558-8563.

CHEN, S. L. & MOUNTS, P. 1989. Detection by antibody probes of human papillomavirus type-6 proteins in repiratory papillomata *Journal of Medical Virology,* 29**,** 273-283.

CHEN, S. L. & MOUNTS, P. 1990. Transforming activity of E5A protein of human papillomavirus type-6 in NIH-3T3 and C127 cells. *Journal of Virology,* 64**,** 3226-3233.

CHEN, S. L., TSAI, T. C., HAN, C. P. & TSAO, Y. P. 1996d. Mutational analysis of human papillomavirus type 11 E5a oncoprotein. *Journal of Virology,* 70**,** 3502-3508.

CHIN, M. T., HIROCHIKA, R., HIROCHIKA, H., BROKER, T. R. & CHOW, L. T. 1988. Regulation of human papillomavirus type 11 enhancer and E6 promoter by activating and repressing proteins from the E2 open reading frame: Functional and biochemical studies. *Journal of Virology,* 62**,** 2994-3002.

CHOO, K. B., PAN, C. C. & HAN, S. H. 1987. Integration of human papillomavirus type-16 into cellular DNA of cervical-carcinoma - preferential deletion of the E2 gene and invariable retention of the long control region and the E6/E7 open reading frames *Virology,* 161**,** 259-261.

CLEMENTS, A., JOHNSTON, K., MAZZARELLI, J. M., RICCIARDI, R. P. & MARMORSTEIN, R. 2000. Oligomerization Properties of the Viral Oncoproteins Adenovirus E1A and Human Papillomavirus E7 and Their Complexes with the Retinoblastoma Protein†. *Biochemistry,* 39**,** 16033-16045.

CLOWER, R. V., FISK, J. C. & MELENDY, T. 2006. Papillomavirus E1 Protein Binds to and Stimulates Human Topoisomerase I. *Journal of Virology,* 80**,** 1584-1587.

COHEN, B. D., GOLDSTEIN, D. J., RUTLEDGE, L., VASS, W. C., LOWY, D. R., SCHLEGEL, R. & SCHILLER, J. T. 1993. Transformation-specific interaction of the bovine papillomavirus E5 oncoprotein with the platelet-derived growth-factor receptor transmembrane domain and the epidermal growth-factor receptor cytoplasmic domain *Journal of Virology,* 67**,** 5303-5311.

COLEMAN, N., BIRLEY, H. D. L., RENTON, A. M., HANNA, N. F., RYAIT, B. K., BYRNE, M., TAYLORROBINSON, D. & STANLEY, M. A. 1994. Immunological events in regressing genital warts *American Journal of Clinical Pathology,* 102**,** 768-774.

COLLINS, A. S., NAKAHARA, T., DO, A. & LAMBERT, P. F. 2005. Interactions with pocket proteins contribute to the role of human papillomavirus type 16 E7 in the papillomavirus life cycle. *Journal of Virology,* 79**,** 14769-14780.

CONDJELLA, R., LIU, X., SUPRYNOWICZ, F., YUAN, H., SUDARSHAN, S., DAI, Y. & SCHLEGEL, R. 2009. The Canine Papillomavirus E5 Protein Signals from the Endoplasmic Reticulum. *Journal of Virology,* 83**,** 12833-12841.

CONRAD, M., BUBB, V. J. & SCHLEGEL, R. 1993. The Human Papillomavirus Type-6 and 16-E5 Proteins are Membrane-associated Proteins which Associate with the 16-Kilodalton Pore-forming Protein *Journal of Virology,* 67**,** 6170-6178.

CONRAD, M., GOLDSTEIN, D., ANDRESSON, T. & SCHLEGEL, R. 1994. The E5 Protein of HPV-6, but Not HPV-16, Associates Efficiently with Cellular Growth Factor Receptors. *Virology,* 200**,** 796-800.

CONWAY, M. J., ALAM, S., CHRISTENSEN, N. D. & MEYERS, C. 2009a. Overlapping and independent structural roles for human papillomavirus type 16 L2 conserved cysteines. *Virology,* 393**,** 295-303.

CONWAY, M. J., ALAM, S., RYNDOCK, E. J., CRUZ, L., CHRISTENSEN, N. D., RODEN, R. B. S. & MEYERS, C. 2009b. Tissue-Spanning Redox Gradient-Dependent Assembly of Native Human Papillomavirus Type 16 Virions. *Journal of Virology,* 83**,** 10515-10526.

CORDEN, S. A., SANT-CASSIA, L. J., EASTON, A. J. & MORRIS, A. G. 1999. The integration of HPV-18 DNA in cervical carcinoma. *Molecular Pathology,* 52**,** 275-282.

CORTESE, M. S., ASHRAFI, G. H. & CAMPO, M. S. 2010. All 4 di-leucine motifs in the first hydrophobic domain of the E5 oncoprotein of human papillomavirus type 16 are essential for surface MHC class I downregulation activity and E5 endomembrane localization. *International Journal of Cancer,* 126**,** 1675-1682.

CROMME, F. V., AIREY, J., HEEMELS, M. T., PLOEGH, H. L., KEATING, P. J., STERN, P. L., MEIJER, C. & WALBOOMERS, J. M. M. 1994. Loss of transporter protein, encoded by the TAP-1 gene, is highly correlated with the loss of HLA expression in cervical carcinomas *Journal of Experimental Medicine,* 179**,** 335-340.

CROMME, F. V., SNIJDERS, P. J. F., VANDENBRULE, A. J. C., KENEMANS, P., MEIJER, C. & WALBOOMERS, J. M. M. 1993. MHC class-I expression in HPV-16 positive carcinomas is posttranscriptionally controlled and independent from c-myc overexpression. *Oncogene,* 8**,** 2969-2975.

CROOKS, G. E., HON, G., CHANDONIA, J. M. & BRENNER, S. E. 2004. WebLogo: A sequence logo generator. *Genome Research,* 14**,** 1188-1190.

CRUSIUS, K., AUVINEN, E. & ALONSO, A. 1997. Enhancement of EGF- and PMA-mediated MAP kinase activation in cells expressing the human papillomavirus type 16 E5 protein. *Oncogene,* 15**,** 1437-1444.

CRUSIUS, K., AUVINEN, E., STEUER, B., GAISSERT, H. & ALONSO, A. 1998. The human papillomavirus type 16 E5-protein modulates ligand-dependent activation of the EGF receptor family in the human epithelial cell line HaCaT. *Experimental Cell Research,* 241**,** 76-83.

CRUSIUS, K., KASZKIN, M., KINZEL, V. & ALONSO, A. 1999. The human papillomavirus type 16 E5 protein modulates phospholipase C-gamma-1 activity and phosphatidyl inositol turnover in mouse fibroblasts. *Oncogene,* 18**,** 6714-6718.

CRUSIUS, K., RODRIGUEZ, I. & ALONSO, A. 2000. The human papillomavirus type 16 E5 protein modulates ERK1/2 and p38 MAP kinase activation by an EGFR-Independent process in stressed human keratinocytes. *Virus Genes,* 20**,** 65-69.

CUBIE, H. A. 2013. Diseases associated with human papillomavirus infection. *Virology,* 445**,** 21-34.

CULLEN, A. P., REID, R., CAMPION, M. & LORINCZ, A. T. 1991. Analysis of the physical state of different human papillomavirus DNAs in intraepithelial and invasive cervical neoplasia. *Journal of Virology,* 65**,** 606-612.

D'SOUZA, G. & DEMPSEY, A. 2011. The role of HPV in head and neck cancer and review of the HPV vaccine. *Preventive Medicine,* 53**,** S5-S11.

DALL, K. L., SCARPINI, C. G., ROBERTS, I., WINDER, D. M., STANLEY, M. A., MURALIDHAR, B., HERDMAN, M. T., PETT, M. R. & COLEMAN, N. 2008.

Characterization of Naturally Occurring HPV16 Integration Sites Isolated from Cervical Keratinocytes under Noncompetitive Conditions. *Cancer Research,* 68**,** 8249-8259.

DANOS, O., KATINKA, M. & YANIV, M. 1982. Human papillomavirus 1a complete DNA sequence: a novel type of genome organization among papovaviridae. *Embo Journal,* 1**,** 231-236.

DAO, L. D., DUFFY, A., VAN TINE, B. A., WU, S.-Y., CHIANG, C.-M., BROKER, T. R. & CHOW, L. T. 2006. Dynamic localization of the human papillomavirus type 11 origin binding protein E2 through mitosis while in association with the spindle apparatus. *Journal of Virology,* 80**,** 4792-4800.

DAVY, C., MCINTOSH, P., JACKSON, D. J., SORATHIA, R., MIELL, M., WANG, Q., KHAN, J., SONEJI, Y. & DOORBAR, J. 2009. A novel interaction between the human papillomavirus type 16 E2 and E1^E4 proteins leads to stabilization of E2. *Virology,* 394**,** 266-275.

DAVY, C. E., JACKSON, D. J., RAJ, K., PEH, W. L., SOUTHERN, S. A., DAS, P., SORATHIA, R., LASKEY, P., MIDDLETON, K., NAKAHARA, T., WANG, Q., MASTERSON, P. J., LAMBERT, P. F., CUTHILL, S., MILLAR, J. B. A. & DOORBAR, J. 2005. Human Papillomavirus Type 16 E1∧E4-Induced G2 Arrest Is Associated with Cytoplasmic Retention of Active Cdk1/Cyclin B1 Complexes. *Journal of Virology,* 79**,** 3998-4011.

DAVY, C. E., JACKSON, D. J., WANG, Q., RAJ, K., MASTERSON, P. J., FENNER, N. F., SOUTHERN, S., CUTHILL, S., MILLAR, J. B. A. & DOORBAR, J. 2002. Identification of a G2 Arrest Domain in the E1∧E4 Protein of Human Papillomavirus Type 16. *Journal of Virology,* 76**,** 9806-9818.

DAY, P. M., BAKER, C. C., LOWY, D. R. & SCHILLER, J. T. 2004. Establishment of papillomavirus infection is enhanced by promyelocytic leukemia protein (PML) expression. *Proceedings of the National Academy of Sciences of the United States of America,* 101**,** 14252-14257.

DAY, P. M., LOWY, D. R. & SCHILLER, J. T. 2003. Papillomaviruses infect cells via a clathrin-dependent pathway. *Virology,* 307**,** 1-11.

DAY, P. M., RODEN, R. B. S., LOWY, D. R. & SCHILLER, J. T. 1998. The papillomavirus minor capsid protein, L2, induces localization of the major capsid protein, L1, and the viral transcription/replication protein, E2, to PML oncogenic domains. *Journal of Virology,* 72**,** 142-150.

DAY, P. M. & SCHILLER, J. T. 2009. The role of furin in papillomavirus infection. *Future Microbiology,* 4**,** 1255-1262.

DAY, P. M., THOMPSON, C. D., SCHOWALTER, R. M., LOWY, D. R. & SCHILLER, J. T. 2013. Identification of a Role for the trans-Golgi Network in Human Papillomavirus 16 Pseudovirus Infection. *Journal of Virology,* 87**,** 3862-3870.

DE JONG, A., VAN DER BURG, S. H., KWAPPENBERG, K. M. C., VAN DER HULST, J. M., FRANKEN, K., GELUK, A., VAN MEIJGAARDEN, K. E., DRIJFHOUT, J. W., KENTER, G., VERMEIJ, P., MELIEF, C. J. M. & OFFRINGA, R. 2002. Frequent detection of human papillomavirus 16 E2-specific T-helper immunity in healthy subjects. *Cancer Research,* 62**,** 472-479.

DE MARTEL, C., FERLAY, J., FRANCESCHI, S., VIGNAT, J., BRAY, F., FORMAN, D. & PLUMMER, M. 2012. Global burden of cancers attributable to infections in 2008: a review and synthetic analysis. *The lancet oncology,* 13**,** 607-15.

DE SANJOSE, S., DIAZ, M., CASTELLSAGUE, X., CLIFFORD, G., BRUNI, L., MUNOZ, N. & BOSCH, F. X. 2007. Worldwide prevalence and genotype distribution of cervical human papillomavirus DNA in women with normal cytology: a meta-analysis. *Lancet Infectious Diseases,* 7**,** 453-459.

DE VILLIERS, E.-M. 2013. Cross-roads in the classification of papillomaviruses. *Virology,* 445**,** 2-10.

DE VILLIERS, E. M., FAUQUET, C., BROKER, T. R., BERNARD, H. U. & ZUR HAUSEN, H. 2004. Classification of papillomaviruses. *Virology,* 324**,** 17-27.

DE VINCENZO, R., RICCI, C., CONTE, C. & SCAMBIA, G. 2013. HPV vaccine cross-protection: Highlights on additional clinical benefit. *Gynecologic Oncology,* 130**,** 642-651.

DEDO, H. H. & YU, K. C. Y. 2001. CO2 laser treatment in 244 patients with respiratory papillomas. *Laryngoscope,* 111**,** 1639-1644.

DELL, G., WILKINSON, K. W., TRANTER, R., PARISH, J., BRADY, L. & GASTON, K. 2003. Comparison of the structure and DNA-binding properties of the E2 proteins from an

oncogenic and a non-oncogenic human papillomavirus. *Journal of Molecular Biology,* 334**,** 979-991.

DENG, W., LIN, B. Y., JIN, G., WHEELER, C. G., MA, T., HARPER, J. W., BROKER, T. R. & CHOW, L. T. 2004. Cyclin/CDK Regulates the Nucleocytoplasmic Localization of the Human Papillomavirus E1 DNA Helicase. *Journal of Virology,* 78**,** 13954-13965.

DENNY, L. 2013. Safety of HPV vaccination: A FIGO statement. *International Journal of Gynecology & Obstetrics*.

DIMAIO, D., GURALSKI, D. & SCHILLER, J. T. 1986. Translocation of open reading frame E5 of bovine papillomavirus is required for its transforming activity *Proceedings of the National Academy of Sciences of the United States of America,* 83**,** 1797-1801.

DIMAIO, D. & PETTI, L. M. 2013. The E5 proteins. *Virology,* 445**,** 99-114.

DING, D.-C., CHIANG, M.-H., LAI, H.-C., HSIUNG, C. A., HSIEH, C.-Y. & CHU, T.-Y. 2009. Methylation of the long control region of HPV16 is related to the severity of cervical neoplasia. *European Journal of Obstetrics & Gynecology and Reproductive Biology,* 147**,** 215-220.

DISBROW, G. L., SUNITHA, I., BAKER, C. C., HANOVER, J. & SCHLEGEL, R. 2003. Codon optimization of the HPV-16 E5 gene enhances protein expression. *Virology,* 311**,** 105-114.

DOORBAR, J. 2006. Molecular biology of human papillomavirus infection and cervical cancer. *Clinical Science,* 110**,** 525-541.

DOORBAR, J. 2013. The E4 protein; structure, function and patterns of expression. *Virology,* 445**,** 80-98.

DOORBAR, J., CAMPBELL, D., GRAND, R. J. & GALLIMORE, P. H. 1986. Identification of the human papilloma virus-1a E4 gene products. *The EMBO journal,* 5**,** 355-362.

DOORBAR, J., ELY, S., STERLING, J., MCLEAN, C. & CRAWFORD, L. 1991. Specific interaction between HPV-16 E1-E4 and cytokeratins results in collapse of the epithelial-cell intermediate filament network *Nature,* 352**,** 824-827.

DOORBAR, J., FOO, C., COLEMAN, N., MEDCALF, L., HARTLEY, O., PROSPERO, T., NAPTHINE, S., STERLING, J., WINTER, G. & GRIFFIN, H. 1997. Characterization of events during the late stages of HPV16 infection in vivo using high-affinity synthetic Fabs to E4. *Virology,* 238**,** 40-52.

DOORBAR, J., PARTON, A., HARTLEY, K., BANKS, L., CROOK, T., STANLEY, M. & CRAWFORD, L. 1990. Detection of novel splicing patterns in a HPV16-containing keratinocyte cell line. *Virology,* 178**,** 254-262.

DOORBAR, J., QUINT, W., BANKS, L., BRAVO, I. G., STOLER, M., BROKER, T. R. & STANLEY, M. A. 2012. The Biology and Life-Cycle of Human Papillomaviruses. *Vaccine,* 30**,** F55-F70.

DRUMMOND-BARBOSA, D., VAILLANCOURT, R. R., KAZLAUSKAS, A. & DIMAIO, D. 1995. Ligand-independent activation of the platelet-derived grwoth-factor-beta receptor - requirements for bovine papollomavirus E5-induced mitogenic signaling *Molecular and Cellular Biology,* 15**,** 2570-2581.

DUGAN, G. E. & HEWITT, E. W. 2008. Structural and functional dissection of the human cytomegalovirus immune evasion protein US6. *Journal of Virology,* 82**,** 3271-3282.

DUGAN, G. E. & HEWITT, E. W. 2009. Dependence of the localization and function of the human cytomegalovirus protein US6 on the transporter associated with antigen processing. *Journal of General Virology,* 90**,** 2234-2238.

DYKSTRA, K. M., POKUSA, J. E., SUHAN, J. & LEE, T. H. 2010. Yip1A Structures the Mammalian Endoplasmic Reticulum. *Molecular Biology of the Cell,* 21**,** 1556-1568.

DYKSTRA, K. M., ULENGIN, I., DELROSE, N. & LEE, T. H. 2013. Identification of Discrete Sites in Yip1A Necessary for Regulation of Endoplasmic Reticulum Structure. *Plos One,* 8.

DYSON, N., GUIDA, P., MÜNGER, K. & HARLOW, E. 1992. Homologous sequences in adenovirus E1A and human papillomavirus E7 proteins mediate interaction with the same set of cellular proteins *Journal of Virology,* 66**,** 6893-6902.

EBERHARD, J., ONDER, Z. & MOROIANU, J. 2013. Nuclear import of high risk HPV16 E7 oncoprotein is mediated by its zinc-binding domain via hydrophobic interactions with Nup62. *Virology,* 446**,** 334-345.

EDWARDS, M. C., LIEGEOIS, N., HORECKA, J., DEPINHO, R. A., SPRAGUE, G. F., TYERS, M. & ELLEDGE, S. J. 1997. Human CPR (Cell Cycle Progression Restoration) Genes Impart a Far– Phenotype on Yeast Cells. *Genetics,* 147**,** 1063-1076.

EGAWA, K. 1994. New types of human papillomaviruses and intracytoplasmic inclusion bodies: a classification of inclusion warts according to clinical features, histology and associated HPV types. *British Journal of Dermatology,* 130**,** 158-166.

EGAWA, N., NAKAHARA, T., OHNO, S.-I., NARISAWA-SAITO, M., YUGAWA, T., FUJITA, M., YAMATO, K., NATORI, Y. & KIYONO, T. 2012. The E1 Protein of Human Papillomavirus Type 16 Is Dispensable for Maintenance Replication of the Viral Genome. *Journal of Virology,* 86**,** 3276-3283.

EISENBERG, D., SCHWARZ, E., KOMAROMY, M. & WALL, R. 1984. Analysis of membrane and surface protein sequences with the hydrophobic moment plot. *Journal of Molecular Biology,* 179**,** 125-142.

EKSTRÖM, J., MÜHR, L. S. A., BZHALAVA, D., SÖDERLUND-STRAND, A., HULTIN, E., NORDIN, P., STENQUIST, B., PAOLI, J., FORSLUND, O. & DILLNER, J. 2013. Diversity of human papillomaviruses in skin lesions. *Virology,* 447**,** 300-311.

EKSTROM, J. L., PAULY, T. A., CARTY, M. D., SOELLER, W. C., CULP, J., DANLEY, D. E., HOOVER, D. J., TREADWAY, J. L., GIBBS, E. M., FLETTERICK, R. J., DAY, Y. S. N., MYSZKA, D. G. & RATH, V. L. 2002. Structure-Activity Analysis of the Purine Binding Site of Human Liver Glycogen Phosphorylase. *Chemistry & Biology,* 9**,** 915-924.

ENEMARK, E. J., CHEN, G., VAUGHN, D. E., STENLUND, A. & JOSHUA-TOR, L. 2000. Crystal Structure of the DNA Binding Domain of the Replication Initiation Protein E1 from Papillomavirus. *Molecular Cell,* 6**,** 149-158.

ENEMARK, E. J., STENLUND, A. & JOSHUA-TOR, L. 2002. Crystal structures of two intermediates in the assembly of the papillomavirus replication initiation complex. *EMBO J,* 21**,** 1487-1496.

ERICKSON, B. K., ALVAREZ, R. D. & HUH, W. K. 2013. Human papillomavirus: what every provider should know. *American Journal of Obstetrics and Gynecology,* 208**,** 169-175.

EVANDER, M., FRAZER, I. H., PAYNE, E., QI, Y. M., HENGST, K. & MCMILLAN, N. A. J. 1997. Identification of the α6 integrin as a candidate receptor for papillomaviruses. *Journal of Virology,* 71**,** 2449-2456.

FAN, X., LIU, Y., HEILMAN, S. A. & CHEN, J. J. 2013. Human Papillomavirus E7 Induces Rereplication in Response to DNA Damage. *Journal of Virology,* 87**,** 1200-1210.

FAUQUET, C. M., MAYO, M. A., MANILOFF, J., DESSELBERGER, U. & BALL, L. A. 2005. Virus Taxonomy: VIIIth Report of the International Committee on Taxonomy of Viruses

FEHRMANN, F., KLUMPP, D. J. & LAIMINS, L. A. 2003. Human papillomavirus type 31 E5 protein supports cell cycle progression and activates late viral functions upon epithelial differentiation. *Journal of Virology,* 77**,** 2819-2831.

FIGUEROA, C., TAYLOR, J. & VOJTEK, A. B. 2001. Prenylated Rab acceptor protein is a receptor for prenylated small GTPases. *Journal of Biological Chemistry,* 276**,** 28219-28225.

FILIPPOVA, M., JOHNSON, M. M., BAUTISTA, M., FILIPPOV, V., FODOR, N., TUNGTEAKKHUN, S. S., WILLIAMS, K. & DUERKSEN-HUGHES, P. J. 2007. The Large and Small Isoforms of Human Papillomavirus Type 16 E6 Bind to and Differentially Affect Procaspase 8 Stability and Activity. *Journal of Virology,* 81**,** 4116-4129.

FINNEN, R. L., ERICKSON, K. D., CHEN, X. J. S. & GARCEA, R. L. 2003. Interactions between papillomavirus L1 and L2 capsid proteins. *Journal of Virology,* 77**,** 4818-4826.

FLORES, E. R., ALLEN-HOFFMANN, B. L., LEE, D. & LAMBERT, P. F. 2000. The human papillomavirus type 16 E7 oncogene is required for the productive stage of the viral life cycle. *Journal of Virology,* 74**,** 6622-6631.

FLORES, E. R. & LAMBERT, P. F. 1997. Evidence for a switch in the mode of human papillomavirus type 16 DNA replication during the viral life cycle. *Journal of Virology,* 71**,** 7167-7179.

FLORIN, L., BECKER, K. A., LAMBERT, C., NOWAK, T., SAPP, C., STRAND, D., STREECK, R. E. & SAPP, M. 2006. Identification of a Dynein Interacting Domain in the Papillomavirus Minor Capsid Protein L2. *Journal of Virology,* 80**,** 6691-6696.

FORMAN, D., DE MARTEL, C., LACEY, C. J., SOERJOMATARAM, I., LORTET-TIEULENT, J., BRUNI, L., VIGNAT, J., FERLAY, J., BRAY, F., PLUMMER, M. & FRANCESCHI, S. 2012. Global Burden of Human Papillomavirus and Related Diseases. *Vaccine,* 30**,** F12-F23.

FREEMAN, A. K. & MORRISON, D. K. 2011. 14-3-3 Proteins: Diverse functions in cell proliferation and cancer progression. *Seminars in Cell & Developmental Biology,* 22**,** 681-687.

FRENCH, A. P., MILLS, S., SWARUP, R., BENNETT, M. J. & PRIDMORE, T. P. 2008. Colocalization of fluorescent markers in confocal microscope images of plant cells. *Nature Protocols,* 3**,** 619-628.

FUCHS, E. 1990. Epidermal differentiation: the bare essentials. *The Journal of Cell Biology,* 111**,** 2807-2814.

FUNK, J. O., WAGA, S., HARRY, J. B., ESPLING, E., STILLMAN, B. & GALLOWAY, D. A. 1997. Inhibition of CDK activity and PCNA-dependent DNA replication by p21 is blocked by interaction with the HPV-16 E7 oncoprotein. *Genes & Development,* 11**,** 2090-2100.

GAO, P. & ZHENG, J. 2010. High-risk HPV E5-induced cell fusion: a critical initiating event in the early stage of HPV-associated cervical cancer. *Virology Journal,* 7.

GARCIA-RANEA, J. A. & VALENCIA, A. 1998. Distribution and functional diversification of the ras superfamily in Saccharomyces cerevisiae. *Febs Letters,* 434**,** 219-225.

GARIGLIO, P., GUTIERREZ, J., CORTES, E. & VAZQUEZ, J. 2009. The Role of Retinoid Deficiency and Estrogens as Cofactors in Cervical Cancer. *Archives of Medical Research,* 40**,** 449-465.

GAUTHIER, J. M., DILLNER, J. & YANIV, M. 1991. Structural analysis of the human papillomavirus type 16-E2 transactivator with antipeptide antibodies reveals a high mobility region linking the transactivation and the DNA-binding domains. *Nucleic Acids Research,* 19**,** 7073-7079.

GENG, J., SHIN, M. E., GILBERT, P. M., COLLINS, R. N. & BURD, C. G. 2005. Saccharomyces cerevisiae Rab-GDI Displacement Factor Ortholog Yip3p Forms Distinct Complexes with the Ypt1 Rab GTPase and the Reticulon Rtn1p. *Eukaryotic Cell,* 4**,** 1166-1174.

GENTHER, S. M., STERLING, S., DUENSING, S., MÜNGER, K., SATTLER, C. & LAMBERT, P. F. 2003. Quantitative role of the human papillomavirus type 16 E5 gene during the productive stage of the viral life cycle. *Journal of Virology,* 77**,** 2832-2842.

GENTHER WILLIAMS, S. M., DISBROW, G. L., SCHLEGEL, R., LEE, D., THREADGILL, D. W. & LAMBERT, P. F. 2005. Requirement of epidermal growth factor receptor for hyperplasia induced by E5, a high-risk human papillomavirus oncogene. *Cancer Research,* 65**,** 6534-6542.

GEORGOPOULOS, N. T., PROFFITT, J. L. & BLAIR, G. E. 2000. Transcriptional regulation of the major histocompatibility complex (MHC) class I heavy chain, TAP1 and LMP2 genes by the human papillomavirus (HPV) type 6b, 16 and 18 E7 oncoproteins. *Oncogene,* 19**,** 4930-4935.

GEREIN, V., RASTORGUEV, E., GEREIN, J., DRAF, W. & SCHIRREN, J. 2005. Incidence, age at onset, and potential reasons of malignant transformation in recurrent respiratory papillomatosis patients: 20 years experience. *Otolaryngology-Head and Neck Surgery,* 132**,** 392-394.

GEWURZ, B. E., GAUDET, R., TORTORELLA, D., WANG, E. W., PLOEGH, H. L. & WILEY, D. C. 2001. Antigen presentation subverted: Structure of the human cytomegalovirus protein US2 bound to the class I molecule HLA-A2. *Proceedings of the National Academy of Sciences of the United States of America,* 98**,** 6794-6799.

GIAMPIERI, S., GARCIA-ESCUDERO, R., GREEN, J. & STOREY, A. 2004. Human papillomavirus type 77 E6 protein selectively inhibits p53-dependent transcription of proapoptotic genes following UV-B irradiation. *Oncogene,* 23**,** 5864-5870.

GIBSON, T. J. 2012. RACK1 research – ships passing in the night? *Febs Letters,* 586**,** 2787-2789.

GIESWEIN, C. E., SHAROM, F. J. & WILDEMAN, A. G. 2003. Oligomerization of the E5 protein of human papillomavirus type 16 occurs through multiple hydrophobic regions. *Virology,* 313**,** 415-426.

GILLISON, M. L., ALEMANY, L., SNIJDERS, P. J. F., CHATURVEDI, A., STEINBERG, B. M., SCHWARTZ, S. & CASTELLSAGUÉ, X. 2012. Human Papillomavirus and Diseases of the Upper Airway: Head and Neck Cancer and Respiratory Papillomatosis. *Vaccine,* 30, Supplement 5**,** F34-F54.

GOLDSTEIN, D. J., LI, W. Q., WANG, L. M., HEIDARAN, M. A., AARONSON, S., SHINN, R., SCHLEGEL, R. & PIERCE, J. H. 1994. The bovine papillomavirus type-1 E5 transforming protein specifically binds and activates the beta-type receptor for the platelet-derived growth-factor but not other related tyrosine kinase-containing receptors to induce cellular-transformation. *Journal of Virology,* 68**,** 4432-4441.

GOTTSCHLING, M., GOEKER, M., STAMATAKIS, A., BININDA-EMONDS, O. R. P., NINDL, I. & BRAVO, I. G. 2011. Quantifying the Phylodynamic Forces Driving Papillomavirus Evolution. *Molecular Biology and Evolution,* 28**,** 2101-2113.

GRASSMANN, K., RAPP, B., MASCHEK, H., PETRY, K. U. & IFTNER, T. 1996. Identification of a differentiation-inducible promoter in the E7 open reading frame of human papillomavirus type 16 (HPV-16) in raft cultures of a new cell line containing high copy numbers of episomal HPV-16 DNA. *Journal of Virology,* 70**,** 2339-2349.

GRIFFIN, H., WU, Z., MARNANE, R., DEWAR, V., MOLIJN, A., QUINT, W., VAN HOOF, C., STRUYF, F., COLAU, B., JENKINS, D. & DOORBAR, J. 2012. E4 Antibodies Facilitate Detection and Type-Assignment of Active HPV Infection in Cervical Disease. *Plos One,* 7**,** e49974.

GRUENER, M., BRAVO, I. G., MOMBURG, F., ALONSO, A. & TOMAKIDI, P. 2007. The E5 protein of the human papillomavirus type 16 down-regulates HLA-I surface expression in calnexin-expressing but not in calnexin-deficient cells. *Virology Journal,* 4.

GU, Z. M. & MATLASHEWSKI, G. 1995. Effect of human papillomavirus type-16 oncogenes on MAP kinase-activity *Journal of Virology,* 69**,** 8051-8056.

GUCCIONE, E., MASSIMI, P., BERNAT, A. & BANKS, L. 2002. Comparative analysis of the intracellular location of the high- and low-risk human papillomavirus oncoproteins. *Virology,* 293**,** 20-25.

HADASCHIK, D., HINTERKEUSER, K., OLDAK, M., PFISTER, H. J. & SMOLA-HESS, S. 2003. The papillomavirus E2 protein binds to and synergizes with C/EBP factors involved in keratinocyte differentiation. *Journal of Virology,* 77**,** 5253-5265.

HALBERT, C. L., DEMERS, G. W. & GALLOWAY, D. A. 1992. The E6 and E7 genes of human papillomavirus type 6 have weak immortalizing activity in human epithelial cells. *Journal of Virology,* 66**,** 2125-2134.

HALIM, A., NILSSON, J., RÜETSCHI, U., HESSE, C. & LARSON, G. 2012a. Human Urinary Glycoproteomics; Attachment Site Specific Analysis of N- and O-Linked Glycosylations by CID and ECD. *Molecular & Cellular Proteomics,* 11.

HALIM, A., RÜETSCHI, U., LARSON, G. & NILSSON, J. 2012b. LC–MS/MS Characterization of O-Glycosylation Sites and Glycan Structures of Human Cerebrospinal Fluid Glycoproteins. *Journal of Proteome Research,* 12**,** 573-584.

HAN, R., CLADEL, N. M., REED, C. A. & CHRISTENSEN, N. D. 1998. Characterization of transformation function of cottontail rabbit papillomavirus E5 and E8 genes. *Virology,* 251**,** 253-263.

HAN, Y., LOO, Y. M., MILITELLO, K. T. & MELENDY, T. 1999. Interactions of the papovavirus DNA replication initiator proteins, bovine papillomavirus type 1 E1 and simian virus 40 large T antigen, with human replication protein A. *Journal of Virology,* 73**,** 4899-4907.

HANAHAN, D. 1983. Studies on Transformation of Escherichia-Coli with Plasmids. *Journal of Molecular Biology,* 166**,** 557-580.

HARTWIG, S., SYRJAENEN, S., DOMINIAK-FELDEN, G., BROTONS, M. & CASTELLSAGUE, X. 2012. Estimation of the epidemiological burden of human papillomavirus-related cancers and non-malignant diseases in men in Europe: a review. *Bmc Cancer,* 12.

HASAN, U. A., ZANNETTI, C., PARROCHE, P., GOUTAGNY, N., MALFROY, M., ROBLOT, G., CARREIRA, C., HUSSAIN, I., MÜLLER, M., TAYLOR-PAPADIMITRIOU, J., PICARD, D., SYLLA, B. S., TRINCHIERI, G., MEDZHITOV, R. & TOMMASINO, M. 2013. The Human papillomavirus type 16 E7 oncoprotein induces a transcriptional repressor complex on the Toll-like receptor 9 promoter. *The Journal of Experimental Medicine,* 210**,** 1369-1387.

HEIDTMAN, M., CHEN, C. Z., COLLINS, R. N. & BARLOWE, C. 2003. A role for Yip1p in COPII vesicle biogenesis. *Journal of Cell Biology,* 163**,** 57-69.

HEIDTMAN, M., CHEN, C. Z., COLLINS, R. N. & BARLOWE, C. 2005. Yos1p is a novel subunit of the Yip1p-Yif1p complex and is required for transport between the endoplasmic reticulum and the golgi complex. *Molecular Biology of the Cell,* 16**,** 1673-1683.

HELLER, C., WEISSER, T., MUELLER-SCHICKERT, A., RUFER, E., HOH, A., LEONHARDT, R. M. & KNITTLER, M. R. 2011. Identification of Key Amino Acid Residues That Determine the Ability of High Risk HPV16-E7 to Dysregulate Major Histocompatibility Complex Class I Expression. *Journal of Biological Chemistry,* 286**,** 10983-10997.

HERDMAN, M. T., PETT, M. R., ROBERTS, I., ALAZAWI, W. O. F., TESCHENDORFF, A. E., ZHANG, X.-Y., STANLEY, M. A. & COLEMAN, N. 2006. Interferon-beta treatment of cervical keratinocytes naturally infected with human papillomavirus 16 episomes

promotes rapid reduction in episome numbers and emergence of latent integrants. *Carcinogenesis,* 27**,** 2341-2353.

HEWITT, E. W., SEN GUPTA, S. & LEHNER, P. J. 2001. The human cytomegalovirus gene product US6 inhibits ATP binding by TAP. *Embo Journal,* 20**,** 387-396.

HICKMAN, A. B. & DYDA, F. 2005. Binding and unwinding: SF3 viral helicases. *Current Opinion in Structural Biology,* 15**,** 77-85.

HINDMARSH, P. L. & LAIMINS, L. A. 2007. Mechanisms regulating expression of the HPV 31 L1 and L2 capsid proteins and pseudovirion entry. *Virology Journal,* 4.

HINES, C. S., MEGHOO, C., SHETTY, S., BIBURGER, M., BRENOWITZ, M. & HEGDE, R. S. 1998. DNA structure and flexibility in the sequence-specific binding of papillomavirus E2 proteins. *Journal of Molecular Biology,* 276**,** 809-818.

HIROKAWA, T., BOON-CHIENG, S. & MITAKU, S. 1998. SOSUI: classification and secondary structure prediction system for membrane proteins. *Bioinformatics,* 14**,** 378-379.

HORNBECK, P. V., CHABRA, I., KORNHAUSER, J. M., SKRZYPEK, E. & ZHANG, B. 2004. PhosphoSite: A bioinformatics resource dedicated to physiological protein phosphorylation. *Proteomics,* 4**,** 1551-1561.

HSU, C.-Y., MECHALI, F. & BONNE-ANDREA, C. 2007. Nucleocytoplasmic Shuttling of Bovine Papillomavirus E1 Helicase Downregulates Viral DNA Replication in S Phase. *Journal of Virology,* 81**,** 384-394.

HU, L., PLAFKER, K., VOROZHKO, V., ZUNA, R. E., HANIGAN, M. H., GORBSKY, G. J., PLAFKER, S. M., ANGELETTI, P. C. & CERESA, B. P. 2009. Human papillomavirus 16 E5 induces bi-nucleated cell formation by cell–cell fusion. *Virology,* 384**,** 125-134.

HU, L., POTAPOVA, T. A., LI, S., RANKIN, S., GORBSKY, G. J., ANGELETTI, P. C. & CERESA, B. P. 2010. Expression of HPV16 E5 produces enlarged nuclei and polyploidy through endoreplication. *Virology,* 405**,** 342-351.

HU, L. L. & CERESA, B. P. 2009. Characterization of the plasma membrane localization and orientation of HPV16 E5 for cell-cell fusion. *Virology,* 393**,** 135-143.

HUANG, H.-S. & LAMBERT, P. F. 2012. Use of an in vivo animal model for assessing the role of integrin α6β4 and Syndecan-1 in early steps in papillomavirus infection. *Virology,* 433**,** 395-400.

HUANG, P. S., PATRICK, D. R., EDWARDS, G., GOODHART, P. J., HUBER, H. E., MILES, L., GARSKY, V. M., OLIFF, A. & HEIMBROOK, D. C. 1993. Protein domains governing interactions between E2F, the retinoblastoma gene-product, and human papillomavirus type-16 E7 protein *Molecular and Cellular Biology,* 13**,** 953-960.

HUBBERT, N. L., SCHILLER, J. T., LOWY, D. R. & ANDROPHY, E. J. 1988. Bovine papilloma virus-transformed cells contain multiple E2 proteins. *Proceedings of the National Academy of Sciences,* 85**,** 5864-5868.

HUDSON, J. B., BEDELL, M. A., MCCANCE, D. J. & LAIMINS, L. A. 1990. Immortalization and altered differentiation of human keratinocytes in vitro by the E6 and E7 open reading frames of human papillomavirus type 18. *Journal of Virology,* 64**,** 519-526.

HUIBREGTSE, J. M., SCHEFFNER, M. & HOWLEY, P. M. 1993. Cloning and expression of the cDNA for E6-AP, a protein that mediates the interaction of the human papillomavirus E6 oncoprotein with p53. *Molecular and Cellular Biology,* 13**,** 775-784.

HUTAGALUNG, A. H. & NOVICK, P. J. 2011. Role of Rab GTPases in Membrane Traffic and Cell Physiology. *Physiological Reviews,* 91**,** 119-149.

HWANG, E. S., NOTTOLI, T. & DIMAIO, D. 1995. The HPV16 E5 protein-expression, detection, and stable complex-formation with transmembrane proteins in COS cells *Virology,* 211**,** 227-233.

HWANG, S. G., LEE, D. Y., KIM, J. Y., SEO, T. G. & CHOE, J. H. 2002. Human papillomavirus type 16 E7 binds to E2F1 and activates E2F1-driven transcription in a retinoblastoma protein-independent manner. *Journal of Biological Chemistry,* 277**,** 2923-2930.

ILVES, I., MÄEMETS, K., SILLA, T., JANIKSON, K. & USTAV, M. 2006. Brd4 Is Involved in Multiple Processes of the Bovine Papillomavirus Type 1 Life Cycle. *Journal of Virology,* 80**,** 3660-3665.

INADOME, H., NODA, Y., KAMIMURA, Y., ADACHI, H. & YODA, K. 2007. Tvp38, Tvp23, Tvp18 and Tvp15: Novel membrane proteins in the Tlg2-containing Golgi/endosome compartments of Saccharomyces cerevisiae. *Experimental Cell Research,* 313**,** 688-697.

ITO, T., CHIBA, T., OZAWA, R., YOSHIDA, M., HATTORI, M. & SAKAKI, Y. 2001. A comprehensive two-hybrid analysis to explore the yeast protein interactome. *Proceedings of the National Academy of Sciences of the United States of America,* 98**,** 4569-4574.

ITO, T., TASHIRO, K., MUTA, S., OZAWA, R., CHIBA, T., NISHIZAWA, M., YAMAMOTO, K., KUHARA, S. & SAKAKI, Y. 2000. Toward a protein-protein interaction map of the budding yeast: A comprehensive system to examine two-hybrid interactions in all possible combinations between the yeast proteins. *Proceedings of the National Academy of Sciences of the United States of America,* 97**,** 1143-1147.

JANG, M. K., KWON, D. & MCBRIDE, A. A. 2009. Papillomavirus E2 Proteins and the Host Brd4 Protein Associate with Transcriptionally Active Cellular Chromatin. *Journal of Virology,* 83**,** 2592-2600.

JEONG, K. W., KIM, H. Z., KIM, S., KIM, Y. S. & CHOE, J. 2007. Human papillomavirus type 16 E6 protein interacts with cystic fibrosis transmembrane regulator-associated ligand and promotes E6-associated protein-mediated ubiquitination and proteasomal degradation. *Oncogene,* 26**,** 487-499.

JIN, C., ZHANG, Y., ZHU, H., AHMED, K., FU, C. & YAO, X. 2005. Human Yip1A specifies the localization of Yif1 to the Golgi apparatus. *Biochemical and Biophysical Research Communications,* 334**,** 16-22.

JOHANNSEN, E. & LAMBERT, P. F. 2013. Epigenetics of human papillomaviruses. *Virology,* 445**,** 205-212.

JOHANSSON, C. & SCHWARTZ, S. 2013. Regulation of human papillomavirus gene expression by splicing and polyadenylation. *Nat Rev Micro,* 11**,** 239-251.

JOHANSSON, C., SOMBERG, M., LI, X., WINQUIST, E. B., FAY, J., RYAN, F., PIM, D., BANKS, L. & SCHWARTZ, S. 2012. HPV-16 E2 contributes to induction of HPV-16 late gene expression by inhibiting early polyadenylation. *Embo Journal,* 31**,** 3212-3227.

JOHNSON, K. M., KINES, R. C., ROBERTS, J. N., LOWY, D. R., SCHILLER, J. T. & DAY, P. M. 2009. Role of Heparan Sulfate in Attachment to and Infection of the Murine Female Genital Tract by Human Papillomavirus. *Journal of Virology,* 83**,** 2067-2074.

JONES, D. T. 2007. Improving the accuracy of transmembrane protein topology prediction using evolutionary information. *Bioinformatics,* 23**,** 538-544.

KABSCH, K. & ALONSO, A. 2002a. The human papillomavirus type 16 (HPV-16) E5 protein sensitizes human keratinocytes to apoptosis induced by osmotic stress. *Oncogene,* 21**,** 947-953.

KABSCH, K. & ALONSO, A. 2002b. The human papillomavirus type 16 E5 protein impairs TRAIL- and FasL-mediated apoptosis in HaCaT cells by different mechanisms. *Journal of Virology,* 76**,** 12162-12172.

KABSCH, K., MOSSADEGH, N., KOHL, A., KOMPOSCH, G., SCHENKEL, J., ALONSO, A. & TOMAKIDI, P. 2004. The HPV-16 E5 protein inhibits TRAIL- and FasL-mediated apoptosis in human keratinocyte raft cultures. *Intervirology,* 47**,** 48-56.

KÄLL, L., KROGH, A. & SONNHAMMER, E. L. L. 2004. A Combined Transmembrane Topology and Signal Peptide Prediction Method. *Journal of Molecular Biology,* 338**,** 1027-1036.

KAMIDE, K., ASAYAMA, K., KATSUYA, T., OHKUBO, T., HIROSE, T., INOUE, R., METOKI, H., KIKUYA, M., OBARA, T., HANADA, H., THIJS, L., KUZNETSOVA, T., NOGUCHI, Y., SUGIMOTO, K., OHISHI, M., MORIMOTO, S., NAKAHASHI, T., TAKIUCHI, S., ISHIMITSU, T., TSUCHIHASHI, T., SOMA, M., HIGAKI, J., MATSUURA, H., SHINAGAWA, T., SASAGURI, T., MIKI, T., TAKEDA, K., SHIMAMOTO, K., UENO, M., HOSOMI, N., KATO, J., KOMAI, N., KOJIMA, S., SASE, K., MIYATA, T., TOMOIKE, H., KAWANO, Y., OGIHARA, T., RAKUGI, H., STAESSEN, J. A. & IMAI, Y. 2013. Genome-wide response to antihypertensive medication using home blood pressure measurements: a pilot study nested within the HOMED-BP study. *Pharmacogenomics,* 14**,** 1709-1721.

KÄMPER, N., DAY, P. M., NOWAK, T., SELINKA, H.-C., FLORIN, L., BOLSCHER, J., HILBIG, L., SCHILLER, J. T. & SAPP, M. 2006. A Membrane-Destabilizing Peptide in Capsid Protein L2 Is Required for Egress of Papillomavirus Genomes from Endosomes. *Journal of Virology,* 80**,** 759-768.

KANO, F., TANAKA, A. R., YAMAUCHI, S., KONDO, H. & MURATA, M. 2004. Cdc2 Kinase-dependent Disassembly of Endoplasmic Reticulum (ER) Exit Sites Inhibits ER-to-Golgi Vesicular Transport during Mitosis. *Molecular Biology of the Cell,* 15**,** 4289-4298.

KANO, F., YAMAUCHI, S., YOSHIDA, Y., WATANABE-TAKAHASHI, M., NISHIKAWA, K., NAKAMURA, N. & MURATA, M. 2009. Yip1A regulates the COPI-independent retrograde transport from the Golgi complex to the ER. *Journal of Cell Science,* 122**,** 2218-2227.

KANODIA, S., FAHEY, L. M. & KAST, W. M. 2007. Mechanisms used by human papillomaviruses to escape the host immune response. *Current Cancer Drug Targets,* 7**,** 79-89.

KARIM, R., MEYERS, C., BACKENDORF, C., LUDIGS, K., OFFRINGA, R., VAN OMMEN, G.-J. B., MELIEF, C. J. M., VAN DER BURG, S. H. & BOER, J. M. 2011. Human Papillomavirus Deregulates the Response of a Cellular Network Comprising of Chemotactic and Proinflammatory Genes. *Plos One,* 6.

KAWANA, Y., KAWANA, K., YOSHIKAWA, H., TAKETANI, Y., YOSHIIKE, K. & KANDA, T. 2001. Human Papillomavirus Type 16 Minor Capsid Protein L2 N-Terminal Region Containing a Common Neutralization Epitope Binds to the Cell Surface and Enters the Cytoplasm. *Journal of Virology,* 75**,** 2331-2336.

KELL, B., JEWERS, R. J., CASON, J., PAKARIAN, F., KAYE, J. N. & BEST, J. M. 1994. Detection of E5 oncoprotein in human papillomavirus type 16-positive cervical scrapes using antibodies raised to synthetic peptides. *Journal of General Virology,* 75**,** 2451-2456.

KEMP, T. J., HILDESHEIM, A., SAFAEIAN, M., DAUNER, J. G., PAN, Y. J., PORRAS, C., SCHILLER, J. T., LOWY, D. R., HERRERO, R. & PINTO, L. A. 2011. HPV16/18 L1 VLP vaccine induces cross-neutralizing antibodies that may mediate cross-protection. *Vaccine,* 29**,** 2011-2014.

KEMP, T. J., SAFAEIAN, M., HILDESHEIM, A., PAN, Y., PENROSE, K. J., PORRAS, C., SCHILLER, J. T., LOWY, D. R., HERRERO, R. & PINTO, L. A. 2012. Kinetic and HPV infection effects on cross-type neutralizing antibody and avidity responses induced by Cervarix®. *Vaccine,* 31**,** 165-170.

KESSIS, T. D., CONNOLLY, D. C., HEDRICK, L. & CHO, K. R. 1996. Expression of HPV16 E6 or E7 increases integration of foreign DNA. *Oncogene,* 13**,** 427-431.

KHO, E.-Y., WANG, H.-K., BANERJEE, N. S., BROKER, T. R. & CHOW, L. T. 2013. HPV-18 E6 mutants reveal p53 modulation of viral DNA amplification in organotypic cultures. *Proceedings of the National Academy of Sciences of the United States of America,* 110**,** 7542-7549.

KIM, G. E., KIM, Y. B., CHO, N. H., CHUNG, H. C., PYO, H. R., LEE, J. D., PARK, T. K., KOOM, W. S., CHUN, M. & SUB, C. O. 2004. Synchronous coexpression of epidermal growth factor receptor and cyclooxygenase-2 in carcinomas of the uterine cervix: A potential predictor of poor survival. *Clinical Cancer Research,* 10**,** 1366-1374.

KIM, S. H., OH, J. M., NO, J. H., BANG, Y. J., JUHNN, Y. S. & SONG, Y. S. 2009. Involvement of NF-kappa B and AP-1 in COX-2 upregulation by human papillomavirus 16 E5 oncoprotein. *Carcinogenesis,* 30**,** 753-757.

KING, G., OATES, J., PATEL, D., VAN DEN BERG, H. A. & DIXON, A. M. 2011. Towards a structural understanding of the smallest known oncoprotein: Investigation of the bovine papillomavirus E5 protein using solution-state NMR. *Biochimica Et Biophysica Acta-Biomembranes,* 1808**,** 1493-1501.

KIVI, N., GRECO, D., AUVINEN, P. & AUVINEN, E. 2008. Genes involved in cell adhesion, cell motility and mitogenic signaling are altered due to HPV 16 E5 protein expression. *Oncogene,* 27**,** 2532-2541.

KIVIAT, N. B. 1999. Papillomaviruses in non-melanoma skin cancer: epidemiological aspects. *Seminars in Cancer Biology,* 9**,** 397-403.

KJAER, S. K., SIGURDSSON, K., IVERSEN, O.-E., HERNANDEZ-AVILA, M., WHEELER, C. M., PEREZ, G., BROWN, D. R., KOUTSKY, L. A., TAY, E. H., GARCIA, P., AULT, K. A., GARLAND, S. M., LEODOLTER, S., OLSSON, S.-E., TANG, G. W. K., FERRIS, D. G., PAAVONEN, J., LEHTINEN, M., STEBEN, M., XAVIER BOSCH, F., DILLNER, J., JOURA, E. A., MAJEWSKI, S., MUNOZ, N., MYERS, E. R., VILLA, L. L., TADDEO, F. J., ROBERTS, C., TADESSE, A., BRYAN, J., MAANSSON, R., LU, S., VUOCOLO, S., HESLEY, T. M., SAAH, A., BARR, E. & HAUPT, R. M. 2009. A Pooled Analysis of Continued Prophylactic Efficacy of Quadrivalent Human Papillomavirus (Types 6/11/16/18) Vaccine against High-grade Cervical and External Genital Lesions. *Cancer Prevention Research,* 2**,** 868-878.

KLEIN, O., KEGLER-EBO, D., SU, J., SMITH, S. & DIMAIO, D. 1999. The bovine papillomavirus E5 protein requires a juxtamembrane negative charge for activation of the platelet-derived growth factor beta receptor and transformation of C127 cells. *Journal of Virology,* 73**,** 3264-3272.

KLINGELHUTZ, A. J., FOSTER, S. A. & MCDOUGALL, J. K. 1996. Telomerase activation by the E6 gene product of human papillomavirus type 16. *Nature,* 380**,** 79-82.

KLUCEVSEK, K., WERTZ, M., LUCCHI, J., LESZCZYNSKI, A. & MOROIANU, J. 2007. Characterization of the nuclear localization signal of high risk HPV16 E2 protein. *Virology,* 360**,** 191-198.

KNAPP, A. A., MCMANUS, P. M., BOCKSTALL, K. & MOROIANU, J. 2009. Identification of the nuclear localization and export signals of high risk HPV16 E7 oncoprotein. *Virology,* 383**,** 60-68.

KNAPPE, M., BODEVIN, S., SELINKA, H.-C., SPILLMANN, D., STREECK, R. E., CHEN, X. S., LINDAHL, U. & SAPP, M. 2007. Surface-exposed Amino Acid Residues of HPV16 L1 Protein Mediating Interaction with Cell Surface Heparan Sulfate. *Journal of Biological Chemistry,* 282**,** 27913-27922.

KNIGHT, G. L., GRAINGER, J. R., GALLIMORE, P. H. & ROBERTS, S. 2004. Cooperation between Different Forms of the Human Papillomavirus Type 1 E4 Protein To Block Cell Cycle Progression and Cellular DNA Synthesis. *Journal of Virology,* 78**,** 13920-13933.

KNIGHT, G. L., TURNELL, A. S. & ROBERTS, S. 2006. Role for Wee1 in Inhibition of G2-to-M Transition through the Cooperation of Distinct Human Papillomavirus Type 1 E4 Proteins. *Journal of Virology,* 80**,** 7416-7426.

KRAWCZYK, E., HANOVER, J. A., SCHLEGEL, R. & SUPRYNOWICZ, F. A. 2008a. Karyopherin beta 3: A new cellular target for the HPV-16 E5 oncoprotein. *Biochemical and Biophysical Research Communications,* 371**,** 684-688.

KRAWCZYK, E., SUPRYNOWICZ, F. A., HEBERT, J. D., KAMONJOH, C. M. & SCHLEGEL, R. 2011. The Human Papillomavirus Type 16 E5 Oncoprotein Translocates Calpactin I to the Perinuclear Region. *Journal of Virology,* 85**,** 10968-10975.

KRAWCZYK, E., SUPRYNOWICZ, F. A., LIU, X., DAI, Y., HARTMANN, D. P., HANOVER, J. & SCHLEGEL, R. 2008b. Koilocytosis - A cooperative interaction between the human papillomavirus E5 and E6 oncoproteins. *American Journal of Pathology,* 173**,** 682-688.

KRAWCZYK, E., SUPRYNOWICZ, F. A., SUDARSHAN, S. R. & SCHLEGEL, R. 2010. Membrane Orientation of the Human Papillomavirus Type 16 E5 Oncoprotein. *Journal of Virology,* 84**,** 1696-1703.

KREIMER, A. R., CLIFFORD, G. M., BOYLE, P. & FRANCESCHI, S. 2005. Human Papillomavirus Types in Head and Neck Squamous Cell Carcinomas Worldwide: A Systematic Review. *Cancer Epidemiology Biomarkers & Prevention,* 14**,** 467-475.

KROGH, A., LARSSON, B., VON HEIJNE, G. & SONNHAMMER, E. L. L. 2001. Predicting transmembrane protein topology with a hidden Markov model: Application to complete genomes. *Journal of Molecular Biology,* 305**,** 567-580.

KRUSTRUP, D., JENSEN, H. L., VAN DEN BRULE, A. J. C. & FRISCH, M. 2009. Histological characteristics of human papilloma-virus-positive and -negative invasive and in situ squamous cell tumours of the penis. *International Journal of Experimental Pathology,* 90**,** 182-189.

KUBOTA, H., HYNES, G., CARNE, A., ASHWORTH, A. & WILLISON, K. 1994. Identification of six Tcp-1-related genes encoding divergent subunits of the TCP-1-containing chaperonin. *Current Biology,* 4**,** 89-99.

KÜHNLE, S., KOGEL, U., GLOCKZIN, S., MARQUARDT, A., CIECHANOVER, A., MATENTZOGLU, K. & SCHEFFNER, M. 2011. Physical and Functional Interaction of the HECT Ubiquitin-protein Ligases E6AP and HERC2. *Journal of Biological Chemistry,* 286**,** 19410-19416.

KUIJPERS, M., YU, K. L., TEULING, E., AKHMANOVA, A., JAARSMA, D. & HOOGENRAAD, C. C. 2013. The ALS8 protein VAPB interacts with the ER-Golgi recycling protein YIF1A and regulates membrane delivery into dendrites. *EMBO J,* 32**,** 2056-2072.

KURG, R., TEKKEL, H., ABROI, A. & USTAV, M. 2006. Characterization of the Functional Activities of the Bovine Papillomavirus Type 1 E2 Protein Single-Chain Heterodimers. *Journal of Virology,* 80**,** 11218-11225.

KURG, R., UUSEN, P., VÕSA, L. & USTAV, M. 2010. Human papillomavirus E2 protein with single activation domain initiates HPV18 genome replication, but is not sufficient for long-term maintenance of virus genome. *Virology,* 408**,** 159-166.

KYRITSIS, C., GORBULEV, S., HUTSCHENREITER, S., PAWLITSCHKO, K., ABELE, R. & TAMPE, R. 2001. Molecular mechanism and structural aspects of transporter associated with antigen processing inhibition by the cytomegalovirus protein US6. *Journal of Biological Chemistry,* 276**,** 48031-48039.

KYTE, J. & DOOLITTLE, R. F. 1982. A simple method for displaying the hydrophatic character of a protein *Journal of Molecular Biology,* 157**,** 105-132.

LACE, M. J., ANSON, J. R., KLUSSMANN, J. P., WANG, D. H., SMITH, E. M., HAUGEN, T. H. & TUREK, L. P. 2011. Human Papillomavirus Type 16 (HPV-16) Genomes Integrated in Head and Neck Cancers and in HPV-16-Immortalized Human Keratinocyte Clones Express Chimeric Virus-Cell mRNAs Similar to Those Found in Cervical Cancers. *Journal of Virology,* 85**,** 1645-1654.

LAI, C. C., EDWARDS, A. P. B. & DIMAIO, D. 2005. Productive interaction between transmembrane mutants of the bovine papillomavirus E5 protein and the platelet-derived growth factor beta receptor. *Journal of Virology,* 79**,** 1924-1929.

LAI, C. C., HENNINGSON, C. & DIMAIO, D. 1998. Bovine papillomavirus E5 protein induces oligomerization and trans-phosphorylation of the platelet-derived growth factor beta receptor. *Proceedings of the National Academy of Sciences of the United States of America,* 95**,** 15241-15246.

LAI, M.-C., TEH, B. H. & TARN, W.-Y. 1999. A Human Papillomavirus E2 Transcriptional Activator: the interactions with cellular splicing factors and potential function in pre-mRNA processing *Journal of Biological Chemistry,* 274**,** 11832-11841.

LANGER, J. D., ROTH, C. M., BÉTHUNE, J., STOOPS, E. H., BRÜGGER, B., HERTEN, D.-P. & WIELAND, F. T. 2008. A Conformational Change in the α-subunit of Coatomer Induced by Ligand Binding to γ-COP Revealed by Single-pair FRET. *Traffic,* 9**,** 597-607.

LAZAR, T., GOTTE, M. & GALLWITZ, D. 1997. Vesicular transport: how many Ypt/Rab-GTPases make a eukaryotic cell? *Trends in Biochemical Sciences,* 22**,** 468-472.

LAZARCZYK, M., CASSONNET, P., PONS, C., JACOB, Y. & FAVRE, M. 2009. The EVER Proteins as a Natural Barrier against Papillomaviruses: a New Insight into the Pathogenesis of Human Papillomavirus Infections. *Microbiology and Molecular Biology Reviews,* 73**,** 348-+.

LAZARCZYK, M. & FAVRE, M. 2008. Role of Zn(2+) Ions in Host-Virus Interactions. *Journal of Virology,* 82**,** 11486-11494.

LAZARCZYK, M., PONS, C., MENDOZA, J. A., CASSONNET, P., JACOB, Y. & FAVRE, M. 2008. Regulation of cellular zinc balance as a potential mechanism of EVER-mediated protection against pathogenesis by cutaneous oncogenic human papillomaviruses. *Journal of Experimental Medicine,* 205**,** 35-42.

LEE, D., HWANG, S. G., KIM, J. & CHOE, J. 2002. Functional interaction between p/CAF and human papillomavirus E2 protein. *Journal of Biological Chemistry,* 277**,** 6483-6489.

LEE, D., KIM, H., LEE, Y. & CHOE, J. 1997. Identification of sequence requirement for the origin of DNA replication in human papillomavirus type 18. *Virus Research,* 52**,** 97-108.

LEE, D., LEE, B., KIM, J., KIM, D. W. & CHOE, J. 2000. cAMP response element-binding protein-binding protein binds to human papillomavirus E2 protein and activates E2-dependent transcription. *Journal of Biological Chemistry,* 275**,** 7045-7051.

LEE, M. T. G., MISHRA, A. & LAMBRIGHT, D. G. 2009. Structural Mechanisms for Regulation of Membrane Traffic by Rab GTPases. *Traffic,* 10**,** 1377-1389.

LEECHANACHAI, P., BANKS, L., MOREAU, F. & MATLASHEWSKI, G. 1992. The E5 gene from human papillomavirus type-16 is an oncogene which enhances growth factor-mediated signal transduction to the nucleus *Oncogene,* 7**,** 19-25.

LEPTAK, C., CAJAL, S. R. Y., KULKE, R., HORWITZ, B. H., RIESE, D. J., DOTTO, G. P. & DIMAIO, D. 1991. Tumorigenic transformation of murine keratinocytes by the E5-genes of bovine papillomavirus type-16. *Journal of Virology,* 65**,** 7078-7083.

LEWIS, C., BARO, M. F., MARQUES, M., GRUENER, M., ALONSO, A. & BRAVO, I. G. 2008. The first hydrophobic region of the HPV16 E5 protein determines protein cellular location and facilitates anchorage-independent growth. *Virology Journal,* 5.

LI, H., OU, X., XIONG, J. & WANG, T. 2006. HPV16E7 mediates HADC chromatin repression and downregulation of MHC class I genes in HPV16 tumorigenic cells through interaction with an MHC class I promoter. *Biochemical and Biophysical Research Communications,* 349**,** 1315-1321.

LI, H., ZHAN, T. L., LI, C., LIU, M. G. & WANG, Q. K. 2009. Repression of MHC class I transcription by HPV16E7 through interaction with a putative RXR beta motif and NF-kappa B cytoplasmic sequestration. *Biochemical and Biophysical Research Communications,* 388**,** 383-388.

LI, N., FRANCESCHI, S., HOWELL-JONES, R., SNIJDERS, P. J. F. & CLIFFORD, G. M. 2011. Human papillomavirus type distribution in 30,848 invasive cervical cancers worldwide: Variation by geographical region, histological type and year of publication. *International Journal of Cancer,* 128**,** 927-935.

LIANG, Y.-J., CHANG, H.-S., WANG, C.-Y. & YU, W. C. Y. 2008. DYRK1A stabilizes HPV16E7 oncoprotein through phosphorylation of the threonine 5 and threonine 7 residues. *The International Journal of Biochemistry & Cell Biology,* 40**,** 2431-2441.

LIPARI, F., MCGIBBON, G. A., WARDROP, E. & CORDINGLEY, M. G. 2001. Purification and Biophysical Characterization of a Minimal Functional Domain and of an N-Terminal Zn2+-Binding Fragment from the Human Papillomavirus Type 16 E6 Protein†. *Biochemistry,* 40**,** 1196-1204.

LIU, D.-W., YANG, Y.-C., LIN, H.-F., LIN, M.-F., CHENG, Y.-W., CHU, C.-C., TSAO, Y.-P. & CHEN, S.-L. 2007. Cytotoxic T-Lymphocyte Responses to Human Papillomavirus Type 16 E5 and E7 Proteins and HLA-A*0201-Restricted T-Cell Peptides in Cervical Cancer Patients. *Journal of Virology,* 81**,** 2869-2879.

LIU, W. J., GAO, F. G., ZHAO, K. N., ZHAO, W. M., FERNANDO, G. J. G., THOMAS, R. & FRAZER, I. H. 2002. Codon modified human papillomavirus type 16 E7 DNA vaccine enhances cytotoxic T-lymphocyte induction and anti-tumour activity. *Virology,* 301**,** 43-52.

LIVAK, K. J. & SCHMITTGEN, T. D. 2001. Analysis of relative gene expression data using real-time quantitative PCR and the $2^{-\Delta\Delta CT}$ method. *Methods,* 25**,** 402-408.

LONGWORTH, M. S. & LAIMINS, L. A. 2004. Pathogenesis of human papillomaviruses in differentiating epithelia. *Microbiology and Molecular Biology Reviews,* 68**,** 362-+.

LORENZON, L., MAZZETTA, F., VENUTI, A., FREGA, A., TORRISI, M. R. & FRENCH, D. 2011. In vivo HPV 16 E5 mRNA: Expression pattern in patients with squamous intra-epithelial lesions of the cervix. *Journal of Clinical Virology,* 52**,** 79-83.

LOWY, D. R. & SCHILLER, J. T. 2012. Reducing HPV-Associated Cancer Globally. *Cancer Prevention Research,* 5**,** 18-23.

MAGLENNON, G. A., MCINTOSH, P. & DOORBAR, J. 2011. Persistence of viral DNA in the epithelial basal layer suggests a model for papillomavirus latency following immune regression. *Virology,* 414**,** 153-163.

MALCLES, M.-H., CUEILLE, N., MECHALI, F., COUX, O. & BONNE-ANDREA, C. 2002. Regulation of Bovine Papillomavirus Replicative Helicase E1 by the Ubiquitin-Proteasome Pathway. *Journal of Virology,* 76**,** 11350-11358.

MALLON, R. G., WOJCIECHOWICZ, D. & DEFENDI, V. 1987. DNA-binding activity of papillomavirus proteins. *Journal of Virology,* 61**,** 1655-1660.

MARCHETTI, B., ASHRAFI, G. H., DORNAN, E. S., ARAIBI, E. H., ELLIS, S. A. & CAMPO, M. S. 2005. The E5 protein of BPV-4 interacts with the heavy chain of MHC class I and irreversibly retains the MHC complex in the Golgi apparatus. *Oncogene,* 25**,** 2254-2263.

MARCHETTI, B., ASHRAFI, G. H., TSIRIMONAKI, E., O'BRIEN, P. M. & CAMPO, M. S. 2002. The bovine papillomavirus oncoprotein E5 retains MHC class I molecules in the Golgi apparatus and prevents their transport to the cell surface. *Oncogene,* 21**,** 7808-7816.

MARUR, S., D'SOUZA, G., WESTRA, W. H. & FORASTIERE, A. A. 2010. HPV-associated head and neck cancer: a virus-related cancer epidemic. *The lancet oncology,* 11**,** 781-789.

MASSIMI, P. & BANKS, L. 2000. Differential Phosphorylation of the HPV-16 E7 Oncoprotein during the Cell Cycle. *Virology,* 276**,** 388-394.

MATERN, H., YANG, X. P., ANDRULIS, E., STERNGLANZ, R., TREPTE, H. H. & GALLWITZ, D. 2000. A novel Golgi membrane protein is part of a GTPase-binding protein complex involved in vesicle targeting. *Embo Journal,* 19**,** 4485-4492.

MATHUR, S. P., MATHUR, R. S. & YOUNG, R. C. 2000. Cervical epidermal growth factor-receptor (EGF-R) and serum insulin-like growth factor II (IGF-II) levels are potential markers for cervical cancer. *American Journal of Reproductive Immunology,* 44**,** 222-230.

MAUFORT, J. P., SHAI, A., PITOT, H. C. & LAMBERT, P. F. 2010. A Role for HPV16 E5 in Cervical Carcinogenesis. *Cancer Research,* 70**,** 2924-2931.

MAUFORT, J. P., WILLIAMS, S. M. G., PITOT, H. C. & LAMBERT, P. F. 2007. Human papillomavirus 16 E5 oncogene contributes to two stages of skin cardnogenesis. *Cancer Research,* 67**,** 6106-6112.

MCBRIDE, A. A. 2013. The Papillomavirus E2 proteins. *Virology,* 445**,** 57-79.

MCBRIDE, A. A., BYRNE, J. C. & HOWLEY, P. M. 1989. E2 polypeptides encoded by bovine papillomavirus type 1 form dimers through the common carboxyl-terminal domain: transactivation is mediated by the conserved amino-terminal domain. *Proceedings of the National Academy of Sciences,* 86**,** 510-514.

MCBRIDE, A. A., OLIVEIRA, J. G. & MCPHILLIPS, M. G. 2006. Partitioning viral genomes in mitosis - Same idea, different targets. *Cell Cycle,* 5**,** 1499-1502.

MCINTOSH, P. B., MARTIN, S. R., JACKSON, D. J., KHAN, J., ISAACSON, E. R., CALDER, L., RAJ, K., GRIFFIN, H. M., WANG, Q., LASKEY, P., ECCLESTON, J. F. & DOORBAR, J. 2008. Structural analysis reveals an amyloid form of the human papillomavirus type 16 E1^E4 protein and provides a molecular basis for its accumulation. *Journal of Virology,* 82**,** 8196-8203.

MCLAUGHLIN-DRUBIN, M. E., BROMBERG-WHITE, J. L. & MEYERS, C. 2005. The role of the human papillomavirus type 18 E7 oncoprotein during the complete viral life cycle. *Virology,* 338**,** 61-68.

MCLAUGHLIN-DRUBIN, M. E., CHRISTENSEN, N. D. & MEYERS, C. 2004. Propagation, infection, and neutralization of authentic HPV16 virus. *Virology,* 322**,** 213-219.

MCLAUGHLIN-DRUBIN, M. E., HUH, K.-W. & MÜNGER, K. 2008. Human papillomavirus type 16 E7 oncoprotein associates with E2F6. *Journal of Virology,* 82**,** 8695-8705.

MCLAUGHLIN-DRUBIN, M. E. & MÜNGER, K. 2009. The human papillomavirus E7 oncoprotein. *Virology,* 384**,** 335-344.

MCLAUGHLIN-DRUBIN, M. E., WILSON, S., MULLIKIN, B., SUZICH, J. & MEYERS, C. 2003. Human papillomavirus type 45 propagation, infection, and neutralization. *Virology,* 312**,** 1-7.

MEHANNA, H., BEECH, T., NICHOLSON, T., EL-HARIRY, I., MCCONKEY, C., PALERI, V. & ROBERTS, S. 2013. Prevalence of human papillomavirus in oropharyngeal and nonoropharyngeal head and neck cancer—systematic review and meta-analysis of trends by time and region. *Head & Neck,* 35**,** 747-755.

MELSHEIMER, P., VINOKUROVA, S., WENTZENSEN, N., BASTERT, G. & DOEBERITZ, M. V. 2004. DNA aneuploidy and integration of human papillomavirus type 16 E6/E7 oncogenes in Intraepithelial neoplasia and invasive squamous cell carcinoma of the cervix uteri. *Clinical Cancer Research,* 10**,** 3059-3063.

MENDOZA-VILLANUEVA, D., DIAZ-CHAVEZ, J., URIBE-FIGUEROA, L., RANGEL-ESCAREAO, C., HIDALGO-MIRANDA, A., MARCH-MIFSUT, S., JIMENEZ-SANCHEZ, G., LAMBERT, P. F. & GARIGLIO, P. 2008. Gene expression profile of cervical and skin tissues from human papillomavirus type 16 E6 transgenic mice. *Bmc Cancer,* 8.

MESHER, D., SOLDAN, K., HOWELL-JONES, R., PANWAR, K., MANYENGA, P., JIT, M., BEDDOWS, S. & GILL, O. N. 2013. Reduction in HPV 16/18 prevalence in sexually active young women following the introduction of HPV immunisation in England. *Vaccine*.

MEYER, A. N., XU, Y. F., WEBSTER, M. K., SMITH, A. E. & DONOGHUE, D. J. 1994. Cellular-transformation by a transmembrane peptide - structural requirements for the bovine papillomavirus E5 oncoprotein *Proceedings of the National Academy of Sciences of the United States of America,* 91**,** 4634-4638.

MEYER, M. F., HUEBBERS, C. U., SIEFER, O. G., VENT, J., ENGBERT, I., ESLICK, G. D., VALTER, M., KLUSSMANN, J. P. & PREUSS, S. F. 2013. Prevalence and risk factors for oral human papillomavirus infection in 129 women screened for cervical HPV infection. *Oral Oncology*.

MEYERS, C., MAYER, T. J. & OZBUN, M. A. 1997. Synthesis of infectious human papillomavirus type 18 in differentiating epithelium transfected with viral DNA. *Journal of Virology,* 71**,** 7381-7386.

MEYERS, J. M., SPANGLE, J. M. & MÜNGER, K. 2013. The Human Papillomavirus Type 8 E6 Protein Interferes with NOTCH Activation during Keratinocyte Differentiation. *Journal of Virology,* 87**,** 4762-4767.

MGC, P. T. 2004. The Status, Quality, and Expansion of the NIH Full-Length cDNA Project: The Mammalian Gene Collection (MGC). *Genome Research,* 14**,** 2121-2127.

MI, H., MURUGANUJAN, A., CASAGRANDE, J. T. & THOMAS, P. D. 2013. Large-scale gene function analysis with the PANTHER classification system. *Nat. Protocols,* 8**,** 1551-1566.

MIDDLETON, K., PEH, W., SOUTHERN, S., GRIFFIN, H., SOTLAR, K., NAKAHARA, T., EL-SHERIF, A., MORRIS, L., SETH, R., HIBMA, M., JENKINS, D., LAMBERT, P., COLEMAN, N. & DOORBAR, J. 2003. Organization of human papillomavirus productive cycle during neoplastic progression provides a basis for selection of diagnostic markers. *Journal of Virology,* 77**,** 10186-10201.

MILEO, A. M., ABBRUZZESE, C., VICO, C., BELLACCHIO, E., MATARRESE, P., ASCIONE, B., FEDERICO, A., DELLA BIANCA, S., MATTAROCCI, S., MALORNI, W. & PAGGI, M. G. 2013. The human papillomavirus-16 E7 oncoprotein exerts antiapoptotic effects via its physical interaction with the actin-binding protein gelsolin. *Carcinogenesis,* 34**,** 2424-2433.

MILLIGAN, S. G., VEERAPRADITSIN, T., AHAMET, B., MOLE, S. & GRAHAM, S. V. 2007. Analysis of novel human papillomavirus type 16 late mRNAs in differentiated W12 cervical epithelial cells. *Virology,* 360**,** 172-181.

MIURA, S., KAWANA, K., SCHUST, D. J., FUJII, T., YOKOYAMA, T., IWASAWA, Y., NAGAMATSU, T., ADACHI, K., TOMIO, A., TOMIO, K., KOJIMA, S., YASUGI, T., KOZUMA, S. & TAKETANI, Y. 2010. CD1d, a Sentinel Molecule Bridging Innate and Adaptive Immunity, Is Downregulated by the Human Papillomavirus (HPV) E5 Protein: a Possible Mechanism for Immune Evasion by HPV. *Journal of Virology,* 84**,** 11614-11623.

MODIS, Y., TRUS, B. L. & HARRISON, S. C. 2002. Atomic model of the papillomavirus capsid. *EMBO J,* 21**,** 4754-4762.

MOLE, S., MILLIGAN, S. G. & GRAHAM, S. V. 2009. Human Papillomavirus Type 16 E2 Protein Transcriptionally Activates the Promoter of a Key Cellular Splicing Factor, SF2/ASF. *Journal of Virology,* 83**,** 357-367.

MOODY, C. A., FRADET-TURCOTTE, A., ARCHAMBAULT, J. & LAIMINS, L. A. 2007. Human papillomaviruses activate caspases upon epithelial differentiation to induce viral genome amplification. *Proceedings of the National Academy of Sciences,* 104**,** 19541-19546.

MORI, K., EMOTO, M. & INABA, M. 2011. Fetuin-A: a multifunctional protein. *Recent patents on endocrine, metabolic & immune drug discovery,* 5**,** 124-46.

MOSCICKI, A.-B., SCHIFFMAN, M., BURCHELL, A., ALBERO, G., GIULIANO, A. R., GOODMAN, M. T., KJAER, S. K. & PALEFSKY, J. 2012. Updating the Natural History of Human Papillomavirus and Anogenital Cancers. *Vaccine,* 30**,** F24-F33.

MÜLLER, C., YANG, R., BECK-VON-PECCOZ, L., IDOS, G., VERBEEK, W. & KOEFFLER, H. P. 1999. Cloning of the cyclin A1 genomic structure and characterization of the promoter region - GC boxes are essential for cell cycle-regulated transcription of the cyclin A1 gene. *Journal of Biological Chemistry,* 274**,** 11220-11228.

MULLIS, K., FALOONA, F., SCHARF, S., SAIKI, R., HORN, G. & ERLICH, H. 1986. Specific enzymatic amplification of DNA in vitro - the polymerase chain-reaction. *Cold Spring Harbor Symposia on Quantitative Biology,* 51**,** 263-273.

MÜNGER, K., WERNESS, B. A., DYSON, N., PHELPS, W. C., HARLOW, E. & HOWLEY, P. M. 1989. Complex-formation of human papillomavirus-E7 proteins with the retinoblastoma tumor suppressor gene-product *Embo Journal,* 8**,** 4099-4105.

MUTO, V., STELLACCI, E., LAMBERTI, A. G., PERROTTI, E., CARRABBA, A., MATERA, G., SGARBANTI, M., BATTISTINI, A., LIBERTO, M. C. & FOCA, A. 2011. Human Papillomavirus Type 16 E5 Protein Induces Expression of Beta Interferon through Interferon Regulatory Factor 1 in Human Keratinocytes. *Journal of Virology,* 85**,** 5070-5080.

NAKAHARA, T., PEH, W. L., DOORBAR, J., LEE, D. & LAMBERT, P. F. 2005. Human Papillomavirus Type 16 E1^E4 Contributes to Multiple Facets of the Papillomavirus Life Cycle. *Journal of Virology,* 79**,** 13150-13165.

NASIR, L. & CAMPO, M. S. 2008. Bovine papillomaviruses: their role in the aetiology of cutaneous tumours of bovids and equids. *Veterinary Dermatology,* 19**,** 243-254.

NATH, R., MANT, C. A., KELL, B., CASON, J. & BIBLE, J. M. 2006. Analyses of variant human papillomavirus type-16 E5 proteins for their ability to induce mitogenesis of murine fibroblasts. *Cancer Cell Int,* 6**,** 19.

NEES, M., GEOGHEGAN, J. M., HYMAN, T., FRANK, S., MILLER, L. & WOODWORTH, C. D. 2001. Papillomavirus type 16 oncogenes downregulate expression of interferon-responsive genes and upregulate proliferation-associated and NF-kappa B-responsive genes in cervical keratinocytes. *Journal of Virology,* 75**,** 4283-4296.

NELSON, L. M., ROSE, R. C. & MOROIANU, J. 2002. Nuclear Import Strategies of High Risk HPV16 L1 Major Capsid Protein. *Journal of Biological Chemistry,* 277**,** 23958-23964.

NICHOLLS, P. K., DOORBAR, J., MOORE, R. A., PEH, W., ANDERSON, D. M. & STANLEY, M. A. 2001. Detection of Viral DNA and E4 Protein in Basal Keratinocytes of Experimental Canine Oral Papillomavirus Lesions. *Virology,* 284**,** 82-98.

NILSON, L. A. & DIMAIO, D. 1993. Platelet-derived growth-factor receptor can mediate tumorigenic transformation by the bovine papillomavirus E5 protein *Molecular and Cellular Biology,* 13**,** 4137-4145.

NILSON, L. A., GOTTLIEB, R. L., POLACK, G. W. & DIMAIO, D. 1995. Mutational analysis of the interaction between the bovine papillomavirus E5 transforming protein and the endogenous β receptor for platelet-derived growth factor in mouse C127 cells. *Journal of Virology,* 69**,** 5869-5874.

NISHIO, M., TAJIMA, O., FURUKAWA, K., URANO, T. & FURUKAWA, K. 2005. Over-expression of GM1 enhances cell proliferation with epidermal growth factor without affecting the receptor localization in the microdomain in PC12 cells. *International Journal of Oncology,* 26**,** 191-199.

OATES, J., HICKS, M., DAFFORN, T. R., DIMAIO, D. & DIXON, A. M. 2008. In vitro dimerization of the bovine papillomavirus E5 protein transmembrane domain. *Biochemistry,* 47**,** 8985-8992.

OBALEK, S., JABLONSKA, S., FAVRE, M., WALCZAK, L. & ORTH, G. 1990. Condylomata acuminata in children - frequent association with human papillomavirus responsible for cutaneous warts *Journal of the American Academy of Dermatology,* 23**,** 205-213.

OELZE, I., KARTENBECK, J., CRUSIUS, K. & ALONSO, A. 1995. Human papillomavirus type-16 E5 protein affects cell-cell communication in an epithelial-cell line *Journal of Virology,* 69**,** 4489-4494.

OETKE, C., AUVINEN, E., PAWLITA, M. & ALONSO, A. 2000. Human papillomavirus type 16 E5 protein localizes to the Golgi apparatus but does not grossly affect cellular glycosylation. *Archives of Virology,* 145**,** 2183-2191.

OH, J.-M., KIM, S.-H., CHO, E.-A., SONG, Y.-S., KIM, W.-H. & JUHNN, Y.-S. 2010. Human papillomavirus type 16 E5 protein inhibits hydrogen peroxide-induced apoptosis by stimulating ubiquitin–proteasome-mediated degradation of Bax in human cervical cancer cells. *Carcinogenesis,* 31**,** 402-410.

OH, J.-M., KIM, S.-H., LEE, Y.-I., SEO, M., KIM, S.-Y., SONG, Y.-S., KIM, W.-H. & JUHNN, Y.-S. 2009. Human papillomavirus E5 protein induces expression of the EP4 subtype of prostaglandin E2 receptor in cyclic AMP response element-dependent pathways in cervical cancer cells. *Carcinogenesis,* 30**,** 141-149.

OH, M. J., CHOI, J. H., KIM, I. H., LEE, Y. H., HUH, J. Y., PARK, Y. K., LEE, K. W., CHOUGH, S. Y., JOE, P. S., KU, B. S. & SAW, H. S. 2000. Detection of epidermal growth factor receptor in the serum of patients with cervical carcinoma. *Clinical Cancer Research,* 6**,** 4760-4763.

OH, S. T., LONGWORTH, M. S. & LAIMINS, L. A. 2004. Roles of the E6 and E7 proteins in the life cycle of low-risk human papillomavirus type 11. *Journal of Virology,* 78**,** 2620-2626.

OHIRA, M., MOROHASHI, A., NAKAMURA, Y., ISOGAI, E., FURUYA, K., HAMANO, S., MACHIDA, T., AOYAMA, M., FUKUMURA, M., MIYAZAKI, K., SUZUKI, Y., SUGANO, S., HIRATO, J. & NAKAGAWARA, A. 2003. Neuroblastoma oligo-capping cDNA project: toward the understanding of the genesis and biology of neuroblastoma. *Cancer Letters,* 197**,** 63-68.

OLAHARSKI, A. J., SOTELO, R., SOLORZA-LUNA, G., GONSEBATT, M. E., GUZMAN, P., MOHAR, A. & EASTMOND, D. A. 2006. Tetraploidy and chromosomal instability are early events during cervical carcinogenesis. *Carcinogenesis,* 27**,** 337-343.

OLIVEIRA, J. G., COLF, L. A. & MCBRIDE, A. A. 2006. Variations in the association of papillomavirus E2 proteins with mitotic chromosomes. *Proceedings of the National Academy of Sciences of the United States of America,* 103**,** 1047-1052.

OPREA, G. E., KRÖBER, S., MCWHORTER, M. L., ROSSOLL, W., MÜLLER, S., KRAWCZAK, M., BASSELL, G. J., BEATTIE, C. E. & WIRTH, B. 2008. Plastin 3 Is a Protective Modifier of Autosomal Recessive Spinal Muscular Atrophy. *Science,* 320**,** 524-527.

ORTH, G. 2008. Host defenses against human papillomaviruses: Lessons from epidermodysplasia verruciformis. *Immunology, Phenotype First: How Mutations Have Established New Principles and Pathways in Immunology,* 321**,** 59-83.

OTA, T., SUZUKI, Y., NISHIKAWA, T., OTSUKI, T., SUGIYAMA, T., IRIE, R., WAKAMATSU, A., HAYASHI, K., SATO, H., NAGAI, K., KIMURA, K., MAKITA, H., SEKINE, M., OBAYASHI, M., NISHI, T., SHIBAHARA, T., TANAKA, T., ISHII, S., YAMAMOTO, J.-I., SAITO, K., KAWAI, Y., ISONO, Y., NAKAMURA, Y., NAGAHARI, K., MURAKAMI, K., YASUDA, T., IWAYANAGI, T., WAGATSUMA, M., SHIRATORI, A., SUDO, H., HOSOIRI, T., KAKU, Y., KODAIRA, H., KONDO, H., SUGAWARA, M., TAKAHASHI, M., KANDA, K., YOKOI, T., FURUYA, T., KIKKAWA, E., OMURA, Y., ABE, K., KAMIHARA, K., KATSUTA, N., SATO, K., TANIKAWA, M., YAMAZAKI, M., NINOMIYA, K., ISHIBASHI, T., YAMASHITA, H., MURAKAWA, K., FUJIMORI, K., TANAI, H., KIMATA, M., WATANABE, M., HIRAOKA, S., CHIBA, Y., ISHIDA, S., ONO, Y., TAKIGUCHI, S., WATANABE, S., YOSIDA, M., HOTUTA, T., KUSANO, J., KANEHORI, K., TAKAHASHI-FUJII, A., HARA, H., TANASE, T.-O., NOMURA, Y., TOGIYA, S., KOMAI, F., HARA, R., TAKEUCHI, K., ARITA, M., IMOSE, N., MUSASHINO, K., YUUKI, H., OSHIMA, A.,

SASAKI, N., AOTSUKA, S., YOSHIKAWA, Y., MATSUNAWA, H., ICHIHARA, T., SHIOHATA, N., SANO, S., MORIYA, S., MOMIYAMA, H., SATOH, N., TAKAMI, S., TERASHIMA, Y., SUZUKI, O., NAKAGAWA, S., SENOH, A., MIZOGUCHI, H., GOTO, Y., SHIMIZU, F., WAKEBE, H., HISHIGAKI, H., WATANABE, T., SUGIYAMA, A., et al. 2004. Complete sequencing and characterization of 21,243 full-length human cDNAs. *Nat Genet,* 36**,** 40-45.

OTTE, S., BELDEN, W. J., HEIDTMAN, M., LIU, J., JENSEN, O. N. & BARLOWE, C. 2001. Erv41p and Erv46p: New Components of Copii Vesicles Involved in Transport between the ER and Golgi Complex. *The Journal of Cell Biology,* 152**,** 503-518.

OUHOUMMANE, N., STEBEN, M., COUTLÉE, F., VUONG, T., FOREST, P., RODIER, C., LOUCHINI, R., DUARTE, E. & BRASSARD, P. 2013. Squamous anal cancer: Patient characteristics and HPV type distribution. *Cancer Epidemiology*.

OZBUN, M. A. & MEYERS, C. 1997. Characterization of late gene transcripts expressed during vegetative replication of human papillomavirus type 31b. *Journal of Virology,* 71**,** 5161-5172.

OZBUN, M. A. & MEYERS, C. 1998. Human Papillomavirus Type 31b E1 and E2 Transcript Expression Correlates with Vegetative Viral Genome Amplification. *Virology,* 248**,** 218-230.

PAAVONEN, J., NAUD, P., SALMERON, J., WHEELER, C. M., CHOW, S. N., APTER, D., KITCHENER, H., CASTELLSAGUE, X., TEIXEIRA, J. C., SKINNER, S. R., HEDRICK, J., JAISAMRARN, U., LIMSON, G., GARLAND, S., SZAREWSKI, A., ROMANOWSKI, B., AOKI, F. Y., SCHWARZ, T. F., POPPE, W. A. J., BOSCH, F. X., JENKINS, D., HARDT, K., ZAHAF, T., DESCAMPS, D., STRUYF, F., LEHTINEN, M., DUBIN, G. & GROUP, H. P. S. 2009. Efficacy of human papillomavirus (HPV)-16/18 AS04-adjuvanted vaccine against cervical infection and precancer caused by oncogenic HPV types (PATRICIA): final analysis of a double-blind, randomised study in young women. *Lancet,* 374**,** 301-14.

PARISH, J. L., BEAN, A. M., PARK, R. B. & ANDROPHY, E. J. 2006. ChIR1 is required for loading papillomavirus E2 onto mitotic chromosomes and viral genome maintenance. *Molecular Cell,* 24**,** 867-876.

PARK, P., COPELAND, W., YANG, L., WANG, T., BOTCHAN, M. R. & MOHR, I. J. 1994. The cellular DNA polymerase alpha-primase is required for papillomavirus DNA replication and associates with the viral E1 helicase. *Proceedings of the National Academy of Sciences,* 91**,** 8700-8704.

PATEL, V. J., THALASSINOS, K., SLADE, S. E., CONNOLLY, J. B., CROMBIE, A., MURRELL, J. C. & SCRIVENS, J. H. 2009. A Comparison of Labeling and Label-Free Mass Spectrometry-Based Proteomics Approaches. *Journal of Proteome Research,* 8**,** 3752-3759.

PATER, M. M. & PATER, A. 1985. Human papillomavirus type-16 and type-18 sequences in carcinoma cell-lines of the cervix *Virology,* 145**,** 313-318.

PEDROZA-SAAVEDRA, A., LAM, E. W. F., ESQUIVEL-GUADARRAMA, F. & GUTIERREZ-XICOTENCATL, L. 2010. The human papillomavirus type 16 E5 oncoprotein synergizes with EGF-receptor signaling to enhance cell cycle progression and the down-regulation of $p27^{Kip1}$. *Virology,* 400**,** 44-52.

PEH, W. L., BRANDSMA, J. L., CHRISTENSEN, N. D., CLADEL, N. M., WU, X. & DOORBAR, J. 2004. The viral E4 protein is required for the completion of the cottontail rabbit papillomavirus productive cycle in vivo. *Journal of Virology,* 78**,** 2142-2151.

PENNIE, W. D., GRINDLAY, G. J., CAIRNEY, M. & CAMPO, M. S. 1993. Analysis of the transforming functions of bovine papillomavirus type-4. *Virology,* 193**,** 614-620.

PENROSE, K. J., GARCIA-ALAI, M., DE PRAT-GAY, G. & MCBRIDE, A. A. 2004. Casein Kinase II Phosphorylation-induced Conformational Switch Triggers Degradation of the Papillomavirus E2 Protein. *Journal of Biological Chemistry,* 279**,** 22430-22439.

PERKINS, D. N., PAPPIN, D. J. C., CREASY, D. M. & COTTRELL, J. S. 1999. Probability-based protein identification by searching sequence databases using mass spectrometry data. *Electrophoresis,* 20**,** 3551-3567.

PETO, J., GILHAM, C., FLETCHER, O. & MATTHEWS, F. E. 2004. The cervical cancer epidemic that screening has prevented in the UK. *Lancet,* 364**,** 249-256.

PETT, M. & COLEMAN, N. 2007. Integration of high-risk human papillomavirus: a key event in cervical carcinogenesis? *Journal of Pathology,* 212**,** 356-367.

PETTI, L. & DIMAIO, D. 1994. Specififc interaction between the bovine papillomavirus E5 transforming protein and the beta-receptor for platelet-derived growth-factor receptor in stably transformed and acutely transfected cells *Journal of Virology,* 68**,** 3582-3592.

PETTI, L., NILSON, L. A. & DIMAIO, D. 1991. Activation of the platelet-derived growth-factor receptor by the bovine papillomavirus-E5 transforming protein *Embo Journal,* 10**,** 845-855.

PETTI, L. M. & RAY, F. A. 2000. Transformation of mortal human fibroblasts and activation of a growth inhibitory pathway by the bovine papillomavirus E5 oncoprotein. *Cell Growth & Differentiation,* 11**,** 395-408.

PFEFFER, S. & AIVAZIAN, D. 2004. Targeting Rab GTPases to distinct membrane compartments. *Nature Reviews Molecular Cell Biology,* 5**,** 886-896.

PFEFFER, S. R. 2013. Rab GTPase regulation of membrane identity. *Current Opinion in Cell Biology,* 25**,** 414-419.

PHELPS, W. C., YEE, C. L., MÜNGER, K. & HOWLEY, P. M. 1988. The human papillomavirus type 16 E7 gene encodes transactivation and transformation functions similar to those of adenovirus E1A. *Cell,* 53**,** 539-547.

PIETENPOL, J. A., STEIN, R. W., MORAN, E., YACIUK, P., SCHLEGEL, R., LYONS, R. M., PITTELKOW, M. R., MÜNGER, K., HOWLEY, P. M. & MOSES, H. L. 1990. TGF-beta-1 inhibition of c-myc transcription and growth in keratinocytes is abrogated by viral transforming proteins with pRB binding domains *Cell,* 61**,** 777-785.

PIGUET, V. 2005. Receptor modulation in viral replication: HIV, HSV, HHV-8 and HPV: Same goal, different techniques to interfere with MHC-I antigen presentation. *In:* MARSH, M. (ed.) *Membrane Trafficking in Viral Replication.*

PIM, D., COLLINS, M. & BANKS, L. 1992. Human papillomavirus type-16 E5 gene stimulates the transforming activity of the epidermal growth-factor receptor. *Oncogene,* 7**,** 27-32.

PIM, D., MASSIMI, P. & BANKS, L. 1997. Alternatively spliced HPV-18 E6* protein inhibits E6 mediated degradation of p53 and suppresses transformed cell growth. *Oncogene,* 15**,** 257-264.

POLJAK, M., CUZICK, J., KOCJAN, B. J., IFTNER, T., DILLNER, J. & ARBYN, M. 2012. Nucleic Acid Tests for the Detection of Alpha Human Papillomaviruses. *Vaccine,* 30**,** F100-F106.

PROST, S., LEDISCORDE, M., HADDAD, R., GLUCKMAN, J.-C., CANQUE, B. & KIRSZENBAUM, M. 2002. Characterization of a Novel Hematopoietic Marker Expressed from Early Embryonic Hematopoietic Stem Cells to Adult Mature Lineages. *Blood Cells, Molecules, and Diseases,* 29**,** 236-248.

PYEON, D., PEARCE, S. M., LANK, S. M., AHLQUIST, P. & LAMBERT, P. F. 2009a. Establishment of Human Papillomavirus Infection Requires Cell Cycle Progression. *PLoS Pathog,* 5**,** e1000318.

PYEON, D., PEARCE, S. M., LANK, S. M., AHLQUIST, P. & LAMBERT, P. F. 2009b. Establishment of Human Papillomavirus Infection Requires Cell Cycle Progression. *Plos Pathogens,* 5.

QUINLAN, E. J., CULLETON, S. P., WU, S.-Y., CHIANG, C.-M. & ANDROPHY, E. J. 2013. Acetylation of Conserved Lysines in Bovine Papillomavirus E2 by p300. *Journal of Virology,* 87**,** 1497-1507.

RAGIN, C. C. R. & TAIOLI, E. 2007. Survival of squamous cell carcinoma of the head and neck in relation to human papillomavirus infection: Review and meta-analysis. *International Journal of Cancer,* 121**,** 1813-1820.

RAMIREZ-SALAZAR, E., CENTENO, F., NIETO, K., VALENCIA-HERNANDEZ, A., SALCEDO, M. & GARRIDO, E. 2011. HPV16 E2 could act as down-regulator in cellular genes implicated in apoptosis, proliferation and cell differentiation. *Virology Journal,* 8.

RAMOZ, N., RUEDA, L. A., BOUADJAR, B., MONTOYA, L. S., ORTH, G. & FAVRE, M. 2002. Mutations in two adjacent novel genes are associated with epidermodysplasia verruciformis. *Nature Genetics,* 32**,** 579-581.

RAPPSILBER, J., MANN, M. & ISHIHAMA, Y. 2007. Protocol for micro-purification, enrichment, pre-fractionation and storage of peptides for proteomics using StageTips. *Nature Protocols,* 2**,** 1896-1906.

REGAN, J. A. & LAIMINS, L. A. 2008. Bap31 Is a Novel Target of the Human Papillomavirus E5 Protein. *Journal of Virology,* 82**,** 10042-10051.

REINSTEIN, E., SCHEFFNER, M., OREN, M., CIECHANOVER, A. & SCHWARTZ, A. 2000. Degradation of the E7 human papillomavirus oncoprotein by the ubiquitin-proteasome system: targeting via ubiquitination of the N-terminal residue. *Oncogene,* 19**,** 5944-5950.

RESHKIN, S. J., BELLIZZI, A., CALDEIRA, S., ALBARANI, V., MALANCHI, I., POIGNEE, M., ALUNNI-FABBRONI, M., CASAVOLA, V. & TOMMASINO, M. 2000. Na^+/H^+ exchanger-dependent intracellular alkalinization is an early event in malignant transformation and plays an essential role in the development of subsequent transformation-associated phenotypes. *Faseb Journal,* 14**,** 2185-2197.

RICHARDS, K. F., BIENKOWSKA-HABA, M., DASGUPTA, J., CHEN, X. S. & SAPP, M. 2013. Multiple Heparan Sulfate Binding Site Engagements Are Required for the Infectious Entry of Human Papillomavirus Type 16. *Journal of Virology,* 87**,** 11426-11437.

RICHARDS, R. M., LOWY, D. R., SCHILLER, J. T. & DAY, P. M. 2006. Cleavage of the papillomavirus minor capsid protein, L2, at a furin consensus site is necessary for infection. *Proceedings of the National Academy of Sciences of the United States of America,* 103**,** 1522-1527.

RILEY, R. R., DUENSING, S., BRAKE, T., MÜNGER, K., LAMBERT, P. F. & ARBEIT, J. M. 2003. Dissection of human papillomavirus E6 and E7 function in transgenic mouse models of cervical carcinogenesis. *Cancer Research,* 63**,** 4862-4871.

RITZ, U., MOMBURG, F., PILCH, H., HUBER, C., MAEURER, M. J. & SELIGER, B. 2001. Deficient expression of components of the MHC class I antigen processing machinery in human cervical carcinoma. *International Journal of Oncology,* 19**,** 1211-1220.

ROBERTS, S., ASHMOLE, I., ROOKES, S. M. & GALLIMORE, P. H. 1997. Mutational analysis of the human papillomavirus type 16 E1 E4 protein shows that the C-terminus is dispensable for keratin cytoskeleton association but is involved in inducing disruption of the keratin filaments. *Journal of Virology,* 71**,** 3554-3562.

RODRIGUEZ, C. A., SCHIFFMAN, M., HERRERO, R., HILDESHEIM, A., BRATTI, C., SHERMAN, M. E., SOLOMON, D., GUILLEN, D., ALFARO, M., MORALES, J., HUTCHINSON, M., KATKI, H., CHEUNG, L., WACHOLDER, S. & BURK, R. D. 2010. Longitudinal Study of Human Papillomavirus Persistence and Cervical Intraepithelial Neoplasia Grade 2/3: Critical Role of Duration of Infection. *Journal of the National Cancer Institute,* 102**,** 315-324.

RODRIGUEZ, M. I., FINBOW, M. E. & ALONSO, A. 2000. Binding of human papillomavirus 16 E5 to the 16 kDa subunit c (proteolipid) of the vacuolar H^+-ATPase can be dissociated from the E5-mediated epidermal growth factor receptor overactivation. *Oncogene,* 19**,** 3727-3732.

ROMAN, A. & MÜNGER, K. 2013. The papillomavirus E7 proteins. *Virology,* 445**,** 138-168.

ROMBALDI, R. L., SERAFINI, E. P., MANDELLI, J., ZIMMERMANN, E. & LOSQUIAVO, K. P. 2008. Transplacental transmission of Human Papillomavirus. *Virology Journal,* 5.

ROMBALDI, R. L., SERAFINI, E. P., MANDELLI, J., ZIMMERMANN, E. & LOSQUIAVO, K. P. 2009. Perinatal transmission of human papilomavirus DNA. *Virology Journal,* 6**,** 83-83.

RONCO, L. V., KARPOVA, A. Y., VIDAL, M. & HOWLEY, P. M. 1998. Human papillomavirus 16 E6 oncoprotein binds to interferon regulatory factor-3 and inhibits its transcriptional activity. *Genes & Development,* 12**,** 2061-2072.

ROPERTO, S., BORZACCHIELLO, G., BRUN, R., LEONARDI, L., MAIOLINO, P., MARTANO, M., PACIELLO, O., PAPPARELLA, S., RESTUCCI, B., RUSSO, V., SALVATORE, G., URRARO, C. & ROPERTO, F. 2010. A Review of Bovine Urothelial Tumours and Tumour-Like Lesions of the Urinary Bladder. *Journal of Comparative Pathology,* 142**,** 95-108.

ROZENBLATT-ROSEN, O., DEO, R. C., PADI, M., ADELMANT, G., CALDERWOOD, M. A., ROLLAND, T., GRACE, M., DRICOT, A., ASKENAZI, M., TAVARES, M., PEVZNER, S. J., ABDERAZZAQ, F., BYRDSONG, D., CARVUNIS, A.-R., CHEN, A. A., CHENG, J., CORRELL, M., DUARTE, M., FAN, C., FELTKAMP, M. C., FICARRO, S. B., FRANCHI, R., GARG, B. K., GULBAHCE, N., HAO, T., HOLTHAUS, A. M., JAMES, R., KORKHIN, A., LITOVCHICK, L., MAR, J. C., PAK, T. R., RABELLO, S., RUBIO, R., SHEN, Y., SINGH, S., SPANGLE, J. M., TASAN, M., WANAMAKER, S., WEBBER, J. T., ROECKLEIN-CANFIELD, J., JOHANNSEN, E., BARABASI, A.-L., BEROUKHIM, R., KIEFF, E., CUSICK, M. E., HILL, D. E., MÜNGER, K., MARTO, J. A., QUACKENBUSH, J., ROTH, F. P., DECAPRIO, J. A. & VIDAL, M. 2012. Interpreting cancer genomes using systematic host network perturbations by tumour virus proteins. *Nature,* 487**,** 491-495.

RUESCH, M. N., STUBENRAUCH, F. & LAIMINS, L. A. 1998. Activation of papillomavirus late gene transcription and genome amplification upon differentiation in semisolid medium is coincident with expression of involucrin and transglutamine but not keratin-10. *Journal of Virology,* 72**,** 5016-5024.

RUMBOLD, A. R., TAN, S. E., CONDON, J. R., TAYLOR-THOMSON, D., NICKELS, M., TABRIZI, S. N., DAVY, M. L. J., O'BRIEN, M. M., CONNORS, C. M., ZARDAWI, I., STANKOVICH, J. & GARLAND, S. M. 2012. Investigating a cluster of vulvar cancer in young women: a cross-sectional study of genital human papillomavirus prevalence. *Bmc Infectious Diseases,* 12.

SAFAEIAN, M., PORRAS, C., SCHIFFMAN, M., RODRIGUEZ, A. C., WACHOLDER, S., GONZALEZ, P., QUINT, W., VAN DOORN, L.-J., SHERMAN, M. E., XHENSEVAL, V., HERRERO, R., HILDESHEIM, A. & COSTA RICAN VACCINE TRIAL, G. 2010. Epidemiological Study of Anti-HPV16/18 Seropositivity and Subsequent Risk of HPV16 and -18 Infections. *Journal of the National Cancer Institute,* 102**,** 1653-1662.

SAHAB, Z., SUDARSHAN, S. R., LIU, X., ZHANG, Y., KIRILYUK, A., KAMONJOH, C. M., SIMIC, V., DAI, Y., BYERS, S. W., DOORBAR, J., SUPRYNOWICZ, F. A. & SCHLEGEL, R. 2012. Quantitative Measurement of Human Papillomavirus Type 16 E5 Oncoprotein Levels in Epithelial Cell Lines by Mass Spectrometry. *Journal of Virology,* 86**,** 9465-9473.

SAMBROOK, J. & RUSSELL, D. W. 2006. The Inoue Method for Preparation and Transformation of Competent E. Coli: "Ultra-Competent" Cells. *CSH protocols,* 2006.

SANDERS, C. M. & STENLUND, A. 2001. Mechanism and Requirements for Bovine Papillomavirus, Type 1, E1 Initiator Complex Assembly Promoted by the E2 Transcription Factor Bound to Distal Sites. *Journal of Biological Chemistry,* 276**,** 23689-23699.

SCHÄFER, F., FLORIN, L. & SAPP, M. 2002. DNA Binding of L1 Is Required for Human Papillomavirus Morphogenesis in Vivo. *Virology,* 295**,** 172-181.

SCHAPIRO, F., SPARKOWSKI, J., ADDUCI, A., SUPRYNOWICZ, F., SCHLEGEL, R. & GRINSTEIN, S. 2000. Golgi alkalinization by the papillomavirus E5 oncoprotein. *Journal of Cell Biology,* 148**,** 305-315.

SCHEFFER, K. D., GAWLITZA, A., SPODEN, G. A., ZHANG, X. A., LAMBERT, C., BERDITCHEVSKI, F. & FLORIN, L. 2013. Tetraspanin CD151 Mediates Papillomavirus Type 16 Endocytosis. *Journal of Virology,* 87**,** 3435-3446.

SCHEFFNER, M., HUIBREGTSE, J. M., VIERSTRA, R. D. & HOWLEY, P. M. 1993. The HPV-16 E6 and E6-AP complex functions as a ubiquitin-protein ligase in the ubiquitination of p53. *Cell,* 75**,** 495-505.

SCHELHAAS, M., SHAH, B., HOLZER, M., BLATTMANN, P., KUEHLING, L., DAY, P. M., SCHILLER, J. T. & HELENIUS, A. 2012. Entry of Human Papillomavirus Type 16 by Actin-Dependent, Clathrin- and Lipid Raft-Independent Endocytosis. *Plos Pathogens,* 8.

SCHILLER, J. T., CASTELLSAGUE, X. & GARLAND, S. M. 2012. A Review of Clinical Trials of Human Papillomavirus Prophylactic Vaccines. *Vaccine,* 30**,** F123-F138.

SCHILLER, J. T., DAY, P. M. & KINES, R. C. 2010. Current understanding of the mechanism of HPV infection. *Gynecologic Oncology,* 118**,** S12-7.

SCHILLER, J. T., VASS, W. C., VOUSDEN, K. H. & LOWY, D. R. 1986. E5 open reading frame of bovine papillomavirus type-1 encodes a transforming gene *Journal of Virology,* 57**,** 1-6.

SCHLEGEL, R., WADEGLASS, M., RABSON, M. S. & YANG, Y. C. 1986. The E5 transforming gene of bovine papillomavirus encodes a small, hydrophobic polypeptide *Science,* 233**,** 464-467.

SCHMITT, M. & PAWLITA, M. 2011. The HPV transcriptome in HPV16 positive cell lines. *Molecular and Cellular Probes,* 25**,** 108-113.

SCHNEIDER, M. A., SCHEFFER, K. D., BUND, T., BOUKHALLOUK, F., LAMBERT, C., COTARELO, C., PFLUGFELDER, G. O., FLORIN, L. & SPODEN, G. A. 2013. The Transcription Factors TBX2 and TBX3 Interact with Human Papillomavirus 16 (HPV16) L2 and Repress the Long Control Region of HPVs. *Journal of Virology,* 87**,** 4461-4474.

SCHOELL, W. M. J., MIRHASHEMI, R., LIU, B., JANICEK, M. F., PODACK, E. R., PENALVER, M. A. & AVERETTE, H. E. 1999. Generation of Tumor-Specific Cytotoxic T Lymphocytes by Stimulation with HPV Type 16 E7 Peptide-Pulsed Dendritic Cells: An Approach to Immunotherapy of Cervical Cancer. *Gynecologic Oncology,* 74**,** 448-455.

SCHREVEL, M., GORTER, A., KOLKMAN-ULJEE, S. M., TRIMBOS, J., FLEUREN, G. J. & JORDANOVA, E. S. 2011. Molecular mechanisms of epidermal growth factor receptor overexpression in patients with cervical cancer. *Modern Pathology,* 24**,** 720-728.

SCHUCK, S., RUSE, C. & STENLUND, A. 2013. CK2 Phosphorylation Inactivates DNA Binding by the Papillomavirus E1 and E2 Proteins. *Journal of Virology,* 87**,** 7668-7679.

SCHUCK, S. & STENLUND, A. 2005. Assembly of a Double Hexameric Helicase. *Molecular Cell,* 20**,** 377-389.

SCHUCK, S. & STENLUND, A. 2011. Mechanistic Analysis of Local Ori Melting and Helicase Assembly by the Papillomavirus E1 Protein. *Molecular Cell,* 43**,** 776-787.

SCHUST, D. J., TORTORELLA, D., SEEBACH, J., PHAN, C. & PLOEGH, H. L. 1998. Trophoblast class I major histocompatibility complex (MHC) products are resistant to rapid degradation imposed by the human cytomegalovirus (HCMV) gene products US2 and US11. *Journal of Experimental Medicine,* 188**,** 497-503.

SCHWARTZ, S. 2013. Papillomavirus transcripts and posttranscriptional regulation. *Virology,* 445**,** 187-196.

SCHWARZ, E., FREESE, U. K., GISSMANN, L., MAYER, W., ROGGENBUCK, B., STREMLAU, A. & HAUSEN, H. Z. 1985. Structure and transcription of human papillomavirus sequences in cervical-carcinoma cells *Nature,* 314**,** 111-114.

SEDMAN, J. & STENLUND, A. 1996. The initiator protein E1 binds to the bovine papillomavirus origin of replication as a trimeric ring-like structure. *Embo Journal,* 15**,** 5085-5092.

SEIWERT, T. 2013. Accurate HPV testing: a requirement for precision medicine for head and neck cancer. *Annals of Oncology,* 24**,** 2711-2713.

SEKHAR, V. & MCBRIDE, A. A. 2012. Phosphorylation Regulates Binding of the Human Papillomavirus Type 8 E2 Protein to Host Chromosomes. *Journal of Virology,* 86**,** 10047-10058.

SHAFTI-KERAMAT, S., SCHELLENBACHER, C., HANDISURYA, A., CHRISTENSEN, N., REININGER, B., BRANDT, S. & KIRNBAUER, R. 2009. Bovine papillomavirus type 1 (BPV1) and BPV2 are closely related serotypes. *Virology,* 393**,** 1-6.

SHAH, S. D., DOORBAR, J. & GOLDSTEIN, R. A. 2010. Analysis of Host-Parasite Incongruence in Papillomavirus Evolution Using Importance Sampling. *Molecular Biology and Evolution,* 27**,** 1301-1314.

SHAI, A., NGUYEN, M. L., WAGSTAFF, J., JIANG, Y. H. & LAMBERT, P. F. 2007. HPV16 E6 confers p53-dependent and p53-independent phenotypes in the epidermis of mice deficient for E6AP. *Oncogene,* 26**,** 3321-3328.

SHAKOORI, A., FUJII, G., YOSHIMURA, S., KITAMURA, M., NAKAYAMA, K., ITO, T., OHNO, H. & NAKAMURA, N. 2003. Identification of a five-pass transmembrane protein family localizing in the Golgi apparatus and the ER. *Biochemical and Biophysical Research Communications,* 312**,** 850-857.

SHOPE, R. E. & HURST, E. W. 1933. Infectious papillomatosis of rabbits: with a note on the histopathology *The Journal of Experimental Medicine,* 58**,** 607-624.

SILVA, M. A., ALTAMURA, G., CORTEGGIO, A., ROPERTO, F., BOCANETI, F., VELESCU, E., FREITAS, A. C., CARVALHO, C. C. R., CAVALCANTI, K. P. S. & BORZACCHIELLO, G. 2013. Expression of connexin 26 and bovine papillomavirus E5 in cutaneous fibropapillomas of cattle. *The Veterinary Journal,* 195**,** 337-343.

SILVERBERG, M. J., THORSEN, P., LINDEBERG, H., GRANT, L. A. & SHAH, K. V. 2003. Condyloma in pregnancy is strongly predictive of juvenile-onset recurrent respiratory papillomatosis. *Obstetrics and Gynecology,* 101**,** 645-652.

SILVESTRE, O., BORZACCHIELLO, G., NAVA, D., IOVANE, G., RUSSO, V., VECCHIO, D., D'AUSILIO, F., GAULT, E. A., CAMPO, M. S. & PACIELLO, O. 2009. Bovine Papillomavirus Type 1 DNA and E5 Oncoprotein Expression in Water Buffalo Fibropapillomas. *Veterinary Pathology Online,* 46**,** 636-641.

SIMPSON, J. C., WELLENREUTHER, R., POUSTKA, A., PEPPERKOK, R. & WIEMANN, S. 2000. Systematic subcellular localization of novel proteins identified by large-scale cDNA sequencing. *EMBO Rep,* 1**,** 287-292.

SINGLETON, M. R., DILLINGHAM, M. S. & WIGLEY, D. B. 2007. Structure and Mechanism of Helicases and Nucleic Acid Translocases. *Annual Review of Biochemistry,* 76**,** 23-50.

SIVARS, U., AIVAZIAN, D. & PFEFFER, S. R. 2003. Yip3 catalyses the dissociation of endosomal Rab-GDI complexes. *Nature,* 425**,** 856-859.

SMITH, E. M., RITCHIE, J. M., PAWLITA, M., RUBENSTEIN, L. M., HAUGEN, T. H., TUREK, L. P. & HAMSIKOVA, E. 2007. Human papillomavirus seropositivity and risks of head and neck cancer. *International Journal of Cancer,* 120**,** 825-832.

SMITH, J. L., CAMPOS, S. K., WANDINGER-NESS, A. & OZBUN, M. A. 2008. Caveolin-1-dependent infectious entry of human papillomavirus type 31 in human keratinocytes

proceeds to the endosomal pathway for pH-dependent uncoating. *Journal of Virology,* 82**,** 9505-9512.

SMOTKIN, D. & WETTSTEIN, F. O. 1986. Transcription of human papillomavirus type-16 early genes in a cervical-cancer and a cancer-derived cell-line and identification of the E7-protein *Proceedings of the National Academy of Sciences of the United States of America,* 83**,** 4680-4684.

SMOTKIN, D. & WETTSTEIN, F. O. 1987. The major human papillomavirus protein in cervical cancers is a cytoplasmic phosphoprotein *Journal of Virology,* 61**,** 1686-1689.

STAEBLER, A., PIERCE, J. H., BRAZINSKI, S., HEIDARAN, M. A., LI, W. Q., SCHLEGEL, R. & GOLDSTEIN, D. J. 1995. Mutational analysis of the beta-type platelet-derived growth-factor receptor defines the site of interaction with the bovine papillomavirus type-1 E5 transforming protein. *Journal of Virology,* 69**,** 6507-6517.

STANLEY, M. 2006. Immune responses to human papillomavirus. *Vaccine,* 24**,** 16-22.

STANLEY, M. 2010. Pathology and epidemiology of HPV infection in females. *Gynecologic Oncology,* 117**,** S5-S10.

STANLEY, M. A. 1994. Replication of human papillomaviruses in cell-culture. *Antiviral Research,* 24**,** 1-15.

STANLEY, M. A. 2012. Epithelial Cell Responses to Infection with Human Papillomavirus. *Clinical Microbiology Reviews,* 25**,** 215-222.

STENLUND, A. 2003. E1 initiator DNA binding specificity is unmasked by selective inhibition of non-specific DNA binding. *EMBO J,* 22**,** 954-963.

STERLING, J. C. 2005. Human papillomaviruses and skin cancer. *Journal of Clinical Virology,* 32**,** S67-S71.

STERLING, J. C., HANDFIELD-JONES, S. & HUDSON, P. M. 2001. Guidelines for the management of cutaneous warts. *British Journal of Dermatology,* 144**,** 4-11.

STERLING, J. C., SKEPPER, J. N. & STANLEY, M. A. 1993. Immunoelectron microscopic localization of human papilomavirus type-16 L1-proteins and E4-proteins in cervical keratinocytes cultured *in vivo*. *Journal of Investigative Dermatology,* 100**,** 154-158.

STERN, P. L., VAN DER BURG, S. H., HAMPSON, I. N., BROKER, T. R., FIANDER, A., LACEY, C. J., KITCHENER, H. C. & EINSTEIN, M. H. 2012. Therapy of Human Papillomavirus-Related Disease. *Vaccine,* 30**,** F71-F82.

STOLER, M. H., RHODES, C. R., WHITBECK, A., WOLINSKY, S. M., CHOW, L. T. & BROKER, T. R. 1992. Human papillomavirus type-16 and type-18 gene expression in cervical neoplasia. *Human Pathology,* 23**,** 117-128.

STOLLE, K., SCHNOOR, M., FUELLEN, G., SPITZER, M., ENGEL, T., SPENER, F., CULLEN, P. & LORKOWSKI, S. 2005. Cloning, cellular localization, genomic organization, and tissue-specific expression of the TGFβ1-inducible SMAP-5 gene. *Gene,* 351**,** 119-130.

STÖPPLER, M. C., STRAIGHT, S. W., TSAO, G., SCHLEGEL, R. & MCCANCE, D. J. 1996. The E5 Gene of HPV-16 Enhances Keratinocyte Immortalization by Full-Length DNA. *Virology,* 223**,** 251-254.

STRAIGHT, S. W., HERMAN, B. & MCCANCE, D. J. 1995. The E5 oncoprotein of human papillomavirus type-16 inhibits the acidification of endosomes in human keratinocytes. *Journal of Virology,* 69**,** 3185-3192.

STRAIGHT, S. W., HINKLE, P. M., JEWERS, R. J. & MCCANCE, D. J. 1993. The E5 oncoprotein of human papillomavirus type-16 transforms fibroblasts and effects the down-regulation of the epidermal growth-factor receptor in keratinocytes. *Journal of Virology,* 67**,** 4521-4532.

STRAUSS, M. J., SHAW, E. W., BUNTING, H. & MELNICK, J. L. 1949. Crystalline virus-like particles from skin papillomas characterized by intranuclear inclusion bodies *Proceedings of the Society for Experimental Biology and Medicine,* 72**,** 46-50.

STUBENRAUCH, F., HUMMEL, M., IFTNER, T. & LAIMINS, L. A. 2000. The E8^E2C Protein, a Negative Regulator of Viral Transcription and Replication, Is Required for Extrachromosomal Maintenance of Human Papillomavirus Type 31 in Keratinocytes. *Journal of Virology,* 74**,** 1178-1186.

STUBENRAUCH, F., STRAUB, E., FERTEY, J. & IFTNER, T. 2007. The E8 repression domain can replace the E2 transactivation domain for growth inhibition of HeLa cells by papillomavirus E2 proteins. *International Journal of Cancer,* 121**,** 2284-2292.

STUBENRAUCH, F., ZOBEL, T. & IFTNER, T. 2001. The E8 domain confers a novel long-distance transcriptional repression activity on the E8-over-cap-E2C protein of high-risk human papillomavirus type 31. *Journal of Virology,* 75**,** 4139-4149.

SUBBARAMAIAH, K. & DANNENBERG, A. J. 2007. Cyclooxygenase-2 transcription is regulated by human papillomavirus 16 E6 and E7 oncoproteins: Evidence of a corepressor/coactivator exchange. *Cancer Research,* 67**,** 3976-3985.

SUDARSHAN, S. R., SCHLEGEL, R. & LIU, X. F. 2010. The HPV-16 E5 protein represses expression of stress pathway genes XBP-1 and COX-2 in genital keratinocytes. *Biochemical and Biophysical Research Communications,* 399**,** 617-622.

SUN, Y.-N., LU, J. Z. J. & MCCANCE, D. J. 1996. Mapping of HPV-11 E1 Binding Site and Determination of Other Important cis Elements for Replication of the Origin. *Virology,* 216**,** 219-222.

SUPRYNOWICZ, F. A., BAEGE, A., SUNITHA, I. & SCHLEGEL, R. 2002. c-Src Activation by the E5 oncoprotein enables transformation independently of PDGF receptor activation. *Oncogene,* 21**,** 1695-1706.

SUPRYNOWICZ, F. A., DISBROW, G. L., KRAWCZYK, E., SIMIC, V., LANTZKY, K. & SCHLEGEL, R. 2008. HPV-16 E5 oncoprotein upregulates lipid raft components caveolin-1 and ganglioside GM1 at the plasma membrane of cervical cells. *Oncogene,* 27**,** 1071-1078.

SUPRYNOWICZ, F. A., KRAWCZYK, E., HEBERT, J. D., SUDARSHAN, S. R., SIMIC, V., KAMONJOH, C. M. & SCHLEGEL, R. 2010. The Human Papillomavirus Type 16 E5 Oncoprotein Inhibits Epidermal Growth Factor Trafficking Independently of Endosome Acidification. *Journal of Virology,* 84**,** 10619-10629.

SURTI, T., KLEIN, O., ASCHHEIM, K., DIMAIO, D. & SMITH, S. O. 1998. Structural models of the bovine papillomavirus E5 protein. *Proteins-Structure Function and Genetics,* 33**,** 601-612.

TAN, C. L., GUNARATNE, J., LAI, D., CARTHAGENA, L., WANG, Q., XUE, Y. Z., QUEK, L. S., DOORBAR, J., BACHELERIE, F., THIERRY, F. & BELLANGER, S. 2012a. HPV-18 E2^E4 chimera: 2 new spliced transcripts and proteins induced by keratinocyte differentiation. *Virology,* 429**,** 47-56.

TAN, M. J. A., WHITE, E. A., SOWA, M. E., HARPER, J. W., ASTER, J. C. & HOWLEY, P. M. 2012b. Cutaneous beta-human papillomavirus E6 proteins bind Mastermind-like coactivators and repress Notch signaling. *Proceedings of the National Academy of Sciences of the United States of America,* 109**,** E1473-E1480.

TANG, B. L., ONG, Y. S., HUANG, B., WEI, S., WONG, E. T., QI, R., HORSTMANN, H. & HONG, W. 2001. A Membrane Protein Enriched in Endoplasmic Reticulum Exit Sites Interacts with COPII. *Journal of Biological Chemistry,* 276**,** 40008-40017.

TANIMOTO, K., SUZUKI, K., JOKITALO, E., SAKAI, N., SAKAGUCHI, T., TAMURA, D., FUJII, G., AOKI, K., TAKADA, S., ISHIDA, R., TANABE, M., ITOH, H., YONEDA, Y., SOHDA, M., MISUMI, Y. & NAKAMURA, N. 2011. Characterization of YIPF3 and YIPF4, cis-Golgi Localizing Yip Domain Family Proteins. *Cell Structure and Function,* 36**,** 171-185.

TEN HAVE, S., BOULON, S., AHMAD, Y. & LAMOND, A. I. 2011. Mass spectrometry-based immuno-precipitation proteomics - The user's guide. *Proteomics,* 11**,** 1153-1159.

TERADA, K. & MORI, M. 2000. Human DnaJ homologs dj2 and dj3, and bag-1 are positive cochaperones of hsc70. *The Journal of biological chemistry,* 275**,** 24728-24734.

THIERRY, F. 2009. Transcriptional regulation of the papillomavirus oncogenes by cellular and viral transcription factors in cervical carcinoma. *Virology,* 384**,** 375-379.

THOMAS, J. T., HUBERT, W. G., RUESCH, M. N. & LAIMINS, L. A. 1999. Human papillomavirus type 31 oncoproteins E6 and E7 are required for the maintenance of episomes during the viral life cycle in normal human keratinocytes. *Proceedings of the National Academy of Sciences of the United States of America,* 96**,** 8449-8454.

THOMAS, M. & BANKS, L. 1999. Human papillomavirus (HPV) E6 interactions with Bak are conserved amongst E6 proteins from high and low risk HPV types. *Journal of General Virology,* 80**,** 1513-7.

THOMAS, M., MASSIMI, P., NAVARRO, C., BORG, J.-P. & BANKS, L. 2005. The hScrib//Dlg apico-basal control complex is differentially targeted by HPV-16 and HPV-18 E6 proteins. *Oncogene,* 24**,** 6222-6230.

THOMAS, M. C. & CHIANG, C.-M. 2005. E6 Oncoprotein Represses p53-Dependent Gene Activation via Inhibition of Protein Acetylation Independently of Inducing p53 Degradation. *Molecular Cell,* 17**,** 251-264.

THOMSEN, P., VAN DEURS, B., NORRILD, B. & KAYSER, L. 2000. The HPV16 E5 oncogene inhibits endocytic trafficking. *Oncogene,* 19**,** 6023-6032.

THORLAND, E. C., MYERS, S. L., GOSTOUT, B. S. & SMITH, D. I. 2003. Common fragile sites are preferential targets for HPV16 integrations in cervical tumors. *Oncogene,* 22**,** 1225-1237.

TITOLO, S., BRAULT, K., MAJEWSKI, J., WHITE, P. W. & ARCHAMBAULT, J. 2003. Characterization of the Minimal DNA Binding Domain of the Human Papillomavirus E1 Helicase: Fluorescence Anisotropy Studies and Characterization of a Dimerization-Defective Mutant Protein. *Journal of Virology,* 77**,** 5178-5191.

TITOLO, S., PELLETIER, A., PULICHINO, A.-M., BRAULT, K., WARDROP, E., WHITE, P. W., CORDINGLEY, M. G. & ARCHAMBAULT, J. 2000. Identification of Domains of the Human Papillomavirus Type 11 E1 Helicase Involved in Oligomerization and Binding to the Viral Origin. *Journal of Virology,* 74**,** 7349-7361.

TOMAKIDI, P., CHENG, H., KOHL, A., KOMPOSCH, G. & ALONSO, A. 2000a. Connexin 43 expression is downregulated in raft cultures of human keratinocytes expressing the human papillomavirus type 16 E5 protein. *Cell and Tissue Research,* 301**,** 323-327.

TOMAKIDI, P., CHENG, H., KOHL, A., KOMPOSCH, G. & ALONSO, A. 2000b. Modulation of the epidermal growth factor receptor by the human papillomavirus type 16 E5 protein in raft cultures of human keratinocytes. *European Journal of Cell Biology,* 79**,** 407-412.

TOMITA, Y., OGAWA, T., JIN, Z. & SHIRASAWA, H. 2007. Genus specific features of bovine papillomavirus E6, E7, E5 and E8 proteins. *Virus Research,* 124**,** 231-236.

TOWLER, M. C., PRESCOTT, A. R., JAMES, J., LUCOCQ, J. M. & PONNAMBALAM, S. 2000. The manganese cation disrupts membrane dynamics along the secretory pathway. *Experimental Cell Research,* 259**,** 167-179.

TRINKLE-MULCAHY, L., BOULON, S., LAM, Y. W., URCIA, R., BOISVERT, F.-M., VANDERMOERE, F., MORRICE, N. A., SWIFT, S., ROTHBAUER, U., LEONHARDT, H. & LAMOND, A. 2008. Identifying specific protein interaction partners using quantitative mass spectrometry and bead proteomes. *Journal of Cell Biology,* 183**,** 223-239.

TSAO, Y. P., LI, L. Y., TSAI, T. C. & CHEN, S. L. 1996. Human papillomavirus type 11 and 16 E5 represses $p21^{WafI/SdiI/CipI}$ gene expression in fibroblasts and keratinocytes. *Journal of Virology,* 70**,** 7535-7539.

TUNGTEAKKHUN, S. S. & DUERKSEN-HUGHES, P. J. 2008. Cellular binding partners of the human papillomavirus E6 protein. *Archives of Virology,* 153**,** 397-408.

TUNGTEAKKHUN, S. S., FILIPPOVA, M., FODOR, N. & DUERKSEN-HUGHES, P. J. 2010. The Full-Length Isoform of Human Papillomavirus 16 E6 and Its Splice Variant E6* Bind to Different Sites on the Procaspase 8 Death Effector Domain. *Journal of Virology,* 84**,** 1453-1463.

UNDERBRINK , M. P., HOWIE, H. L., BEDARD, K. M., KOOP, J. I. & GALLOWAY, D. A. 2008. E6 Proteins from Multiple Human Betapapillomavirus Types Degrade Bak and Protect Keratinocytes from Apoptosis after UVB Irradiation. *Journal of Virology,* 82**,** 10408-10417.

VALDOVINOS-TORRES, H., OROZCO-MORALES, M., PEDROZA-SAAVEDRA, A., PADILLA-NORIEGA, L., ESQUIVEL-GUADARRAMA, F. & GUTIERREZ-XICOTENCATL, L. 2008. Different Isoforms of HPV-16 E7 Protein are Present in Cytoplasm and Nucleus. *The open virology journal,* 2**,** 15-23.

VALENCIA, C., BONILLA-DELGADO, J., OKTABA, K., OCADIZ-DELGADO, R., GARIGLIO, P. & COVARRUBIAS, L. 2008. Human Papillomavirus E6/E7 Oncogenes Promote Mouse Ear Regeneration by Increasing the Rate of Wound Re-epithelization and Epidermal Growth. *Journal of Investigative Dermatology,* 128**,** 2894-2903.

VALLE, G. F. & BANKS, L. 1995. The human papillomavirus (HPV)-6 and HPV-16 E5 proteins co-operate with HPV-16 E7 in the transformation of primary rodent cells. *Journal of General Virology,* 76**,** 1239-1245.

VAMBUTAS, A., BONAGURA, V. R. & STEINBERG, B. M. 2000. Altered expression of TAP-1 and major histocompatibility complex class I in laryngeal papillomatosis: Correlation of TAP-1 with disease. *Clinical and Diagnostic Laboratory Immunology,* 7**,** 79-85.

VAMBUTAS, A., DEVOTI, J., PINN, W., STEINBERG, B. M. & BONAGURA, V. R. 2001. Interaction of human papillomavirus type 11 E7 protein with TAP-1 results in the reduction of ATP-dependent peptide transport. *Clinical Immunology,* 101**,** 94-99.

VAN DOORSLAER, K. 2013. Evolution of the Papillomaviridae. *Virology,* 445**,** 11-20.

VAN DOORSLAER, K., TAN, Q., XIRASAGAR, S., BANDARU, S., GOPALAN, V., MOHAMOUD, Y., HUYEN, Y. & MCBRIDE, A. A. 2013. The Papillomavirus Episteme: a central resource for papillomavirus sequence data and analysis. *Nucleic Acids Research,* 41**,** D571-D578.

VAN KEMPEN, P., NOORLAG, R., BRAUNIUS, W., STEGEMANS, I., WILLEMS, S. & GROLMAN, W. 2013. Differences in methylation profiles between HPV-positive and HPV-negative oropharynx squamous cell carcinoma: A systematic review. *Epigenetics,* 9.

VAN TINE, B. A., DAO, L. D., WU, S. Y., SONBUCHNER, T. M., LIN, B. Y., ZOU, N. X., CHIANG, C. M., BROKER, T. R. & CHOW, L. T. 2004. Human papillomavirus (HPV) origin-binding protein associates with mitotic spindles to enable viral DNA partitioning. *Proceedings of the National Academy of Sciences of the United States of America,* 101**,** 4030-4035.

VANDE POL, S. B. & KLINGELHUTZ, A. J. 2013. Papillomavirus E6 oncoproteins. *Virology,* 445**,** 115-137.

VELDMAN, T., HORIKAWA, I., BARRETT, J. C. & SCHLEGEL, R. 2001. Transcriptional Activation of the Telomerase hTERT Gene by Human Papillomavirus Type 16 E6 Oncoprotein. *Journal of Virology,* 75**,** 4467-4472.

VENUTI, A., MARCANTE, M. L., FLAMINI, S., DICASTRO, V. & BAGNATO, A. 1997. The autonomous growth of human papillomavirus type 16 immortalized keratinocytes is related to endothelin-1 autocrine loop. *Journal of Virology,* 71**,** 6898-6904.

VENUTI, A., PAOLINI, F., NASIR, L., CORTEGGIO, A., ROPERTO, S., CAMPO, M. S. & BORZACCHIELLO, G. 2011. Papillomavirus E5: the smallest oncoprotein with many functions. *Molecular Cancer,* 10.

VENUTI, A., SALANI, D., POGGIALI, F., MANNI, V. & BAGNATO, A. 1998. The E5 Oncoprotein of Human Papillomavirus Type 16 Enhances Endothelin-1-Induced Keratinocyte Growth. *Virology,* 248**,** 1-5.

VOLLERT, C. S. & UETZ, P. 2004. The phox homology (PX) domain protein interaction network in yeast. *Molecular & Cellular Proteomics,* 3**,** 1053-1064.

VÕSA, L., SUDAKOV, A., REMM, M., USTAV, M. & KURG, R. 2012. Identification and Analysis of Papillomavirus E2 Protein Binding Sites in the Human Genome. *Journal of Virology,* 86**,** 348-357.

WANG, H.-K., DUFFY, A. A., BROKER, T. R. & CHOW, L. T. 2009. Robust production and passaging of infectious HPV in squamous epithelium of primary human keratinocytes. *Genes & Development,* 23**,** 181-194.

WANG, J. W. & RODEN, R. B. S. 2013. L2, the minor capsid protein of papillomavirus. *Virology,* 445**,** 175-186.

WANG, Q., GRIFFIN, H., SOUTHERN, S., JACKSON, D., MARTIN, A., MCINTOSH, P., DAVY, C., MASTERSON, P. J., WALKER, P. A., LASKEY, P., OMARY, M. B. & DOORBAR, J. 2004. Functional analysis of the human papillomavirus type 16 E1^E4 protein provides a mechanism for in vivo and in vitro keratin filament reorganization. *Journal of Virology,* 78**,** 821-833.

WANG, X., HELFER, C. M., PANCHOLI, N., BRADNER, J. E. & YOU, J. 2013. Recruitment of Brd4 to the Human Papillomavirus Type 16 DNA Replication Complex Is Essential for Replication of Viral DNA. *Journal of Virology,* 87**,** 3871-3884.

WANG, X., MEYERS, C., WANG, H. K., CHOW, L. T. & ZHENG, Z. M. 2011. Construction of a full transcription map of human papillomavirus type 18 during productive viral infection. *Journal of Virology,* 85**,** 8080-8092.

WELTERS, M. J. P., DE JONG, A., VAN DEN EEDEN, S. J. F., VAN DER HULST, J. M., KWAPPENBERG, K. M. C., HASSANE, S., FRANKEN, K., DRIJFHOUT, J. W., FLEUREN, G. J., KENTER, G., MELIEF, C. J. M., OFFRINGA, R. & VAN DER BURG, S. H. 2003. Frequent display of human papillomavirus type 16 E6-specific memory T-helper cells in the healthy population as witness of previous viral encounter. *Cancer Research,* 63**,** 636-641.

WETHERILL, L. F. 2012. Identification of High-Risk Human Papillomavirus Type 16 E5 Oncoprotein as a Novel Viroporin. *Thesis, University of Leeds*.

WETHERILL, L. F., HOLMES, K. K., VEROW, M., MUELLER, M., HOWELL, G., HARRIS, M., FISHWICK, C., STONEHOUSE, N., FOSTER, R., BLAIR, G. E., GRIFFIN, S. & MACDONALD, A. 2012a. High-Risk Human Papillomavirus E5 Oncoprotein Displays Channel-Forming Activity Sensitive to Small-Molecule Inhibitors. *Journal of Virology,* 86**,** 5341-5351.

WETHERILL, L. F., ROSS, R. & MACDONALD, A. 2012b. *HPV E5: An Enigmatic Oncoprotein*.

WHELAN, F., STEAD, J. A., SHKUMATOV, A. V., SVERGUN, D. I., SANDERS, C. M. & ANTSON, A. A. 2012. A flexible brace maintains the assembly of a hexameric replicative helicase during DNA unwinding. *Nucleic Acids Research,* 40**,** 2271-2283.

WHO & ICO 2010. Information Centre on HPV and Cervical Cancer (HPV Information Centre). Human Papillomavirus
and Related Cancers in World. Summary Report 2010.

WILSON, R., FEHRMANN, F. & LAIMINS, L. A. 2005. Role of the E1^E4 protein in the differentiation-dependent life cycle of human papillomavirus type 31. *Journal of Virology,* 79**,** 6732-6740.

WILSON, R. & LAIMINS, L. A. 2005. Differentiation of HPV-containing cells using organotypic "raft" culture or methylcellulose. *In:* DAVY, C. & DOORBAR, J. (eds.) *Methods in Molecular Medicine.*

WILSON, R., RYAN, G. B., KNIGHT, G. L., LAIMINS, L. A. & ROBERTS, S. 2007. The full-length E1^E4 protein of human papillomavirus type 18 modulates differentiation-dependent viral DNA amplification and late gene expression. *Virology,* 362**,** 453-460.

WILTING, S. M., STEENBERGEN, R. D. M., TIJSSEN, M., VAN WIERINGEN, W. N., HELMERHORST, T. J. M., VAN KEMENADE, F. J., BLEEKER, M. C. G., VAN DE WIEL, M. A., CARVALHO, B., MEIJER, G. A., YLSTRA, B., MEIJER, C. J. L. M. & SNIJDERS, P. J. F. 2009. Chromosomal Signatures of a Subset of High-Grade Premalignant Cervical Lesions Closely Resemble Invasive Carcinomas. *Cancer Research,* 69**,** 647-655.

WINDISCH, D., HOFFMANN, S., AFONIN, S., VOLLMER, S., BENAMIRA, S., LANGER, B., BÜRCK, J., MUHLE-GOLL, C. & ULRICH, A. S. 2010. Structural Role of the Conserved Cysteines in the Dimerization of the Viral Transmembrane Oncoprotein E5. *Biophysical Journal,* 99**,** 1764-1772.

WINER, R. L., HUGHES, J. P., FENG, Q., XI, L. F., CHERNE, S., O'REILLY, S., KIVIAT, N. B. & KOUTSKY, L. A. 2010. Detection of Genital HPV Types in Fingertip Samples from Newly Sexually Active Female University Students. *Cancer Epidemiology Biomarkers & Prevention,* 19**,** 1682-1685.

WINER, R. L., HUGHES, J. P., FENG, Q., XI, L. F., CHERNE, S., O'REILLY, S., KIVIAT, N. B. & KOUTSKY, L. A. 2011. Early Natural History of Incident, Type-Specific Human Papillomavirus Infections in Newly Sexually Active Young Women. *Cancer Epidemiology Biomarkers & Prevention,* 20**,** 699-707.

WINER, R. L., KIVIAT, N. B., HUGHES, J. P., ADAM, D. E., LEE, S. K., KUYPERS, J. M. & KOUTSKY, L. A. 2005. Development and duration of human papillomavirus lesions, after initial infection. *Journal of Infectious Diseases,* 191**,** 731-738.

WINOKUR, P. L. & MCBRIDE, A. A. 1992. Separation of the transcriptional activation and replication functions of the bovine papillomavirus-1 E2 protein. *Embo Journal,* 11**,** 4111-4118.

WISNIEWSKI, J. R., ZOUGMAN, A., NAGARAJ, N. & MANN, M. 2009. Universal sample preparation method for proteome analysis. *Nature Methods,* 6**,** 359-U60.

WOLF, M., GARCEA, R. L., GRIGORIEFF, N. & HARRISON, S. C. 2010. Subunit interactions in bovine papillomavirus. *Proceedings of the National Academy of Sciences of the United States of America,* 107**,** 6298-6303.

WOODHALL, S., RAMSEY, T., CAI, C., CROUCH, S., JIT, M., BIRKS, Y., EDMUNDS, W. J., NEWTON, R. & LACEY, C. J. N. 2008. Estimation of the impact of genital warts on health-related quality of life. *Sexually Transmitted Infections,* 84**,** 161-166.

WOODHAM, A. W., DA SILVA, D. M., SKEATE, J. G., RAFF, A. B., AMBROSO, M. R., BRAND, H. E., ISAS, J. M., LANGEN, R. & KAST, W. M. 2012. The S100A10 Subunit of the Annexin A2 Heterotetramer Facilitates L2-Mediated Human Papillomavirus Infection. *Plos One,* 7**,** e43519.

WU, E. W., CLEMENS, K. E., HECK, D. V. & MÜNGER, K. 1993. The human papillomavirus E7 oncoprotein and the cellular transcription factor E2F bind to separate sites on the retinoblastoma tumor suppressor protein *Journal of Virology,* 67**,** 2402-2407.

WU, M.-H., CHAN, J. Y.-H., LIU, P.-Y., LIU, S.-T. & HUANG, S.-M. 2007a. Human papillomavirus E2 protein associates with nuclear receptors to stimulate nuclear receptor- and E2-dependent transcriptional activations in human cervical carcinoma cells. *The International Journal of Biochemistry & Cell Biology,* 39**,** 413-425.

WU, M.-H., HUANG, C.-J., LIU, S.-T., LIU, P.-Y., HO, C.-L. & HUANG, S.-M. 2007b. Physical and functional interactions of human papillomavirus E2 protein with nuclear receptor coactivators. *Biochemical and Biophysical Research Communications,* 356**,** 523-528.

WU, R., ABRAMSON, A. L., SHIKOWITZ, M. J., DANNENBERG, A. J. & STEINBERG, B. M. 2005. Epidermal growth factor-induced cyclooxygenase-2 expression is mediated through phosphatidylinositol-3 kinase, not mitogen-activated protein/extracellular signal-regulated

kinase kinase, in recurrent respiratory papillomas. *Clinical Cancer Research,* 11**,** 6155-6161.

WU, R., CONIGLIO, S. J., CHAN, A., SYMONS, M. H. & STEINBERG, B. M. 2007c. Up-regulation of Rac1 by epidermal growth factor mediates COX-2 expression in recurrent respiratory papillomas. *Molecular Medicine,* 13**,** 143-150.

WU, Y.-C., BIAN, X.-L., HEATON, P. R., DEYRIEUX, A. F. & WILSON, V. G. 2009. Host cell sumoylation level influences papillomavirus E2 protein stability. *Virology,* 387**,** 176-183.

XI, S. Z. & BANKS, L. M. 1991. Baculovirus expression of the human papillomavirus type-16 capsid proteins - detection of L1-L2 protein complexes *Journal of General Virology,* 72**,** 2981-2988.

YANG, D.-H., WILDEMAN, A. G. & SHAROM, F. J. 2003a. Overexpression, purification, and structural analysis of the hydrophobic E5 protein from human papillomavirus type 16. *Protein Expression and Purification,* 30**,** 1-10.

YANG, R., DAY, P. M., YUTZY, W. H., LIN, K.-Y., HUNG, C.-F. & RODEN, R. B. S. 2003b. Cell Surface-Binding Motifs of L2 That Facilitate Papillomavirus Infection. *Journal of Virology,* 77**,** 3531-3541.

YANG, X. P., MATERN, H. T. & GALLWITZ, D. 1998. Specific binding to a novel and essential Golgi membrane protein (Yip1p) functionally links the transport GTPases Ypt1p and Ypt31p. *Embo Journal,* 17**,** 4954-4963.

YANOFSKY, V., PATEL, R. & GOLDENBERG, G. 2012. Genital warts: a comprehensive review. *J Clin Aesthet Dermatol.,* 5**,** 25-36.

YOSHIDA, Y., SUZUKI, K., YAMAMOTO, A., SAKAI, N., BANDO, M., TANIMOTO, K., YAMAGUCHI, Y., SAKAGUCHI, T., AKHTER, H., FUJII, G., YOSHIMURA, S., OGATA, S., SOHDA, M., MISUMI, Y. & NAKAMURA, N. 2008. YIPF5 and YIF1A recycle between the ER and the Golgi apparatus and are involved in the maintenance of the Golgi structure. *Experimental Cell Research,* 314**,** 3427-3443.

YOUNG, K. H. 1998. Yeast two-hybrid: So many interactions, (in) so little time. *Biology of Reproduction,* 58**,** 302-311.

YU, J.-H., LIN, B. Y., DENG, W., BROKER, T. R. & CHOW, L. T. 2007. Mitogen-Activated Protein Kinases Activate the Nuclear Localization Sequence of Human Papillomavirus Type 11 E1 DNA Helicase To Promote Efficient Nuclear Import. *Journal of Virology,* 81**,** 5066-5078.

YU, T. X., FERBER, M. J., CHEUNG, T. H., CHUNG, T. K. H., WONG, Y. F. & SMITH, D. I. 2005. The role of viral integration in the development of cervical cancer. *Cancer Genetics and Cytogenetics,* 158**,** 27-34.

YU, Y. & MÜNGER, K. 2013. Human papillomavirus type 16 E7 oncoprotein inhibits the anaphase promoting complex/cyclosome activity by dysregulating EMI1 expression in mitosis. *Virology,* 446**,** 251-259.

ZANIER, K., CHARBONNIER, S., SIDI, A. O. M. H. O., MCEWEN, A. G., FERRARIO, M. G., POUSSIN-COURMONTAGNE, P., CURA, V., BRIMER, N., BABAH, K. O., ANSARI, T., MULLER, I., STOTE, R. H., CAVARELLI, J., VANDE POL, S. & TRAVÉ, G. 2013. Structural Basis for Hijacking of Cellular LxxLL Motifs by Papillomavirus E6 Oncoproteins. *Science,* 339**,** 694-698.

ZANIER, K., OULD M'HAMED OULD SIDI, A., BOULADE-LADAME, C., RYBIN, V., CHAPPELLE, A., ATKINSON, A., KIEFFER, B. & TRAVÉ, G. 2012. Solution Structure Analysis of the HPV16 E6 Oncoprotein Reveals a Self-Association Mechanism Required for E6-Mediated Degradation of p53. *Structure,* 20**,** 604-617.

ZERFASS-THOME, K., ZWERSCHKE, W., MANNHARDT, B., TINDLE, R., BOTZ, J. W. & JANSENDURR, P. 1996. Inactivation of the cdk inhibitor $p27^{KIP1}$ by the human papillomavirus type 16 E7 oncoprotein. *Oncogene,* 13**,** 2323-2330.

ZERFASS, K., SCHULZE, A., SPITKOVSKY, D., FRIEDMAN, V., HENGLEIN, B. & JANSEN-DÜRR, P. 1995. Sequential activation of cyclin E and cyclin A gene expression by human papillomavirus type 16 E7 through sequences necessary for transformation. *Journal of Virology,* 69**,** 6389-99.

ZHANG, B. Y., LI, P., WANG, E., BRAHMI, Z., DUNN, K. W., BLUM, J. S. & ROMAN, A. 2003. The E5 protein of human papillomavirus type 16 perturbs MHC class II antigen maturation in human foreskin keratinocytes treated with interferon-gamma. *Virology,* 310**,** 100-108.

ZHANG, B. Y., SPANDAU, D. F. & ROMAN, A. 2002. E5 protein of human papillomavirus type 16 protects human foreskin keratinocytes from UVB-irradiation-induced apoptosis. *Journal of Virology,* 76**,** 220-231.

ZHANG, B. Y., SRIRANGAM, A., POTTER, D. A. & ROMAN, A. 2005. HPV16 E5 protein disrupts the c-Cbl-EGFR interaction and EGFR ubiquitination in human foreskin keratinocytes. *Oncogene,* 24**,** 2585-2588.

ZHAO, K.-N., HENGST, K., LIU, W.-J., LIU, Y. H., LIU, X. S., MCMILLAN, N. A. J. & FRAZER, I. H. 2000. BPV1 E2 Protein Enhances Packaging of Full-Length Plasmid DNA in BPV1 Pseudovirions. *Virology,* 272**,** 382-393.

ZHAO, K. N., GRU, W. Y., FANG, N. X., SAUNDERS, N. A. & FRAZER, I. H. 2005. Gene codon composition determines differentiation-dependent expression of a viral capsid gene in keratinocytes in vitro and in vivo. *Molecular and Cellular Biology,* 25**,** 8643-8655.

ZHENG, Z. M. & BAKER, C. C. 2006. Papillomavirus genome structure, expression, and post-transcriptional regulation. *Frontiers in Bioscience,* 11**,** 2286-2302.

ZHOU, F., CHEN, J. & ZHAO, K.-N. 2013. Human papillomavirus 16-encoded E7 protein inhibits IFN-γ-mediated MHC class I antigen presentation and CTL-induced lysis by blocking IRF-1 expression in mouse keratinocytes. *Journal of General Virology,* 94**,** 2504-2514.

ZHOU, J., DOORBAR, J., XIAO YI, S., CRAWFORD, L. V., MCLEAN, C. S. & FRAZER, I. H. 1991. Identification of the nuclear localization signal of human papillomavirus type 16 L1 protein. *Virology,* 185**,** 625-632.

ZOU, N., LIN, B. Y., DUAN, F., LEE, K.-Y., JIN, G., GUAN, R., YAO, G., LEFKOWITZ, E. J., BROKER, T. R. & CHOW, L. T. 2000. The Hinge of the Human Papillomavirus Type 11 E2 Protein Contains Major Determinants for Nuclear Localization and Nuclear Matrix Association. *Journal of Virology,* 74**,** 3761-3770.